AN ELECTRON SPIN RESONANCE STUDY

OF DRUG BINDING TO NUCLEIC ACIDS.

T. Porumb

A Thesis submitted for the Degree

of Doctor in Philosophy, University

of Keele, England, 1976.

ABSTRACT.

The thesis presents a study of the interaction of paramagnetic derivatives of drugs with the nucleic acids, carried out using the electron spin resonance (ESR) technique. The general principles of ESR (particularly those concerned with the free radicals) are outlined and spin labelling techniques as applied to biological specimens are described. The interaction of nucleic acids with small molecules is also reviewed.

Most of the work was performed using the radical cation of the tranquilizer chlorpromazine (CPZ^+). Measurements were taken at X and Q-band frequencies and were coupled with extensive theoretical simulations of the ESR spectra. The hyperfine tensor elements arising from the ^{14}N atom of the chlorpromazine ion were determined by computer fitting, from the spectrum obtained from a DNA-CPZ^+ gel. The analysis of the spectra obtained from oriented DNA-CPZ^+ fibre specimens led to the formulation of a fibre model according to which the DNA molecules described a Gaussian distribution of orientations about the fibre axis (with a half width in the range from 27 to 40°). The results were compared with data obtained by other techniques (particularly optical linear dichroism).

The measurements were extended to the investigation of other nucleic acid species and drugs and the results were discussed in relation to their biophysical significance.

15 June 1976.

ACKNOWLEDGEMENTS.

CONTENTS

CHAPTER 1.

INTRODUCTION

The nucleic acids function through their interaction with other molecules. For example, the translation, transcription and replication require large enzyme systems, which bind to the nucleic acids in highly specific manners. At the same time, a large number of small drug molecules, such as the acridine mutagens, the antitumor drugs daunomycin and adriamycin or the antibiotic ethydium bromide, owe their therapeutic action (or some of their side effects) to their ability to bind to the nucleic acids. The importance of studying the drug-nucleic acid interactions at a molecular level lies not only in the direct applicability of the results of these studies in pharmacology (to the design and synthesis of better drugs), but also in providing valuable information on the factors responsible for the binding and the specificity; an essential basis for understanding the nature of the binding of more complex molecules.

The object of the present project was to study the interaction of drugs with nucleic acids using the electron spin resonance (ESR) technique, and to investigate the possibility of correlating this information with data obtained from other techniques. Most of the work described in this thesis was performed using the radical cation derivative of the drug chlorpromazine.

Chlorpromazine (CPZ) is the prototype of a class of tranquilizer drugs, derived from phenothiazine (Fig. 4.1.). The psychotropic activity of these drugs is not fully understood. Recent studies showed that CPZ inhibits the cholinergic receptors in the brain (Ref. 1.). It has also been reported that CPZ causes structural alternations of metaphase chromosomes of human lymphocytes in tissue cultures (Ref. 2.), and has a photosensitization effect on skin. It was suggested that the latter phenomenon could be related to the formation of CPZ-DNA complexes under the influence of UV rays (Ref. 3.). A particular feature of the drugs belonging to this class

is their long persistence in the organism after administration (Ref. 7.).

Forrest et al. (Ref. 4.), observing the metabolites of CPZ excreted by the organism, suggested that the biologically active form of the drug was that of a stable free radical, i.e. a molecule possessing an unpaired eletron. The drug could represent an active oxido-reduction system in this state. According to Piette et al. (Ref. 5.), the radical is the cation derivative of chlorpromazine, CPZ^+, which is obtained from the neutral species by a one-step oxidation process (see Section 4.1.). Ohnishi and McConnell (Ref. 6.) showed that the stability of CPZ^+ cation radical was enhanced upon its binding to the DNA, and presented evidence which suggested that the CPZ^+ molecule adopted a definite orientation relative to the DNA helix. (Detailed references to this paper will be made in the subsequent chapters.)

The interaction of CPZ^+ with the DNA is also particularly interesting from the theoretical point of view, since the chlorpromazine molecule is not perfectly planar, thus differing in this respect from the drug molecules mentioned in the beginning of this chapter. It is widely accepted that such planar molecules bind to the nucleic acids by intercalating between adjacent base-pairs of the nucleic acid helix. It would be interesting to see if an intercalation mechanism (which is the one suggested by Ohnishi and McConnell, Ref. 6.) could apply to the CPZ^+-DNA interaction, because the CPZ^+ molecule is "bent" and the existent models of intercalation do not make explicit provisions for such special cases (see also Section 4.2.).

It was considered appropriate to begin the thesis by placing this project in the context of related pieces of work reported in the literature. Although the techniques employed in this project (mainly the spin labelling technique) are sufficiently well established, the context in which they were applied is relatively new. Therefore, it was found necessary to review the background corresponding to these topics separately. Thus, Chapter 2 gives

an outline of the general principles of ESR, emphasising those connected with the free radicals, which are relevant to this piece of work. The recent advances in the field of the spin labelling technique and the biological applications of ESR are reviewed in Chapter 3, which is followed by the presentation of the properties of the nucleic acids and their interactions with small molecules, in Chapter 4.

A summary of the present project is given in Section 4.3., with the emphasis on its practical applicability and the justification of the techniques employed. Part of the information contained in this thesis has already been published (with Dr. E. F. Slade) in the following papers:

"A Computational Method for the Synthesis of ESR Spectra of Systems with One Axis of Symmetry", Journal of Magnetic Resonance, 22, 219-226 (1976).

This topic is discussed in Chapters 5 and 6 and an extension of the method to the simulation of some anisotropic optical properties of fibres (birefringence and linear dichroism) is presented in Chapter 8.

"Electron-Spin-Resonance Studies of a Chlorpromazine Derivative Bound to DNA Fibres", European Journal of Biochemistry, 65, 21-24 (1976).

The full treatment of this topic is found in Chapter 6.

The ESR lineshape computer program (for general use with free radical specimens including fibres), which was developed as a research tool in the present project, has been made available to the University of Indiana, Quantum Chemistry Exchange Programs (library number QCEP 295).

The CPZ^+ binding studies carried out with other nucleic acid species are presented in Chapter 7. The conclusions of this piece of work are presented in Chapter 9, which also describes the attempts made to extend the method developed in the preceding chapters to the study of the interaction of the nucleic acids with ionic forms or paramagnetic derivatives of other drugs.

REFERENCES.

1. M. TRABUCCHI, D. CHENEY, G. RACAGNI, E. COSTA: Nature, 249, 664-666, (1974).

2. P. S. MARFEY, M. G. LI: Z. Naturforsh, 29G, 306, (1974).

3. G. KAHN, B. P. DAVIS: J. Invest. Dermatol., 55, 47, (1970).

4. I. S. FORREST, F. M. FORREST, M. BERGER: Biochim. Biophys. Acta., 29, 441-442, (1958).

5. L. H. PIETTE, G. BULOW, I. YAMAZAKI: Biochim. Biophys. Acta, 88, 120, (1964).

6. S. OHNISHI, M. M. McCONNEL: J. Amer. Chem. Soc., 87, 2293, (1965).

7. British Pharmaceutical Codex, 1959, The Pharmaceutical Press.

CHAPTER 2.

THE THEORY AND THE DETECTION OF ELECTRON SPIN RESONANCE.

The contents of this chapter serves as a theoretical background for the thesis. This chapter gives an outline of the general principles of ESR, emphasising those connected with the properties of the free radicals which are relevant to this piece of work. At the same time, it was designed so that it can be used as a practical source of reference in the future. All the formulae and the numerical constants quoted in the chapter conform to the SI system of units.

As the general field is well documented (see Bibliography, Refs. 1. - 5.) it was found appropriate to present the concepts in a concise form, reference being made to the basic textbooks for detailed arguments.

2.1. The Phenomenon of Electron Spin Resonance.

A free electron that possesses a spin angular momentum of $\hbar \underline{S}$ (where $\underline{S}$ is the electronic spin vector, $|\underline{S}| = [S(S+1)]^{\frac{1}{2}}$, and $\hbar = 1.05459 \times 10^{-34}$ J.S. is Planck's constant divided by 2π) has a magnetic moment $\underline{\mu}_e$ associated with it, so that:

$$\underline{\mu}_e = -g\,\beta\,\underline{S} \tag{1}$$

In this expression g is a dimensionless constant (the g factor) which in the case of the free electron is equal to 2.002322, and $\beta = e\hbar/(2m)$ (with -e and m the electronic charge and mass) is the Bohr magneton and is equal to 9.27410×10^{-24} J T^{-1}. The magnetic moment $\underline{\mu}_e$ is measured in J T^{-1} = A m^2. An equivalent statement to Equation (1) is:

$$\underline{\mu}_e = -\gamma\,\hbar\,\underline{S} \tag{2}$$

with $\gamma = g\beta/\hbar$ being the gyromagnetic ratio of the electron (T^{-1} s^{-1}).

The energy of interaction with an applied magnetic field $\underline{B}$ assumed to be along the Z direction is represented by the "Zeeman" Hamiltonian:
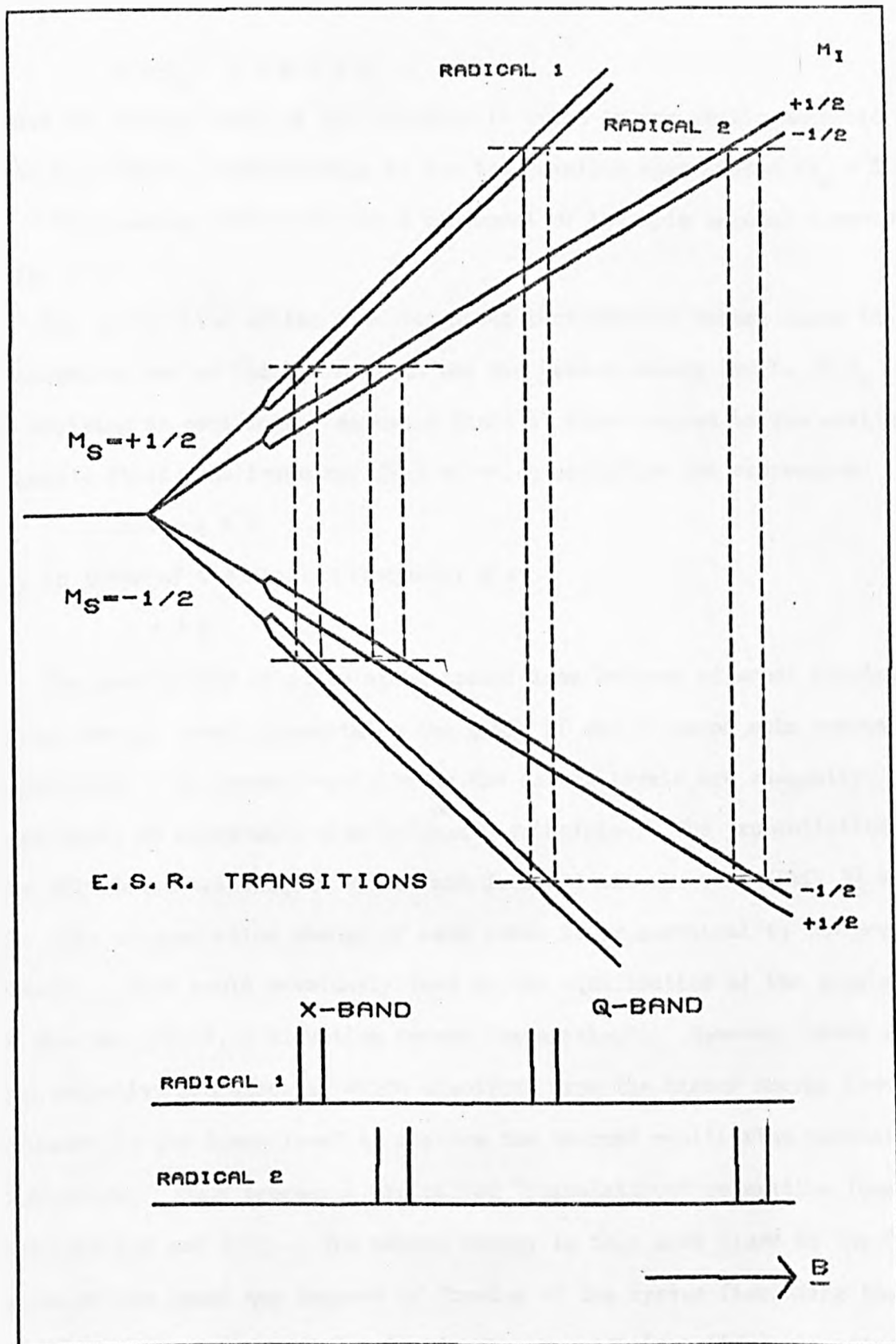
FIG. 2.1 SCHEMATIC REPRESENTATION OF THE SPLITTING OF THE SPIN
ENERGY LEVEL IN A MAGNETIC FIELD (B). TWO RADICALS (OF ELECTRONIC SPIN
1/2) ARE CONSIDERED, DIFFERRING IN THEIR G-VALUES $(G_1 > G_2)$. THE HYPER-
FINE STRUCTURE DUE TO A NUCLEUS OF NUCLEAR SPIN 1/2 WITH POSITIVE
COUPLING CONSTANT IS INCLUDED AND THE POSITION OF THE ESR TRANSITIONS
IS INDICATED. THE SEPARATION OF THE HYPERFINE LINES OF A RADICAL IS
INDEPENDENT OF THE FREQUENCY (X VS. Q BAND). THE SEPARATION OF TWO
SIGNALS OF DIFFERENT G-VALUE IS HIGHER IF RECORDED AT A HIGHER FREQUENCY.

$$H = -\underline{\mu}_e \cdot \underline{B} = g \beta B S_z \tag{3}$$

Hence the energy level of the electron is split in the static magnetic field into two levels, corresponding to the two possible spin states ($m_s = \pm \frac{1}{2}$, m_s = the quantum number for the Z component of the spin angular momentum). (Fig. 2.1).

The application of the time dependent perturbation theory shows that transitions can be induced between the two Zeeman energy levels ($\Delta m_s = \pm 1$) by applying an oscillatory magnetic field at right angles to the static magnetic field, the frequency (γ) of which satisfies the expression:

$$h\gamma = g\beta B \tag{4}$$

or, in terms of the angular frequency ω :

$$\omega = \gamma B \tag{5}$$

The possibility of stimulating transitions between adjacent electronic Zeeman energy levels constitutes the basis of the electron spin resonance experiment. In thermal equilibrium the energy levels are unequally populated, in accordance with Boltman's principle. The probabilities of the stimulated transitions upward and downward are the same (Ref. 5) and the rate of population change of each level is proportional to the population itself. This would eventually lead to the equalization of the population of the two levels, a situation termed "saturation". However, there are non-radiative processes by which electrons from the higher energy level are returned to the lower level to restore the thermal equilibrium population difference. Such processes are called "spin-lattice" relaxation (see also Sections 2.2 and 2.4). The excess energy in this case flows to the "lattice", by which one means any degrees of freedom of the system (including the vibrations of the crystal lattice in the case of the solids) other than those directly concerned with the spin. The system can be in solid, liquid or gaseous states.

Thus absorption of energy takes place at resonance.   In an ESR experiment one monitors the energy absorption as the field is varied at a fixed frequency which is usually in the X-band (9.5 G H_z) or Q-band (35 G H_z) range.

In cases when both orbital and spin angular momentum are present and if the L S coupling is applicable, the resultant angular momentum is associated with the quantum number $\underline{J}$ where $\underline{J} = \underline{L} + \underline{S}$ and g is given by the Landé g factor:

$$g_J = 1 + \frac{J\,(J + 1) + S\,(S + 1) - L\,(L + 1)}{2\,J\,(J + 1)}$$

so that Equation (1) becomes:

$$\mu\, J = -\, g_J\, \beta\, \underline{J}$$

This thesis is concerned primarily with free radicals i.e. molecules which have at least one unpaired electron.   The essential property of a free radical is that the magnetism of the radical is largely due to the spin. Thus the free radicals give g values close to the free electron value. Deviations from this value indicate orbital contributions to the effective magnetic moment of the unpaired electron.

A useful free radical, often used as g marker, is diphenyl picryl hydrazyl (DPPH), which has a g value equal to 2.0036 (Ref. 12).

2.2.   The ESR Lineshape.

The finite "width" of the ESR signal follows from the uncertainty principle as a result of the broadening of the energy levels due to the finite lifetime of the excited spin states.

The spin-lattice relaxation has already been mentioned as an essential factor for the success of an ESR experiment.   This is one of the possible interactions of the spin system with its surroundings ("relaxations") which lead to limiting the lifetime of the spin states.

There is a classical theory due to Bloch, which predicts an actual lineshape.

Bloch's treatment is in terms of the macroscopic property of the sample, $\underline{M}$, the magnetization, which is the sum over all the spins in a unit volume of the individual spin magnetic momenta $\underline{\mu}_e$. The basic assumptions of the theory are: 1) In the magnetic field both $\underline{\mu}_e$ and $\underline{M}$ behave like classical gyroscopes, hence the gyroscopic equations of motion can be applied; 2) $\underline{M}$ tends to approach its thermal equilibrium value $\underline{M}_0$, proportional to the static magnetic susceptibility χ_0 ($M_0 = \chi_0 B/\mu_0$).

These assumptions lead to "Bloch's equations" of motion:

$$\frac{dM_z}{dt} = \gamma \, (\underline{B} \times \underline{M})_z + \frac{M_0 - M_z}{T_1} \tag{6a}$$

$$\frac{dM_{x,y}}{dt} = \gamma \, (\underline{B} \times \underline{M})_{x,y} - \frac{M_{x,y}}{T_2} \tag{6b}$$

They describe a damped precession motion of $\underline{M}$ about $\underline{B}$, in which the transverse components of $\underline{M}$ decay to zero with a characteristic time T_2 while M_z relaxes towards its equilibrium value M_0 with a characteristic time T_1.

As the magnetic energy ($-\underline{M}.\underline{B}$) depends on M_z, it can be seen that T_1 is a measure of the rate at which energy flows from the spin system to the lattice when the system approaches thermal equilibrium and thus T_1 is called the "spin-lattice" relaxation time.

No energy need flow out of the system for the relaxation of M_x and M_y. T_2 can be regarded as a dephasing time, measuring the time in which the individual spins remain in phase with each other. It is called the "spin-spin", or longitudinal relaxation time because the interaction between the

various spins, causing different local magnetic fields at each spin is the main cause of randomising the precessional phases.

Bloch's equations can be solved to give the power absorbed from an oscillatory magnetic field of amplitude $2 B_1$ and angular frequency ω :

$$P(\omega) = \frac{B_1^2 \chi_0 \omega \omega_0 T_2}{1 + T_2^2 (\omega_0 - \omega)^2 + \gamma^2 T_1 T_2 B_1^2} \tag{7}$$

In this expression $\omega_0 = \gamma B$ is the resonant ("Larmor") angular frequency. Equation (7) gives the "saturated" lineshape.

Far from saturation (achieved by using small microwave amplitudes so that the term $\gamma^2 B_1^2 T_1 T_2$ is negligible), one obtains the "Lorentzian" lineshape (Equation (8)), which depends only on T_2 and not on T_1. The normalised "unsaturated" lineshape, the width at half height ($\Delta \omega_{\frac{1}{2}}$) and the width between the points of maximum slope ($\Delta \omega$) are given by:

$$g(\omega) = \frac{T_2}{\pi} \cdot \frac{1}{1 + T_2^2 (\omega - \omega_0)^2}$$

$$\Delta \omega_{\frac{1}{2}} = \frac{2}{T_2} , \quad \Delta \omega = \frac{2}{T_2 3^{\frac{1}{2}}} \tag{8}$$

Therefore T_1 determines the degree of saturation and T_2 the unsaturated linewidth.

Another common lineshape is the Gaussian, given by:

$$g(\omega) = \frac{T_2}{(2\pi)^{\frac{1}{2}}} e^{-\frac{1}{2} T_2^2 (\omega - \omega_0)^2} \tag{9}$$

$$\Delta \omega_{\frac{1}{2}} = \frac{2.35}{T_2} , \quad \Delta \omega = \frac{2}{T_2}$$

Such lineshapes are usually obtained from solids or concentrated solutions

in which dipolar interactions (of the form shown in Equation (12) of Section 2.3.1) are taking place between the neighbouring paramagnetic ions (Ref. 9). These interactions produce a spread in the magnitude of the magnetic fields experienced by the various ions, which leads to the broadening of the resonance. The dipolar broadening effect is treated in greater detail in Section 2.4.2.

2.3. The Hamiltonian for a Free Radical.

2.3.1. Introduction.

To write the full Hamiltonian applicable to a free radical, one must take into account the effects of the nuclear interactions. The effects of the electric quadrupole moment of nuclei of nuclear spin 1 or greater and of the nuclear Zeeman interaction are small and will be neglected.

The most important term which leads to splitting of the electronic Zeeman energy levels is the hyperfine interaction which derives from the interaction between the electron and magnetic nuclei. The hyperfine interaction brings extra terms of the form $\underline{S} . \underline{A} . \underline{I}$ in the Hamiltonian, where $\underline{A}$ is the hyperfine tensor which takes into account the magnitude and the orientation dependence of the interaction energy. $\underline{S}$ and $\underline{I}$ are the electronic and nuclear spin vectors.

In general the Zeeman interaction (Equation (3)) between the electron spin and the applied magnetic field $\underline{B}$ is anisotropic and can be represented in terms of the $\underline{g}$ tensor by a term $\beta \underline{B} . \underline{g} . \underline{S}$. Hence the expression for the Hamiltonian, incorporating the hyperfine interaction with one magnetic nucleus and including g value anistropy is given by:

$$H = \beta \underline{B} . \underline{g} . \underline{S} + \underline{S} . \underline{A} . \underline{I} \tag{10}$$

The $\underline{g}$ and $\underline{A}$ tensors can usually be diagonalized although not necessarily in terms of the same axis system (see also Section 2.3.5 and Ref. 1.,pp 107, 133). Considering the first term in Equation (10), it can be represented

in the molecular frame of reference that diagonalize the $\underline{g}$ tensor as:

$$\beta \left(g_{xx} B_x S_x + g_{yy} B_y S_y + g_{zz} B_z S_z \right) \tag{11}$$

A similar expression can be written for the hyperfine term.

The hyperfine energy consists of two parts:

1) An isotropic part, a $\underline{S} \cdot \underline{I}$ arising from the "Fermi contact interaction" which can only occur if the electron has a finite probability density at the nucleus.

2) An anisotropic part, arising from the electron – nuclear dipolar interaction. This has the form:

$$\frac{\mu_o}{4\pi} \left[\frac{\underline{\mu}_e \cdot \underline{\mu}_n}{r^3} - \frac{3 \left(\underline{\mu}_e \cdot \underline{r} \right) \left(\underline{\mu}_n \cdot \underline{r} \right)}{r^5} \right] \tag{12}$$

where $\underline{\mu}_e$ and $\underline{\mu}_n$ are the electronic and nuclear spin moments and $\underline{r}$ is the radius vector between the two moments. It can be shown that this term follows a $(3 \cos^2 \theta - 1)$ variation, where θ is the angle between the direction of the applied magnetic field and the line joining the electron and the nucleus.

In the liquid phase, where the radicals perform a fast and random tumbling motion, the dipolar term is averaged to zero (providing the tumbling rate is greater than the largest anisotropic component) and the observed hyperfine splitting gives the isotropic coupling constant a (Ref. 7.). In the same conditions the g tensor is averaged to 1/3 of its trace, which is the isotropic g value.

2.3.2. Isotropic Hyperfine Spectra.

Considering the Hamiltonian:

$$H = g \beta \underline{B} \underline{S} + a \underline{I} \cdot \underline{S} \tag{13}$$

one can demonstrate the splitting of the Zeeman energy levels under the

isotropic hyperfine interaction by treating the a $\underline{I} \cdot \underline{S}$ term as a first order perturbation on the Zeeman energy levels. Considering only the interaction between the unpaired electron and one proton ($I = \frac{1}{2}$) the following four energy levels are obtained:

$$E_1 = \frac{1}{2} g \beta B + \frac{1}{4} a \qquad | \alpha_e \alpha_n >$$

$$E_2 = \frac{1}{2} g \beta B - \frac{1}{4} a \qquad | \alpha_e \beta_n >$$

$$E_3 = -\frac{1}{2} g \beta B - \frac{1}{4} a \qquad | \beta_e \alpha_n > \qquad (14)$$

$$E_4 = -\frac{1}{2} g \beta B + \frac{1}{4} a \qquad | \beta_e \beta_n >$$

where the right hand column shows the corresponding basis spin functions constructed with the possible electronic and nuclear spin states.

It can be further shown that two equally likely ESR transitions can take place between the energy levels 1 - 3 and 2 - 4 (obeying the selection rules $\Delta m_s = \pm 1, \Delta m_I = 0$) and the two lines will be separated by a, the hyperfine coupling constant. This situation is illustrated in Fig. 2.1.

In a more rigorous treatment the nuclear Zeeman energy ($g_n \beta_n \underline{B} \cdot \underline{I}$) should be included in the Hamiltonian from Equation (13). This term brings shifts in the energy levels, of the order of $\pm \frac{1}{2} g_n \beta_n B$. Following the treatment by the perturbation theory to second order, one obtains correction terms to the energy levels 2 and 3 of the form $\pm \dfrac{a^2}{4 (g \beta B + g_n \beta_n B)}$. The "allowed" ESR transitions will then occur at slightly different energies but their separation is unaltered and equal to a. However, a transition ($\Delta m_s = 1, \Delta m_I = 1$) forbidden under the simple treatment becomes possible under this treatment if the oscillatory field is parallel to the static magnetic field $\underline{B}$. Most of the free radical spectra in solution can be adequately interpreted using the simple treatment by first order perturbation theory and neglecting the nuclear Zeeman effect.

The treatment can be extended to more hyperfine interactions and for nuclear spins greater than $\frac{1}{2}$. The resonant frequencies are given in the general case by:

$$h \gamma = g \beta B + a_k m_k + \ldots + a_k m_k + \ldots \qquad (15)$$
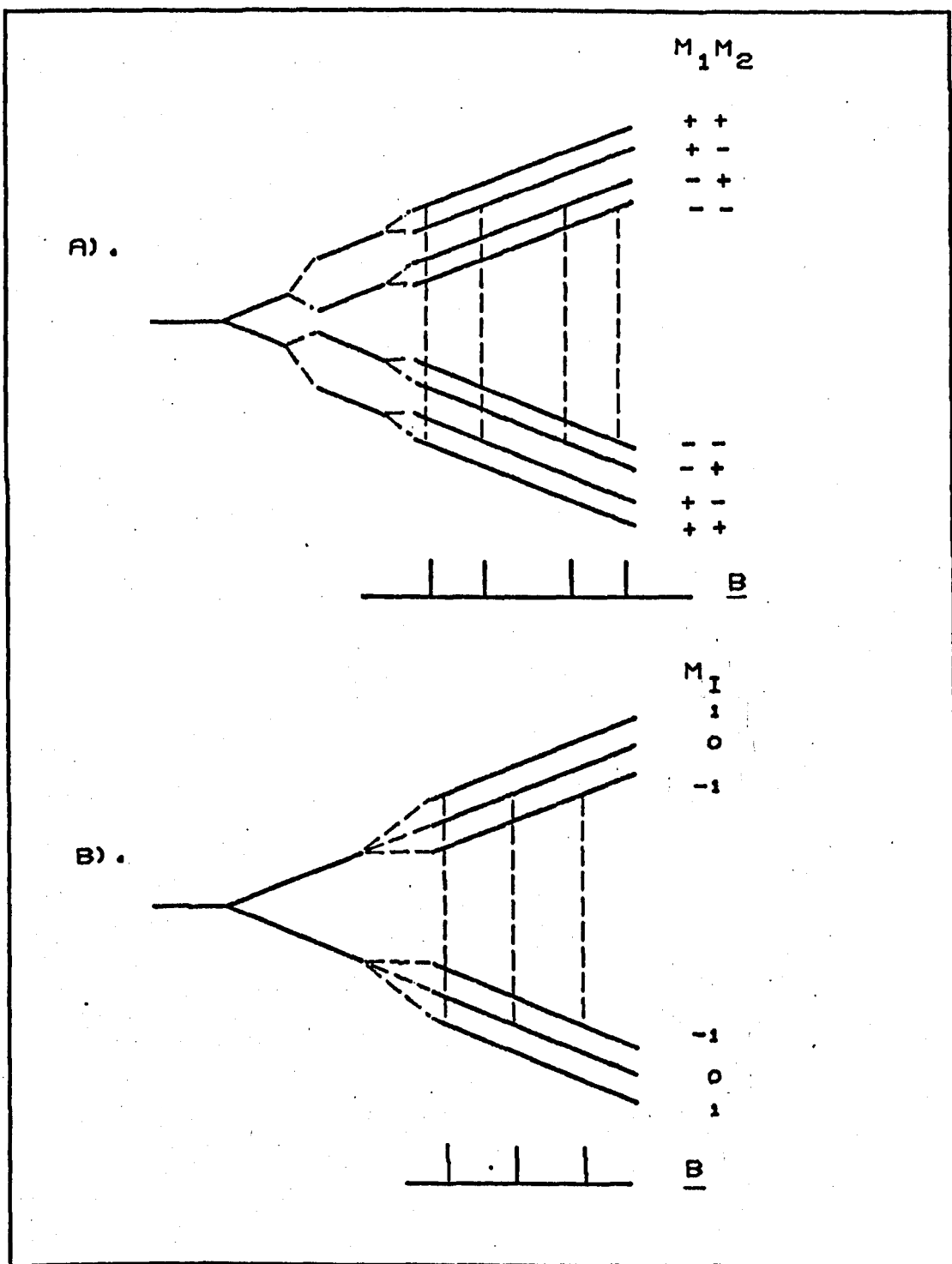
FIG. 2. 2 HYPERFINE ENERGY LEVELS AND TRANSITIONS FOR : A). TWO
UNEQUIVALENT PROTONS, B). A SINGLE NUCLEUS OF SPIN I=1. ALL THE
COUPLING CONSTANTS WERE ASSUMED POSITIVE.

where a_k is the hyperfine coupling constant with the kth nucleus and m_k is

one of the allowed values of the nuclear spin quantum number. The a's are

expressed in energy units.

Thus two unequivalent protons would split the ESR spectrum into four

equal lines (3 lines in the ratio 1:2:1 if they had the same coupling constant)

(Fig. 2a.) and ^{14}N, with a nuclear spin I = 1, would give 3 equal lines

separated by a_N, the hyperfine coupling constant (Fig. 2b.).

2.3.3. Information Available from Isotropic Hyperfine Spectra.

This section explains the origin of the isotropic hyperfine structure of

the free radical spectra and shows how this can be related to the electronic

structure of the particular free radicals.

As it was mentioned before, such spectra are obtained from free radicals

in solution, where the molecules can perform rapid tumbling motions (charact-

erised by rotational correlation times of the order of $10^{-7} - 10^{-11}$s), that

result in the averaging out of the dipolar contribution. Well resolved

hyperfine spectra are obtained at sufficiently low free radical concentrations

(usually less than 10^{-3}M), when the exchange interactions between the free

radicals are almost completely eliminated. The topics of line broadening

mechanisms and exchange interactions, together with their practical applic-

ations will be treated separately.

The analysis of the hyperfine spectra can provide information about the

nature of the free radical. As the common carbon isotope (^{12}C) has zero

nuclear spin, the observed hyperfine splittings in the radical spectra

usually come from protons or the ^{14}N atoms. The emergence of complicated

hyperfine structures in many organic radicals is explained by the substantial

delocalization of the unpaired electron which interacts with several of the

nuclei of the molecule.

In many cases where the Fermi contact term is expected to vanish and

no hyperfine splittings to occur it is necessary to consider small admixtures

of excited states with the ground state. An example is provided by the aromatic radicals where the unpaired electron is delocalized in the π molecular orbital. This has a node in the plane of the molecule and hence the electron density at the place where the protons are expected to be zero (Fig2.3.). However, proton splittings do occur and this is explained (Ref. 1., p 83) in terms of the π orbital of the unpaired electron acquiring some σ character from the anti bonding C – H orbital. Alternatively one can invoke a mechanism of indirect coupling of the π electrons of the ring with the spins of the σ electrons in the C – H bond by virtue of exchange forces, according to which the unpaired spin in the π system induces unpaired spin of opposite polarisation at the proton (Fig2.3.). For this reason the unpaired spin density and the proton hyperfine coupling constant are negative.

It follows from this theory that the hyperfine splitting (in Tesla) produced by a proton bonded to an aromatic carbon atom is directly proportional to the unpaired electron density ρ_e at the C atom (McConnell's relationship):

$$a_H = Q \, \rho_e \tag{16}$$

with Q negative and equal to about -2.25 mT.

Another common mechanism of hyperfine coupling in substituted aromatic radicals is "hyperconjugation", which results from the direct penetration of the H orbitals of the substituted groups that stick up and down out of the plane of the molecule, into the π system. Thus a freely rotating methyl ($-CH_3$) substituent gives a contribution characteristic of three equivalent protons. The recorded hyperfine splittings are usually of the same order of magnitude as those given by the ring protons.

The splittings arising from aromatic ^{14}N nuclei are roughly proportional to the unpaired electron density in their $2p_z$ orbitals, with Q values about +2.5 mT.
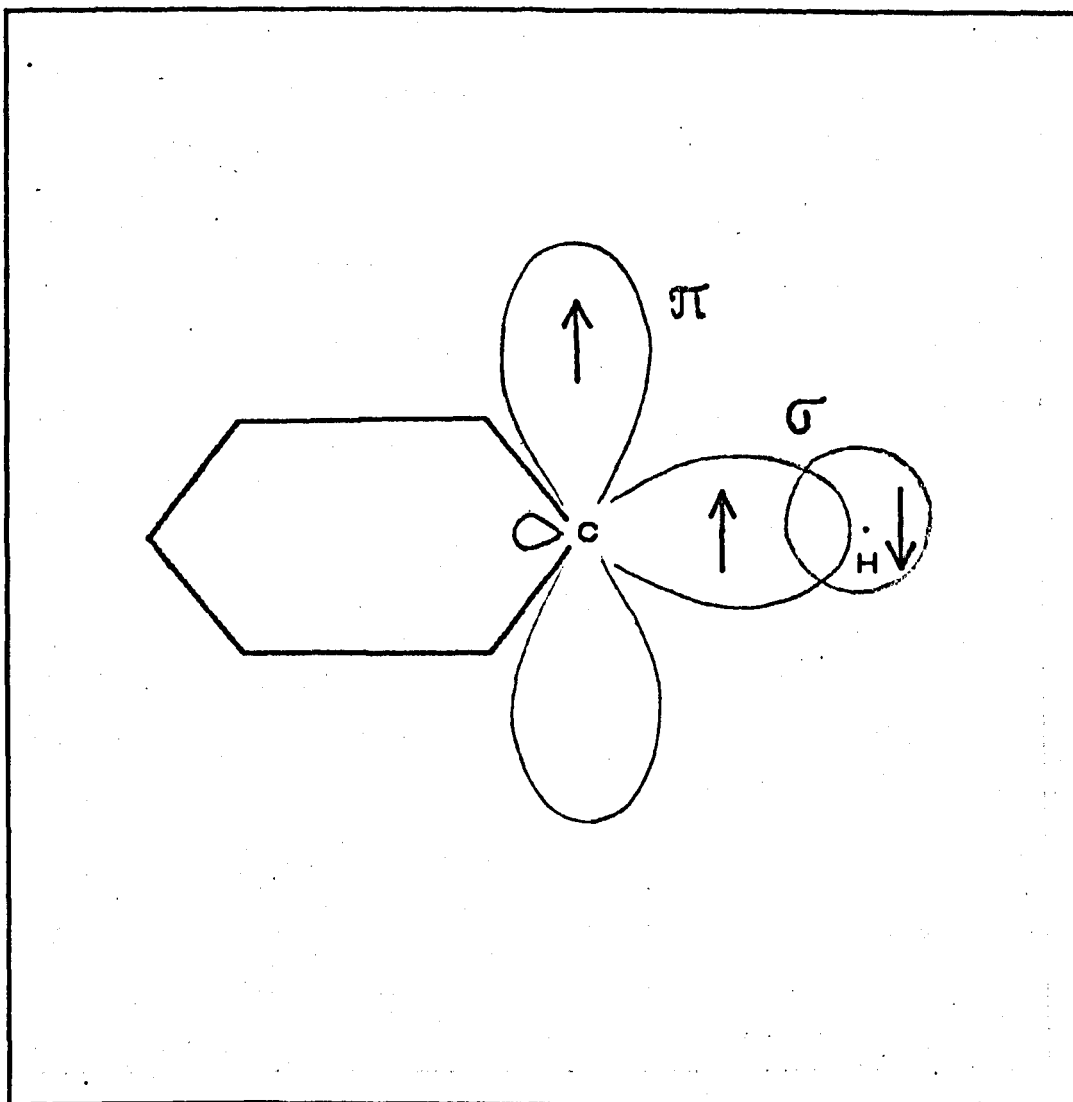
FIG. 2. 3 INDIRECT HYPERFINE COUPLING THROUGH A C-H BOND IN AN AROMATIC RADICAL. A 2PZ CARBON ORBITAL BELONGING TO THE AROMATIC π ORBITAL AS WELL AS A C-H σ BOND (IN THE PLANE OF THE MOLECULE) ARE SHOWN. THE POLARIZATION OF THE SPINS IS INDICATED BY ARROWS.

A large number of free radicals have been studied, which have their unpaired electron either localized on to one particular atom (such as N, S or C) or delocalized over aromatic or conjugated double bond systems. A number of such radicals will be described in Section 2.3.5. and in Chapter 3. In addition, one often encounters biradicals (Refs. 13., 14.) (molecules with two paramagnetic centres, usually fairly separated) or organic molecules in triplet states (Ref. 1.), which will not be further discussed here.

A consultation of the Atlas of ESR Spectra (Ref. 15.) reveals that ^{14}N gives isotropic hyperfine splittings in the range of 0.5 - o.8 mT if ^{14}N is part of an aromatic system, or higher, (up to 1.7 mT), in the case of introxides (Ref. 18.). The overall spread of the proton hyperfine pattern in the case of the aromatic radicals is comparable to McConnell's constant Q. This property derives from the fact that the unpaired spin densities in the radical should add up to unity. The spread of the isotropic hyperfine pattern tends to be considerably greater than Q if both negative and positive spin densities are present (e.g. in odd alternant aromatic radicals - Ref. 1.). In heterocycles containing ^{14}N, the proton splittings are normally smaller than the ^{14}N splittings.

It should be mentioned that as the hyperfine interaction is independent of the applied magnetic field or the microwave frequency, the splittings recorded at different microwave frequencies should be the same. It is common practice to check that a splitting arose solely from hyperfine interactions and not from the presence of two different species, by running ESR spectra at X and Q-band frequencies and the spectra should be identical. For isotropic hyperfine spectra this statement is correct only in the limit of fast tumbling motions when no asymmetric broadening of the lineshape takes place.

2.3.4. Anisotropic Hyperfine and g Tensors.

Considering the "anisotropic" Hamiltonian:

$$H = \beta \ \underline{B} \cdot \underline{g} \cdot \underline{S} + \underline{S} \cdot \underline{A} \cdot \underline{I} \qquad (10)$$

the ESR spectrum can be determined for a particular orientation of the molecule relative to the applied magnetic field.

The $\underline{A}$ and $\underline{g}$ are the hyperfine and g tensors, which can be diagonalized as shown in Equation (11) of Section 2.3.1. Let's assume for simplicity that the two sets of principal tensor axes coincide. The g value and the hyperfine splitting can then be worked out as functions of the principal g and A tensor values and the coordinates of the magnetic field in the molecular frame defined by the principal tensor axes. We adopt the formalism set up by Van, Birrell and Griffith (Ref. 6.) and let (x, y, z) denote the molecular frame of reference while (X, Y, Z) is a laboratory based system of reference.

Specifying Z to be the direction of the applied magnetic field and neglecting the less important off diagonal terms in Sx and Sy (that is to say, considering only the first order effects of the hyperfine term (Ref. 1.; p 100))the Hamiltonian (10) can be rewritten as:

$$H = \beta \ g_{ZZ} \ B \ S_Z + A_{ZZ} \ S_Z \ I_Z + A_{XZ} \ S_Z \ I_X + A_{YZ} \ S_Z \ I_Y \qquad (17)$$

with

$$g_{ZZ} = g_{xx} \ l^2_{Zx} + g_{yy} \ l^2_{Zy} + g_{zz} \ l^2_{Zz}$$

$$A_{ZZ} = A_{xx} \ l^2_{Zx} + A_{yy} \ l^2_{Zy} + A_{ZZ} \ l^2_{Zz}$$

$$A_{XZ} = A_{xx} \ l_{Xx} \ l_{Zx} + A_{yy} \ l_{Xy} \ l_{Zy} + A_{ZZ} \ l_{Xz} \ l_{Zz} \qquad (18)$$

$$A_{YZ} = A_{xx} \ l_{Yx} \ l_{Zx} + A_{yy} \ l_{Yy} \ l_{Zy} + A_{ZZ} \ l_{Yz} \ l_{Zz}$$

In these expressions g_{xx}, ... A_{xx}, ... are the principal g and A tensor values and the l's are the direction cosines between the molecular (x, y, z) axes and the laboratory (X, Y, Z) axes.

The matrix elements of the Hamiltonian (17) in the $| m_s, m_I \rangle$ basis can be worked out and used to determine the energy levels, eigenfunctions and the relative transition probabilities (Ref. 6.). In the "high field" approximation, the $S_Z I_X$ and $S_Z I_Y$ terms of Equation (17) are neglected, corresponding to a case in which the electron and nuclear spins are independently aligned along the magnetic field vector. As the Hamiltonian is diagonal under the above representation, the observed g value and splitting will be given by the simple expressions $g = g_{ZZ}$ and $A = A_{ZZ}$.

In the "intermediate field" approximation (with the H given by Equation (17)), $g = g_{ZZ}$ (as before) and $A = (A_{ZZ}^2 + A_{XZ}^2 + A_{YZ}^2)^{\frac{1}{2}}$, or, in terms of the principal tensor values and the direction cosines of the magnetic field in the molecular frame:

$$g = g_{xx} \, l_{Zx}^2 + g_{yy} \, l_{Zy}^2 + g_{zz} \, l_{Zz}^2$$

$$A = (A_{xx}^2 \, l_{Zx}^2 + A_{yy}^2 \, l_{Zy}^2 + A_{zz}^2 \, l_{Zz}^2)^{\frac{1}{2}}$$

(19)

This case corresponds to the nuclear spin being quantized along the direction of the effective magnetic field produced by the unpaired electron at the nucleus.

The allowed ESR transitions within both approximations are equally probable, and isotropic.

As the second order effects of the hyperfine term are usually unimportant compared to the effects of the nuclear Zeeman energy, the most general treatment should also include the nuclear Zeeman term (Ref. 1.).

The anisotropy formulae and the transition probabilities for the most general case are given by Pake (Ref. 2.).

2.3.5. Information Available from Anisotropic Spectra.

It could be inferred from the previous discussion, that in order to detect the anisotropic terms in the Hamiltonian one has to work with

immobilized specimens.   The spectra described in the previous section

would correspond to those obtained from single crystals of diluted para-

magnetic species, in which all the paramagnetic ions have the same

orientation relative to the magnetic field.   The work with single crystals

can provide the principal g and A tensor values, by studying the angular

variation of the g value and hyperfine splitting, as well as the orient-

ation of the molecular axes inside the crystal.

The principal g and A tensor axes need not coincide in the general case

and this makes the interpretation of the spectra more difficult.   However,

it turns out that they often do coincide and they can also be directly

related to some unique directions in the molecule (e.g. the P_z orbital axis

in the case of a ^{14}N atom) or directions of chemical bonds.

The "powder" spectrum is a superposition of spectra corresponding to

all the possible orientations.   This means that most of the information

that could be obtained from a single crystal is obscured in the powder case.

However, it turns out that if one of the hyperfine tensor components

is much larger than the other two, a feature corresponding to that splitting

can be recognised in the spectrum, thus enabling that principal hyperfine.

value to be determined.   The feature mentioned above consists of character-

istic bell-like shapes (Fig. 2.4a).   McConnell's treatment (Ref. 7.) gives

a description of how these shapes arise from the summation of "first

derivative" lineshapes.   Whether the tensors are axial or not can be

sometimes inferred from the number of inflexions in the powder spectrum,

as shown by Kneubuhl (Ref. 8.).   At the same time, estimates can be made

of the principal g values by examining the way the intensity builds up in

certain regions of the powder spectra, as shown by the same author.   For

example, for an axial (or near axial g tensor) a strong peak will occur in

the $g_\perp$ region, thus enabling one to estimate $g_\perp$ (Fig. 2.4b). $(g_\perp = g_{xx} = g_{yy})$.
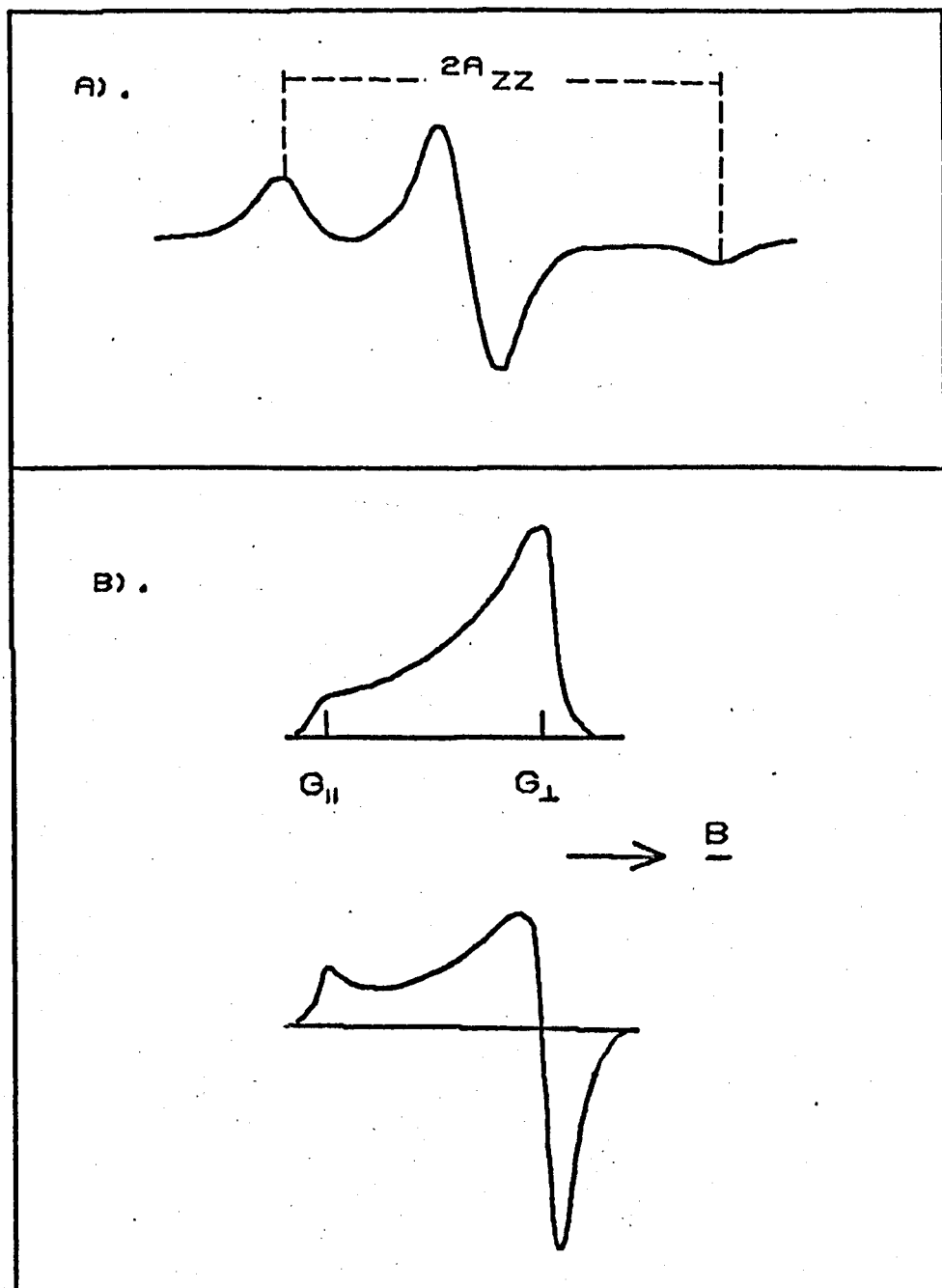
FIG. 2. 4 ESR SPECTRA FROM STRONGLY IMMOBILIZED SPECIMENS.
A). A NITROXIDE SPIN LABEL (16-DOXYL STEARIC ACID) IN ETHANOL. THE
SEPARATION OF THE BELL-LIKE FEATURES IS EQUAL TO THE LARGEST ANISOTROPI
COMPONENT (A_{zz}) OF THE NITROXIDE TENSOR. (AFTER REF. 3. 15).
B). THE ABSORPTION AND FIRST DERIVATIVE LINESHAPES OF A POLYCRYSTALLINE
SAMPLE WITH TWO PRINCIPAL G VALUES. (AFTER REF. 3. 13)

The hyperfine coupling constants can only be determined experimentally in absolute value and the determination of the sign represents a separate problem (Ref. 1.). The knowledge of the absolute value of the isotropic coupling constant a, from solution work, helps the asignment because it should be close to the average of the diagonal elements of the A tensor, allowing for some discrepancy due to the different polarity of the two media.

The relationship between the principal A tensor values and its isotropic and anisotropic parts is given by:

$$A_{xx} = t_{xx} + a$$
$$A_{yy} = t_{yy} + a$$
$$A_{zz} = t_{zz} + a \quad (20)$$
$$a = \frac{A_{xx} + A_{yy} + A_{zz}}{3}$$

where t_{xx}, ... are the principal values of the traceless dipolar (T) tensor, which has the same principal axes as $\underline{A}$.

While A and a are obtained by experiment, T is more related to theory (as one can often predict theoretically the sign and relative magnitude of its principal values). For example, if the unpaired electron is localized in a p_z orbital (of, for example, ^{14}N or ^{13}C), the dipolar tensor should be necessarily axially symmetric and $t_{||} = -2t_{\perp}$ with $t_{||} > 0$ (Ref. 1., p 110). The deviations from axial symmetry are due to unpaired spin density onto the neighbouring atoms.

This situation can be illustrated by giving the 5-doxyl stearic acid free radical as example (Ref. 16. and Fig. 2.5). This is a representative example for the class of nitroxide spin labels, which will enjoy considerable attention in Chapter 3. The nitroxides give rise to ESR spectra consisting of three equal lines, which can be attributed to the interaction of the unpaired spin with the ^{14}N nucleus (of nuclear spin 1). Both the isotropic

ISOTROPIC SPECTRUM   2.0058 1.51 MT

FIELD ALONG X AXIS   2.0088 0.59

FIELD ALONG Y AXIS   2.0058 0.54

FIELD ALONG Z AXIS   2.0022 3.29

POWDER SPECTRUM

MAGNETIC CHARACTERISTICS OF A NITROXIDE RADICAL

FIG. 2. 5 MAGNETIC CHARACTERISTICS OF THE NITROXIDE RADICAL 5-DOXYL STEARIC ACID. (THE PARAMETERS WERE TAKEN FROM REF. 2.16).

and anisotropic spectra are well resolved, which enables the accurate

determination of the spectral parameters.

The magnetic characteristics of the 5-doxyl stearic acid radical,

including the orientation of the principal tensor axes in the molecule, are

shown in Fig. 2.5. The near axial symmetry of the g and A tensors is

consistent with the localization of the unpaired spin mainly in the ^{14}N P_z

orbital. The application of Equations (20) leads to the following set of

parameters: t_{xx} = -0.883 mT, t_{yy} = -0.933 mT and t_{zz} = +1.817 mT. If we

define t_{11} = t_{zz} and $t_\perp$ = $(t_{xx} + t_{yy})/2$ = 0.908 mT, we see that the

relationship t_{11} = $-2t_\perp$, with t_{11} greater than zero, is ~~almost~~ exactly

obeyed. This is what one would have predicted for the signs and the

relative magnitude of the principal values of the dipolar tensor if the

spin was localized in the ^{14}N p_z orbital.

The observed deviations from axial symmetry are largely due to the

delocalization of the unpaired spin density towards the oxygen atom. This

was revealed by a more careful study (involving molecular orbital calculations

- Ref. 18. - and the analysis of the solvent effect on the absorption and

ESR spectra - Refs. 18, 20.), which showed that the nitroxide radical can be

described as an intermediate structure between the two canonical forms:

$$ \overset{..}{\underset{/}{\diagup}\!\!N} - \overset{.}{\underset{..}{O}}: \quad \longrightarrow \quad \overset{+}{\overset{.}{\underset{/}{\diagup}\!\!N}} - \overset{-}{\overset{..}{\underset{..}{O}}}: $$

$$ (A) \qquad\qquad (B) $$

Structure (A) localizes the unpaired electron on the oxygen atom (of zero

nuclear spin) whereas structure (B) localizes the unpaired electron on the

nitrogen atom, and is primarily responsible for the three-line ^{14}N splitting.

A consequence of this description that is worth being noted is that polar

solvents (such as water) that tend to stabilize the ionic structure (B), will

increase the unpaired spin density on nitrogen and, therefore, increase the

isotropic and anisotropic hyperfine splittings (Ref. 18.).

2.4. Relaxation and Line Broadening Mechanisms.

2.4.1. The Physical Origin of the Relaxation.

In the treatment of the phenomenon of ESR Bloch introduced two relaxation times, T_1 and T_2 (see Section 2.2.). The "spin-lattice" relaxation time, T_1, determines the degree of saturation and is a measure of the rate at which energy flows from the excited spin system to the lattice when the system approaches thermal equilibrium. On the other hand, the "spin-spin" relaxation time, T_2, is regarded as the "dephasing time" of the individual spins in the system and it determines the "unsaturated" line-width (Equation (8), Section 2.2.). The processes causing spin-spin relaxation act by varying the relative energies of the spin levels rather than their lifetimes and there is no exchange of energy with the lattice. The physical origin of the relaxation processes will be discussed in this section.

Both kinds of relaxation are caused by time dependent magnetic or electric fields at the electron which in turn come from the random thermal motions present in any form of matter.

The spin-lattice relaxation results from the phonon modulation of the crystalline electric field and there are three principal processes by which this proceeds: direct (emission or absorption of a phonon), Raman (scattering of a phonon) and Orbach (intervention of a third state).

The spin-spin relaxation derives from the fluctuating magnetic fields due to all the other paramagnetic ions.

The theory of relaxation (based on the time dependent perturbation theory) (Ref. 1., p 183) shows that the interactions contributing to T_1 must fluctuate strongly at the resonant frequency ω_0 while those contributing to T_2 are fluctuating forces which modulate the spin energy levels at frequencies close to zero, without causing transitions between them.

Although the two relaxation processes sound different they are in fact closely related because they result from the same interactions of the spin system. For example, in the case of the liquids, the fluctuating magnetic interactions due to the Brownian motion cause both the modulation of the energy levels and the finite lifetime of the spin states (see also Section 2.4.3.).

The relaxation is one of the major factors determining the linewidths of the ESR signals. The main relaxation mechanisms which can occur in practical systems will be described in the next sections, distinction being made between those relevant to the solid state and the solution phase.

Out of the two relaxation processes mentioned above, the effect of the spin-lattice relaxation (which broadens the ESR resonance by virtue of the uncertainty principle) is usually small and it only makes appreciable contributions to the linewidth in conditions of extreme narrowing (e.g. in solutions, in the limit of fast tumbling motions). This effect is called "lifetime broadening". Most of the discussion below will be concerned with spin-spin interactions, which usually provide the dominant contribution to the linewidth. Instrumental sources of broadening will also be mentioned.

2.4.2. Relaxation Mechanisms and ESR linewidths in Solids.

Dipolar broadening. The magnetic dipolar interaction which has the form shown in Equation (12) of Section 2.3.1. is usually the most important cause of line broadening in a rigid lattice of magnetic dipoles.

Van Vleck (Ref. 9.) calculated the second moment $< B_p^2 >$ of the z components of the local magnetic fields produced at one ion by all the other identical ions in a simple cubic crystal. The isotropic average of his formula, applicable to cases such as polycrystalline specimens, where one is not interested in the directional properties, has the form:

$$\langle B_p^2 \rangle = \frac{\mu_0}{4\pi} \frac{15.2}{3} (g \beta n)^2 S(S+1) \tag{21}$$

where S is the spin, n is the number of spins/unit volume and μ_0 is the permeability of the free space (equal to $4\pi \times 10^{-7}$ Hm^{-1}). In terms of angular frequency Equation (21) becomes:

$$\langle \omega_p^2 \rangle = \frac{\mu_0}{4\pi} \frac{15.2}{3} \left(\frac{g^2 \beta^2}{h^2}\right)^2 n^2 S(S+1) \tag{22}$$

These formulae can be extended to take into account the effect of other paramagnetic ions which are not at resonance simultaneously with the first kind (Ref. 1., p 34). These ions also contribute to the second moment but their effect is smaller by a factor of 4/9.

The square root of $\langle B_p^2 \rangle$ can be correlated with the half width of the ESR line. The dipolar broadened lineshape, as derived by Van Vleck's treatment is Gaussian (Equation (9) of Section 2.2.), a fact that is confirmed in practice by investigating spectra from paramagnetic diluted cyrstals (Refs. 17., 2.).

Exchange Narrowing. Experimentally it is often found that the width of the resonance line is much narrower than expected from the dipole-dipole interaction. This effect, which is called "exchange narrowing" takes place in magnetically concentrated materials in which the wave functions on different ions can overlap. The exchange interaction arises out of the quantum mechanical principle of the indistinguishability of the two spins upon overlap, which makes the two electrons belonging equally to both atoms. The interaction tends to align the spins, which can only be achieved effectively at very low temperatures (a few degrees K). The exchange energy between two spins S_1 and S_2 has the form $J \underline{S}_1 \cdot \underline{S}_2$, where J is the "exchange interaction" and has the dimensions of energy.

The magnetic Hamiltonian (taking into account the exchange) can be represented following Anderson (Refs. 10,11.) as:

$$H = H_o + H_p + H_e \tag{23}$$

with H_o and H_p the Zeeman and dipolar energies and $H_e = \sum_{ik} J \underline{Si} \cdot \underline{Sk}$,

the exchange term with the sum running over all the nearest neighbour ions.

One can define an "exchange frequency"

$$\omega_e = \frac{J}{\hbar} \tag{24}$$

and can imagine the effect of exchange of being to produce a precession of

the spins at a rate ω_e or to allow the electrons on neighbouring lattice

sites to exchange spin states at the rate ω_e. This causes a time variation

of the local dipolar fields, with direct effect on the ESR linewidth.

Van Vleck (Ref. 9.) showed that the second moment of the lineshape is

not affected by exchange and is given by Equations (21) or (22). However,

the fourth moment contains the exchange and is given by:

$$\langle \omega_p^4 \rangle = \omega_e^2 \langle \omega_p^2 \rangle + \langle \omega_p^2 \rangle^2 \tag{25}$$

Anderson (Refs. 10, 11.) was able to predict a definite lineshape: a

Lorentzian with the width:

$$\Delta\omega = \frac{\omega_p^2}{\omega_e} \tag{26}$$

and a cut-off at ω_e, where $\omega_p = \sqrt{\langle \omega_p^2 \rangle}$ is the amplitude in frequency

of the average dipolar field (the linewidth in absence of exchange) and

ω_e is the exchange rate. As $\omega_e \gg \omega_p$, the lines are usually much

narrower than expected for the dipole-dipole interaction.

The treatment can be extended to account for the effect of exchange

on spectra showing hyperfine structure. Two limiting cases can be disting-

uished. In the first case, of "fast exchange" ($\omega_e \gg \omega_p$) formula (26)

holds, with ω_p now representing the magnitude in frequency of the hyperfine

interaction. The hyperfine structure is averaged out and a single

"exchange narrowed" line at the average frequency occurs.

In the second case, of "slow exchange" ($\omega_e < < \omega_p$), the hyperfine

lines are resolved but each is broadened, with a width:

$$\Delta \omega_e \simeq \omega_e \qquad\qquad (27)$$

An example of exchange narrowing is the DPPH radical in powder state (see

Section 2.1.), which displays an exchange narrowed line of about 0.3 mT c.f.

the predicted 10 mT (Ref. 1.).

2.4.3. ESR Linewidths in Liquids.

In liquids, the magnetic fluctuations are due to the random Brownian

motion of the molecules and they can lead to the averaging out of the time

dependent interactions.   It has already been seen that if the molecules

perform a fast tumbling motion the hyperfine (A) and g tensors are averaged

to their isotropic values, provided the tumbling rate is greater than the

largest anisotropic component.   In the same time the local dipolar fields,

responsible for the dipolar broadened lineshape in solids, are averaged out

to zero (provided the tumbling rate is greater than the dipolar interaction)

and narrowing of the ESR lines occurs.   This effect is called "motional

narrowing".

However, there are two major broadening mechanisms which operate in

liquids.   They come from:

1) The anisotropy of the g and A tensors, which produces a line

dependent broadening.

2) The electron spin exchange, which can cause considerable broadening

in concentrated solutions.

1) The electron spin of a radical which has anisotropic g and A tensors

will see two fluctuating random fields, one from the variation of g and the

other from A.   These fluctuations are correlated because they result from

the same motion.   It can be shown that the linewidth in this case varies

from one line to another as $A + B\, m_I + C\, m_I^2$ (m_I = the nuclear spin

component), i.e. the 2nd term makes the outer lines to be broader on one side of the spectrum while the 3rd term makes the outer lines to be broader than the inner ones. This effect also depends on the microwave frequency.

An explicit version of this formula as applied to nitroxide radicals is given in Section 3.3.

2) Exchange effects can occur if the concentration of the spins in solution is high and collisions occur frequently. During such collisions the electronic wave functions overlap and the exchange interaction $J \underline{S}_1 \cdot \underline{S}_2$ may interchange the spins of the two radicals and this can cause both line broadening or narrowing depending on the collision rate. If we note that the exchange rate ω_e now represents the collision rate (indirectly depending on the concentration and temperature), the formulae (26) and (27) describing the fast and slow exchange can be applied to describe this process as well.

The exchange effects, as seen from the broadening of the lines, can become apparent as soon as the concentration of free radicals exceeds about 10^{-3} M.

There are cases occuring with organic radicals when conformational changes or molecular motions involving only particular groups, cause the modulation of the electronic configuration of the radical, resulting in linewidth effects involving one or more hyperfine splittings. This phenomenon (which is temperature dependent) is similar to the electron spin exchange and, depending on the motional rate, the effect can be the broadening of the lines in question or the collapse of the lines onto one single line, the other lines remaining unchanged (Ref. 1., p 213).

2.4.4. Other Sources of Lineshape Broadening.

The saturation of the resonance can occur in systems with long spin-lattice relaxation times (such as free radicals) if the microwave power is too high. In such cases the $\gamma^2 B_1^2 T_1 T_2$ term in Equation (7) Section 2.2

becomes important.   The saturation affects the centre of the absorption curve and gives rise to an apparent broadening of the lineshape.

The "modulation broadening" occurs as a result of using phase sensitive detection of the ESR signal.   If the modulation frequency is too large, side bands appear at both sides of the true resonant line causing apparent broadening.   Also, if the amplitude of the modulation field is too high, the width of the first derivative lineshapes will be increased and the lineshape eventually distorted.

Other sources of broadening of the resonant line are: i) the inhomogeneity of the steady magnetic field, which results in a spread in the position at which the different spins have their resonances, ii) the instability of the microwave frequency, which shifts the position of the resonances, and iii) the existence of unresolved hyperfine structure.

2.5.   The Detection of the ESR Signal.

In Bloch's treatment of the phenomenon of magnetic resonance (Section 2.2) it was necessary to introduce a complex magnetic susceptibility:

$$\chi(\omega) = \chi'(\omega) + i\,\chi''(\omega) \tag{28}$$

deriving from the existence of two components of the magnetisation $\underline{M}$, oscillating respectively in phase and 90° out of phase with the microwave field $\underline{B}_1$.

The magnetic resonance corresponds to sharp changes both in real and imaginary parts of $\chi(\omega)$.   It can be shown that the power $P(\omega)$ (Equation (7), Section 2.2.) absorbed from the microwaves, which represents, by definition, the ESR lineshape, is proportional to the imaginary part of the susceptibility:

$$P(\omega) = 2\omega\,B_1{}^2\,\chi''(\omega) \tag{29}$$

The ESR spectrometers normally follow the absorptive part of the susceptibility (χ'') which gives the familiar ESR lineshape, but usually they can be set up to observe the dispersion signal (χ') as well.

Most of the modern spectrometer systems employ resonant cavities with the microwave frequency tuned to the resonance of the cavity and one monitors the change in the power transmitted through or reflected from the cavity.

The performance of a resonant cavity depends on the "quality factor" Q, defined as:

$$Q = \omega_0 \frac{\text{energy stored at resonance}}{\text{energy dissipated per cycle}} \tag{30}$$

which can be a very large number and is typically in the range of 5 - 10000, depending on the mode in which they operate. At resonance the power dissipated is increased by an amount equal to the paramagnetic losses, which can be obtained from Equation (7) by integration over the volume of the sample. If the paramagnetic losses are small compared to the cavity losses, the change in the Q factor brought about by the ESR is proportional to the absorptive part of the susceptibility χ'' and given by:

$$\Delta Q = Q_0^2 \chi'' \eta$$

where η is a "filling factor" which is a measure of the fraction of the microwave energy from the cavity that interacts with the sample.

It can be shown (Refs. 2., 12.) that the change in the power transmitted or reflected by the cavity depends directly on the change in the quality factor Q and that the measured power change represents essentially the microwave power absorbed in the ESR experiment (Equation (7)) amplified through Q.

Spectrometer Systems. The essential components required to produce ESR are a magnet, providing the static magnetic field $\underline{B}$ and the microwave circuitry providing the oscillatory field $\underline{B}_1$ perpendicular to $\underline{B}$. An ESR spectrometer would also contain a detection system, a means of sweeping the magnetic field and a system of stabilizing the microwave frequency.

Two conventional ESR spectrometer systems, both of "reflection cavity" type, incorporating the above components (Figs. 2.6a and b) were selected in order to illustrate the principles of the detection of the ESR signal. Further details on this topic can be found in the literature of speciality (Refs. 12., 19.).

The microwave power in both cases is produced by a klystron and is fed into the waveguide run via an isolator. The role of the isolator is to allow the oncoming power to pass unattenuated while absorbing any power reflected in the opposite direction, which might affect the stability of the klystron.
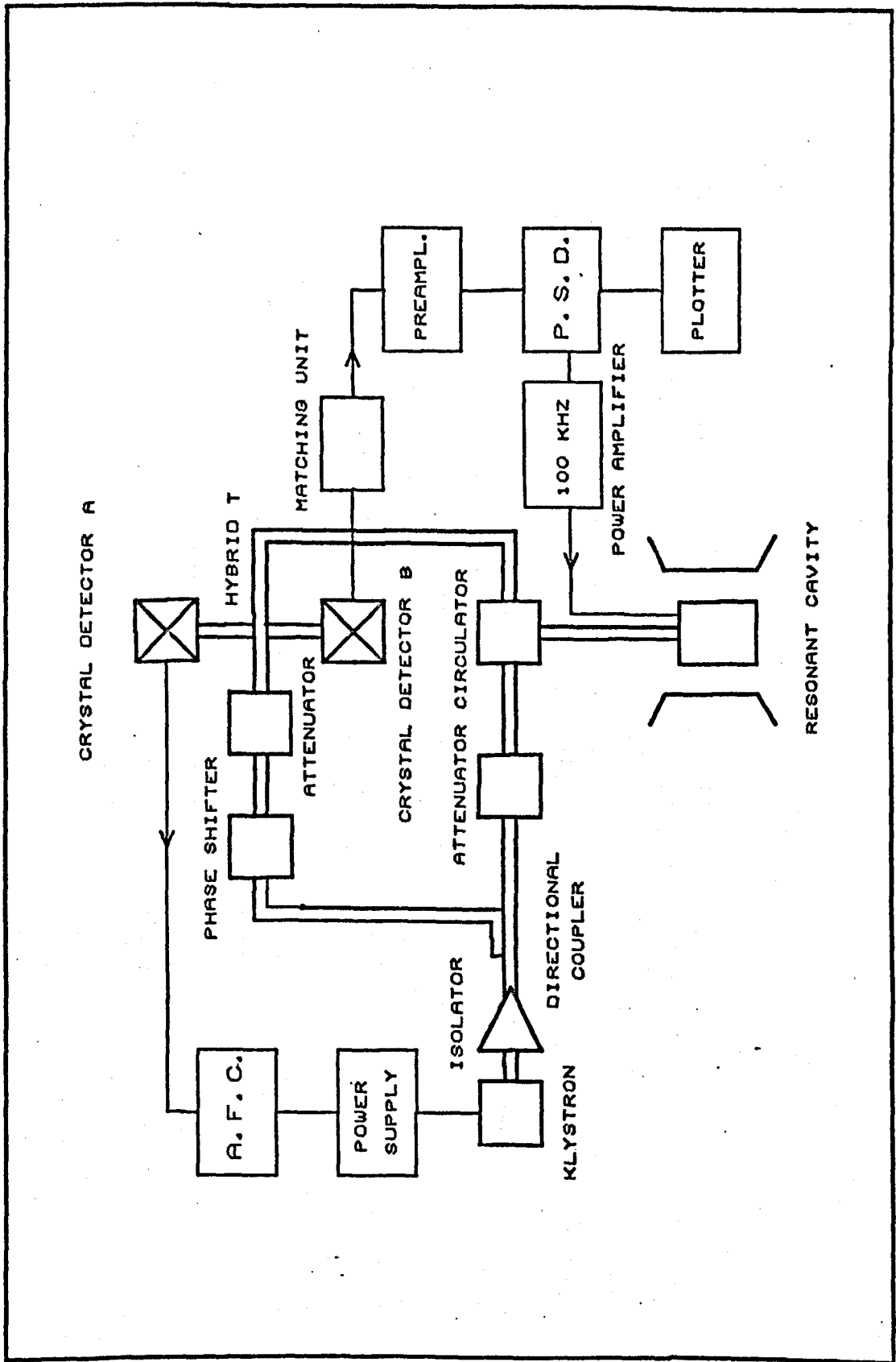
FIG. 2. 6. A. REFLECTION TYPE ESR SPECTROMETER WITH BUCKING ARM
(AS USED FOR THE X-BAND WORK).

FIG. 2.6.B. REFLECTION TYPE ESR SPECTROMETER WITH MAGIC T
(AS USED FOR THE Q-BAND WORK).

ATTENUATOR AND PHASE SHIFTER

POWER SUPPLY AND AFC

PLOTTER

3   MAGIC T

PREAMPL.

1   4

P. S. D.

2

KLYSTRON   ISOLATOR   ATTENUATOR

CRYSTAL DETECTOR

100 KHZ POWER AMPLIFIER

RESONANT CAVITY
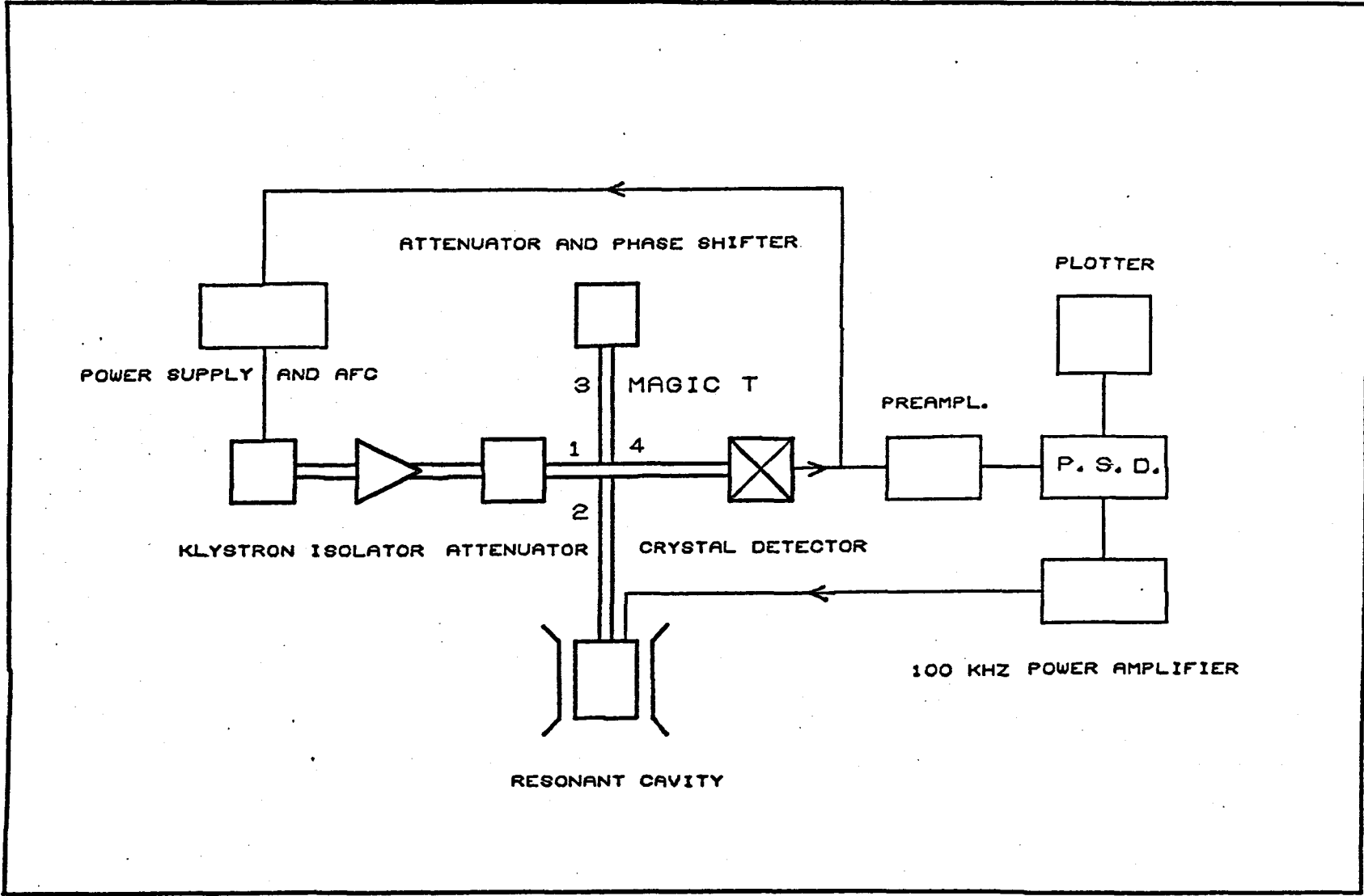
The main feature of the spectrometer a) is the bucking arm which enables a fraction of the power generated by the klystron to be extracted from the main waveguide run and fed separately to the detectors to bias the crystals, the remainder being fed to the microwave cavity via an attenuator. The advantage of this arrangement is that it permits the operation of the spectrometer at low incident powers while still being able to bias the crystal detectors at the optimum microwave power. This level corresponds to a compromise between the two factors affecting the sensitivity of the detection: the crystal noise (which is proportional to the incident power) and the conversion loss (which decreases with increasing power). The bucking arm contains both an attenuator and a phase - shifter, so that the amount of power fed back can be varied in both magnitude and phase to give the desired crystal bias. The system also incorporates a circulator which directs the incident power into the cavity and the reflected power to the crystal detectors A and B (through a hybrid T).

It is usually necessary to prevent the frequency of the klystron from drifting away from the resonant frequency of the cavity. The function of an automatic frequency control (AFC) system is to respond to such changes in the klystron frequency by supplying an error voltage to the klystron reflector, the polarity of which depends on whether the frequency has drifted above or below that of a reference frequency or the resonant frequency of a reference cavity. The AFC system employed in Fig. (2.6 a) locks the klystron frequency to that of the resonant cavity. This is achieved by frequency modulating the output of the klystron. The frequency modulation is converted into amplitude modulation by using the cavity as a discriminator (as illustrated in Fig. (2.7 a)) and after suitable detection a d.c. error voltage is obtained and is fed back to the reflector of the klystron. It can be seen in Fig.(2.7) that the phase of the error signal, and hence the polarity of the d.c. error voltage, depends on the frequency (f) being greater or smaller than the resonant frequency of the cavity (fo). The magnitude of the d.c. voltage is zero if f equals fo (because the error signal produced
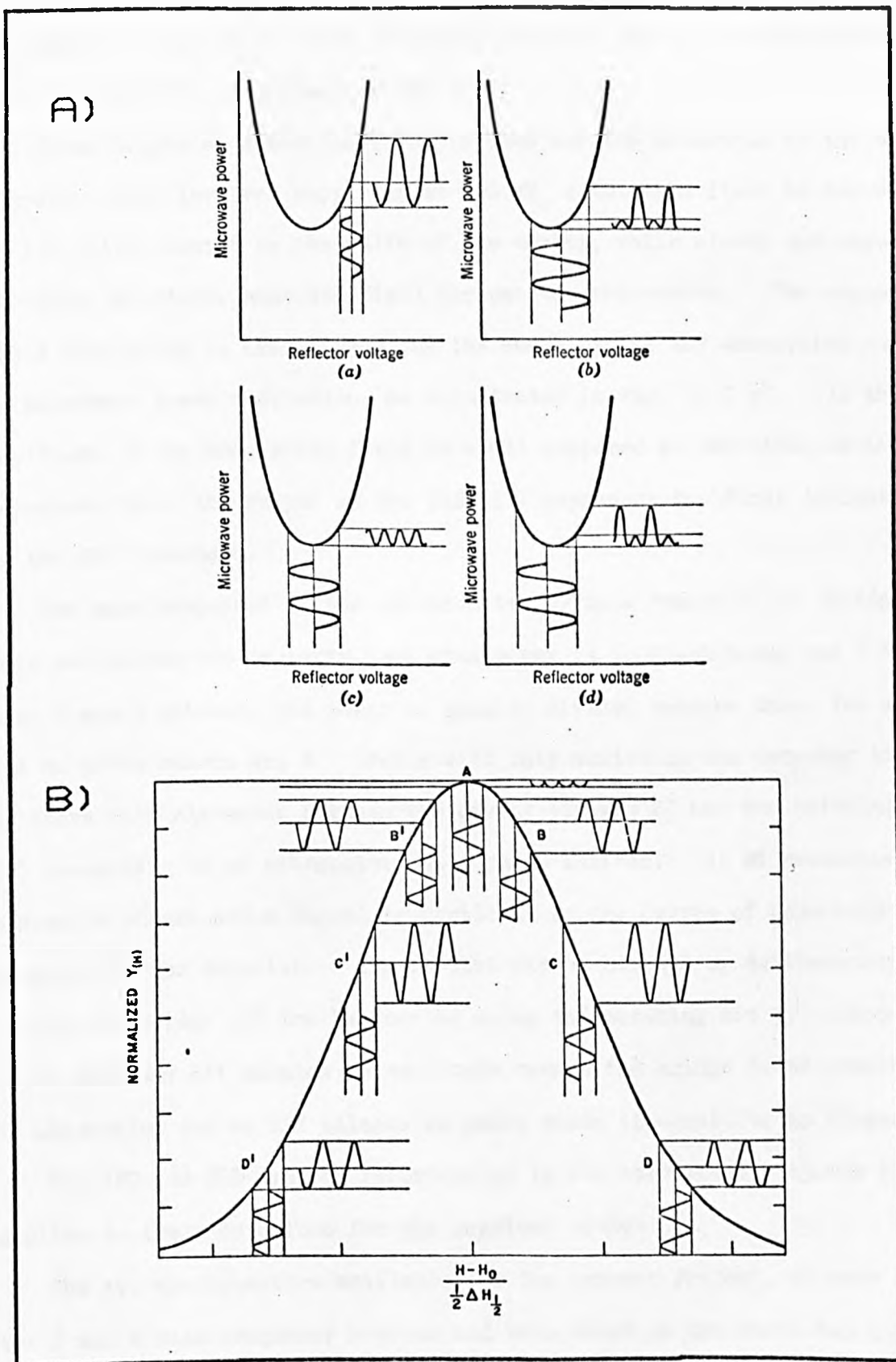
FIG. 2.7 A). ERROR SIGNAL KLYSTRON STABILIZER CLOSE TO RESONANCE.
B). THE ESR SIGNAL PRODUCED IN A MAGNETIC FIELD MODULATED SPECTROMETER.

is twice the frequency of the modulating signal) and it increases with increasing difference between f and fo.

Phase sensitive detection (PSD) is used for the detection of the ESR signal. This involves supplying an 100 KH_z modulation field to the sample by two coils mounted in the walls of the cavity, while slowly and linearly sweeping the static magnetic field through the resonances. The magnetic field modulation is transformed, by the shape of the ESR absorption curve, to microwave power modulation, as illustrated in Fig. (2.7 b). If the amplitude of the modulating field is small compared to the width of the resonance line, the output of the PSD will represent the first derivative of the ESR lineshape.

The main component of the spectrometer b) is a "magic T" or "bridge". This device has the property that when power is incident along arm 1 with arms 2 and 3 matched, the power is equally divided between these two arms and no power enters arm 4. Power will only arrive at the detector in arm 4 if there is a mis-match between the cavity (in arm 2) and the matching arm (3) consisting of an attenuator and a phase shifter. At X resonance a mis-match occurs and a signal proportional to the degree of unbalance is detected by the detector. The crystal can be biassed by deliberately taking the bridge off the balance by using the matching arm 3. It can be shown that any off balance in amplitude causes the bridge to be sensitive to absorption and an off balance in phase makes it sensitive to dispersion.

The AFC and PSD systems incorporated in the spectrometer system b) are similar to those described for the previous system.

The two spectrometers available for the present project, operate in the X and Q band frequency regions and were based on the above two systems (see Section 6.3.1. for further details).

REFERENCES.

1. A. CARRINGTON, A. D. McLACHLAN: Introduction to Magnetic Resonance - with Applications to Chemistry and Chemical Physics, a Harper International Edition, (1969).

2. G. E. PAKE, T. L. ESTLE: The Physical Principles of EPR (2nd Edition), W. A. Benjamin Inc., N.Y., (1973).

3. N. M. ATHERTON: Electron Spin Resonance, John Wiley and Sons Inc., (1973).

4. Ch. P. SLICHTER: Principles of Magnetic Resonance with Examples from Solid State Physics, A Harper Interational Student Reprint, (1964).

5. A. ABRAGAM: The Principles of Nuclear Magnetism, The International Series of Monographs in Physics, Oxford: Clarendon Press, (1961).

6. S. P. VAN, G. B. BIRREL, O. H. GRIFFITH: J. Magn. Reson., 15, 444, (1974).

7. H. M. McCONNELL, B. G. McFARLAND: Quart. Rev. Biophys., 3, 91, (1970).

8. F. K. KNEUBUHL: J. Chem. Phys., 33, 1074-8, (1960).

9. J. H. VAN VLECK: Phys. Rev., 74, 1168-1183, (1948).

10. P. W. ANDERSON, P. R. WEISS: Revs. Modern Phys., 25, 269-276, (1953).

11. P. W. ANDERSON: J. Phys. Soc. Japan, 9, 316-339, (1954).

12. Ch. P. POOLE: Electron Spin Resonance, A comprehensive Treatise on Experimental Techniques, Interscience Publishers, USA, (1967).

13. A. D. KEITH et al.: Biochem. Biophys. Acta, 300, 379-419, (1973).

14. A. V. KULIKOV et al.: Biofizica, 17, 42-48, (1972).

15. B. H. J. BILISKI, J. M. GEBICKI: Atlas of ESR Spectra, Academic Press (New York & London), (1967).

16. L. J. LIBERTINI, C. A. BURKE, P. C. JOST, O. H. GRIFFITH: J. Magn. Reson., 15, 460-476, (1974).

17. C. KITTEL, E. ABRAHAMS: Phys. Rev., 90, 238-239, (1953).

18. O. H. GRIFFITH, P. J. DEHLINGER, S. P. VAN: J. Membrane Biol., 15, 159-192, (1974).

19. H. M. ASSENHEIM: Introduction to Electron Spin Resonance, Higler &
     Watts Ltd., London, (1966).

20. R. BRIERE, H. LEMAIRE, A. RASSAT: Bull. Soc. Chim. Fr., 32, 3273,
     (1965).

CHAPTER 3.

SPIN LABELLING OF BIOLOGICAL MOLECULES.

3.1. Biological Applications of ESR.

The aim of this chapter is to place the present work performed with spin labelled nucleic acids in the context of the biological applications of the ESR technique.

The spin labelling technique has developed in connection with the study of complex biological systems (enzymes, nucleic acids). A spin label is a paramagnetic probe of known characteristics which can be attached at specific sites on to the biological molecule or simply dissolved into the biological system. By monitoring the ESR signal of the spin label one obtains indirect information about the system itself.

This chapter is not a comprehensive account of the biological applications of ESR but it is a concise presentation of the main areas of interest, with particular emphasis on the spin labelling technique. The biological applications of ESR can be grouped together into three major classes: the determination of the molecular structure; the study of fast enzyme catalysed reactions; and spin labelling studies.

The application of ESR to the determination of the molecular structure concerns biological macromolecules (particularly metal proteins) which possess paramagnetic groups in their structure. Such studies (which often involve the use of single crystals) can lead to the determination of the orientation and the environment of the paramagnetic group in the molecule.

A classical example is the work performed by Slade and Ingram (Ref. 1.) with Myoglobin single crystals, which led to the determination of the orientation of the Haem plane in the Myoglobin molecule, an essential step in the determination of the molecular structure of the biological macromolecule. The study was based on the anisotropy of the g-tensor, outlined in Section 2.3.4. If θ is the angle between the symmetry axis of the axial

g tensor and the magnetic field, one has:

$$g_\Theta^2 = g_{||}^2 \cos^2 \Theta + g_\perp^2 \sin^2 \Theta$$

One can write for this particular case: $g_\Theta^2 = 4 (1 + 8 \sin^2 \Theta)$, which yields the observed extreme g values of $g = 2$ and 6. Further details of ESR work with metal-proteins (particularly transition metal ions) are found in Refs. 2 - 4.

An ESR study performed in conjunction with flow or stopped-flow techniques can help in the elucidation of the mechanisms of fast enzyme catalysed reactions, by determining the nature of the radicals formed as reaction intermediates. Such studies have been carried out in connection with electron transfer enzymes, such as Flavoproteins (involved in redox reactions) or those from the photosynthetic pathway. An account of results in this area can be found in Ref. 5.

3.2. Spin Labelling Studies.

The pioneer work in the field of spin labelling macromolecules was performed by McConnell (Ref. 6.). One of the first ordered systems to be studied by this method was the DNA spin labelled with the cation radical of chlorpromazine (Ref. 7.). (Detailed references to this paper will be made in Chapter 6.)

However, the most widely used spin labels are the nitroxides (Fig. 3.1), which were introduced by the same author in 1969. The nitroxides are stable free radicals containing the group $N \doteq O$, with the nitrogen atom bonded to two tertiary carbon atoms (Fig. 1a). With the exception of the di-t-butyl nitroxide which is linear (Fig. 1b), most of the useful nitroxide spin labels are five or six membered ring structures (Fig. 3.1e - f). They are listed in Refs. 8 and 9.

NITROXIDE SPIN LABELS

A).

R$_1$ R$_2$
| |
C — N — C
|
O
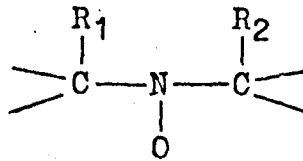
GENERAL FORMULA

B).

C).
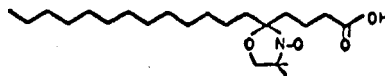
D).
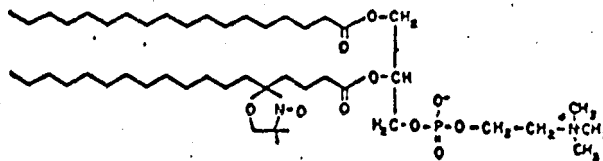
E).
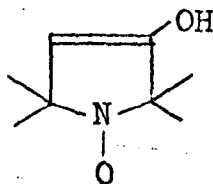
F).
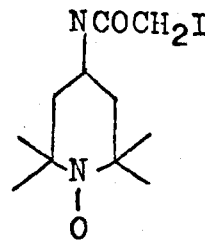
FIG. 8. 1 A). GENERAL FORMULA OF A NITROXIDE SPIN LABEL, B). DI-T-
-BUTYL NITROXIDE, C). 15-DOXYL STEARIC ACID (A FATTY ACID), D). L-ALPHA-
-LECYTHINE (A PHOSPHOLIPID), E). A 5-MEMBERED AND F). A 6-
-MEMBERED RING NITROXIDE LABEL.

The nitroxides display a simple three-line spectrum, due to the interaction of the unpaired electron with the ^{14}N atom (Fig. 3.2.). The magnetic characteristics of a typical nitroxide free radical have been presented in Section 2.3.5. and Fig. 2.5.

Specially prepared nitroxide labels can be diffused in the phase of study (such work has been carried out with membranes - Ref. 10.), or attached to specific sites by reactions involving their sidechains and not the nitroxide group. Such reactions are described in Ref. 11. The main biological materials which have been investigated using this technique are: nucleic acids, proteins, membranes and model membranes.

3.3. Information Available from Spin Labelling Studies.

The analysis of the ESR spectra can provide information about: a) the nature of the mobility of the spin label and b) the polarity of its environment. Both these applications will be discussed with reference to work on membranes or model membranes.

The membranes consist essentially of lipid bilayers, in which the aliphatic chains are oriented perpendicular to the bilayer surface, with their polar terminal groups exposed to the solvent and the apolar chains embedded in the interior of the bilayer. These systems can be spin labelled by diffusing into them specially prepared fatty acid or phospholipid molecules, with nitroxide groups bonded to various positions along the lipid chains (Fig. 3.1.c, d.).

The effect of various degrees of motion on the shape of the ESR spectrum of a nitroxide spin label can be followed from Fig. 3.2. For rapid isotropic motions characterised by very short rotational correlation times ($\tau_c < 10^{-11} - 10^{-12}$s) the nitroxides give three equal hyperfine lines (Fig. 3.2a). For slower motions ($10^{-11} < \tau_c < 10^{-7}$ s) that are still in the rapid isotropic range, one obtains unequal broadening of the three lines, indicating
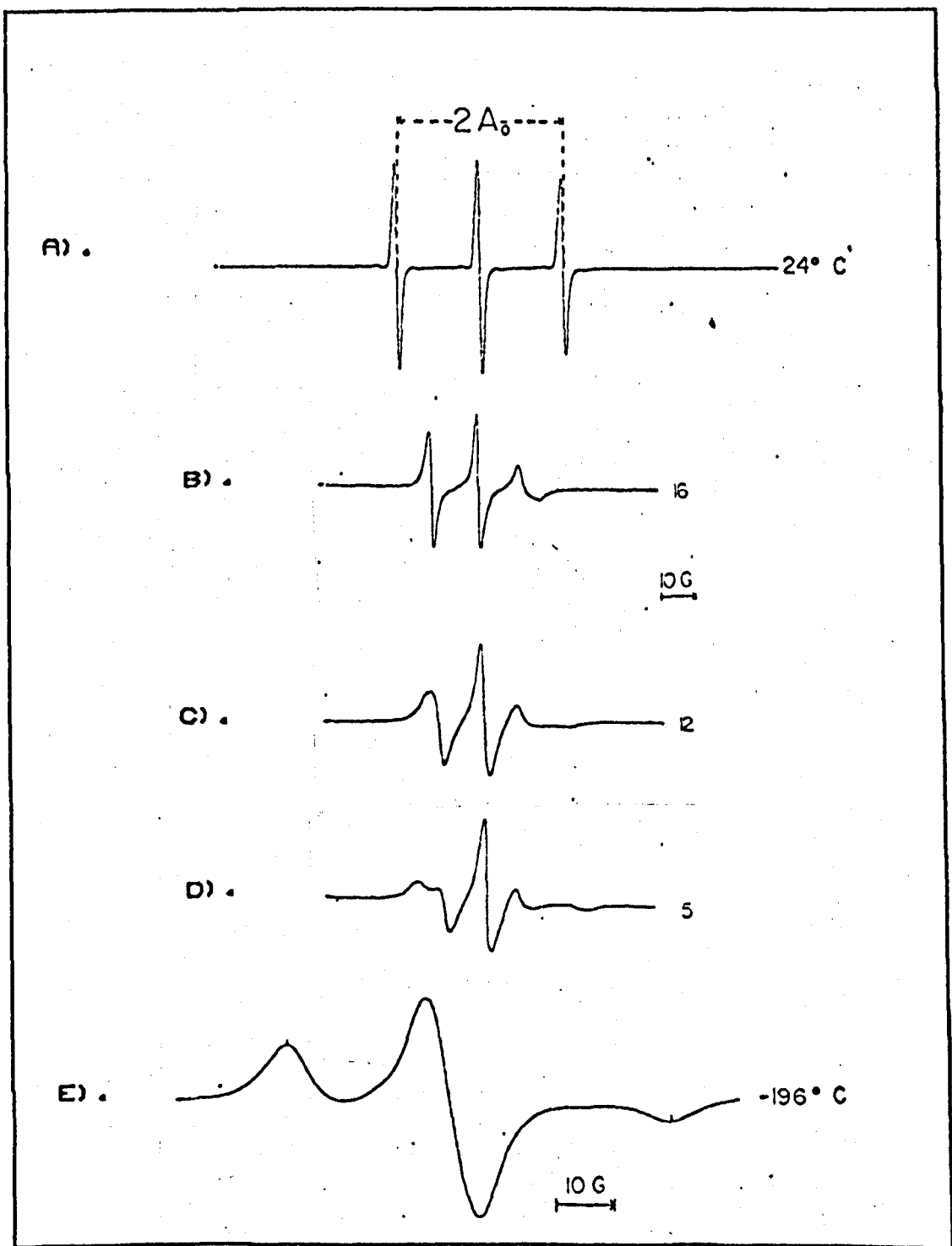
FIG. 8.2 16-DOXYL STEARIC ACID IN ETHANOL AT (A) 24° C AND (E) FROZEN AT -196° C.   (B) - (D) : 5-, 12-, AND 16-DOXYL STEARIC ACID IN MICROSOMAL MEMBRANES, AT ROOM TEMPERATURE. (AFTER REF. 8.15)

a small anisotropic contribution deriving from the incomplete averaging of the dipolar and g tensors (Fig. 3.2b, c, d.). This property has been discussed in Section 2.4.3.

The following relationship quoted by Stone et al. (Ref. 12), which is an explicit version of the relationship presented in the above mentioned section, can be used to calculate the rotational correlation time τ_c of the nitroxide radical:

$$\frac{T_2(0)}{T_2(M)} = 1 - \frac{4\tau_c}{15} \, b\Delta\gamma B_0 \, T_2(0) \, M - \frac{\tau_c}{8} b^2 \, T_2(0) \, M^2$$

where
$$M = \pm 1$$
$$\Delta\gamma = -\frac{|\beta|}{\hbar} \, g_{zz}^{-\frac{1}{2}} \, (g_{xx} + g_{yy})$$
$$b = \frac{4\pi}{3} \, (A_{\parallel} - A_{\perp})$$

$$(3.1)$$

For "strongly immobilized" species, corresponding to correlation times greater than 10^{-4}s one obtains "powder" type of spectra (Fig. 3.2e), as described by McConnell (6), Kneubul (13) and Vängard and Aasa (14).

The spectra b, c and d from Fig. 3.2. reproduce a set of spectra obtained from membrane suspensions, spin labelled at progressively deeper positions along their lipid chains (Ref. 15.). It can be seen that the spectral lines become narrower and the splittings decrease as the nitroxide group is moved along the chain from the C_5 to the C_{12} and finally to the C_{16} position. This behaviour infers the existence of a mobility gradient along the chain, which culminates near the centre of the bilayer. Such results, which were initially obtained by McConnell from model membranes (lecithin and lecithin/cholesterol mixtures) and later, by the same author, from biological membranes (nerve axons and erythrocytes), led to the formulation of the so-called "fluid model" of the membrane (Refs. 10, 15.).

A more careful analysis (Ref. 16.) showed that the motion performed by the spin labels in the above preparations was anisotropic. Such motion

commonly occurs if the molecule is not gravitationally symmetric or if its movement is constrained, and consists of a rapid rotation or large amplitude oscillations about a particular direction (Refs. 6, 17.). The result is that the hyperfine tensor is averaged about that particular axis only. The spectral parameters in this case depend on the inclination of that axis relative to the magnetic field as well as on the degree of order. It was possible to deduce in this way that close to the polar interface, the chains were tilted relative to the plane of the bilayer by about 30° (Ref. 18.).

Translational diffusion processes within the bilayers (Ref. 18.) or the fusion of erythrocyte cells (Ref. 19.) have been equally successfully studied by the spin labelling technique.

The second type of information available from spin labelling studies concerns the polarity of the medium, which can be inferred from shifts in the measured g-values and hyperfine splittings.

The results of Griffith et al. (Ref. 15.) in this field are worth being mentioned in some detail because they are of general interest. The authors showed that the isotropic hyperfine constant of di-t-butyl nitroxide increased from about 1.5 mT to about 1.75 mT when the radical passed from a hydrocarbon environment (hexane) to a polar environment (water or a LiCl aqueous solution). In the same conditions the isotropic g value decreased from about 2.0068 to about 2.0056. A plot of the isotropic hyperfine constant (a) against the g-value for a series of 33 solvents, placed all the points on to the same line, implying that the shift in g and a were both the consequence of the same interactions. It was reckoned that the most important of the solvent effects was the possibility of of hydrogen bonds formation between the solvent and the nitroxide group. The authors also demonstrated the existence of a linear relationship between the isotropic hyperfine splitting (a) of the nitroxide in a particular solvent and the corresponding largest anisotropic splitting (A_{zz}) measured from the glasses obtained by freezing the same solutions.

These considerations were used by the same authors to estimate the shape of the hydrophobic barrier (i.e. the polarity profile) across lipid bilayers. The work involved the use of frozen samples of bilayers, spin labelled by the method already described above. A comparison of the ESR parameters obtained for various positions of the spin label along the fatty acid chains, to the "polarity scale" described above, showed that the hydrophobic barrier was trapezoidal in shape and it also indicated that significant water penetration into the bilayer occurred in both the pure lipid bilayers and in the membrane preparations.

It is however difficult to prove that the water molecules detected by the spin label actually penetrate in the absence of the spin label. This fact points towards the major problem in all the labelling experiments, namely the perturbation introduced by the label itself. One other uncertainty inherent in both two pieces of work described above is whether the labelled lipid molecule was in register with the other lipids and not, perhaps, stretching further into the aqueous interface. However, the identical results obtained with both fatty acid and phospholipid labels seem to indicate that the first was indeed the case.

Nitroxide spin labels have been used in connection with conformational studies of single stranded and double stranded nucleic acids (Refs. 20 - 22). In these studies a suitable spin label (such as label f from Fig. 3.1) was covalently attached to the A and U residues of the polynucleotides (Ref. 21.). The level of binding achieved corresponded to about one spin label to each polynucleotide chain. The spin label bonded to the poly-nucleotides represented in this way a probe for the mobility of the poly-nucleotide chains. The studies involved the measurement of the rotational correlation time (by using formula 3.1) at a series of sample temperatures or pH values. It was thus possible to detect, for example, the existence of a low mobility intermediate in the "melting" (see also Section 4.1.2.)

of the double helical structure of polyU (Ref. 20.). This intermediate would correspond to the original single "hairpin" being broken down into a "multi-hairpin" structure, of high viscosity, and hence corresponding to a long correlation time.

The sharp "melting" of the double stranded polyA . polyU was followed in a similar manner. The plot of the logarithm of the correlation time against the reciprocal of the temperature consisted of two parallel linear regions and the magnitude of the step permitted an estimation of the activation energy of the transition.

Still in the field of the nucleic acids, Ishizu et al. (Ref. 23.) have reported a binding study of the 5-Methyl Phenazinium radical to the DNA. This radical, which is a tricyclic system with two nitrogen atoms in the central ring, can be obtained from the drug Phenazine Methosulphate by chemical reduction in anaerobic conditions. The interaction of this radical (which probably has a planar chromophore) with the DNA is interesting both theoretically (see Section 4.2.) and practically, especially since there is evidence that several similar compounds are physiologically active in reduced form (Ref. 23.). The stability of the radical against oxidation was sensibly enhanced upon binding it to the DNA (but not to RNA or denatured DNA). The immobilization of the radical upon binding could be deduced from the "powder" character of the ESR spectrum of the complex. However, it is apparent that in investigating this interaction, the authors did not take full advantage of the ESR technique, in the sense of obtaining, for example, orientational information, by studying oriented specimens. The use of the technique was confined to measuring drug concentrations in the specimens, in order to produce a Skatchard plot (Ref. 24.) and determine the number of types of binding sites (one), thus confirming the result obtained from a similar plot, produced on the basis of spectrophotometric measurements.

Nitroxide spin labels bound to specific residues in the active site of enzymes (e.g. lysosyme) have provided information about the hydrophobicity and the mobility of the site (Ref. 15.). Recently, the use of Lanthanide ions (e.g. Gd) as spin labels has been reported (Ref. 26.). The study quoted showed that it was possible to combine advantageously the information obtained by ESR with that obtained by NMR (broadening of the peaks corresponding to the residues close to the binding site of the Gd ion), in an attempt to map the binding site of the enzyme.

The main disadvantages of the spin labelling technique arise because the spin labels can perturb the media to which they are added and that one obtains only indirect information on the local interactions and mobilities. However, the brief review above shows that the results obtained by using this technique are remarkable. In some cases (e.g. the membranes) the spin labelling permitted important progress to be done in the study of complex biological systems otherwise uneasily accessible by other techniques. In other cases the possibility of combining advantageously spin labelling studies with other techniques (NMR, X-ray diffraction, optical properties) became evident.

Although the DNA was one of the first biological specimens investigated by spin labelling (when the technique was just being developed), the attention was subsequently shifted towards other species. The present piece of work reconsiders the matter of spin labelling of the nucleic acids in the new context of the interaction of small molecules with the nucleic acids (see also Section 4.2.). The work does not fall exactly into any of the three classes mentioned above, the information gained being both orientational and motional.

One of the materials of study was the radical cation of chlorpromazine (CPZ^+). The binding of this small molecule on to the DNA is interesting both theoretically and practically (see Chapter 1 and 4). The CPZ^+ radical has the special property of being a spin label in itself, so that this was an almost ideal system of study, free of the major inconveniences of the

spin labelling mentioned above.   An attempt was then made to extend and generalise the work with CPZ^+ by synthesising a nitroxide type of spin label, based on to another small molecule, the intercalating drug Proflavine (Chapter 9.).

REFERENCES

1. E. F. SLADE, D. J. INGRAM: Proc. R. Soc. Ser. A., 312, 85, (1969).

2. H. SIGEL (Ed.): Metal Ions in Biological Systems, Vols. I - VI, Marcel Dekker Inc., N.Y.

3. H. NEURATH (Ed.): The Proteins, Vol. V, Academic Press (1970).

4. J. PEISACH, P. AISEN, W. E. BLUMBERG (Eds.): The Biochemistry of Copper, Academic Press (1966).

5. H. BEINERT, G. PALMER in Advances in Engymology, 27, 105-198, (19).

6. H. M. McCONNELL, B. G. McFARLAND: Quart. Rev. Biophys., 3, 91, (1970).

7. S. OHNISHI, H. M. McCONNELL: J. Am. Chem. Soc., 87, 2293, (1965).

8. R. BRIERE, H. LEMAIRE, A. RASSAT: Bul. Soc. Chim. Fr., 32, 3273, (1973).

9. A. D. KEITH et al.: Biochem. Biophys. Acta, 300, 379-419, (1973).

10. H. M. McCONNELL, B. G. McFARLAND: Ann. N.Y. Acad. Sci., 195, 207, (1972).

11. E. G. ROZANTZEV, M. B. NEIMAN: Tetrahedron, 20, 131-137, (1964).

12. T. J. STONE, T. BUCKMAN, P. L. NORDIO, H. M. McCONNELL: Proc. Nat. Acad. Sci., 51, 1010-1017, (1965).

13. F. K. KNEUBÜHL: J. Chem. Phys., 33, 1074-1078, (1960).

14. VÄNGARD and AASA in Paramagnetic Resonance (Low, Ed.), Vol. II, Academic Press, (1963).

15. O. H. GRIFFITH, P. J. DEHLINGER, S. P. VAN: J. Membrane Biol., 15, 159-192, (1974).

16. S. P. VAN, G. B. BIRRELL, O. H. GRIFFITH: J. Magn. Reson., 15, 444, (1974).

17. G. B. BIRRELL, S. P. VAN, O. H. GRIFFITH: J. Amer. Chem. Soc., 95, 2451, (1973).

18. M. PTAK: Biochimie, 57, 483-503, (1975).

19. T. MAEDA, S. OHNISHI: Biochem. Biophys. Res. Com., 60, 1509-1516, (1974).

20. Y. C. E. PAN, A. M. BOBST: Biopolymers, 13, 1979-1083, (1974).

21. A. M. BOBST: Biopolymers, 11, 1421, (1972).

22. E. P. YU-CHING, A. M. BOBST: Biopolymers, 12, 367, (1973).

23. K. ISHIZU et al.: Biochemistry, 8, 1238, (1969).

24. G. SCATCHARD: Ann. N.Y. Acad. Sci., 51, 660, (1949).

25. R. A. DWECK et al.in The Physics and Chemistry of Biological Recognition, Phyl. Trans. Series B, 272, 53-75, (1975).

26. S. K. DOWER et al.: Biochem. J., 149, 73-82, (1975).

CHAPTER 4.

THE NUCLEIC ACIDS AND THEIR INTERACTION WITH SMALL MOLECULES.

Most of this work is concerned with complexes of the drug chlorpromazine (CPZ) with nucleic acids. The properties of such a system are presented in this chapter, with a review of related pieces of work.

The first section presents some of the properties of the basic materials used in the present investigation, as they were known at the moment of the initiation of the project, and is followed by a section dedicated to the nucleic acid - drug interactions. The last section gives an outline description of the project, with the emphasis on its practical applications and the justification of the techniques employed.

4.1. The Basic Materials.

4.1.1. Chlorpromazine.

Chlorpromazine (CPZ) has the chemical formula shown in Fig. 4.1. It belongs to the family of phenothiazine derivatives, the members of which consist of tricyclic structures with Nitrogen and Sulphur in the central ring. Compared to the principal derivative of the class (Phenothiazine), CPZ has in addition a Cl substituent in position 2 and a long sidechain attached to the N in position 10. The sidechain is terminated by a dimethyl-amino group. It is considered (Ref. 1.) that it is the protonation of this group in aqueous solution that is responsible for the water solubility of this compound. CPZ is colourless and diamagnetic.

CPZ is most readily available as a hydrochloride, which is a white amorphous powder. Chemically it represents the same species, with a HCl molecule associated with each CPZ molecule. One will refer to this species as "native CPZ" or CPZ^{o}. The sample used was obtained from May and Baker Ltd .

THE CHLORPROMAZINE RADICAL CATION
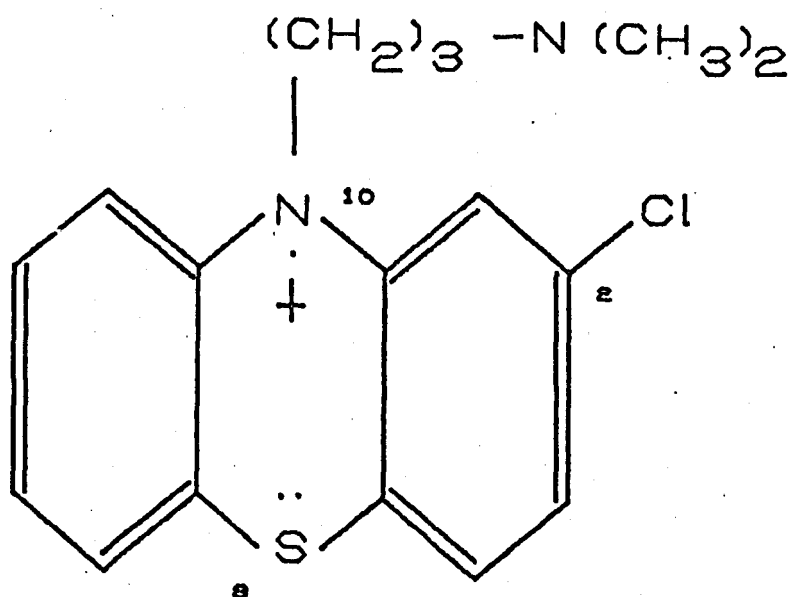
$(CH_2)_3 -N (CH_3)_2$

PHENOTHIAZINE DERIVATIVES

DERIVATIVE	POSITION 10	POSITION 2	POSITION 9
PHENOTHIAZINE	—H	—H	..
CPZ	—$(CH_2)_3$ —N $(CH_3)_2$	—CL	..
CPZ SULPHOXIDE	AS CPZ	—CL	=O
PROMAZINE	AS CPZ	—H	..
10—MET PROMAZINE	—CH_3	—H	..
PROMETHAZINE	—CH_2 —CH (CH_3) —N $(CH_3)_2$	—H	..

FIG. 4. 1

A one step oxidation carried out chemically (Ref. 2.) or electrolitically (Ref. 3.) converts CPZ^o to the red coloured radical cation CPZ^+. Piette (Ref. 3.) verified that the charge carried by the cation radical was +1.

This species is one of the basic materials of this project. The main disadvantage of CPZ^+ is its instability. The conditions of maximum yield of this species were established and they will be presented later (see Section 6.1.3.).

A further oxidation step converts CPZ^+ to the fully oxidised species CPZ sulphoxide which has an O atom attached on to S. This species, like $CPZ^{\oplus}$, is colourless and diamagnetic.

Considering the electronic structure of CPZ, the tricyclic system is not aromatic by Huckel's "4n + 2" rule (Ref. 4.), because the π electronic system of CPZ^o consists of 16 electrons on 14 centres (N and S contributing each with two electrons), the nearest "aromatic" numbers being 14 or 18. Similarly, CPZ^+ has 15 electrons (on 14 centres) and the sulphoxide 16 electrons (on 15 centres).

Alternately one can regard the CPZ molecule as being formed of two orthosubstituted benzoid rings linked together by N and S bridges but this description has the disadvantage of overlooking the participation of N and S to the molecular π system, while the properties of CPZ can be better understood if one assumes the delocalization of the π electron cloud over the whole system. To illustrate this, one should mention that the ESR spectra of CPZ^+ and indeed of the cation radicals of Phenothiazine and other derivatives (see Section 6.3.5.) show contributions from the ring ^{14}N atom as well as from the ring protons, consistent with a delocalization of the electron cloud over the entire structure.

There are no published calculations of the electronic structure of any of the CPZ^+ species. Such calculations would be useful in the interpretation of the ESR spectra of CPZ^+. The nearest compound for which the

electronic structure has been worked out is Phenothiazine (Refs. 5, 6.).

There are two reported structures for the molecular structure of CPZ, based on two different crystallographic forms (Refs. 7, 8.), both of which show the molecule being bent along one axis passing approximately through the N - S atoms so that the two benzoid rings lie in two planes the normals of which make 139 - 137°. The first figure was quoted by McDowell (Ref. 7.). The second was calculated on the basis of the coordinates given by Dorignac-Callas (Ref. 8.). Recently, the molecular geometry of the radical cation (CPZ$^+$) in crystals of charge transfer complex with 7, 7, 8, 8 - tetracyano-quinodimethan has been reported (Ref. 9.). There are two independent radical cations in the asymmetric unit, of slightly different conformations. It is apparent that the ring systems are not planar, the angles between the planes of the two benzoid rings in the two molecules being 143° and 147°, somewhat larger than the angles reported for the neutral species.

CPZ is not a unique example of a bent tricyclic molecule. Hosoya (Ref. 10.) gives examples to show that if the central ring contains any two of the atoms C, O or N, the molecule assumes a flat conformation. However, if the central ring contains one of the atoms S, Se, Te, the molecule is bent. This is valid for molecules, like CPZ^o, containing the S in unoxidized form, as well as for the sulphoxides or dioxides of these molecules.

It is apparent therefore that the bending of the molecule is associated with the presence of the S (or Se or Te) atom, irrespective of its oxidation state. It is thus reasonable to assume that all the CPZ species assume a bent conformation and that this exists not only in crystal state but also in solution.

4.1.2. The Nucleic Acids.

The nucleic acids are linear polymers, the residues of which are the nucleotides (Fig. 4.2.). A unit consists of a purine base (Adenine (A)

NUCLEIC ACIDS

PHOSPHATE

BASE

H8

H2

5' H

H

4'

H

O

1'

H

H

3'

2'

H

O

H

SUGAR

adenine

cytosine

guanine

uracil

inosine
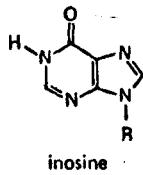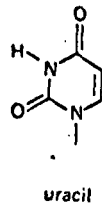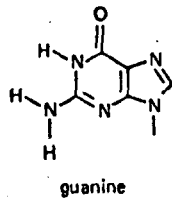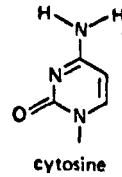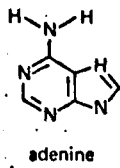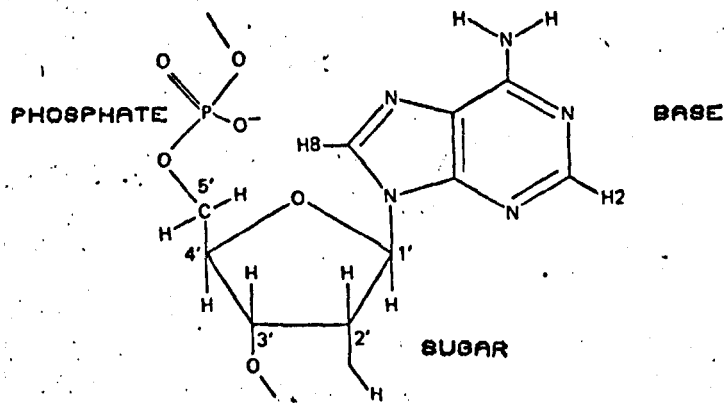
FIG. 4. 2 THE MONOMERIC UNIT OF POLYNUCLEOTIDES (BASE, SUGAR, PHOSPHATE). BELOW (LEFT AND RIGHT) : PURINE AND PYRIMIDINE BASES.

or Guanine (G)) or a pyrimidine base (Cytosine (C), Thymine (T) or Uracil (U)), and a five membered sugar ring. The sugar can be of two kinds, and this determines the two major classes of nucleic acids: DNA (with deoxyribose) and RNA (with ribose). The difference between the two, lies in the presence of OH rather than just H in the 2' position of the deoxyribose, this being sufficient to cause significant structural differences (of steric nature) between the two species. The successive sugar rings are joined together by phosphate groups which form the so called 3'5' diester link.

The double stranded nucleic acids consist of two complementary chains, the bases of each chain forming Hydrogen bonds with those from the opposite chain. In all the natural nucleic acids the base pairs are of Watson-Crick type (i.e. A pairs with T and G with C) and the two chains (i.e. the 3'5' diester links) run in antiparallel fashion. This property and the equal size of the base pairs form the basis for the double stranded nucleic acids having regular double helical structures, in which the residues occupy equivalent positions.

In such a structure, the base-pairs (stacked on top of one another) occupy the interior of the molecule, while the phosphate backbones are exposed to the solvent. The portions between the two interwound phosphate backbones appear to an external observer as two independent groves running in helical paths along the helix. Under physiological conditions the phosphate groups are negatively charged and partially screened by the metal ions present in solution.

The DNA can assume two fundamental forms, A and B, depending on the external conditions such as the relative humidity and to some extent the cation present (Ref. 11, p 121.).

The basic feature of the B type of DNA is that the base pairs are stacked on top of one another, perpendicular to the helical axis. There are exactly 10 base pairs per turn, the pitch of the helix being 33.7 - 34.6 A$^\circ$. In

the A form, the base-pairs are moved away from the helical axis and tilted. Although the separation between the two phosphate backbones is almost equal, the depth of the two independent groves is unequal.

It is considered that in physiological conditions the DNA assumes the B form, because it is this form that is obtained experimentally in high relative humidity conditions. In experimental systems, reversible transitions can be induced from the B to the A form by lowering the relative humidity below about 80%, provided the salt concentration is not too high. Some drugs determine the DNA to assume the B conformation even though the ambient conditions would normally induce the A form (Refs. 12, 15.).

The structure of the double stranded RNA (such as that occuring naturally in some phages) is similar to that of the A form of DNA.

Synthetic single stranded or double stranded polynucleotydes of either the ribo or deoxyribo type and of definite base composition are available. There are structural variations within these species, depending on the base composition and this is why when referring to them it is necessary to state the base composition. For example, poly I . poly C is a synthetic double stranded polynucleotide of RNA type, having C (Cytosine) on one strand and I (Inosine) on the other. Inosine is a base similar to Guanine (Fig. 4.2.). Poly I . Poly C can produce double helices with 11 - 12 base-pairs per turn and tilted base-pairs (Ref. 13.), but never triple helices and this is why this species was preferred for use over the other species, which also give unusual structures.

The structure of the double stranded nucleic acids in aqueous solution is stabilised mainly by the hydrophobic forces (Ref. 11, p 336.) arising from the stacking of the base-pairs and to a smaller extent by the hydrogen-bonding between the two strands. The metal ions (such as Na^+, K^+, Mg^{2+}, Ca^{2+}) which are normally present in the system, play an important stabilizing role, by screening the charges of the phosphate backbones, thus reducing the

repulsion between the two strands.

The double stranded structure can be destroyed by raising the temperature, when the chains separate. The denaturation occurs in a cooperative fashion within a small temperature range, similar to the melting of a crystalline solid. The stability of the double helix is insensitive to the pH (between pH 5 and 9) but if the pH is made more acidic than 5 extensive protonation of the bases takes place, leading to the melting of the structure at low pH (Ref. 14.). The presence of the metal ions mentioned above, results in the stablization of the helix in the region of low pH's (Ref. 11, p 332.).

Extreme values of pH can cause chemical degradation of the nucleic acids. For example, the extreme acidic conditions can result in the hydrolysis of the glycosidic link between the purine bases and the sugars, both in DNA and RNA, resulting in the removal of the purine bases, but this requires high acid concentrations (greater than 1N HCl).

4.2. Complexes of Nucleic Acids with Drug Molecules.

The topic defined by this heading belongs to the general field of the interaction of the nucleic acids with small molecules, which involves the study of the hydration of the nucleic acids as well as the more specific binding of metal ions, drugs or amino and polyaminoacids. Such studies give an insight into the forces responsible for the binding and the specificity, and represent a step towards understanding the nature of the binding of large molecules (e.g. enzymes) on to the nucleic acids. Such an understanding is essential if the biological role of these systems is to be understood.

The study of the binding of a number of drugs having a flat polycyclic structure on to the nucleic acids has enjoyed considerable attention. The reason for this lies in the direct applicability of the results of these

studies in pharmacology e.g. for the design of better drugs.   Such

molecules include the acridines, such as proflavine or acridine orange

and other planar molecules, such as Ethydium Bromide, polycyclic hydro-

carbons, actinomycins, etc. (Ref. 11.).

It is now accepted (Ref. 11, p 429.) on the basis of indirect evidence

obtained by a variety of techniques, that the above drugs can bind on to

the nucleic acids by two mechanisms.

1) The first such mechanism is the intercalation, originally proposed

by Lerman (Ref. 15.) according to which the drug molecule is inserted between

the two successive base-pairs.   The original model suffered refinements due

to Fuller and Waring (Ref. 16.) and Sobel and Jain (Ref. 17.) but the main

points remain the same: i) The DNA is required to be in the B form;

ii) The intercalation involves the movement of the adjacent base-pairs away

from each other to produce a gap that would accommodate the drug, followed

by the local unwinding of the helix at the intercalation site.   The inter-

calated molecules would thus have an orientation perpendicular to the helical

axis.

The stability of such a system is attributed to a hydrophobic (stacking)

effect but many models provide also for some electrostatic contribution or

the possiblity of Hydrogen bonding.   It is likely that the precise orientat-

ion of the drug in the intercalation gap may vary from drug to drug, governed

by the nature and the disposition of the substituents.   Pritchard et al.

(Ref 18.) proposed a model of partial intercalation according to which

only a part of the hydrophobic surface of the molecule is accommodated

inside the intercalation gap but to compensate for this disadvantageous

situation the molecule with charged basic groups can form favourable electro-

static interactions with the phosphate backbone.   The intercalation of

molecules with bulky groups can also be explained by this model but so far

no experimental evidence for this model have been observed.   A review of

the whole topic has been given by Waring (Ref. 19.).

The question of intercalation as applied to CPZ$^+$ is interesting since the CPZ$^+$ molecule is bent and no model makes explicit provision for such cases.   The balance of the forces involved is a delicate one, firstly because a supplementary energy has to be used to produce an intercalation gap larger by about $2 - 2.5_A^o$ than that necessary for a flat molecule (3.4_A^o); secondly because of the bulky Chlorine atom and sidechain present, and thirdly because of the positive charges carried by CPZ$^+$ which must play some role in the interaction.

2) The second mode of binding of the drugs, by attachment of the molecules individually or in clusters at external sites on to the nucleic acids, is well documented (Ref. 11.).   It is widely accepted that at levels of binding of about one drug molecule to each nucleic acid phosphate group, i.e. at "phosphate to drug ratio" (P/D) about 1, stacks of drug molecules can be formed along the exterior of the nucleic acid molecules.   This mode of binding occurs because of the tendency of most of these molecules to aggregate in solution, probably by a stacking mechanism (Ref. 20.).

4.3. Summary - Outline Description of the Project.

The discussion in the previous section revealed that a number of drugs were shown by various techniques to bind to nucleic acids.   Biochemical investigations have further shown that in many cases the binding was correlated with the biological activity of the drug.   In some cases, such as Chlorpromazine (see Chapter 1.) or Phenazine Methosulphate (see Section 3.3.) it appeared that the active forms of the drugs were the radical cation species. In both these two cases the radical cations were shown to be stabilized upon binding to the DNA.

The object of this project is to study the binding of ionic forms of drugs or related derivatives to nucleic acids, by using electron spin

resonance, thus extending the range of information already available from other technqieus. The usefulness of this technique became apparent from Ohnishi and McConnel's work (see Section 6.4.2.), who reported ESR observations on solutions of DNA with CPZ^+ attached. They obtained orientational effects by flowing the solutions through tubes, oriented parallel or perpendicular to the magnetic field. The observed anisotropy of the ESR spectra was found consistent with a preferred orientation of the drug molecules with their planes perpendicular to the flow direction. Most of the work in the present project was performed by using this particular drug, which provided a convenient system of study (see Section 3.3.), but the method of work developed is more generally applicable. The choice of this drug was also determined by both the practical (see Chapter 1.) and theoretical (see Section 4.2) interests related to it.

The nucleic acid-drug interactions were investigated in three phases: in solution, gel and fibres, the latter one being used for orientational studies. The gel represents the sediment obtained from the ultracentrifugation of a solution; the process by which the nucleic acid with the drug attached to it is sedimented while the excess of drug that is not bound remains in the supernatant. The fibres are partially oriented specimens that can be obtained from the gel by placing a small quantity of gel between the ends of two tiny glass rods and allowing it to dry. During the drying, the nucleic acid molecules tend to align themselves parallel to the fibre axis, resulting in a cylindrically symmetric, partially oriented specimen.

By making studies on fibres it is possible to investigate the dependence of the ESR spectrum on the orientation of the fibre relative to the magnetic field and so to determine the orientation of the drug relative to the fibre axis . Where the drug binds externally it has so far not been possible to produce this type of information from other techniques (particularly from

X-ray diffraction).   It will be remembered that the X-ray diffraction (XRD)

has been developed over a number of years as a major technique for invest-

igating the interaction of small molecules with nucleic acids, and the major

models of binding (particularly the intercalation) were based primarily on

information obtained by this technique.   On the other hand (as it became

apparent from the review presented in Chapter 3) a range of spin-label studies

have been pursued using ESR techniques.   The work on nucleic acid fibres

offers the possibility of carrying out ESR and XRD measurements on the same

specimen, thus permitting a direct and valuable compairson between XRD and

ESR data.

Apart from orientational information the ESR technique can provide

information on the mobility of the drug attached to the nucleic acid in the

three phases mentioned above, as well as on the degree of ordering and homo-

geneity within the specimens.   This information can be combined together to

give a picture of the nature of the nucleic acid-drug complexes.

In order to understand better the stereochemical aspects of the binding,

it was proposed to compare the behaviour of a series of complexes obtained

by using different types of nucleic acids and drugs and to investigate these

specimens in a variety of conditions.   Among the parameters that were varied

were: the temperature, the ionic strength, the phosphate to drug ratio and

the relative humidity (which is relevant to comparisons with the XRD studies;

this parameter being one which is often varied in the XRD work).

The major technique employed in this project was the X-band and Q-band

ESR technique.   The experimental methods used are presented in Chapter 6.

The quantitative description of the ESR spectra (i.e. the spectral parameters

and the parameters describing the degree of order), was achieved by simulating

the ESR spectra theoretically.   A computer program for lineshape synthesis

for general use with free radical specimens including fibres was developed,

and this is presented in Chapter 5.

The account of the experimental results starts with the presentation of the properties of CPZ^+ in random environments (Chapter 6) and continues with the investigation of ordered specimens (Chapters 6 - 8). The conclusions of the ESR investigation of fibres were compared with data obtained by other techniques, particularly X-ray fibre diffraction (mentioned in Chapters 6 and 8) and optical dichroism and birefringence (developed in Chapter 7). The final chapter contains a discussion of the significance of the results and of their limitations and makes suggestions for future work.

REFERENCES.

1. D. C. BORG, G. C. COTZIAS: Proc. Natl. Acad. Sci. US., 48, 617-623, (1962).

2. D. C. BORG, G. C. COTZIAS: Proc. Natl. Acad. Sci. US., 48, 623-627, (1962).

3. L. H. PIETTE, I. S. FORREST: Biochem. Biophys. Acta, 57, 419-420, (1962).

4. A. STREITWIESER, Jr.: Molecular Orbital Theory for Organic Chemists, Wiley, N.Y., (1961).

5. H. H. MANTSCH, J. DEHLER: Canad. J. Chem., 47, 3173-3178, (1969).

6. B. C. GILBERT, P. HANSON, R. O. C. NORMAN, B. T. SUTCLIFFE: Chem. Commun., 6, 161-164, (1966).

7. J. J. H. McDOWELL: Acta. Cryst. B 25, 2175, (1969).

8. M. R. DORIGNAC-CALAS, P. MARSAU: C. R. Acad. Sc. Paris, Ser. C, 274, 1806-1809, (1972).

9. R. M. METZGER (Mississippi): Private Communication, (1976).

10. S. HOSOYA: Acta. Cryst., 16, 310-312, (1963).

11. V. A. BLOOMFIELD, D. M. CROTHERS, I. TINOCO: Physical Chemistry of Nucleic Acids, Harper and Row, (1974).

12. D. M. NEVILLE, Jr., D. R. DAVIES: J. Mol. Biol., 17, 57-74, (1966).

13. S. ARNOTT, W. FULLER, A. HODGSON, J. PRUTTON: Nature, 220, 561-564, (1968).

14. C. ZIMMER, H. TRIEBL: Biopolymers, 8, 573-577, (1969).

15. L. S. LERMAN: J. Mol. Biol., 3, 18-30, (1961); J. Mol. Biol., 10, 367, (1964).

16. W. FULLER, M. J. WARING: Ber. Dtsch. Bunsenges.Phys. Chem., 68, 805-808, (1964).

17. H. M. SOBELL, S. C. JAIN: J. Mol. Biol., 68, 21-34, (1972).

18. N. J. PRITCHARD, A. BLAKE, A. R. PEACOCKE: Nature, 212, 1360, (1966).

19. M. J. WARING: Nature, _219_, 1380, (1968).

20. A. R. PEACOCKE, J. N. H. SKERRETT: Trans. Farad. Soc., _52_, 261, (1956).

CHAPTER 5.

A COMPUTER PROGRAM FOR ESR LINESHAPE SYNTHESIS

FOR GENERAL USE WITH FREE RADICAL SPECIMENS INCLUDING FIBRES.

5.1. Introduction.

The need for a computer program to assist the experimental ESR work by the theoretical simulation of the ESR spectra was mentioned in the previous chapter.   The literature does not contain any published program that would be generally and conveniently applicable to this free radical work.

The computer program which is presented in this chapter was developed in order to serve as a research tool in the present project and it was also aimed to fill the existing gap in the literature.   The program contains, for convenience, a package of algorithms that can undertake the task of simulating the ESR spectra of the types of specimen most commonly encountered in free radical work; solutions (isotropic hyperfine spectra), single crystals, powders (or immobilised species) as well as fibres.

For the purpose of comparing the experimental and theoretical spectra, the experimental spectra were recorded on paper tape by using a magnetic follower (Dmac), scaled by computer and replotted.   The computational technique proved to be a powerful way of interpreting rigorously the ESR results.   It made possible the determination of the CPZ^+ principal tensor values from the "gel" spectra and the formulation of the model of a dis-oriented fibre (to be presented in Chapter 6).   This computer program was also used to check the validity of the assignments made in various published papers in conjunction with spectra of different radicals related to CPZ^+. The fact that in most of the cases in which spectral simulations were not performed the published parameters failed to reproduce the features of the experimental spectra illustrates the value of the computational technique in the ESR work.

5.2. The Theoretical Simulation of the ESR Spectra.

The synthesis of the isotropic hyperfine spectra was based on a Hamiltonian of the form given by Equation (13) from Section 2.3.2., while the form used for the anisotropic spectra was that given by Equation (10) from Section 2.3.4.

The position of a particular ESR absorption line in the magnetic field can be calculated in both cases from the formula:

$$B_o = \frac{h\gamma}{g\beta} - \Sigma_1 M_{I_1} A_1 \tag{1}$$

where 1 labels the quantities referring to the hyperfine interaction with the 1th nucleus and the $1\ M_{I_1}$ values represent a combination of the possible nuclear spin components of the nuclei. An ESR absorption line corresponds to each such combination and a lineshape function of Gaussian or Lorentzian type (see Section 2.2.) is attached to each absorption line.

In the isotropic hyperfine case, g and A in Equation (1) represent the isotropic g value and coupling constant (a). In the anisotropic hyperfine case, g and A represent the orientation dependent g value and splitting (A), which are given within the "intermediate field" approximation by the expressions (19) of Section 2.3.4.

The synthesis of an isotropic hyperfine spectrum is the simplest application of the Formula (1) and the only required parameters are those required by this equation.

The synthesis of a "single crystal" type of spectrum is also straightforward because there is just one orientation of the molecule relative to the magnetic field involved and this orientation is specified beforehand.

However, the "powder" and "fibre" spectra represent superpositions of many spectra which are summed so as to conform to the random orientation model in the first case or to the model of the fibre in the second. Clearly the latter case has greater complexity and requires a more detailed

discussion.   A model of a partially oriented fibre in which the misalign-
ment is described by a Gaussian function is developed and presented in the
next section.

5.3.   The Fibre Model.

We shall refer to fibres of spin labelled DNA in an ESR experiment, but
as the model is more general the fibre can be considered as a collection of
"fibrils", preferentially oriented along one axis.   The species of interest
can be either a molecule attached on to the fibril (as the spin label is
attached on to the DNA) or it can be part of the fibril itself.   The
magnetic field direction we shall refer to is a unique direction in the
laboratory frame, the significance of which depends on the particular
experiment in question (e.g. it could be the direction of the electric
vector of the plane polarised light beam, in a linear dichroism experiment).

As a specific example consider a DNA molecule within the fibre with a
small paramagnetic molecule (spin label) attached to it.   For our purpose,
we can regard the DNA molecule as an essentially cylindrical object because
of its random orientation about its axis.   By specifying the position of
one labelling molecule relative to this DNA molecule the positions of other
equivalent labels is defined;   positions that can be obtained from the
initial one by rotating the DNA molecule about its axis.   Needless to say
that the labels in each of these orientations will produce a different ESR
spectrum, the parameters of which would depend also on the orientation of
the particular DNA molecule in the fibre and on the orientation of the
fibre relative to the magnetic field.

In this model it has been assumed that the DNA molecules (or segments
of DNA molecules) describe a Gaussian distribution of orientations about
the fibre axis, so that the probability of a DNA molecule lying on the
surface of a cone of semiangle α is proportional to exp $(-\alpha^2/2\delta^2)$ where δ is

the halfwidth of the distribution (standard deviation). Therefore, the "cylindrical averaging" which takes place at the level of a DNA molecule is followed by a second "cylindrical averaging" process at the level of the fibre. Consequently the only information needed to simulate this fibre specimen are the details of the binding of the label on to the DNA molecule and the width of the Gaussian distribution.

To describe this quantitatively, it is convenient to use the formalism set up by Van et al. (Ref. 1.) and attach Cartesian frames of reference to the label (x,y,z), the DNA molecule (x_2,y_2,z_2), the fibre (X_1,Y_1,Z_1) and the laboratory (X,Y,Z) assuming the magnetic field B to be along the Z axis. We then need the coordinates of B in the label molecular frame.

The orientation of a label molecule relative to the DNA is specified by the transformation:

$$L_2 = \begin{pmatrix} \cos\theta_2\cos\phi_2\cos\psi_2 - \sin\phi_2\sin\psi_2 & \cos\theta_2\sin\phi_2\cos\psi_2 + \cos\phi_2\sin\psi_2 & -\sin\theta_2\cos\psi_2 \\ -\cos\theta_2\cos\phi_2\sin\psi_2 - \sin\phi_2\cos\psi_2 & -\cos\theta_2\sin\phi_2\sin\psi_2 + \cos\phi_2\cos\psi_2 & \sin\theta_2\sin\psi_2 \\ \sin\theta_2\cos\phi_2 & \sin\theta_2\sin\phi_2 & \cos\theta_2 \end{pmatrix}$$

$$\begin{pmatrix} x_2 \\ y_2 \\ z_2 \end{pmatrix} = L_2^\tau \begin{pmatrix} x \\ y \\ z \end{pmatrix}$$

where ϕ_2 describes a rotation of the label about the DNA z_2 axis, θ_2 is a rotation about the DNA y_2 axis specifying the "tilt" of the label relative to the DNA, ψ_2 specifies the "twist" of the label about its own z axis, and L_2^τ denotes the transpose of L_2.

Similarly, one has three angles involved in the transformation from the DNA to the fibre reference frame: ϕ_1, which takes into account the rotation

about the fibre axis, θ_1, the tilt of the DNA molecule relative to the fibre axis and ψ_1 the rotation about the DNA axis, which can be set equal to zero as this rotation has been accounted for by the angle ϕ_2, of the previous transformation.

Finally, the transformation from the fibre to the laboratory reference frame is characterised by the angle θ_0 (between the direction Z of the field and the fibre axis) and we set $\phi_0 = 0$ (due to the invariance of the experiment for rotations about the Z axis) and $\psi_0 = 0$ (since rotations about the fibre axis were taken into account by ϕ_1 of the above transformation).

$$
L_1 = \begin{bmatrix} \cos\theta_1\cos\phi_1 & \cos\theta_1\sin\phi_1 & -\sin\theta_1 \\ -\sin\phi_1 & \cos\phi_1 & 0 \\ \sin\theta_1\cos\phi_1 & \sin\theta_1\sin\phi_1 & \cos\theta_1 \end{bmatrix}
$$

$$
L_0 = \begin{bmatrix} \cos\theta_0 & 0 & -\sin\theta_0 \\ 0 & 1 & 0 \\ \sin\theta_0 & 0 & \cos\theta_0 \end{bmatrix}
$$

Hence,

$$
\begin{bmatrix} X \\ Y \\ Z \end{bmatrix} = L_0^{\tau}\, L_1^{\tau}\, L_2^{\tau} \begin{bmatrix} x \\ y \\ z \end{bmatrix}
\tag{2}
$$

from which the coordinates of the magnetic field direction (Z) in the molecule referenced system can be found.

In the case of an ESR experiment, these coordinates can be used to calculate the Hamiltonian parameters corresponding to this particular orientation, particularly the g-value and the hyperfine splitting A. In this derivation the molecular frame was the frame given by the principal

directions of the A and g-tensors, assumed to be co-linear which is true

for many systems.   In the general case (A and g-tensors non co-linear),

one would need to carry the chain transformation one step further and to

determine the coordinates of B along the principal directions of both these

tensors in a separate calculation.

The fibre spectrum is built up by summation of spectra, which formally

is done in two steps corresponding to the two levels of averaging mentioned

above.   In practice, however, one allows the angles ϕ_2, ϕ_1, and Θ_1 to

sample their allowed ranges (which are $0,360^\circ$ for ϕ_2 and ϕ_1 and $0,180^\circ$ for

Θ_1) by making each of them take systematic equal steps.   The spectrum

corresponding to each orientation defined by ϕ_2, ϕ_1 and Θ_1 is weighted in

the sum by:

$$P\ (\phi_2,\ \phi_1,\ \Theta_1) = \sin \Theta_1\ \exp\ (-\Theta_1^2/2\delta^2)$$

where δ is the width of the distribution, and P is proportional to the

probability of a DNA molecule having an orientation in the vicinity of the

direction defined by Θ_1, ϕ_1.

The first factor in the above equation is the weighting factor associated

with changes in the angle ϕ_1 which is involved in the cylindrical averaging

at the level of the fibre and is consequent upon the use of spherical polar

coordinates.

The normalization of the final spectrum is done in the end by division

of the accumulated spectrum by the sum of the weights of each component

spectrum.   This mode of normalization in one step is possible because the

weighting factor associated with changes in the angles Θ_1 and ϕ_2 are constants.

If the labelling molecule is not bound rigidly on to the DNA as considered

up to here but has a range of possible orientations, then this "play" has to

be described in terms of the two binding angles Θ_2 and ψ_2.   It can be seen

that for each pair Θ_2, ψ_2, one is concerned with essentially a different

label species to which there corresponds a different fibre-type of spectrum.

The final spectrum can be computed as a sum of these fibre spectra, and

weightings will also have to operate at this level. The program is only valid if the inverse correlation time for substantial re-orientation of the principal (z) axis is much less than the largest anisotropic term in the spin Hamiltonian. In dried fibres this will invariably be the case.

5.4. The Powder Case.

In the "powder" case the orientation of the magnetic field in the molecular frame is described using a set of spherical polar coordinates (θ, ϕ), θ being the angle between the z molecular axis and the magnetic field direction. The anisotropy formulae (19) from Section 2.3.4. apply, with l_{zx}, l_{zy} and l_{zz} being equal to cos θ, sin θ cos ϕ and sin θ sin ϕ respectively.

The random distribution of orientations is simulated by allowing the angles θ and ϕ to sample their allowed ranges, the probability associated with an orientation (θ, ϕ) being equal to $| \sin \theta |$. Since the anisotropy formulae are quadradic in the coordinates one can restrict the variation of θ and ϕ to a quarter of the unit sphere $(0,90^{\circ}$ and $0,180^{\circ}$ respectively). If the z molecular axis is a symmetry axis for the A and g tensors, the anisotropy formulae become independent on ϕ and the only angle that has to be varied is θ, the probability associated with orientation being still $| \sin \theta |$.

The "single crystal" case uses the same formalism as above, with the angles θ and ϕ fixed (and specified as input).

5.5. Description of the Computer Program.

5.5.1. The Basic Flow Chart.

The main program prepares the parameters necessary for the computation of the ESR spectra, a task which is undertaken by a subroutine.

The construction of the program can be followed from the flow chart illustrated in Fig. 5.1. and commences by reading a master card, which
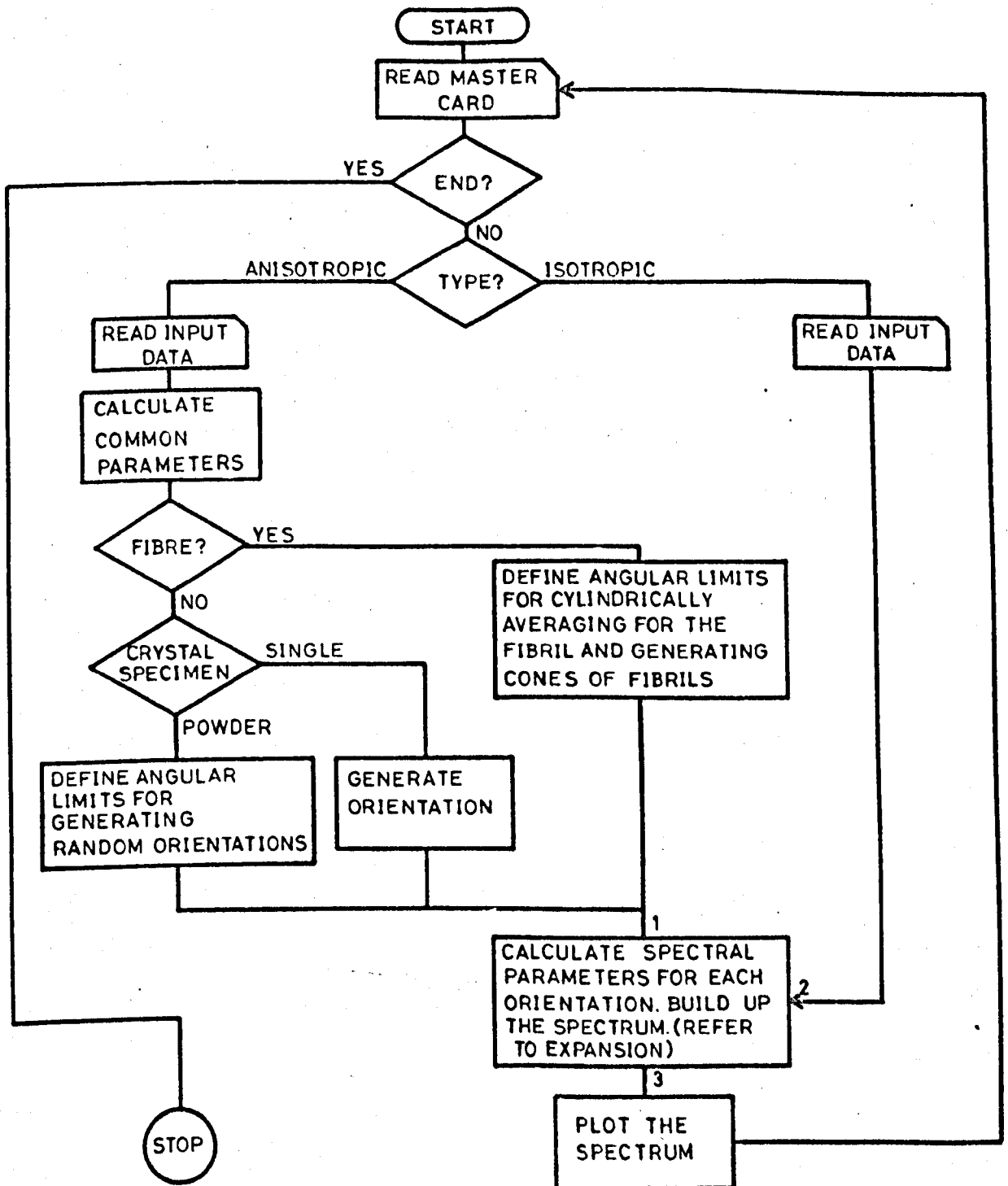
FIG. 5. 1 (A). THE FLOW CHART (REFER TO THE EXPANSION IN FIG. 5. 1B).

specifies the functions to be fulfilled (see Section 5.5.2), in particular the type of spectrum to be computed (isotropic, single crystal, powder or fibre). One subsequently brances according to the type of spectrum and reads in the pertinent input parameters. The "isotropic" branch, where the problem of orientation does not exist is simpler and one can pass directly to building up the spectrum. The anisotropic spectra are treated in common, since in all these cases the spectral parameters (essentially the g-value and hyperfine splitting) are orientation dependent.

The generation of the orientations necessary in the averaging processes described above is done by varying the appropriate angles in predetermined equal steps. The procedure followed in the fibre case is shown expanded in the flow chart from Fig. 5.1b.

The angles θ_1, ϕ_1, ϕ_2 (the program variables ALFA, BETA, FI) are set to sweep their ranges in steps as specified by the input variables ASTEP, BSTEP, FSTEP. The nested loops are so designed as to minimise the computational effort.

The core of the loops deals with the calculation of the magnetic field components in the molecular reference frame, by an expansion of the matrix product (2). This is an expression in terms of the angles θ_1, ϕ_1 and ϕ_2 as well as the given orientation of the fibre relative to the magnetic field θ = GAMMA) and the given details of the orientation of the molecule relative to the DNA (the tilt angle θ - THETA and twist angle ψ_2 - PSI).

For each orientation, the g and A values are calculated, the ESR spectrum is computed, weighted and added to the accumulator. After all the cycles have been performed, the spectrum is normalized by division by the sum of the weights, ready for plotting.

The powder and single crystal are treated as particular cases of the fibre case, some of the variables associated with the fibre properties being reassigned new meanings. Thus the angles ALFA and BETA now define
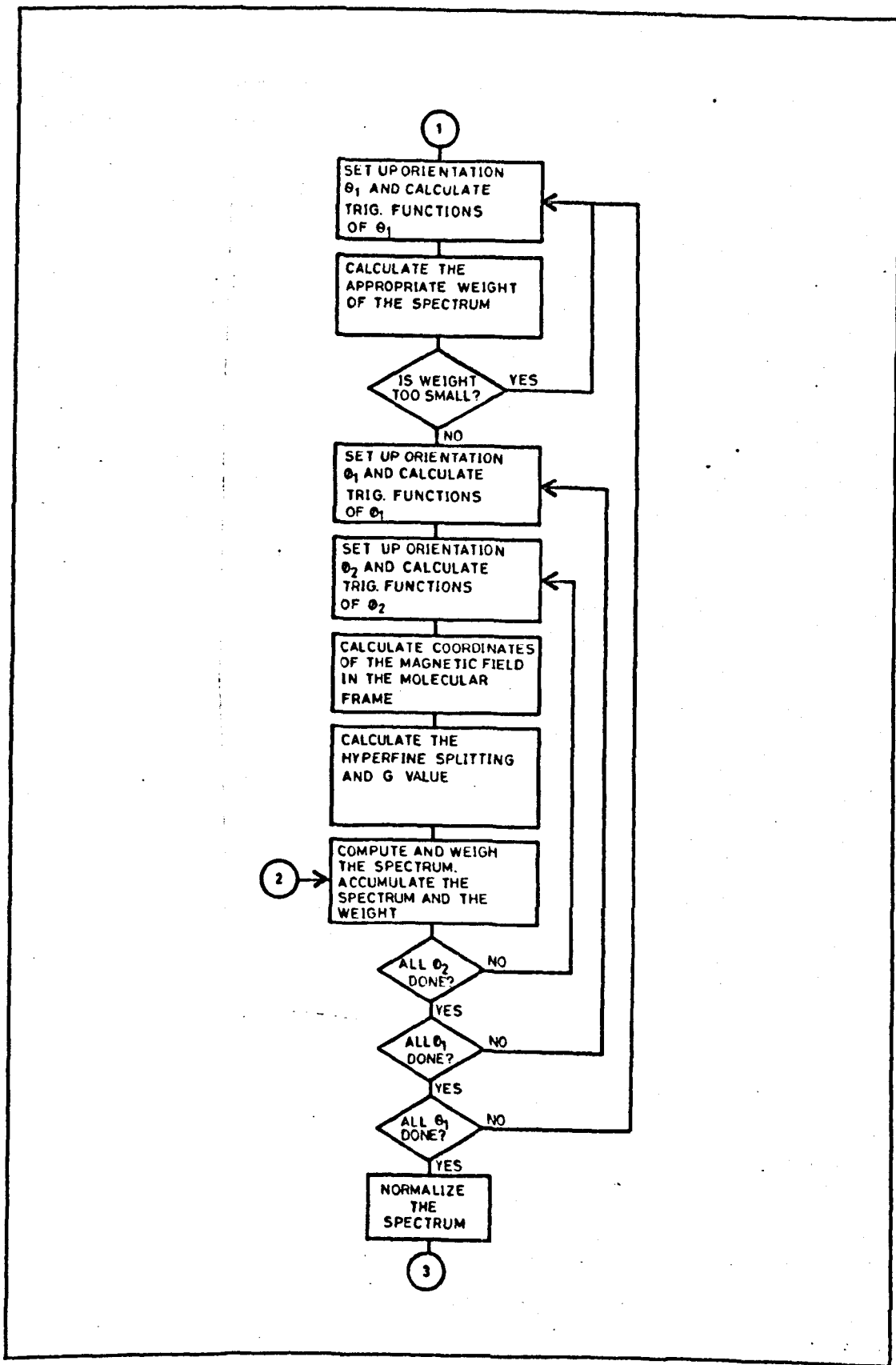
FIG. 5. 1 (B). THE CYLINDRICAL AVERAGING ROUTINES FOR FIBRE TYPES OF SIMULATIONS.

an orientation of the magnetic field in the molecular frame.

5.5.2. Other Functions of the Program.

Several facilities were provided in order to make the use of the program more convenient.   They came into operation after the ESR spectrum of the species is completed and plotted, and they were omitted from the flow chart of Fig. 5.1.   The necessary parameters, NO, IADD, IPRINT, ISHAPE, RA, IREPET, are read in from the master card.

The parameter RA is a fraction by which the normalised spectrum is multiplied and is useful when summing spectra arising from different species (see below).

The program is based on a dual storage system, which functions as specified by IADD.   If IADD is set equal to 0 (as in the normal mode of operation), the newly synthesised spectrum is transferred to the storage register so that at any time before this step one can have access to both the newly synthesised spectrum and the spectrum synthesised previously. This facility is used, for example, when one tries to analyse (by a least squares procedure) an experimental spectrum into a sum of two computed spectra, corresponding to two different species.   If IADD = 1, the newly synthesised spectrum weighted by RA is added to the contents of the storage register.

One has a choice of lineshapes, as specified by ISHAPE, (0 = Lorentzian, 1 = Gaussian).   If ISHAPE = 2, the synthesis is performed using a Gaussian lineshape first and then repeated using a Lorentzian lineshape.   IPRINT = 1 (as opposed to 0) results in the print out of all the intermediate results. IREPET = 1 (as opposed to 0) open the access to a section of the program in which any parameter (including the "master" parameters) can be changed in the desired manner and the synthesis repeated.   One can use this facility to generate a sequence of spectra (corresponding for example to a series of

orientations of the fibre relative to the field) or to sum up spectra of different species (corresponding for example to different orientations of the spin label which is allowed to have a "play" relative to the DNA). In addition, one can specify in this part of the program an alternative microwave frequency so that one can obtain spectra both at X and Q band frequencies.

5.5.3. The Synthesis of the ESR Spectra (The Subroutine SPECTR).

The synthesis of the ESR lineshape is performed by the subroutine SPECTR which takes data (principally the g-value and the hyperfine splitting) from the main program.

The subroutine computes and accumulates spectra from successive calls and returns the accumulated absorption and derivative spectra to the main program. The same algorithm is used to compute both isotropic and anisotropic spectra, and was designed to cope with up to 10 hyperfine interactions. The full absorption spectrum is built up line by line, and the first derivative spectrum is computed simply by calculating the slopes between adjacent points.

Field dependent linewidths have also been provided for, since in many cases one of the hyperfine splittings, say that arising from the nucleus labelled 1, is dominant over the others, and one can associate a linewidth with each of the M_{I_1} values corresponding to this nucleus so that the linewidth of an ESR absorption line will be determined by the value of M_{I_1} contributing to that line. No further provision for orientational dependent linewidths has been included.

A subroutine of original design for line printer plotting is also included in the listing.

5.6. Concise Specification.

The following tupes of ESR spectra can by synthesised:

1) Solution spectra (up to 10 isotropic hyperfine interactions).

2) Single crystal spectra.

3) Powder spectra.

4) Partially oriented fibres.

A single anisotropic hyperfine interaction is accounted for in the cases 2) to 4) above, within the intermediate magnetic field approximation. The theoretical background was presented in the Sections 5.2. to 5.4.

The output consists of a plot of the computed spectrum and/or a table showing the magnetic field values at the positions of the centres of the hyperfine components. Facilities are provided to use either Gaussian or Lorentzian lineshapes or both, and for line dependent linewidths. The mathematical operations involved are based on fundamental principles of magnetic resonance and the program allows for easy interference with its function. It can handle more paramagnetic species, and produce sequences of spectra etc.

The programming language is FORTRAN. The meaning of the program variables is explained in the Sections 5.5.1. and 5.5.2. above. The required input (from cards) is indicated in the listing.

The listing of the program is attached as appendix. The program was also made available to the Quantum Chemistry Exchange Programs, University of Indiana (Reference Number QCEP 295).

REFERENCES.

1. S. P. VAN, G. B. BIRRELL, O. H. GRIFFITH: J. Magn. Reson., $\underline{15}$, 444, (1974).

CHAPTER 6.

ELECTRON SPIN RESONANCE AND OPTICAL MEASUREMENTS

OF CHLORPROMAZINE AND CPZ^+ - DNA COMPLEXES.

The first two sections of this chapter present some of the properties of the CPZ^+ radical in both free state and bound to DNA, as deduced from absorption spectrophotometric measurements. Section 6.3. describes the experimental arrangements for the ESR work, and is followed by the present-ation of the ESR measurements of CPZ^+ in disordered environments (solutions and gels), which led to the determination of the ^{14}N principal tensor para-meters. The final section presents the results of the orientational studies performed with DNA - CPZ^+ fibres.

6.1. The Properties and Preparation of the CPZ^+ Radical.

6.1.1. U.V. and Visible Absorption Spectra.

The U.V. absorption spectra of aqueous solutions of the three CPZ species mentioned in Section 4.1.1. are shown in Fig. 6.1a. The visible absorption spectrum of a solution of CPZ^+ is shown in Fig. 6.1b. The concentration was determined on the basis of the dry quantity of drug used and assuming a molecular weight of 356 for the chlorpromazine hydrochloride. The material was used without preliminary purification.

The cation radical CPZ^+ was obtained in aqueous solution by the chemical oxidation of the CPZ° with equivalent amounts of sodium persulphate. (For the practical method of preparation see Section 6.1.3.) The spectrum of the species thus obtained is similar to the published spectra of CPZ^+ obtained by other techniques (Ref.1.). It can be seen that although there is sodium persulphate in the system, this species does not absorb in the visible and near-U.V. ranges.

The sulphoxide (SO) was obtained directly by the chemical oxidation of CPZ° with excess sodium persulphate. The spectrum of this species from

CHLORPROMAZINE ABSORPTION SPECTRA

MOLAR EXTINCTION

5000
4500
4000
3500
3000
2500
2000
1500
1000
500

8000
7000
6000
5000
4000
3000
2000
1000

420 440 460 480 500 520 540 560 580 600

WAVELENGTH, NM

220 230 240 250 260 270 280 290 300 310 320 330 340 350 360 370 380 390

WAVELENGTH, NM

FIG.6.1 U.V.ABSORPTION SPECTRA OF CHLORPROMAZINE:
——NATIVE, ——RADICAL CATION, ---SULPHOXIDE.
...RADICAL CATION, ----SULPHOXIDE.
IN CAPTION, VISIBLE ABSORPTION SPECTRUM OF THE CATION RADICAL.
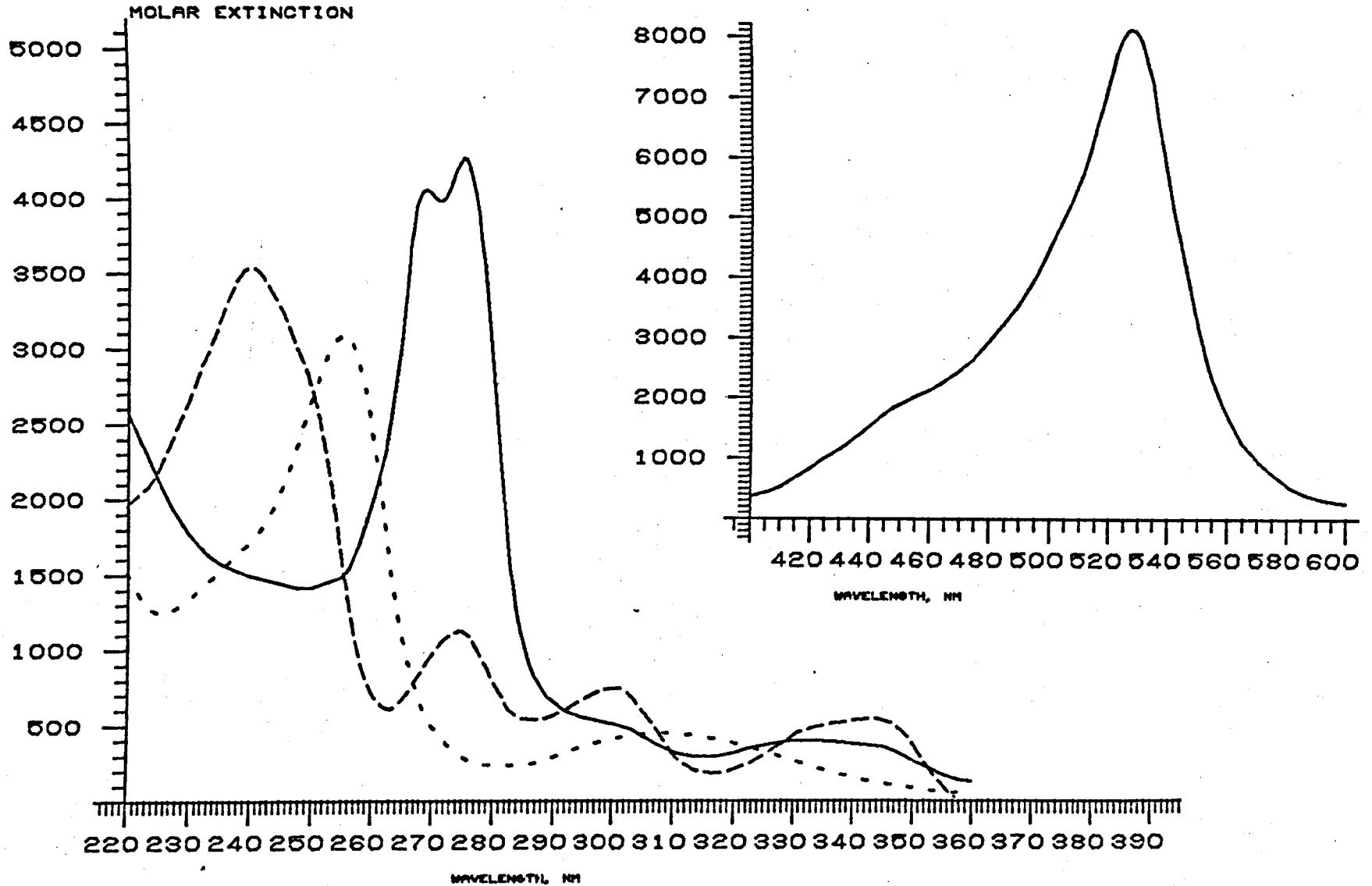
Fig. 6.1a. is similar to that reported previously (Ref. 1.).

The extinction coefficients at the maximum absorption peaks of the three species, as deduced from the spectra from Fig. 6.1 are given below (in $mole^{-1}$ l cm^{-1}):

$$CPZ^o : E_{256} = 31000$$

$$CPZ^+ : E_{270} = 39840, \quad E_{527} = 7980$$

$$SO : E_{240} = 34940, \quad E_{300} = 7550$$

They were used in the determination of the extent of binding of CPZ^+ on to the DNA by a spectrophotometric method (6.2.2.).

6.1.2. The Stability of the CPZ^+ Radical.

The CPZ^+ radical in aqueous solution is unstable. The average lifetime of the radical species ranges between about one hour, for dilute solutions (concentration about $10^{-4}M$) to a few minutes, for more concentrated solutions (about $10^{-2}M$). At even higher concentrations, insoluble aggregates develop in the solution, the dark colour of which remains stable.

Fig. 6.2. represents a family of absorption spectra of a solution of CPZ^+, recorded at various time intervals after the preparation of the radical cation. It can be seen that the spectra have common isosbestic points, which is consistent with the existence of a unique decay reaction. The decay product was identified on the basis of its absorption spectrum as the CPZ sulphoxide.

It was verified that CPZ^+ also decays to the sulphoxide in oxygen free solutions, and that the CPZ recovered in the supernatants obtained from the ultracentrifugation of DNA/CPZ^+ solutions was also in the form of sulphoxide. The decay mechanism cannot be inferred from the present information but it is apparent that it is not the proposed "dismutation" reaction, i.e. two radical cations reacting and resulting in one fully oxidised and one reduced species (Ref. 2.), because this would result in a 1:1 mixture of CPZ^o and sulphoxide, which would exhibit a different absorption spectrum.

THE DECAY OF THE CPZ RADICAL
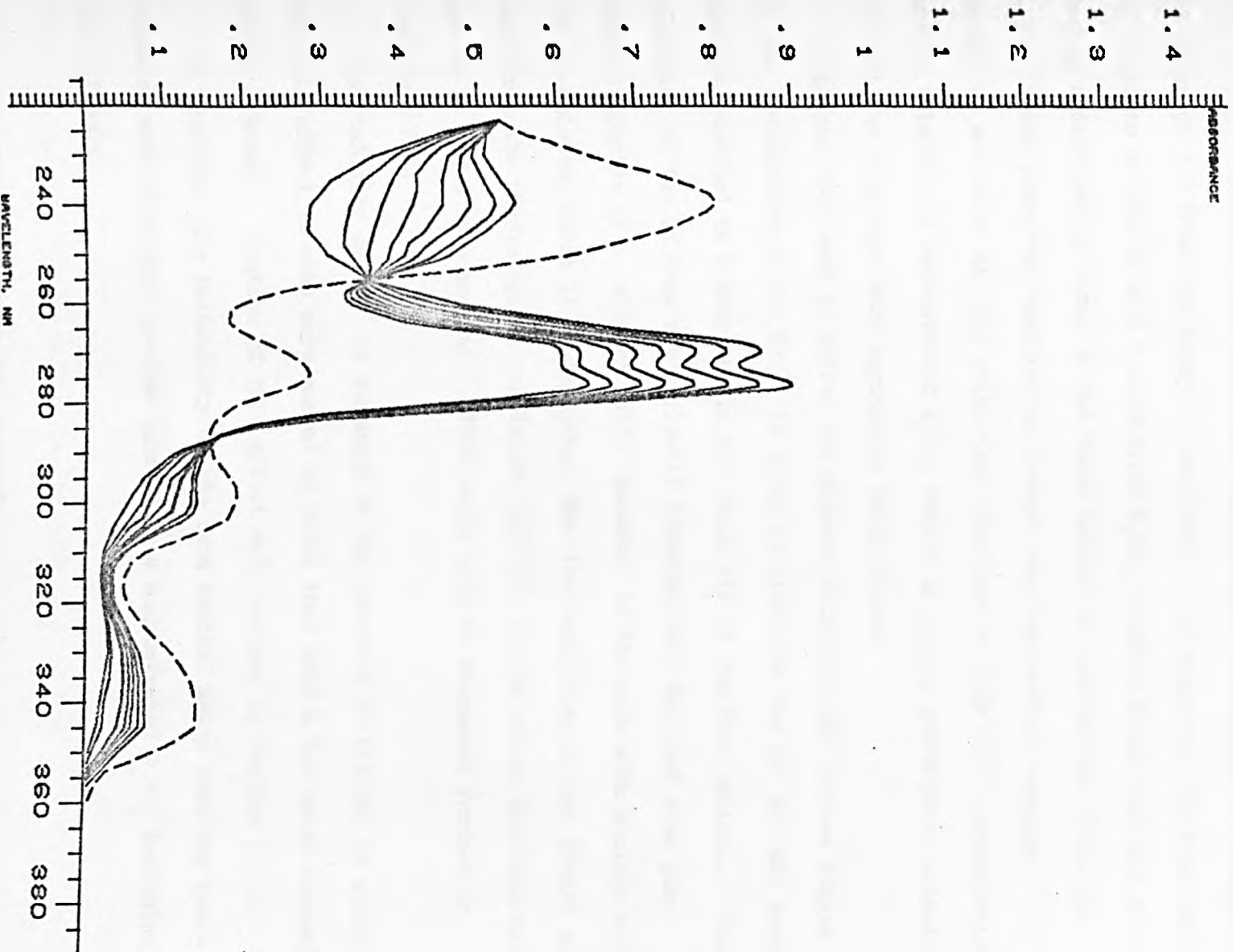
FIG.6.2 ABSORPTION SPECTRA OF AN AQUEOUS CPZ⁺ SOLUTION, RECORDED
AT 8 MIN. INTERVALS AFTER PREPARATION. THE LIMITING SPECTRUM (DASHED)
CORRESPONDS TO CPZ SULPHOXIDE.

The decay of the CPZ^+ in solution is accompanied by a continuous drop in the pH, showing that protons are liberated during the reaction. Thus the pH would decrease from just under neutral (for a fresh CPZ^+ solution) to about pH 3.8 (when the decay is complete). As expected, the free radical is found to be stable in a concentrated H_2SO_4 solution (about 32%) and this can be understood in terms of the "mass action" of the protons (from the H_2SO_4) which force the equilibrium towards the free radical species. It should be mentioned at this point that solutions of high CPZ^+ concentration can be obtained in concentrated H_2SO_4 medium by sodium persulphate oxidation without the insoluble dark aggregates being formed.

Attempts were made to buffer the aqueous solutions (at various stages of the preparation of the CPZ^+) in order to stabilize the pH, but any such attempt resulted in a decrease in the stability of the free radical. The variation of the pH does not seriously inconvenience the work with pure radical species (i.e. without DNA); however, in the work with nucleic acid/ CPZ^+ complexes, where it is important that the conditions do not depart too much from the physiological conditions (pH 7.0), the pH effect outlined above has to be taken into account. This topic will be discussed further in Section 6.2.2.

The stability of CPZ^+ is enhanced by the presence of the DNA in solution and this effect is even more marked in media that have a low water content (gels, fibres). Mention of this effect will be made in Section 6.2.2.

In practice, the instability of the free radical means that any quantitative work with this species (except in a concentrated H_2SO_4 medium) will be difficult.

6.1.3. Preparation of the CPZ^+ Radical.

The practical method for preparation of the CPZ^+ radical in solution is presented in this section. The optimum conditions for the reaction were

established by trial, since both the formation rate of CPZ^+ and its decay rate (Section 6.1.2.) are strongly concentration dependent. If the concentration of the reagents given below are used, the formation rate of the radical is much faster than the decay and the yield is a maximum (practically complete). Also at these concentrations no insoluble aggregates are formed.

The starting materials are $10^{-2}M$ solutions of CPZ hydrochloride (MW = 356) and sodium persulphate (MW = 238). A volume of sodium persulphate solution is poured onto an equal volume of the CPZ^0 solution and allowed to stand for 1 min 15 s, in which time a strong red colour, characteristic of the CPZ^+, develops. At this moment (at which the yield is maximum) the reaction is slowed down by a 10 or 5 fold dilution with water. The solution can be conveniently used in this form for experiments or for preparing nucleic acid/CPZ^+ complexes (Section 6.2.1.).

An attempt to obtain CPZ^+ by sodium persulphate oxidation in solution after CPZ^0 was mixed with the DNA was unsuccessful, as was the attempt to obtain any UV induced paramagnetism in DNA/CPZ complexes (solutions or fibres). A short wavelength Mercury lamp was used for this experiment.

One should mention in this context that the UV irratiation of a CPZ^+ solution in H_2SO_4 (CPZ^+ concn. = $10^{-2}M$; H_2SO_4 concn. about 30%), which gave signs of a slow CPZ^+ decay, resulted in the intensification of the red colour of the solution and an increase of the CPZ^+ ESR signal. The system behaved as if the UV reversed the decay of the free radical. However, irradiation of CPZ^0 solutions resulted in no radical formation unless H_2SO_4 was present and only after prolonged exposures (e.g. overnight). Insoluble dark deposits occurred in the solution and a well resolved ESR signal having a different hyperfine pattern to that of CPZ^+ was observed (compare Figs. 6.3. and 6.9.). The major background lineshape was missing and the hyperfine splitting of the 17 lines was about 0.14 mT. No further mention of this species will be made.
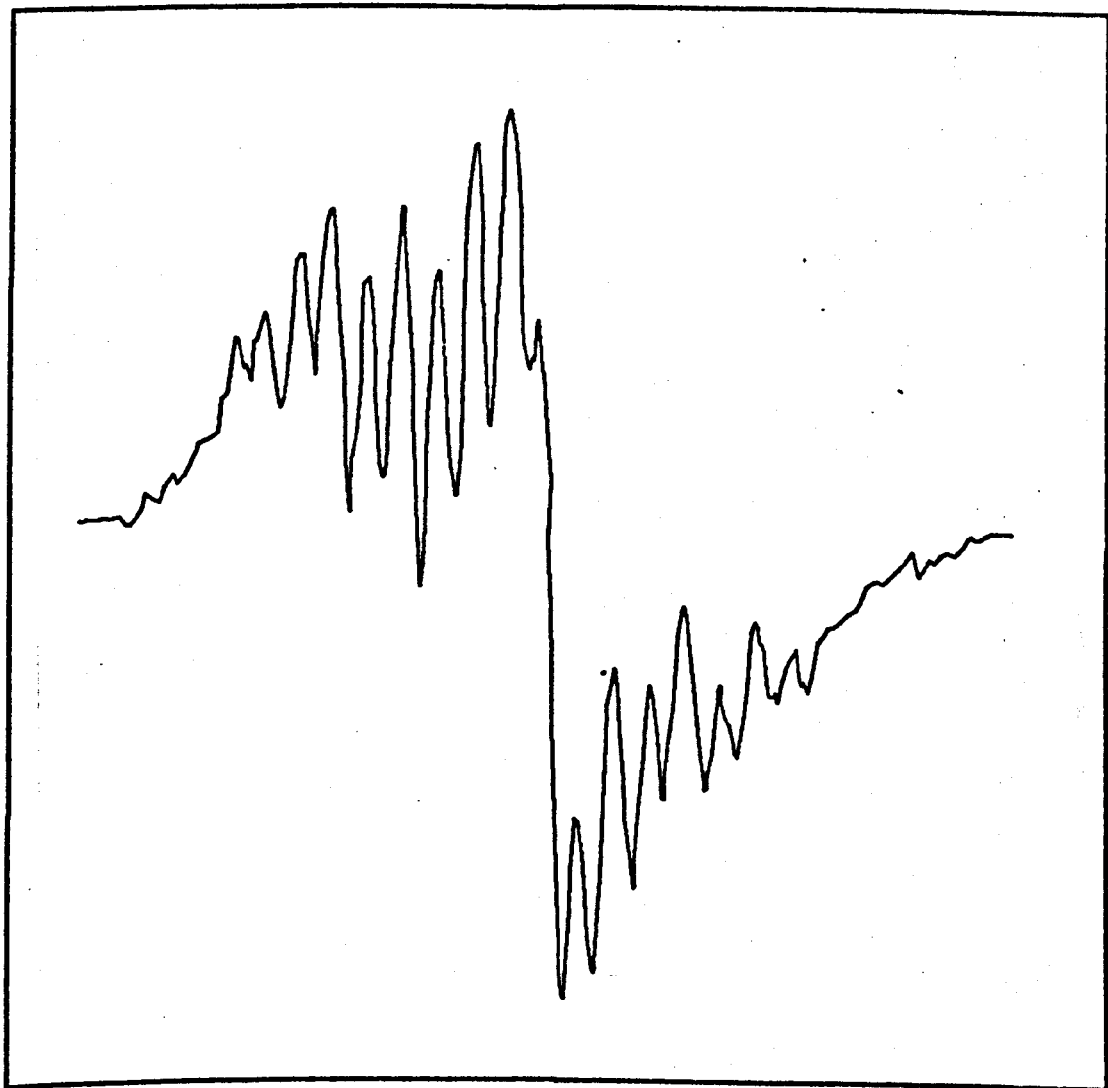
FIG. 6.8 X-BAND SPECTRUM OF A UV IRRADIATED CPZ SPECIES.

6.2. CPZ⁺ Bound to Nucleic Acids.

6.2.1. The Preparation of Solutions, Gels and Fibres of Nucleic Acid/CPZ⁺

Calf thymus DNA supplied by Sigma Chemicals Co. (Type V, Sodium Salt) was used. This is a highly polymerised type of DNA (average molecular weight 1 to 1.3 million). The material contained protein impurities and it was necessary to purify it before use. A phenol extraction method was used, which consisted of shaking equal volumes of a solution of DNA (of concentration 1 mg/ml in 0.15 M NaCl) and freshly distilled phenol (saturated in the above salt solution), for 10 mins. The solution was spun for 15 mins in a bench centrifuge (at 4000 rpm), and the aqueous phase from the top (containing the DNA) was collected. The DNA was precipitated out of the solution by $2\frac{1}{2}$ volumes of cold propanol, collected with a glass rod, washed successively in ethonal/H_2O (70:30), ethanol and acetone, and then vacuum dried.

The DNA solutions were made from the dry material. The DNA concentration in the solution was determined spectrophotometrically ($E_{260} = 6600$ mole^{-1} 1 cm^{-1}).

The synthetic double stranded polynucleotides poly I . poly C were obtained from Sigma chemicals. The phenol extraction removed no apparent impurities and the material was used without purification. Further details are given in Chapter 7.

Nucleic acid/CPZ⁺ complexes of various phosphate to drug (P/D) ratios and salt contents were made by mixing CPZ⁺ solutions (prepared as in Section 6.1.3.) and nucleic acid solutions in the appropriate proportions.

To avoid the precipitation of the material which can occur if the negatively charged phosphate groups become neutralized by the positively charged drug molecules, the CPZ⁺ solution was added gradually to the nucleic acid solution using a Pasteur pipette while agitating the container. The ionic strength was adjusted to the desired one by adding small amounts of a concentration (1M) NaCl solution.

In a typical preparation the P/D was equal to 6 at DNA concentration of 0.7 mM (total base concentration) and ionic strength 0.04 M NaCl. This salt concentration was found to be a reasonable compromise to assure the solubility of the nucleic acids (which is higher at low salt concentrations), the stability of the double helix and the ease of obtaining the gel by sedimentation (the latter two properties require higher salt concentrations).

The "gel" represents a very viscous solution, highly concentrated in the nucleic acid drug complex, free of unbound drug molecules. Two methods were used for the preparation of gels. The first one consisted in spinning the complex down from the solution, in an M.S.E. "Superspeed 70" preparative ultracentrifuge, at 40,000 rpm for about four hours at $4^{\circ}C$.

The second method employed a membrane filtration system (Amicon Diaflo). The device consisted of a container which held the solution, to which a pressure of about 2 atm was applied. The filtrant was passed through a membrane (type PM 10) in the bottom of the container, which retained the high molecular weight components. This method was quicker than the centrifugation for small quantity work and one also had the advantage of being able to stop the process when the desired consistency of the gel was achieved.

The results obtained with the DNA by using this method were comparable in all respects to those obtained by centrifugation. However, for the RNA/CPZ^{+} complexes the centrifugation method gave considerably better preparations (in the respect of the yield of free radical in the gel), probably because a considerable quantity of material is sedimented in the first few minutes of the centrifugation and thus the free radical present in that quantity is prevented from the faster decay in the solution.

The fibres were made by standard techniques (see Section 4.3.) at the temperature and the relative humidity of the laboratory.

6.2.2. The Stability of the CPZ$^+$ Bound to DNA.

When the DNA and CPZ$^+$ solutions are mixed, there is a detectable change of the colour of the solution, from the red of the free CPZ$^+$ to the red-violet of the CPZ$^+$ interacting with the DNA. Spectrophotometrically this represents a 3 n m red shift of the CPZ$^+$ maximum absorption peak (Fig. 6.4.). This effect is similar to that obtained from many dyes and drugs upon their interaction with the DNA (Ref. 3.).

As it has been already mentioned, the binding of CPZ$^+$ on to the DNA has the effect of reducing the instability of the free radical. In practice this means that one has about 3 hours available for using such a solution of the complex before the decrease in the concentration of the free radical becomes appreciable.

As can be seen from Fig. 6.5. the decay consists of a short accelerated step immediately after the preparation of the complex (probably due to the decay of the excess CPZ$^+$ which did not bind on to the DNA), followed by a slower decay of the remaining material. The process continues in the gel and fibre state but at a much slower rate, and this appears to be due either to the reduced hydration or to the restricted freedom of movement of the molecules in these states. Thus, the "half life" of the CPZ$^+$ radical in a fibre varies from a day up to a week and also depends on the treatment of the fibre (variations in the relative humidity and in the temperature have an adverse effect upon the stability).

It is estimated (see below) that only about 15-30% of the initial CPZ$^+$ in DNA/CPZ$^+$ complex is regained in the gel obtained by centrifugation, the remainder either staying in the supernatant (where it is regained as sulphoxide) or being converted to a different species in the gel (probably still sulphoxide).

The curves from Fig. 6.5. were plotted in an attempt to determine the conditions for the best stability of the radical bound on to the DNA. The
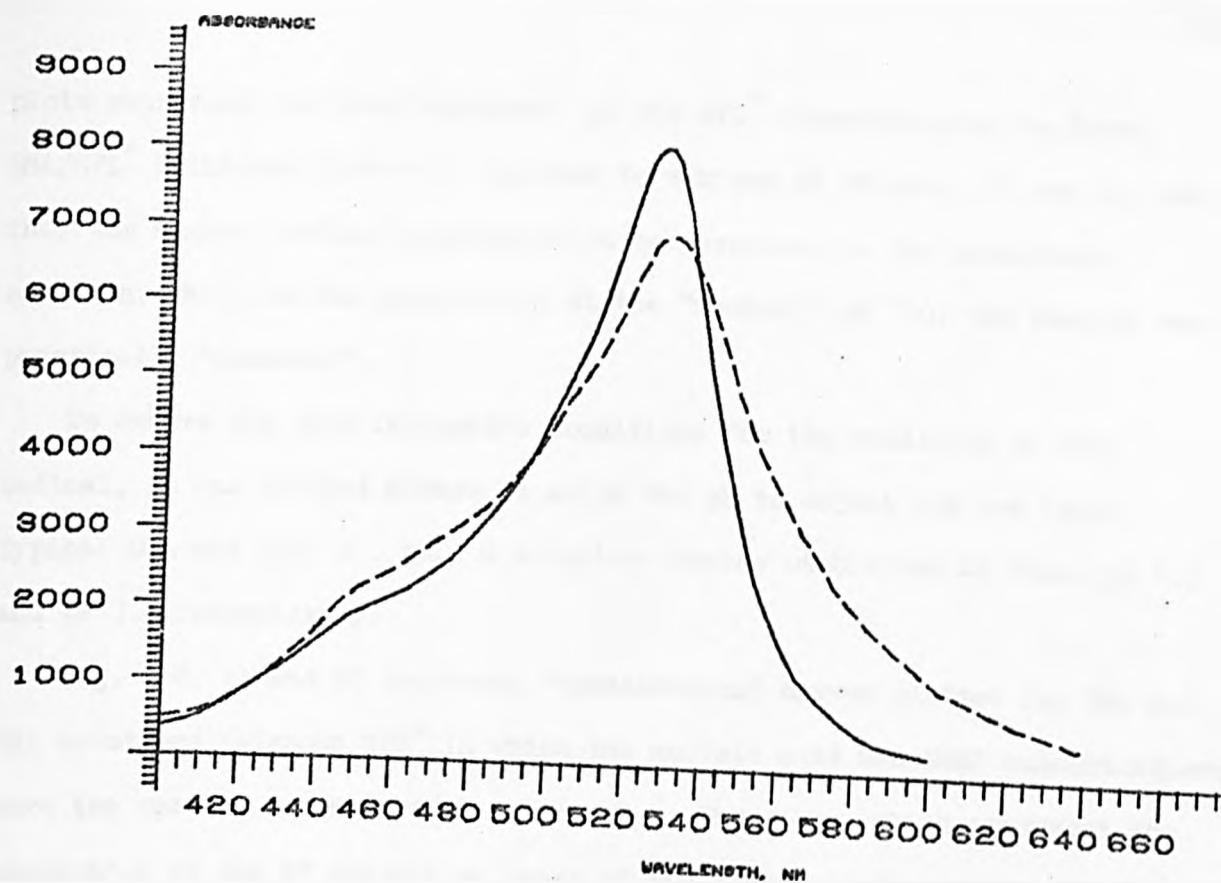
FIG. 8. 4 VIS. ABSORPTION SPECTRA OF SOLUTIONS OF CPZ$^+$ (FULL LINE) AND CPZ$^+$-DNA COMPLEX (DASHED)
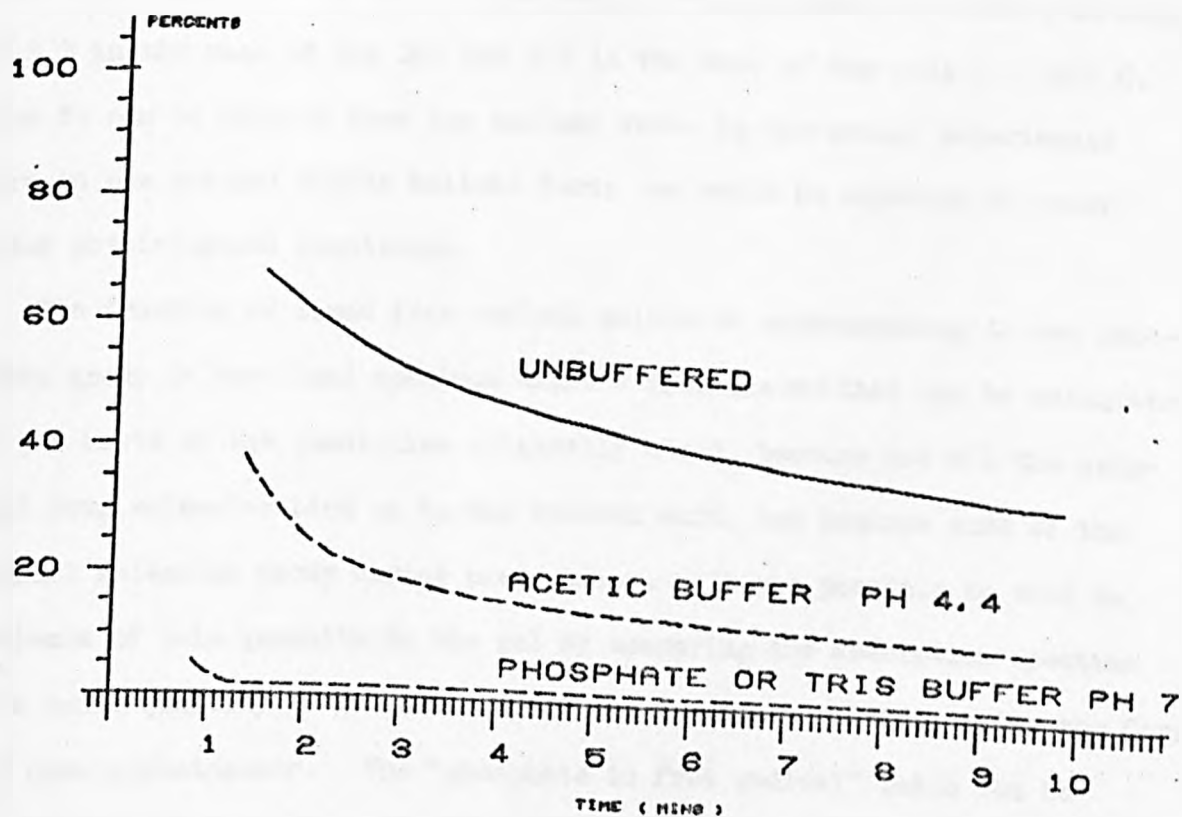
FIG. 8. 5 TIME COURSE OF THE DECAY OF THE RED COLOURED RADICAL FROM CPZ$^+$-DNA COMPLEXES (P/D=4), IN WATER AND DIFFERENT BUFFERS. ONLY THE UNBUFFERED SOLUTION PRODUCED RED COLOURED GELS.

plots represent the time dependence of the CPZ^+ concentrations in fresh DNA/CPZ^+ solutions (P/D = 1) buffered to various pH values. It can be seen that the highest radical concentration corresponded to the unbuffered solution, while in the preparation at the "neutral" pH 7.0, the radical was practically "quenched".

To ensure the most favourable conditions for the stability of the radical, it was decided always to allow the pH to adjust its own level. Typical DNA and poly I . poly C solutions become stabilized at about pH 4.3 and pH 3.8 respectively.

Fig. 6.6. (a and b) represent "denaturation" curves plotted for DNA and RNA solutions (without CPZ^+) in which the nucleic acid and NaCl concentrations were the same as in the actual complexes. The plots, which represent the absorption at the UV absorption peaks of the nucleic acids versus the pH, detect the hyperchromic effect (increase in absorption) which occurs upon the denaturation of the double helical structure (see Section 4.1.2.). Under the conditions of these experiments, the denaturation occured at about pH 3.3 in the case of the DNA and 3.8 in the case of the poly I . poly C. Thus it can be deduced that the nucleic acids in the actual experiments were in the natural double helical form; as would be expected to occur under physiological conditions.

The fraction of bound free radical molecules corresponding to one phosphate group in the final specimen differs from the one that can be calculated on the basis of the quantities originally mixed, because not all the original drug molecules bind on to the nucleic acid, and because some of the radical molecules decay during preparation. It was possible to make an estimate of this quantity in the gel by measuring the absorption spectrum of a small quantity of gel crushed between two quartz plates, using the Cary 118 spectrophotometer. The "phosphate to free radical" ratio can be calculated as the ratio of the absorptions of the UV peak (mainly due to the nucleic acid) and the visible peak (due to the CPZ^+ alone) divided by

PH DENATURATION CURVES (DNA)

(RNA)
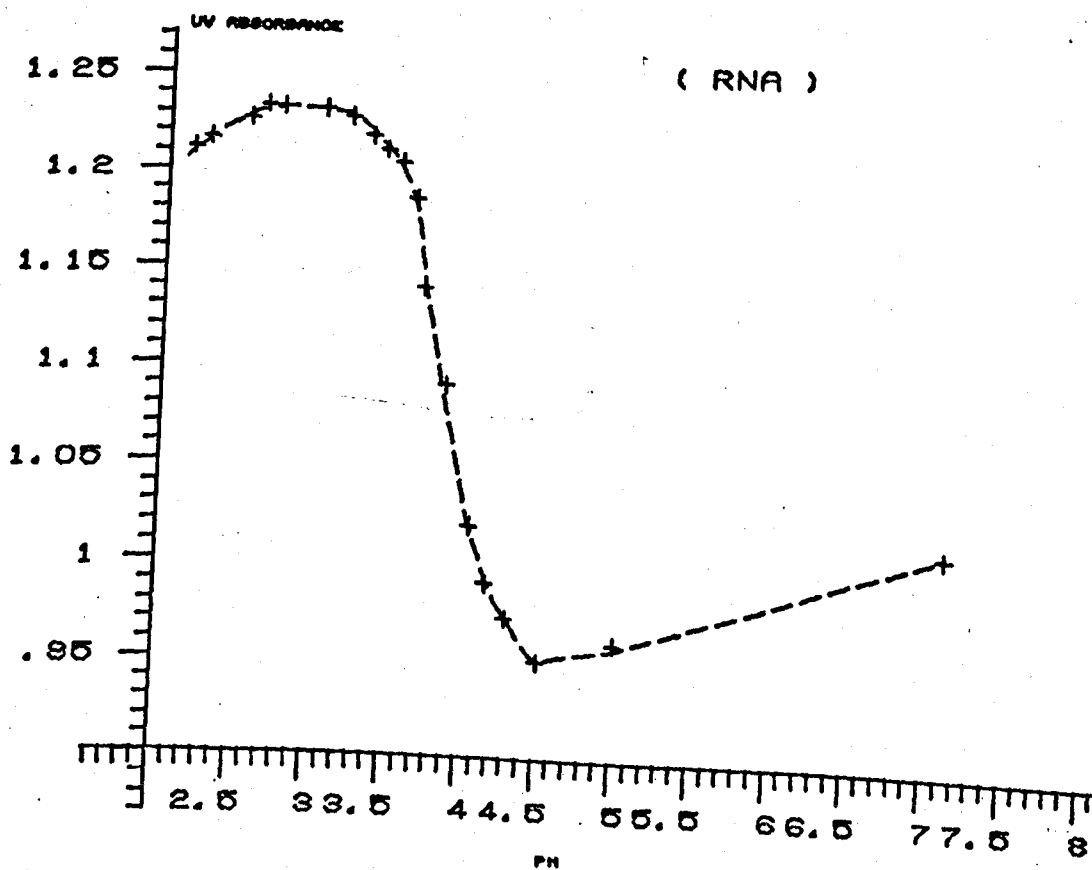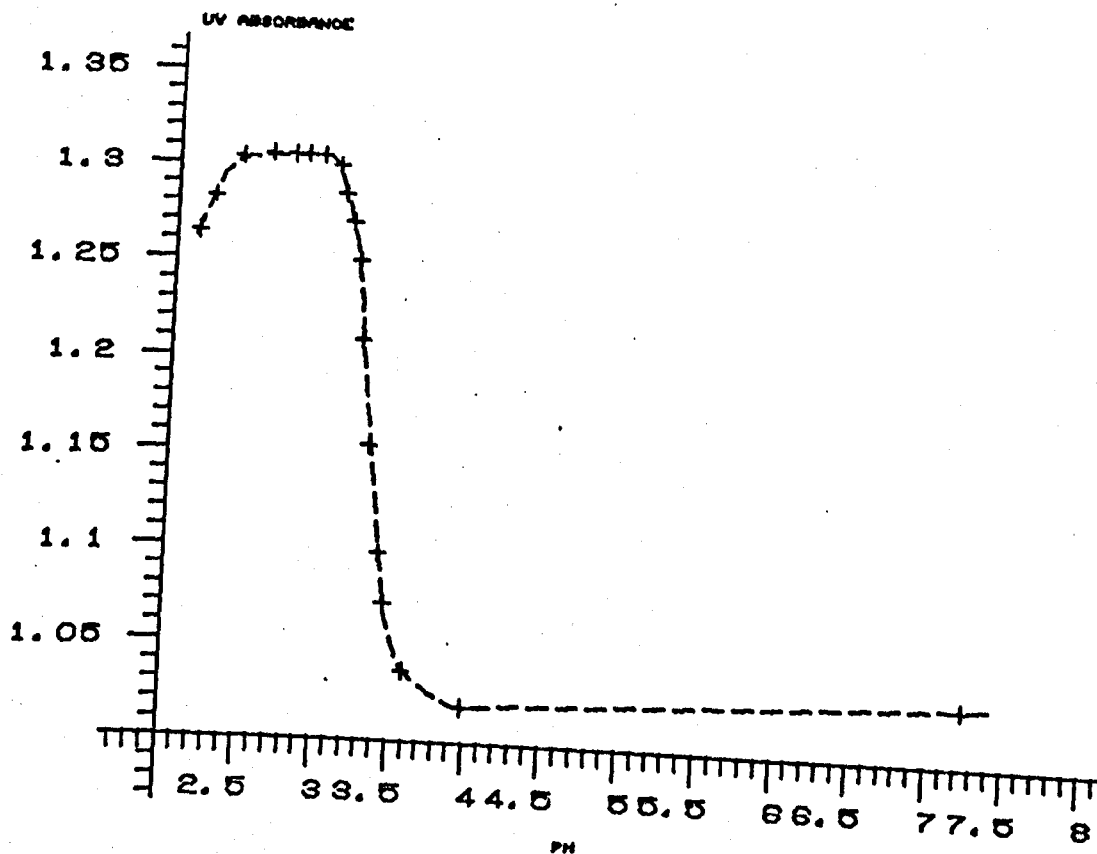
FIG. 8. 8 THE DENATURATION OF POLY I. POLY C UPON LOWERING THE PH,
AS OBSERVED BY FOLLOWING THE HYPERCHROMIC EFFECT AT THEIR U. V.
ABSORPTION PEAKS. THE CONDITIONS (NUCLEIC ACID CONCN. 2 MM IN A
0. 05 M NA CL AQUEOUS SOLUTION) WERE TYPPICAL FOR THE EXPERIMENTS
DESCRIBED IN THE TEXT.

the ratio of the corresponding extinction coefficients. The formula can be improved by taking into account the contribution of the absorptions of CPZ^+ and the sulphoxide to the UV absorption peak. This correction is necessary for low P/D ratios, but even so, the formula should be regarded as approximate, because the extinction coefficients of the bound species being unknown, one had to use those of the free species in aqueous solution:

$$(P/D)_{gel} = \frac{A_{255}}{A_{530}} \cdot \frac{E_{DNA}}{E_{530}\,(CPZ^+)} - \frac{E_{255}\,(isosb)}{E_{DNA}} \cdot (1 + \frac{[SO]}{[CPZ^+]})$$

$$= 0.83 \frac{A_{255}}{A_{530}} - 2.3\,(1 + \frac{[SO]}{[CPZ^+]})$$

In this expression, which is applicable to the DNA - CPZ^+ gels, the UV absorption is measured at 255 n m, which is an isosbestic point for the CPZ^+ radical/sulphoxide system, and is also close to the DNA maximum absorption peak. The ratio $[SO] / [CPZ^+]$ is the unknown relative proportion of chlorpromazine sulphoxide and free radical in the gel at the moment of the measurement. Tests showed that in a fresh DNA-CPZ^+ gel this ratio should be taken equal to about 2 or 3, indicating that under the conditions used, the CPZ^+ radical represented only about 25-33% of the total quantity of drug present in the gel. This total quantity was consistent with that determined by checking the UV absorption spectrum of the supernatant, and represented typically about 75% of the original amount mixed with the DNA.

It is thought that the sulphoxide from the gel resulted from the decay of some of the bound CPZ^+ radicals; decay which occured after the gel was formed. This interpretation is substantiated by the observation that the sulphoxide from a DNA-sulphoxide solution would not sediment by ultracentrifugation. A formula similar to that given above was devised for the RNA (see Section 7.1.1.).

The extent of binding depended on the type of the nucleic acid (DNA or RNA), the initial P/D ratio, the ionic strength (low P/D ratios and high ionic strengths resulting in lower levels of binding), and to a certain extent it varied from specimen to specimen. In this respect the estimates proved to be rather variable. The figures of 15-30% for the level of binding quoted above reflect the range of this variability.

6.3. ESR Spectra of the CPZ^+ Radical.

6.3.1. Experimental Methods.

The X-band and Q-band spectrometers available for the present project were based on the systems described in Section 2.5. (Fig. 2.6a, b.).

In the X-band work the specimens were placed in a Varian rectangular cavity type V-453, operating in the H_{012} mode, or a Microspin W-932 cylindrical cavity, operating in the H_{011} mode. Both were high quality factor cavities. The first one (of loaded Q about 5000) was particularly suitable for solution work, in conjunction with Varian aqueous cells (type E-248). The magnetic field was produced by a Newport Instruments electromagnet type D with 20 cm diameter pole pieces, and swept by using a Newport Instruments slow sweep unit (type A). A 10 kHz AFC system (see Section 2.5.) was used to lock the klystron frequency to the cavity. The detection system consisted of a Shottky barrier crystal, (optimum sensitivity at approximately 1 m A bias level), a low noise preamplifier (PAR type CR4) and a PAR model 120 phase sensitive detector. The 100 kHz reference signal supplied by the phase sensitive detector was fed via a power amplifier to the modulation coils mounted inside the X-band cavities.

A similar arrangement was set up for the Q-band spectrometer. The specimens were placed in a cylindrical Microspin (W-981) tunable cavity, operating in the H_{111} mode. The dielectric losses due to water restricted the use of this cavity to dry specimens (e.g. fibres).

For cooling the specimens down to liquid nitrogen temperatures ($77^{\circ}K$) a gas flow system was used. Dry oxygen-free nitrogen gas was cooled by passing it through a copper coil immersed in liquid nitrogen, and then passed through a Dewar tube in which the sample was placed. The temperature was controlled by adjusting the rate of flow.

For temperatures down to the liquid helium temperatures ($4.2^{\circ}K$) the system showed in Fig. 6.7. was used. The liquid helium was syphoned through a steel Dewar tube, provided with a needle valve. The rate of flow could be controlled by adjusting the current through a small heater, consisting of a resistor immersed in the liquid helium. This system permits obtaining temperatures below $4.2^{\circ}K$, by using the cooling effect resulting from the expansion of the gas after the needle valve (Joule-Thompson effect). The temperatures were measured with an Allen-Bradley resistor.

For temperatures higher than the ~~ambient~~ ambient, a heated gas flow system was devised. The temperature was controlled by a thermocouple, in conjunction with a temperature control unit made by Ether.

Atmospheres of various relative humidities were obtained (at room temperature) by flowing an air stream which was passed through an appropriate saturated salt solution (sodium nitrite for 66%, sodium chlorate for 75%,sodium tartrate for 92% and potassium chlorate for 98% relative humidity).

For the room temperature work the solutions and gels were placed in aqueous sample cells. For the low temperature work, quartz tubes with thick walls were used, in conjunction with the cooling systems described above. The fibres were mounted in a Varian tissue cell (for the X-band measurements), or on the bottom plate of the H_{111} cylindrical cavity (for the Q-band work),(see Section 6.4.1.).

The spectra were recorded at low modulation levels (max. 0.05 mT peak-to-peak). The maximum microwave power level used was about 25 mW, above which saturation effects occured (see Section 2.4.4.), especially at low temperatures.

TO SAMPLE AND RECOVERY

NEEDLE VALVE

SYPHON

HE

HEATER

LIQUID HELIUM COOLING SYSTEM
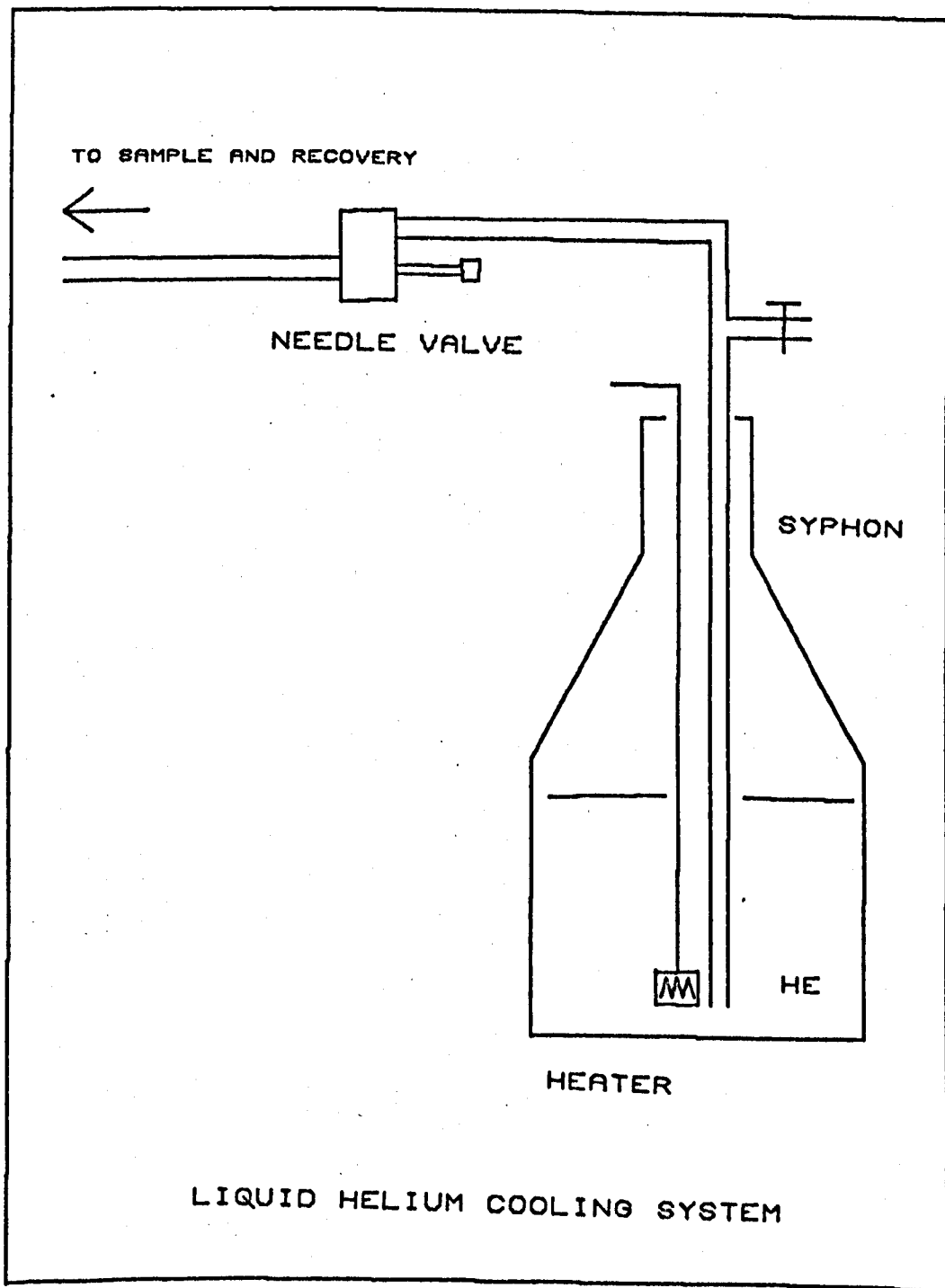
FIG. 6.7 SCHEMATIC DIAGRAM OF THE SYSTEM USED TO COOL THE SPECIMENS SPECIMENS IN THE ESR EXPERIMENTS DOWN TO THE LIQUID HELIUM TEMPERATURE.

The measurement of the hyperfine splittings and linewidths of the recorded spectra, was achieved by using a "field/Cm" calibration of the sweep, obtained by using a proton resonance magnetometer. The magnetometer (which consisted of a ~~limited~~ limiting oscillator and a low noise amplifier) was built by following the design of Robinson (Ref. 5.). The oscillator circuit was mounted in the metal case of an old Newport Instruments magnetometer, the probe head and the slow motion condenser of which were incorporated in the new system. It was also possible to obtain a calibration of the sweep in the region of the CPZ^+ signal by using the central hyperfine lines of the spectrum of a Mn^{++} doped MgO polycrystalline powder. The separation of the two central lines is 8.69 mT.

The g values were determined with reference to the DPPH marker, using the above calibration. The klystron frequency was measured by using a Hewlett Packard counter with a transfer oscillator unit. The accuracy of this method was satisfactory, the greatest source of errors being the broadness of the lineshapes. The measurements quoted in the thesis were reproduceable within 0.04 mT.

In order to enhance the sensitivity of detection, signal averaging equipment was fitted to both the X and Q-band spectrometers. The system is represented schematically in Fig. 6.8. The central part was a Nuclear Measurements (type 546C) computer/averager of transients, which permitted the accumulation of the spectra from recurrent sweeps. The triggering impulse for each sweep was provided by the signal from the proton resonance magnetometer, set to resonate at a predetermined position. The interphase for the triggering system consisted of a phase sensitive detector and a Schmitt trigger (constructed according to the circuit shown in Fig. 6.8.). The phase sensitive detection of the proton resonance signal was performed at the frequency of 1 kHz, the modulation current being fed to a pair of Helmholtz coils (3 Cm diameter) attached to the proton resonance probe.
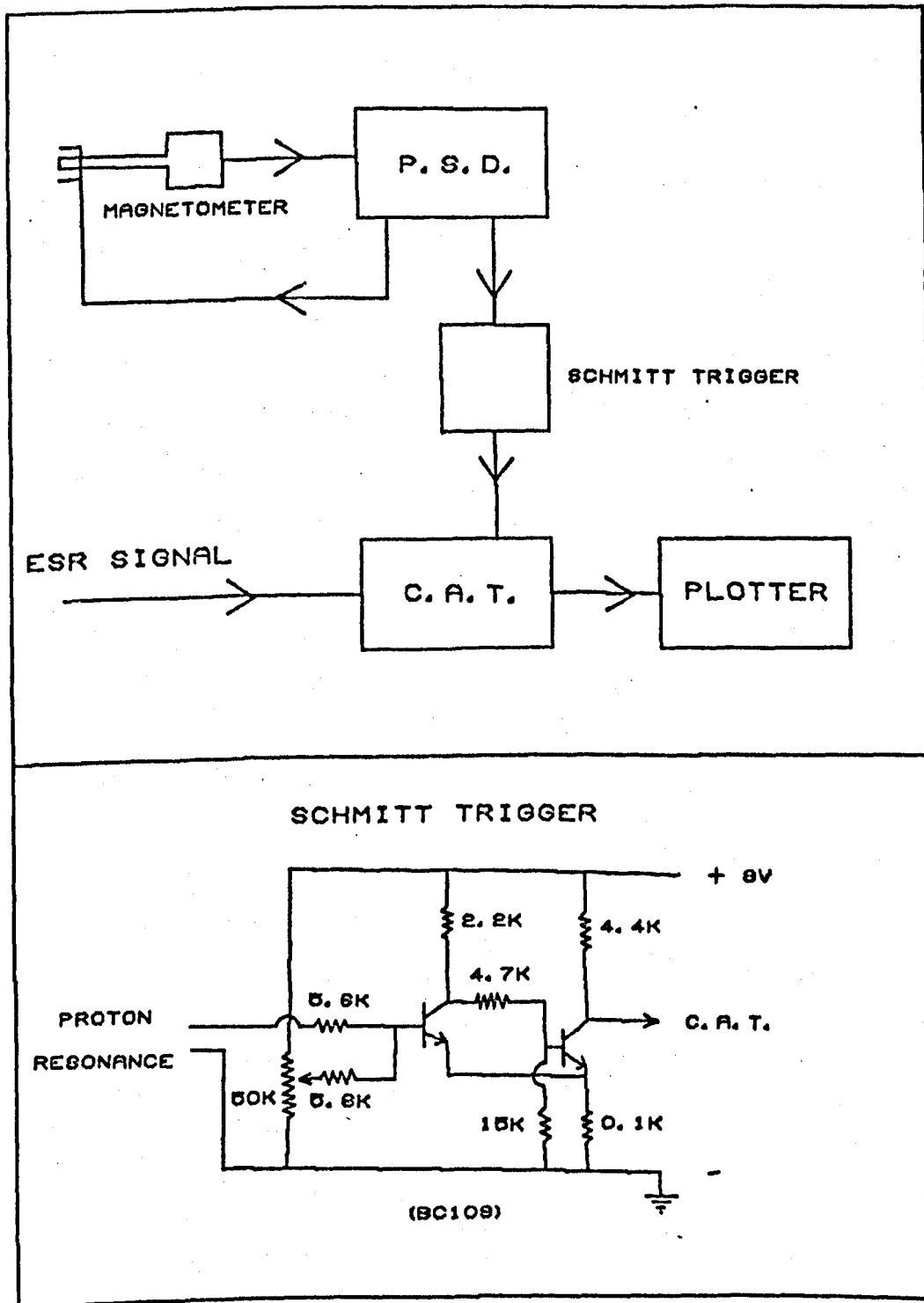
FIG. 6. 8 BLOCK DIAGRAM OF THE SIGNAL AVERAGING SYSTEM.
BELOW: THE SCHMITT TRIGER CIRCUIT, INCORPORATED IN THE ABOVE SYSTEM.

81.

6.3.2. ESR Spectra of CPZ^+ and CPZ^+-DNA Complexes in Disordered Environments.

A common feature of the ESR spectra which are going to be described in this section is that they correspond to samples in which the radical molecules are randomly oriented (either rapidly tumbling in solution or immobilized). These include ESR spectra from solutions of CPZ^+ at various temperatures as well as "gel" spectra (from DNA/CPZ^+ gels). The fibres, in which the radical molecules assume a preferential orientation, will form the object of a subsequent section.

Fig. 6.9. shows the ESR spectrum of a CPZ^+ solution at the room temperature. Such spectra were obtained from CPZ^+ solutions in water or H_2SO_4, at CPZ^+ concentrations below about 2.5×10^{-2} M and at temperatures greater or equal to the room temperature. The same spectra are observed at all temperatures up to $100^\circ C$. About 16 equidistant hyperfine peaks are resolved, apparently superimposed on to a major line (see also 6.3.5.). The g value at the centre of the pattern and the hyperfine splitting are indicated in the figure.

The transition from a "solution" to an "immobilized" type of spectrum upon the freezing of the specimen can be followed from Fig. 6.10 (a to e), which represents the ESR spectra of a viscous CPZ^+/H_2SO_4 solution run at progressively lower temperatures, in the range $0^\circ C$ to $-73^\circ C$ ($200^\circ K$).

The spectra from Fig. 6.10. exhibit a "triplet" feature which can be assigned to the hyperfine interaction with the ring ^{14}N atom of the CPZ^+ radical, as originally suggested by Ohnishi and McConnell (Ref. 4.). This assignment is entirely consistent with the results obtained from the CPZ^+ radicals oriented in fibres (see Section 6.4.), where the spectra ranged from a clear three line spectrum (when the magnetic field was parallel to the fibre axis) to a single broad line (when the field was perpendicular to the fibre). A detailed discussion of this variation will be given in Section 6.4. Here it is sufficient to mention that this is as would be
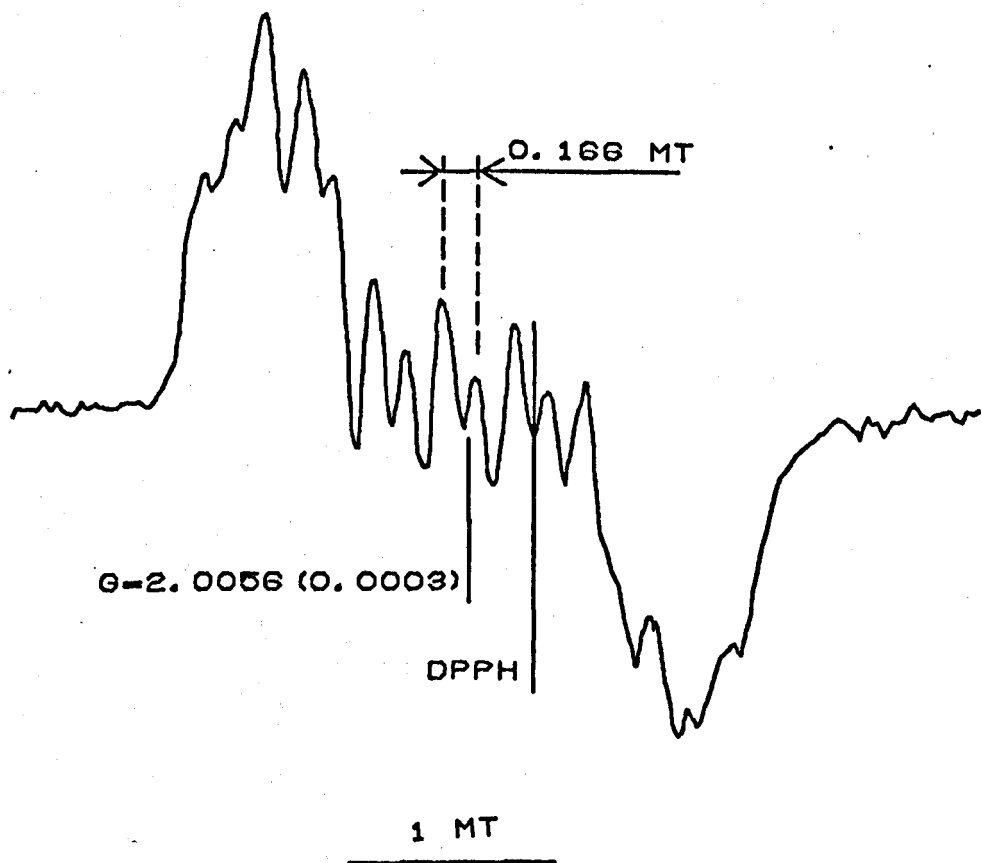
FIG. 6. 9 THE X-BAND ESR SPECTRUM OF A CPZ⁺ SOLUTION IN 82%
SULPHURIC ACID, AT ROOM TEMPERATURE (CPZ⁺ CONCN. 10 MM).
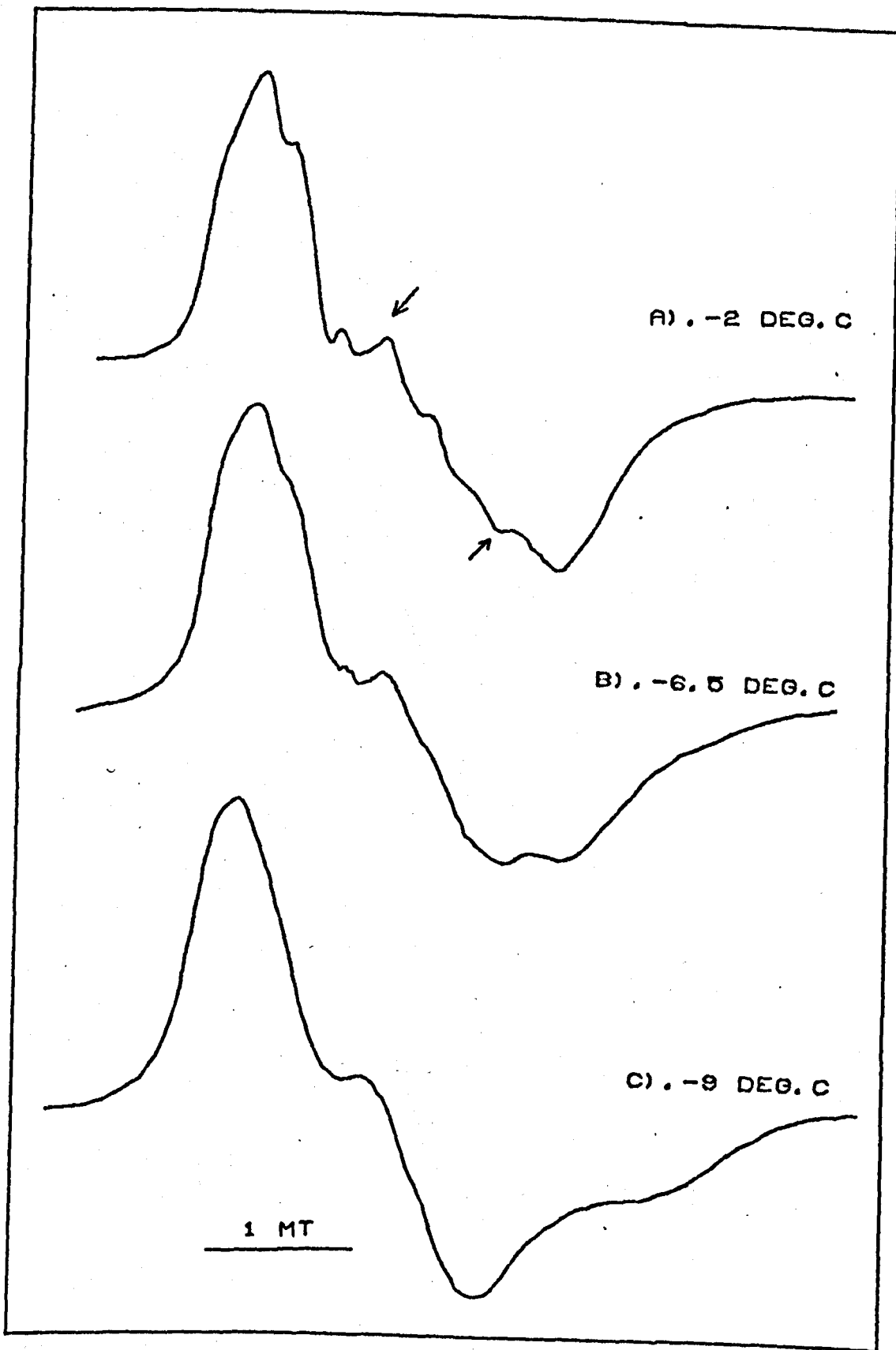
FIG. 8. 10 X-BAND SPECTRA OF A CPZ$^+$ SOLUTION, RECORDED AT
PROGRESSIVELY LOWER TEMPERATURES. (CONTINUED ON NEXT PAGE).

D). -20 DEG C

E). 200 K

1 MT
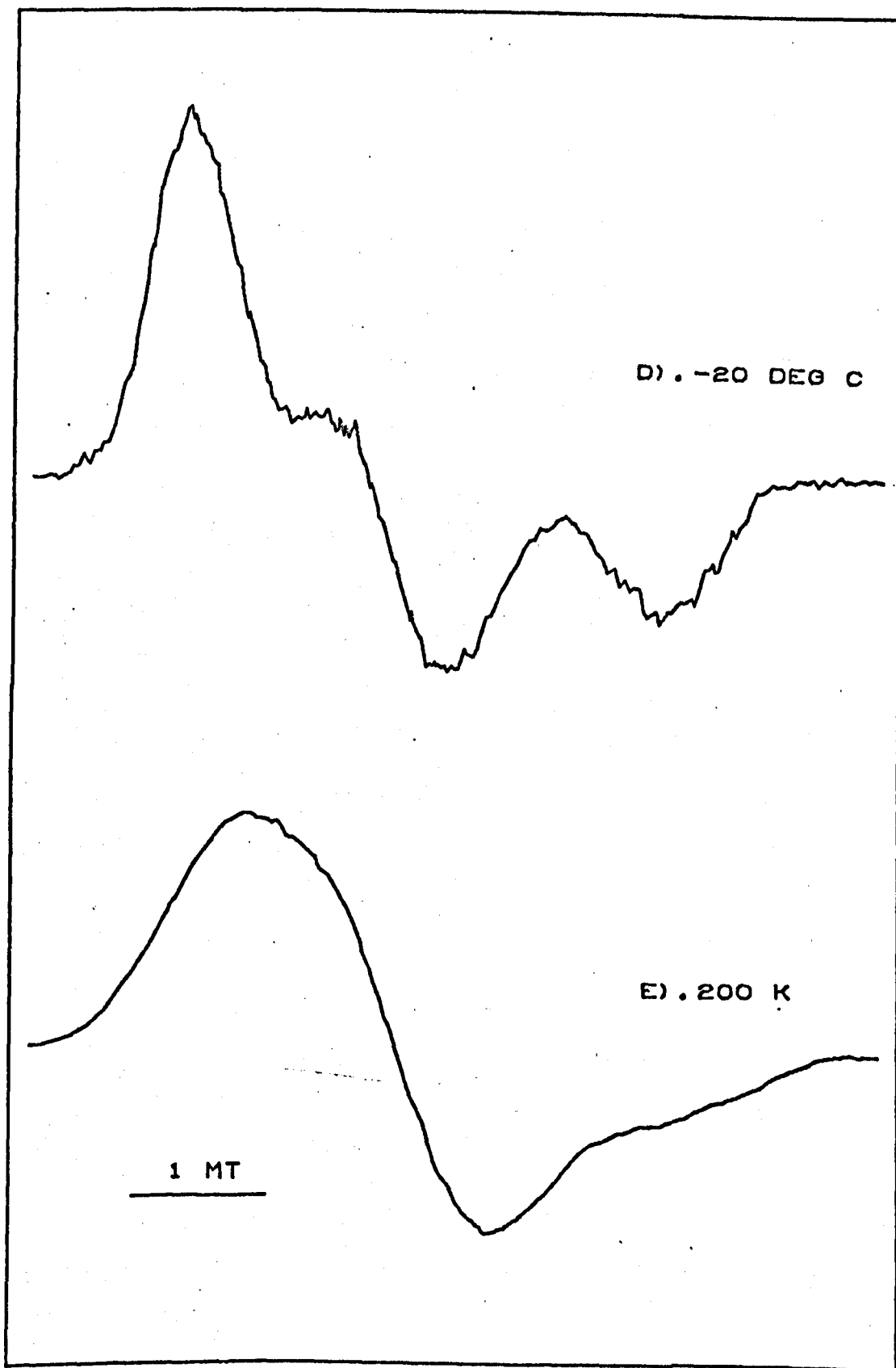
FIG. 6. 10 (D) - (E).

expected if the unpaired spin was localized mainly in the p orbital of the ^{14}N atom of the CPZ^+ and the magnetic field in the two cases above was parallel and respectively perpendicular to the axis of the p orbital (see also Section 2.3.5.).

The anisotropic and isotropic CPZ^+ spectra can thus be interpreted in terms of a radical in which the unpaired spin density is mainly associated with the ^{14}N atom but in which there is also a considerable delocalization of the electron cloud over the rest of the molecule. The numerous proton contributions which are responsible for the complex isotropic hyperfine structure are not apparent in the anisotropic spectra (i.e. of frozen solutions, gels and fibres). The lineshapes in the latter case represent envelopes over unresolved proton splittings.

By observing the spectra from Figs. 6.9. and 6.10. in succession one can follow the stages of the transition from the situation (in Fig. 6.9.) in which the anisotropic terms and the local dipolar fields are averaged to zero due to the rapid molecular motions (Section 2.4.3.) to a situation in which the radicals are practically immobilized. The first anisotropic features to appear are those associated with the ^{14}N hyperfine anisotropy (the two shoulders marked in Fig. 6.10a. correspond to the "kink" and the negative peak of the fully immobilized spectrum), consistent with this being the largest anisotropic component in the system. At the same time the isotropic hyperfine pattern disappears. The dipolar broadening, the next largest anisotropic interaction, becomes apparent as the temperature is lowered (Fig. 6.10b - e) and it continues to operate even below $-20^{\circ}C$ at which point the ^{14}N anisotropic features can be considered to be completely resolved. (This is seen from the fact that below that temperature the peaks no longer change their position.) In fact a transition towards a very broad, feature-less spectrum, takes place around $200^{\circ}K$ (Fig. 6.10e), illustrating a further restriction in the molecular motion.

Two ESR spectra of DNA/CPZ$^+$ complexes, both of "immobilized" type were obtained from DNA/CPZ$^+$ complexes.

The first one (Fig. 6.11.) was obtained from a DNA/CPZ$^+$ gel at room temperature. It shows a well resolved spectrum, similar to that of the frozen CPZ$^+$/H$_2$SO$_4$ solution at -20°C (Fig. 6.10d). The gel spectrum suffers a transition towards a broad, featureless signal upon cooling similar to the CPZ$^+$/H$_2$SO$_4$ specimen, except that this transition takes place as soon as the temperature is lowered below about +9 or +10°C (Fig. 6.12.).

The second spectrum was obtained from a solution of a DNA/CPZ$^+$ complex at the room temperature (Fig. 6.13.) and exhibits several features consistent with an "immobilized" radical.

The ESR signals shown in Figs.6.11 - 13. were obtained from CPZ$^+$ radicals that are bound on to the DNA. It is unlikely that in any of the two cases (gel and solution) unbound radicals were present along with the bound ones. In the case of the gel this is because only the bound species sediments with the DNA during the centrifugation while the unbound species remains in the supernatant and in the case of the solution it is because the unbound radicals decay very fast so that only those which are stabilized by binding on to the DNA remain (see Section 6.2.2.). Thus the immobilization revealed by the ESR spectra in these two cases can be attributed to the binding of the small radical molecule on to the large and less mobile DNA molecule and not to a simple viscosity effect.

6.3.3. Fitting the ^{14}N Principal Tensor Values by Computer Simulation
of the "Gel" Spectrum.

The principal g and A tensor values of the ^{14}N atom (I = 1) of CPZ$^+$ were determined by computer simulation of the DNA/CPZ$^+$ gel spectrum (Fig. 6.11.). This particular specimen was selected because it gave one of the best resolved "immobilized" ESR spectra and also because the gel conditions were directly

ESR SPECTRUM (X-BAND) OF A DNA-CPZ GEL
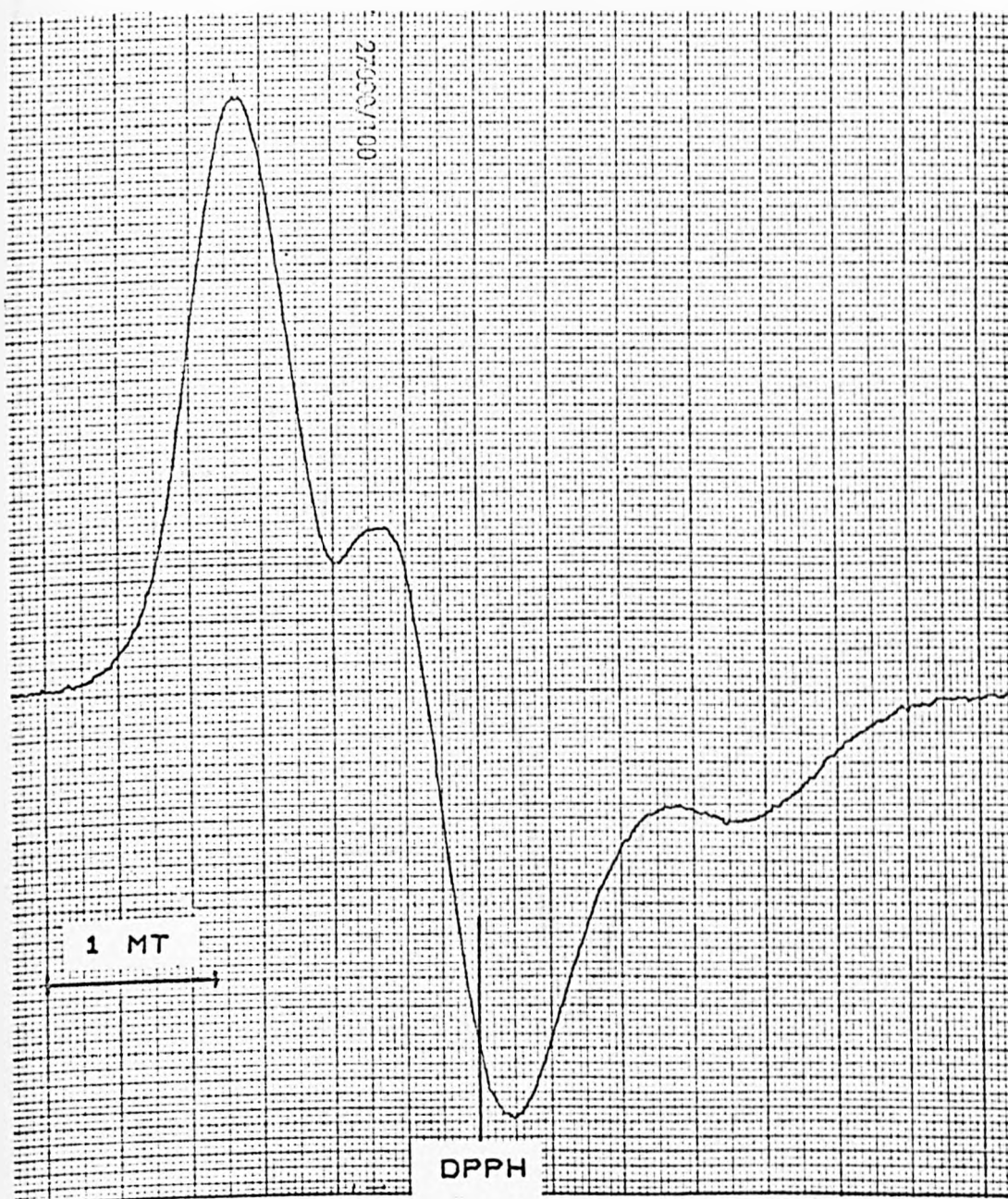
FIG. 6. 11 EXPERIMENTAL X-BAND SPECTRUM (9. 5 GHZ) OF A DNA-CPZ$^+$
GEL, RECORDED AT ROOM TEMPERATURE.
(THE THEORETICAL SPECTRUM IS SHOWN IN FIG. 6. 14).
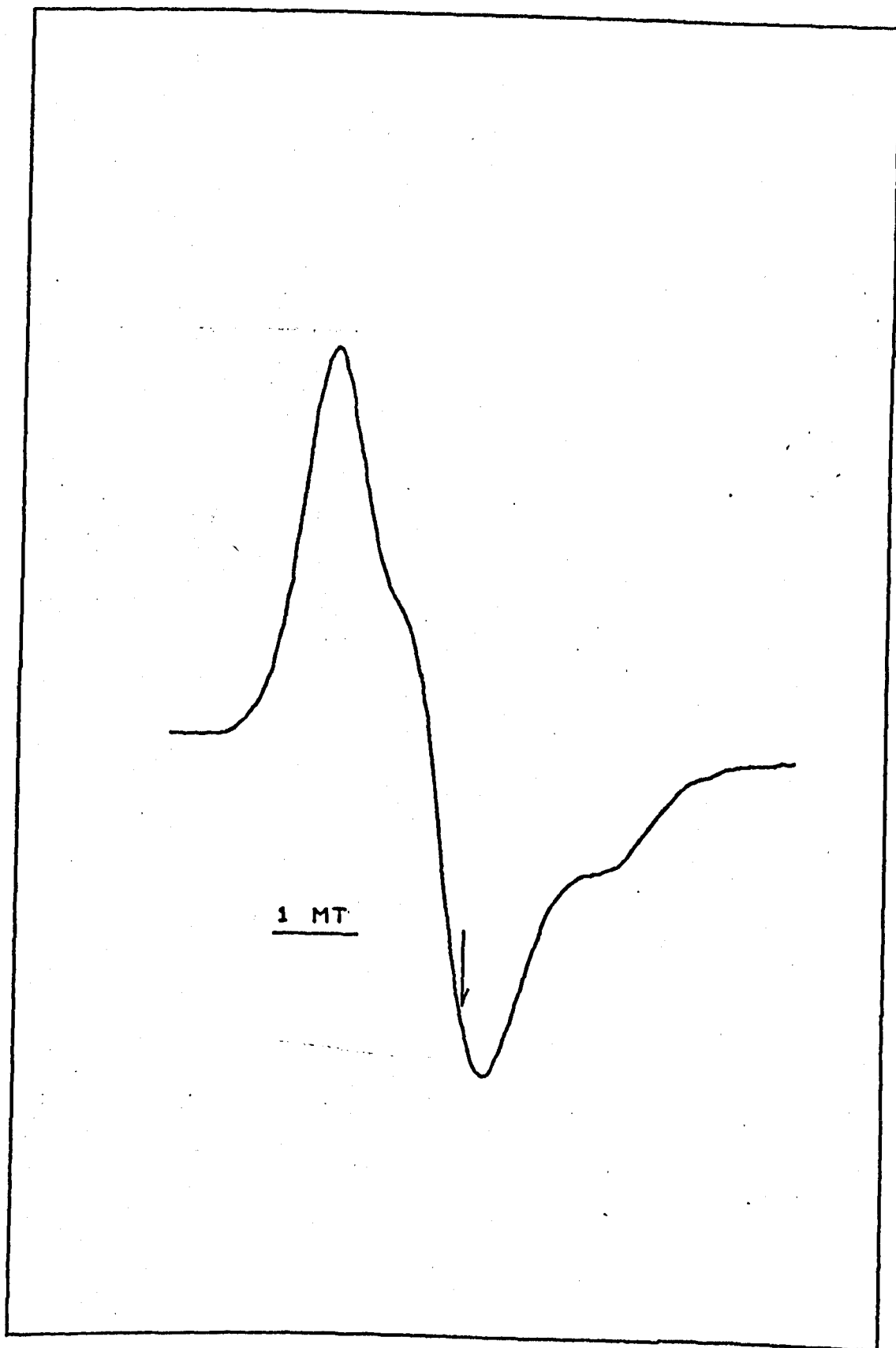
FIG. 6. 12 EXPERIMENTAL X-BAND SPECTRUM OF A DNA-CPZ$^+$ GEL, RECORDED AT 4°C.
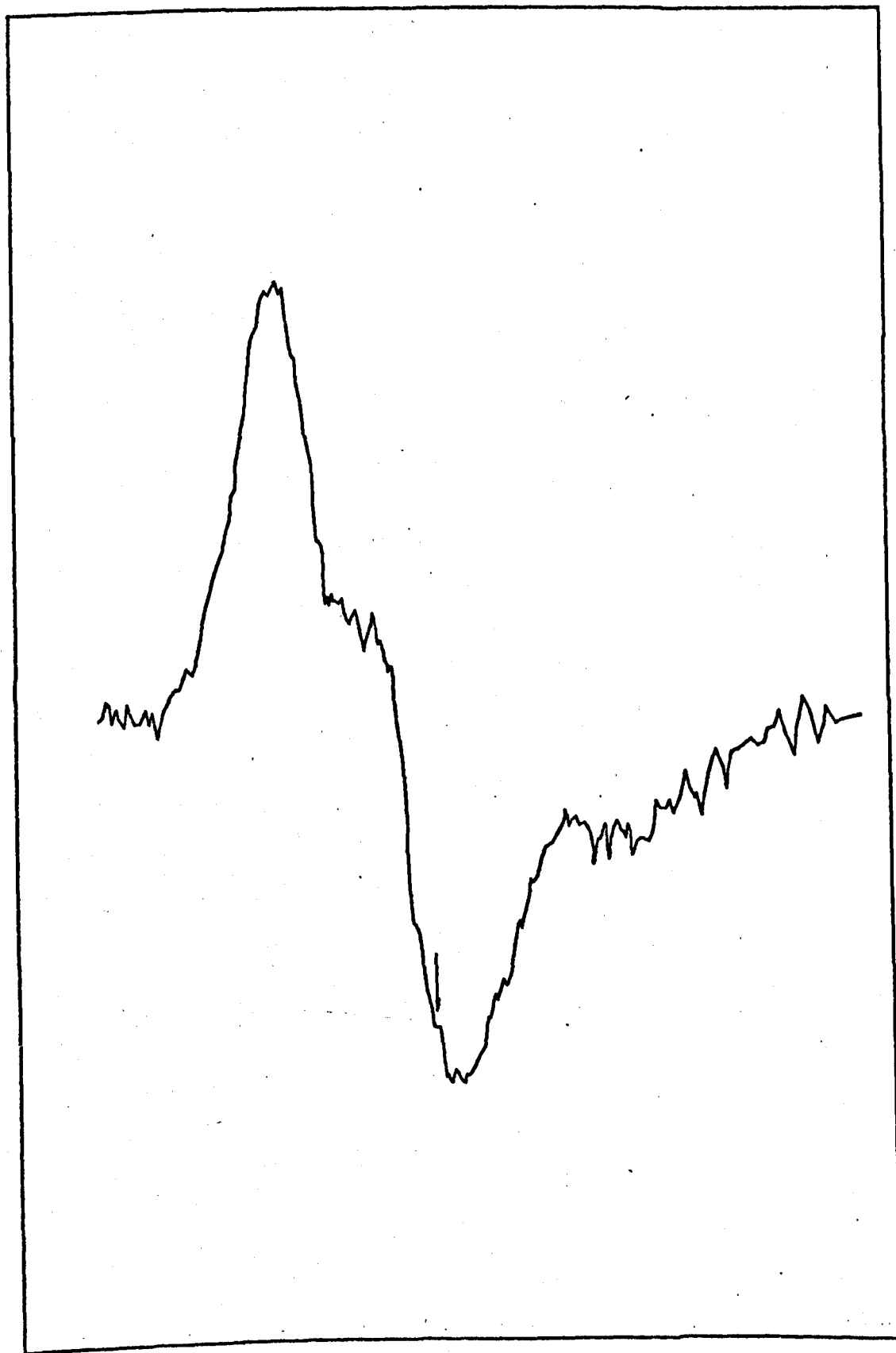
FIG. 8. 13 THE ROOM TEMPERATURE X-BAND SPECTRUM OF A DNA-CPZ$^+$
SOLUTION (P/D=8), RECORDED 80 MINS AFTER PREPARATION.

relevant to the DNA/CPZ$^+$ system of interest, as opposed to a CPZ$^+$ system in the absence of DNA.

The "gel" gave a "powder" type of spectrum. This system of random orientations was preferred for the computer simulation to the "fibres", because of the fewer parameters involved: it is necessary to fit only the principal tensor values and the linewidth, whereas for the "fibres" one also has to assume a particular model of the fibre (see Section 6.4.3.). The parameters which were obtained at the end of this work fit in a satisfactory manner the ESR spectra presented in the previous section as well as the X and Q band ESR spectra of the fibres.

The main simplifying assumptions were: 1) The g and A tensors were axially symmetric, i.e. $g_{xx} = g_{yy} = g_\perp$, $A_{xx} = A_{yy} = A_\perp$, and g_{zz} was set equal to $g_{||}$ and $A_{zz} = A_{||}$. 2) The directions of the principal axes of the g and A tensors coincided.

Three of the necessary parameters could be estimated from the "fibre" spectra (Section 6.4.3.). These were $g_{||}$, $g_\perp$ and $A_{||}$. The trial parameters were fed into the computer program set for "powder" type of simulations and made to vary within specified ranges. The effect of the various changes in the parameters was appreciated by the visual examination of the computer generated plots. It was realized at an early stage that Gaussian lineshapes, which rose sharply and didn't have the extended "wings" of the Lorentzian lineshapes reproduced the experimental lineshapes more accurately. The fitting of the spectral parameters proceeded by trial and error until a good fit to the experimental spectrum was obtained. This was achieved by the following set of parameters and a Gaussian lineshape:

$$g_{||} = 2.0025 \pm 0.0002$$
$$g_\perp = 2.0069 \pm 0.0002$$
$$| A_{||} | = 1.63 \pm 0.03 \text{ mT}$$
$$| A_\perp | = 0.35 \pm 0.05 \text{ mT}$$

MAGNETIC CHARACTERISTICS OF THE CPZ$^+$ RADICAL
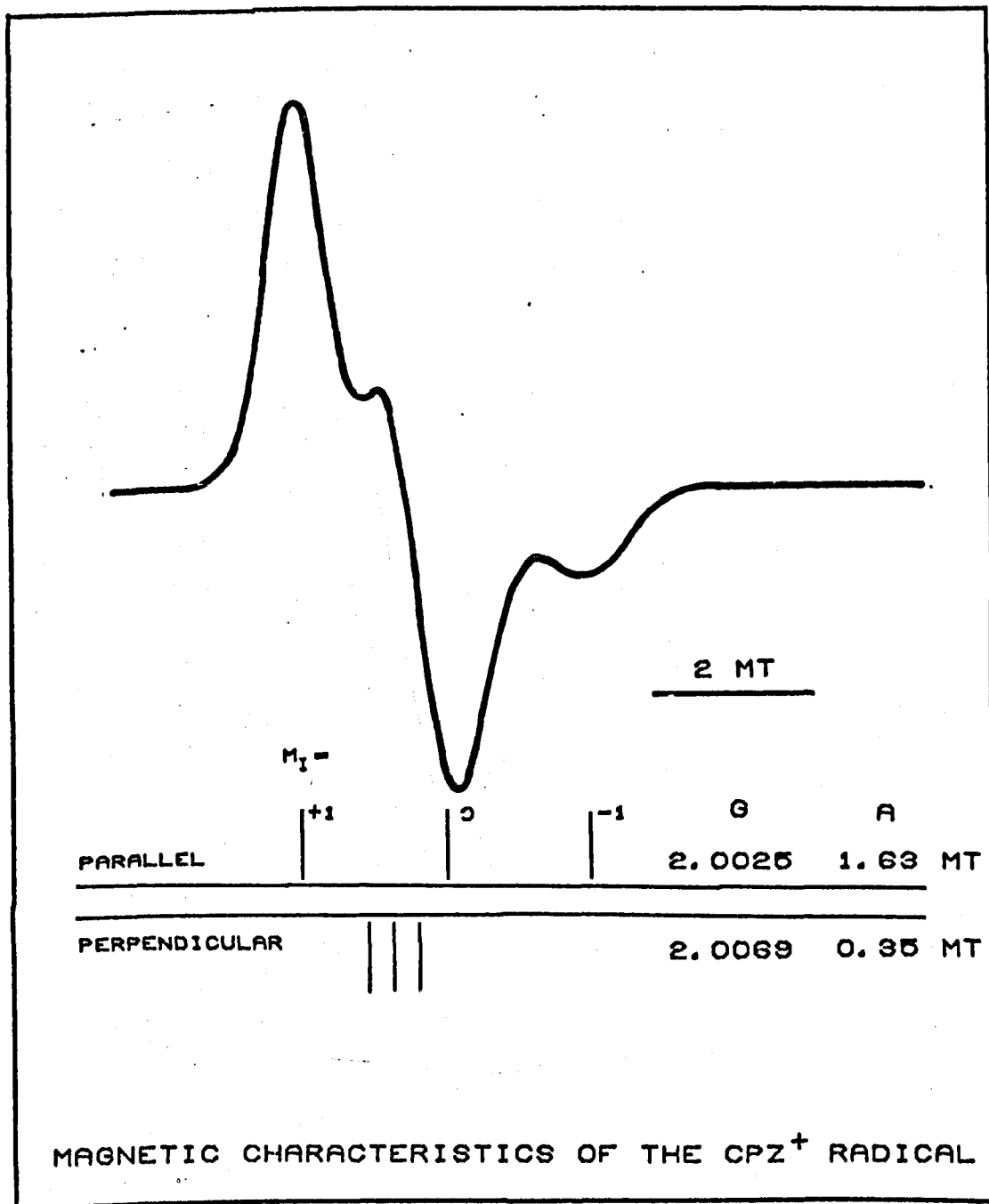
FIG. 8.14 THEORETICAL SIMULATION OF THE X-BAND SPECTRUM OF A DNA-CPZ$^+$ GEL, INDICATING THE PRINCIPAL TENSOR VALUES AND THE CORRESPONDING POSITIONS OF THE HYPERFINE LINES.
(GAUSSIAN LINESHAPE, THE WIDTH OF THE THREE LINES=0.8, 0.8, 0.85 MT).

The fit was improved if one introduced a differential broadening of the three hyperfine components so that the line which occurs at the highest field (see Fig. 6.14.) is broader than the other two.

$$\Delta B_{+1} = 0.8 \text{ mT}, \qquad \Delta B_{0} = 0.8 \text{ mT}, \qquad \Delta B_{-1} = 0.95 \text{ mT} \qquad (2)$$

This feature had to be introduced in order to make it possible to reproduce simultaneously the $g_{||}$ and $g_{\perp}$ regions of the spectrum with the same set of parameters and the significance of this assignment will be discussed below.

Fig. 6.14. shows the simulation of the spectrum of the DNA/CPZ^{+} gel from Fig. 6.12. obtained using the parameters given above. The polar angle θ (see Section 5.4.) was varied in steps of 2° while the angle ϕ was automatically kept constant as the g and A tensors were axial. A further reduction of the angular steps did not result in changes in the lineshape. The detailed shape of the simulated spectrum from Fig. 6.14., particularly the "kink" in the central region and the ratio of the heights of the positive and negative peaks, proved to be very sensitive to any deviations from the above set of parameters. The X and Q-band spectra of a disoriented collection of crushed fibres, which are also "powder" type of spectra, could be simulated using the same set of parameters, except that the linewidth in the latter case was larger by about 10%.

The calculations were carried out within the "intermediate" field approximation (Section 2.2.). It was checked that when the most general formulae for the anisotropic g value and hyperfine splitting were used (Section 2.3.4.), the corrections introduced were negligibly small (for example the g value for a particular orientation would suffer a correction in its sixth decimal position).

The unequal linewidth of the three hyperfine components may originate from one, or possibly both of the following causes: One possibility is an inhomogeneous broadening of the three hyperfine lines by the mechanism

presented in Section 2.4.3., which is consistent with the fact that the gel represents a state in which molecular motions still exist (see 6.3.2.). The second possibility arises from small deviations from the axial symmetry of the g and A tensors. Indeed, the m_s = +1 and 0 hyperfine lines (see Fig. 6.14) contribute mainly to the intensity in the $g_\perp$ region of the spectrum so that the apparent broadening of that region is dependent on the values of $g_\perp$ and $A_\perp$. A practical demonstration of this effect was difficult to achieve because of the large number of variables needing to be adjusted, which increased the complexity of the problem.

The good fit to the experimental spectrum provided on the basis of assuming the axial symmetry of the g and A tensors shows that the model is essentially correct and that the adjustments proposed should necessarily be small. They would probably not be greater than the variations in the parameters corresponding to different preparations (differing, for example, in the consistency of the gel). Such variations, which can be assigned to differences in the local polarity of the environment related to the availability of water were small and were normally neglected. The errors quoted with the parameters above correspond to the ranges within which most of the spectra (both of gels and fibres) can be accounted for. It is felt that a more accurate answer to the problem of axial symmetry could only be obtained from single crystal studies (see Section 2.3.5.).

6.3.4. Discussion.

The principal values of the hyperfine tensor ($A_\parallel$ and $A_\perp$) were determined in the previous section only in absolute value. There are essentially two choices to make: in the first case $A_\parallel$ and $A_\perp$ have both the same sign, say positive; in the second case they have opposite signs, with, say $A_\parallel$ positive. A further two possibilities would be the above two cases with the signs changed.

Considering the first case and applying the formula (20) from Section 2.3.4, one obtains the following set of parameters:

$$t_{||} = +8.5 \text{ Gauss} \quad (1 \text{ Gauss} = 10^4 \text{ Tesla})$$

$$t_{\perp} = -4.3 \quad "$$

$$a = +7.8 \quad "$$

which has the remarkable properties (see below) that $t_{||} \approx -2t_{\perp}$, with $t > 0$ and $a > 0$.

In the second case, one obtains a different set of parameters:

$$t_{||} = +13.2 \text{ Gauss}$$

$$t_{\perp} = -6.6 \quad "$$

$$a = +3.1 \quad "$$

which coincidentally has identical properties to the previous set.

These three properties, together with the axial symmetry of the hyperfine and g tensors (all deduced experimentally) reproduce the necessary conditions stated in the Sections 2.3.3. and 2.3.5. for the localization of the unpaired electron in a ^{14}N $2p$ orbital and represent a beautiful confirmation of the assignment of the unpaired spin density mainly to the ring ^{14}N atom of CPZ^+ made in Section 6.3.2.

The alternative choice of signs can be disregarded as there is no physical interpretation that could justify such a set of parameters. One is thus left with the problem of deciding which of the two cases above corresponds to the real situation, i.e. which is the relative sign of the hyperfine tensor components $A_{||}$ and $A_{\perp}$.

The solution could be obtained experimentally by studying the second order effects on the anisotropic ESR and ENDOR spectra (Ref. 6., p 102), but such a study would require perfectly oriented specimens (magnetically diluted CPZ^+ single crystals), which are not available.

The question could also be answered if the ^{14}N isotropic hyperfine coupling constant was known from the CPZ^+ solution spectrum, but this

information is not available either. However, a comparison with other radical species is very useful at this stage. One observation arising from such a comparison is that in the case of the $^{13}C_\pi$ -electron hyperfine interactions the anisotropic hyperfine splitting parallel to the p orbital $(A_{||})$ is usually approximately equal to twice the isotropic splitting a (Ref. 4.), and this is also found to be true in the case of the nitroxides (Ref. 7; see also Fig. 2.5.). On the basis of such considerations one can see that the first case above, with a = 7.8 ($\pm$0.4) Gauss and $A_{||}$ = 16.3 Gauss, closely conforms to the empirical rule and thus it represents the preferred choice. This value of the ^{14}N isotropic coupling constant is also close to the values of 6.52 and 7.06 Gauss corresponding respectively to the Phenothiazine cation radical and Phenothiazine neutral radical (Ref. 8.). The average of the principal tensor values (g = 2.0054 $\pm$0.0002) is close to the experimental g value measured on the isotropic hyperfine spectra of the CPZ^+ in solution (2.0056 $\pm$ 0.0003), and also the relative magnitude of the g values ($g_{||} \approx g_{free\ electron}$ and $g_\perp > g_{free}$) is consistent with the theory of the aromatic π radicals (Ref. 9.).

6.3.5. Interpretation of the Isotropic Hyperfine Spectrum of CPZ^+.

No analysis of the CPZ^+ isotropic hyperfine structure is available from the literature although ESR spectra of CPZ^+ have been published. These spectra refer to CPZ^+ radicals obtained under a variety of conditions: by chemical oxidation (Refs. 1, 10, 11.), by electrolytical generation (Refs. 1, 12.), on acid columns (Refs. 1, 10, 11.), or by enzymic oxidation (Ref. 13.)

The discussion above showed that the ring ^{14}N atom is expected to contribute to the isotropic hyperfine pattern with a major splitting. The assessment of the contributions due to the other atoms of the radical is not possible at this stage but it is likely that both the ring protons and the side chain will be involved. Such considerations are borne out by

comparisons between the ESR spectra of various Phenothiazine derivatives.

The first example concerns Phenothiazine itself, which has no sidechain. A convincing assignment of the hyperfine splittings to the various positions in the Phenothiazine molecule, confirmed by Molecular Orbital Theory calculations and by spectral simulations has been given by Piette and Forrest (Ref. 8.). Hyperfine splittings have been assigned to all the protons of the ring, some of which make substantial contributions (up to 3.67 Gauss splittings).

A second example shows that changes in the sidechain do affect the hyperfine structure. Promazine$^+$ is a radical similar to CPZ$^+$ except that it lacks the Cl substituent. Its "immobilized" spectrum (Ref. 11.) exhibits a triplet feature similar to that of CPZ$^+$; however, there is another derivative, Promethazine, which is similar to Promazine except that it has a CH$_3$ branch in the sidechain (Fig. 4.1.). The "immobilized" spectrum of this species shows a four line feature (Ref. 11.) which demonstrates that changes in the sidechain, even when fairly remote from the ring system, do affect the hyperfine pattern. Possibly a hyperconjugation mechanism involving the CH$_3$ protons is responsible for this effect.

A more detailed correlation between the hyperfine patterns and the molecular structure based on published ESR spectra is difficult because of the differences in the systems used by the various authors and because of the generally poor resolution of the published experimental spectra (Ref. 14.).

An attempt was made to simulate the isotropic hyperfine spectrum of CPZ$^+$. Although the attempt was not successful due to the insufficient background information, some points still emerged and are worth noting.

The major "background" lineshape, with its positive and negative peaks and a "horizontal" section in the middle (Fig. 6.9.) can arise from the overlap of a large number of hyperfine lines, provided the linewidth is comparable to the separation between these lines. This observation

COMPUTER SIMULATION

OF THE CPZ$^+$ ISOTROPIC HYPERFINE SPECTRUM
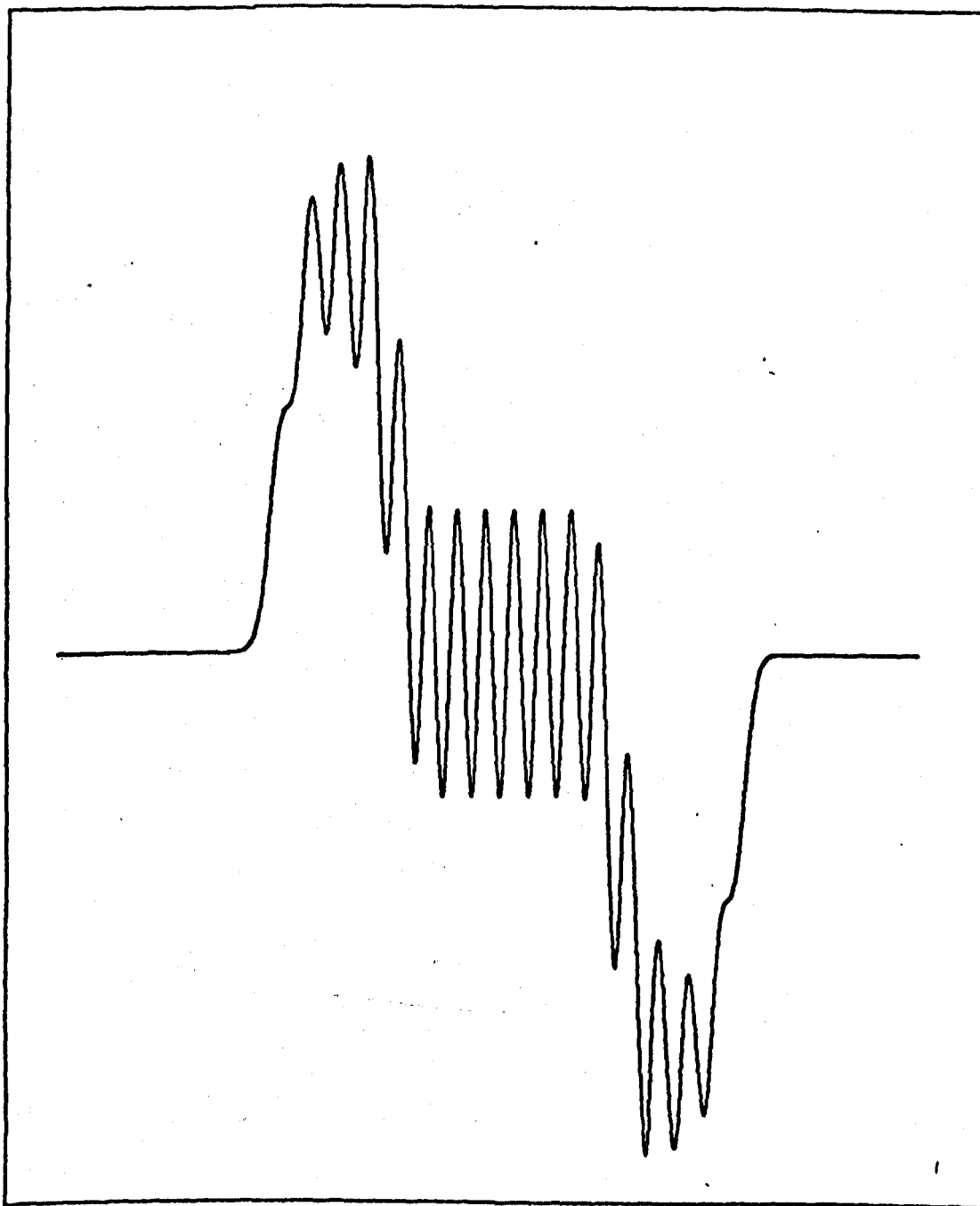
FIG. 6. 10 THEORETICAL ISOTROPIC HYPERFINE SPECTRUM OBTAINED
ASSUMING THE FOLLOWING COUPLING CONSTANTS,

NITROGEN 0. 640 MT

3 EQUIVALENT PROTONS 0. 166 MT

2 EQUIVALENT PROTONS 0. 332 MT

(GAUSSIAN LINESHAPE, LINEWIDTH 0. 166 MT)

(COMPARE TO FIG. 6. 9)

indicates that the "background" shape is a feature of the isotropic hyperfine spectrum itself and is not due to other causes (e.g. a different species or an incompletely averaged anisotropic contribution).

Gaussian lineshape functions reproduce these features considerably better than Lorentzian lineshape functions. It was also realised that in order to reproduce the regularity of the hyperfine pattern (particularly the 1.66 Gauss periodicity apparent over the entire spectrum) there must be some simple relationship between the various hyperfine splittings. The general features of the experimental spectrum mentioned above could be obtained by using sets of equivalent protons, with the hyperfine coupling constants multiples of 1.66 (Fig. 6.15.) but the fit was not particularly good. The observed alternation of height of the hyperfine lines in the centre of the pattern is thought to arise from small deviations from the equivalence of the protons or in the relationship between the hyperfine coupling constants.

The problem of interpreting the hyperfine structure of CPZ^+ in solution remains an interesting one, because it promises to clarify the participation of the sidechain of the radical to the hyperfine interactions. Two suggestions are made for the future: a) to use the ENDOR technique to investigate the hyperfine structure of CPZ^+ in solutions, or b) to use the computer simulation technique to interpret the isotropic hyperfine spectrum of the CPZ^+ analogue Promazine (Fig. 4.1.). The analysis of this spectrum should be considerably simpler because of the symmetry of the Promazine molecule. A high resolution ESR spectrum of this compound has been published (Ref. 10.).

6.4. Studies of CPZ$^+$-DNA Fibres.

This section presents the results of orientational studies performed on DNA-CPZ$^+$ fibres. The fibres represent essentially cylindrically symmetric specimens, in which the long DNA helices, with the drug molecules attached to them, are preferentially aligned along one direction (see also Sections 4.3. and 5.3.).

The analysis of the dependence of the X-band and Q-band spectra on the orientation of the fibres relative to the magnetic field, combined with the rigorous theoretical simulation of the spectra, permitted the determination of the preferential orientation of the drug molecules relative to the DNA, as well as the quantitative description of the degree of order in the fibres.

In order to illustrate the method, a particular example (that corresponding to a DNA-CPZ$^+$ complex of P/D ≈ 6) will be presented in greater detail in sub-sections 1-3, followed by the discussion and generalisation of the results (in sub-sections 4 and 5). The work presented in this section is closely related to the work on DNA-CPZ$^+$ gels, presented in the previous section, and the investigation of some optical properties of the fibres, presented in Chapter 8.

6.4.1. ESR Spectra from DNA/CPZ$^+$ Fibres.

Fibres of DNA were made from the gel obtained (see Section 4.2.) by the ultracentrifugation of a DNA/CPZ$^+$ solution of P/D equal to 6. The DNA concentration in the solution was 6.6×10^{-4} M and the ionic strength 0.044 NaCl. The pH of the original solution stabilized about 4.3 at which the DNA is not denatured (see Section 6.2.2.). It was estimated that in this preparation about 20% of the original CPZ$^+$ remained as CPZ$^+$ in the gel (see 6.2.2.).

The actual specimen consisted of 15 fibres (each of about 350 μm diameter and about 3 mm long), mounted side by side on the sticky face of a

small piece of Selotape. The operations of cutting the fibres from the glass rods on which they were dried (Section 4.3.) and of mounting, were carried out under a stereoscopic microscope. The specimen thus obtained was suitable for use in the resonant cavities, where it was mounted using a small quantity of silicone grease, on the wall of a Varian tissue cell (for the X-band measurements), or on the bottom plate of an H_{111} cylindrical cavity for the (Q-band work). This mode of mounting, with the fibres exposed to the atmosphere, permitted the relative humidity of the fibres to come in equilibrium with the chosen relative humidity of the environment (see Section 6.3.1.).

The X-band and Q-band spectra were recorded at about 9.5 and 32.8 GHz microwave frequencies respectively, at power levels of about 5 mW and an amplitude of the 100 KHz modulation field of about 50 - 80 μT peak-to-peak. The orientation of the fibres relative to the magnetic field was varied by rotating the tissue cell, in the X-band case, or by rotating the magnet, in the Q-band case.

The spectra obtained at X and Q-bands from the DNA/CPZ$^+$ fibres are shown in Figs. 6.16. and 6.17. for a range of orientations of the fibre axis relative to the magnetic field. These spectra were recorded at the laboratory relative humidity (about 60%) but little change was observed over a wide range of relative humidities produced as explained in Section 6.3.1.

Spectra similar to those obtained at Q-band with the field parallel to and perpendicular to the fibre axis, but less well resolved, have been obtained from solutions by Ohnishi and McConnell (Ref. 4.), where the orientational effects were obtained by passing the solutions through capillary tubes and not from fibres.

The examination of the spectra for intermediary angles reveals more detail of the specific state of orientation of the chlorpromazine ions in the fibre than is available from the two "extreme" spectra.

X-BAND SPECTRA OF DNA-CPZ FIBRES

EXPERIMENTAL

THEORETICAL

4 MT

0

30

60

90
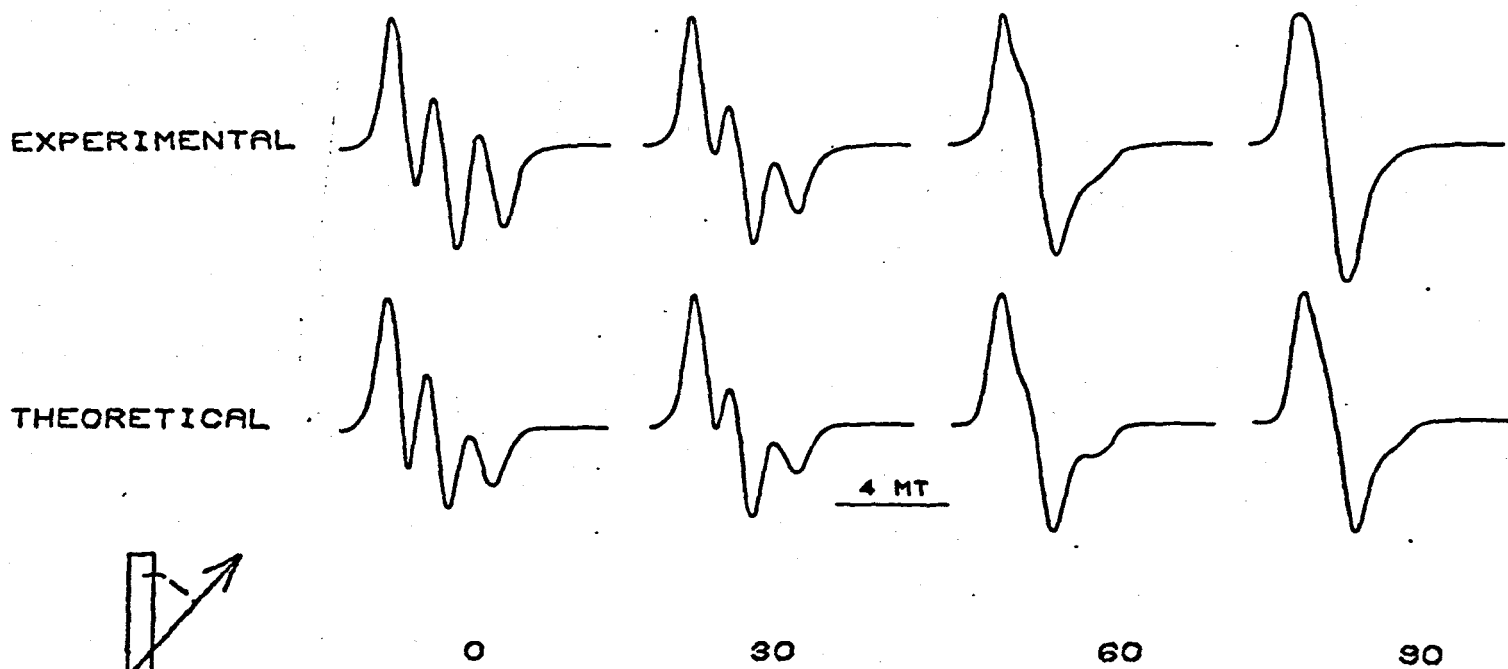
FIG.6.18 EXPERIMENTAL AND COMPUTER SIMULATED ESR SPECTRA OF DNA--CPZ⁺ FIBRES, RECORDED AT X-BAND FREQUENCY AS A FUNCTION OF THE ANGLE BETWEEN THE MAGNETIC FIELD AND THE FIBRE AXIS.

Q-BAND SPECTRA OF DNA-CPZ FIBRES

EXPERIMENTAL

THEORETICAL

4 MT

0   30   60   90

6.4.2. The Interpretation of the Fibre Spectra.

The triplet features of the spectra from Figs. 6.16. and 6.17. are assigned to the ^{14}N hyperfine interaction and sufficient evidence to support this was gained in the previous chapter, where the principal ^{14}N tensor values were determined and compared to the theory and other published data, (see discussion in Section 6.3.4.). It was seen that the ^{14}N hyperfine interaction produced a large triplet splitting if the field was along the p orbital axis and a small splitting for the perpendicular direction.

Thus, assuming the ring ^{14}N is responsible for this interaction, a large triplet splitting displayed in the "fibre parallel to the field" case, as opposed to a small splitting corresponding to the "fibre perpendicular to the field" case is consistent with the binding of the chlorpromazine ion on to the DNA so that the plane defined by the g_x and g_y, that is the general plane of the tricyclic system, is perpendicular to the DNA helical axis. This observation was made by Ohnishi and McConnell (Ref. 4.),who proposed that an intercalation mechanism (see Section 4.2.) could be responsible for the binding.

A careful examination of the spectra recorded at intermediate orientations shows that the triplet splitting is approximately constant. The intensity of the triplet feature measured over the background major lineshape decreases as the angle made by the fibre with the magnetic field increases from 0 to 90°. The spectrum taken parallel to the fibre axis itself shows a pronounced asymmetry.

While the variation of the spectrum between a "triplet" to a "single line" shape can be taken as an indication of a preferential orientation of the drug perpendicular to the fibre axis, the constancy of the hyperfine splitting as well as the asymmetry of the spectra infer the existence of a degree of misorientation of the drug molecules inside the fibre.
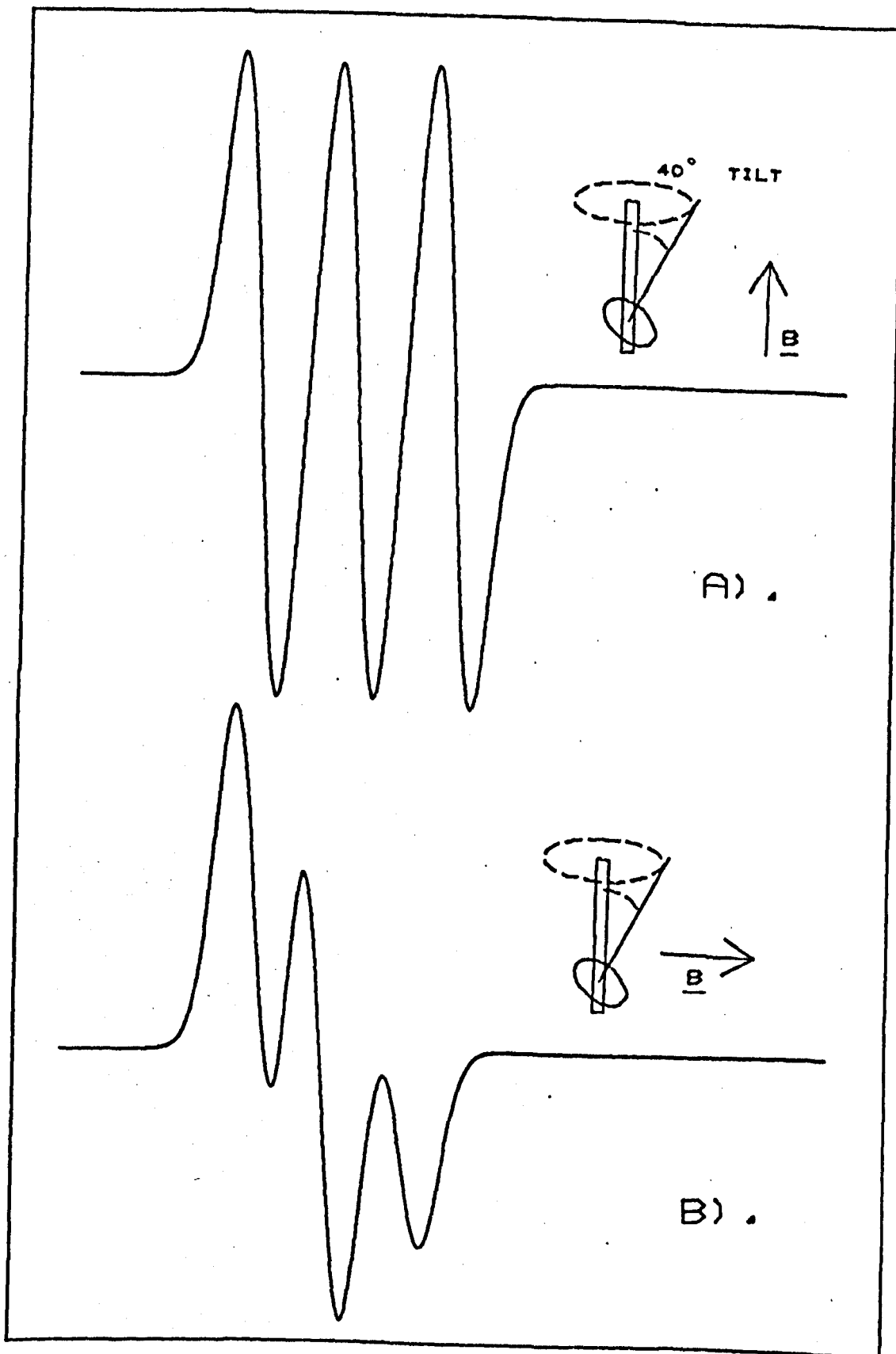
FIG. 6.18 THEORETICAL ESR SPECTRA FROM A PERFECTLY ALIGNAD DNA-OPZ$^+$ FIBRE, WITH DRUG MOLECULE TILTED BY 40 DEG. RELATIVE TO THE FIBRE AXIS. THE PARALLEL TO THE FIBRE SPECTRUM IS SYMMETRIC, WHILE THE PERPENDI-CULAR TO THE FIBRE SPECTRUM IS ASYMMETRIC.

If the drug was bound rigidly on to the DNA in any well defined manner and if all the DNA molecules in the fibre were aligned parallel to the fibre axis, one would expect to obtain a perfectly symmetric "parallel to the field" spectrum from such an "ideal" fibre. This is so because the magnetic field, which is the symmetry axis of the Hamiltonian, coincides with the symmetry axis of the fibre, so that the drug molecules have a unique orientation relative to the magnetic field. This situation is illustrated in Fig. (6.18a), for a perfectly oriented fibre with the drug molecule making an angle of tilt of 40° relative to the fibre axis. (The angle of tilt is defined in Fig. 6.19.) Deviations from the symmetry of the spectrum could only occur if there was some disorder present, so that there was no unique orientation of the drug molecules relative to the magnetic field.

Fig. 6.18b. shows the "perpendicular to the field" spectrum expected from the same fibre. It can be seen that the spectrum is no longer symmetric, because the radicals that are bound at different positions around the DNA molecule have a different orientation relative to the magnetic field (e.g. the angle between the field and the z molecular axis varies in this case between 50 and 130°). The recorded spectrum would represent in this case a superposition of different individual spectra. Thus, quite generally, the spectra recorded from fibres with the field perpendicular to the fibre axis (as opposed to those recorded with the field parallel to the fibre axis) are expected to by asymmetric and less informative on the degree of ordering inside the specimen. The only particular case when the two "extreme" spectra would be both symmetrical is for axial tensors, with the symmetry axis of the tensors parallel to the fibre axis.

Therefore, the asymmetry of the "fibre parallel to the field" spectrum is the first indication of the misorientation within the DNA-CPZ$^+$ fibre. At the same time, the observation that the hyperfine splitting recorded at various orientations of the fibre is approximately constant and equal to
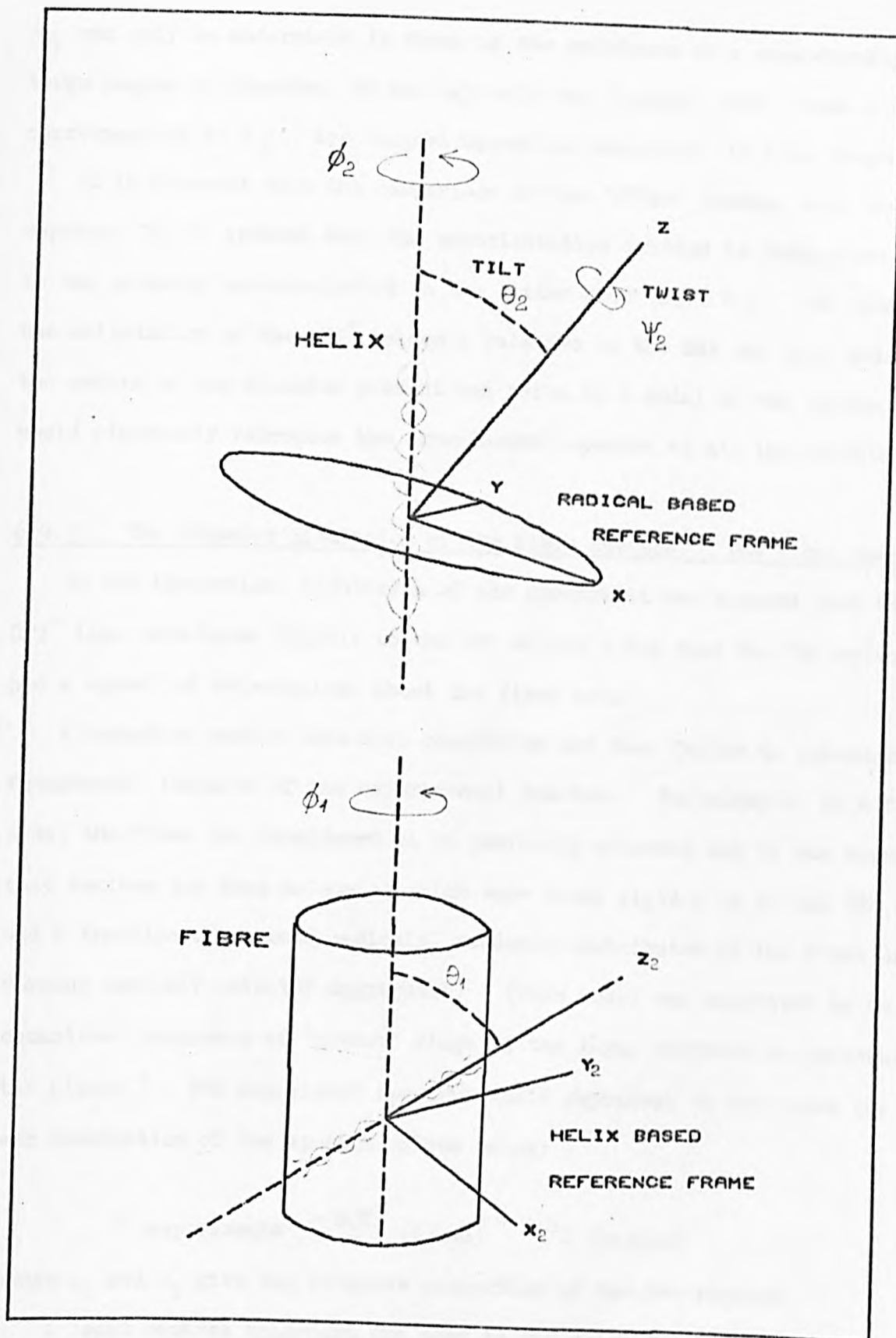
FIG. 0.19 REFERENCE FRAMES AND EULERIAN ANGLES USED TO DEFINE THE ORIENTATION OF A DRUG MOLECULE RELATIVE TO A DNA HELIX (ABOVE) AND OF A HELIX INSIDE THE FIBRE (BELOW).

$A_{||}$ can only be understood in terms of the existence of a considerably large degree of disorder, by analogy with the "powder" case, where a feature corresponding to $A_{||}$, the largest hyperfine component, is also displayed.

It is apparent from the comparison of the "fibre" spectra with the reported "flow" spectra that the misorientation existed in both cases, but it was probably underestimated in the latter case (Ref. 4.). To specify the orientation of the CPZ^+ molecule relative to the DNA one must understand the nature of the disorder present and build up a model of the system which would rigorously reproduce the experimental spectra at all the orientations.

6.4.3.   The Computer Simulation of the Fibre Spectra.   The Fibre Model.

In the theoretical simulation of the spectra it was assumed that the CPZ^+ ions were bound rigidly to the DNA molecule but that the DNA molecules had a spread of orientations about the fibre axis.

Alternative models were also considered but they failed to reproduce the fundamental features of the experimental spectra. For example, in a first model the fibre was considered to be perfectly oriented and it was assumed that besides the drug molecules which were bound rigidly on to the DNA there was a fraction of unbound radicals, randomly distributed in the fibre or forming randomly oriented aggregates. (This model was suggested by the occasional occurence of "powder" rings in the X-ray diffraction patterns of the fibres.) The experiment spectrum would represent in this case the linear combination of two spectra, given below:

$$S_{experimental} = c_1 S_1 \text{ (bound)} + c_2 S_2 \text{ (random)}$$

where c_1 and c_2 give the relative proportion of the two species.

A least squares procedure was used to decompose the experimental spectra into two components. The first one, represented a symmetrical three line spectrum corresponding to the rigidly bound radicals. The second one,
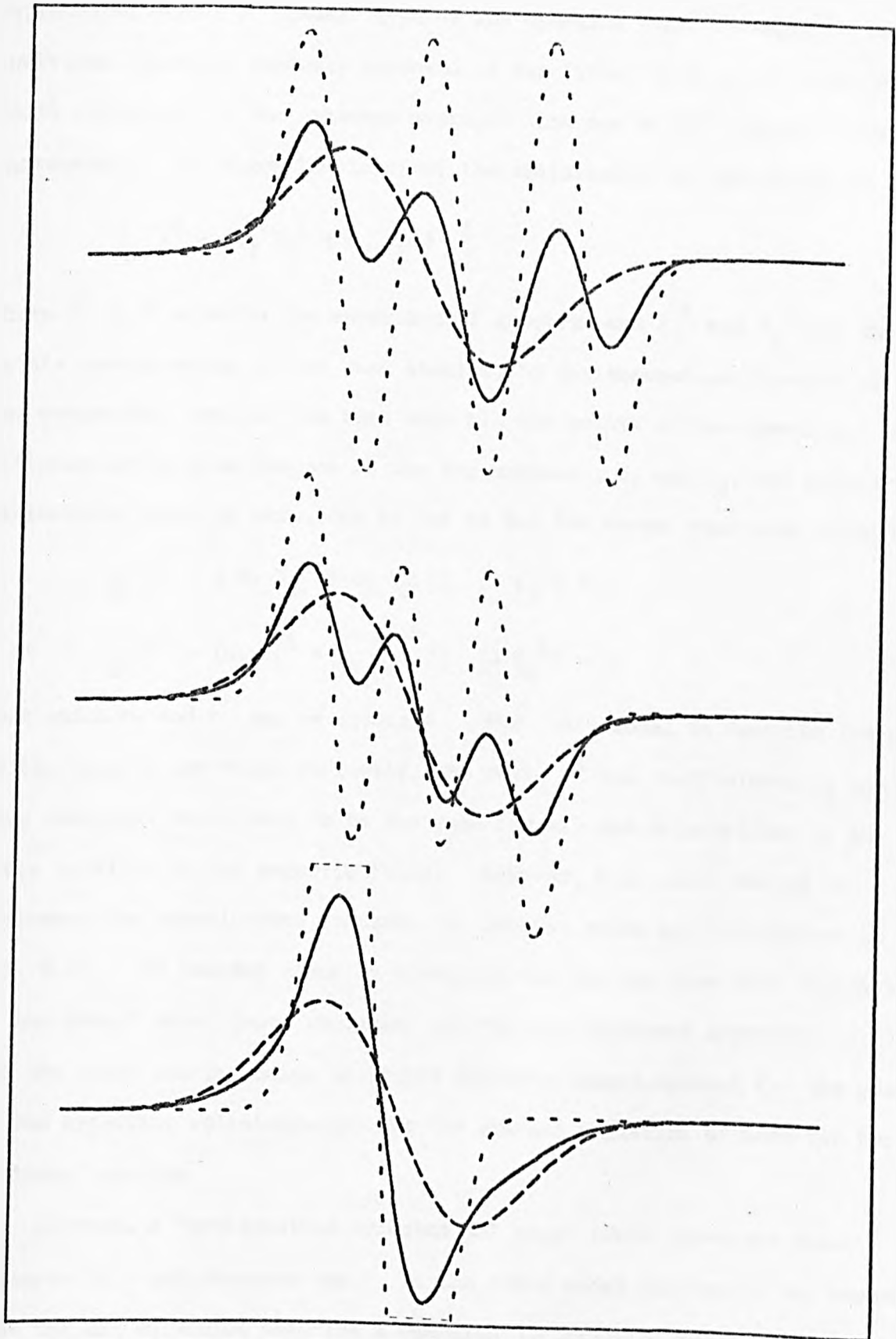
FIG. 6.20 HYPOTHETICAL FIBRE ESR SPECTRA (FULL LINE) CONFORMING TO
A MODEL IN WHICH ONLY A FRACTION (33%) OF THE CPZ RADICALS WERE
ORIENTED (DOTTED LINE). THE CONTRIBUTION OF THE RANDOM PHASE (A BROAD
LINESHAPE CENTERED AT THE ISOTROPIC G VALUE) IS SHOWN DASHED.
THE MODEL FAILS TO PRODUCE CONSTANT HYPERFINE SPLITTINGS AND TO RE-
PRODUCE THE ASYMMETRY OF THE EXPERIMENTAL SPECTRA AT ALL THE ORIENTATIONS.

represented either a "powder" type of ESR spectrum (corresponding to the individual radicals randomly oriented in the fibre) or a single line (which would correspond to the exchange averaged line due to the radicals forming aggregates). The algorithm involved the minimization of the function:

$$\sum_i [Y^i - (c_1 Y_1^i + c_2 Y_2 i)]^2$$

where Y^i is a point in the experimental spectrum and Y_1^i and Y_2^i are the points corresponding to the same abscisa, in the theoretical spectra of the two components, and the sum runs over all the points of the spectrum. By differentiating with respect to the two unknowns, c_1 and c_2, and setting the derivatives equal to zero, one is led to the two normal equations given below:

$$\sum_i [Y^i - (c_1 Y_1^i + c_2 Y_2 i)] \; (- Y_1^i) = 0$$

$$\sum_i [Y^i - (c_1 Y_1^i + c_2 Y_2^i)] \; (- Y_2^i) = 0$$

from which c_1 and c_2 can be obtained. For this model to describe the state of the drug in the fibre correctly, the ratio of the coefficients c_1 and c_2 thus obtained, would have to be the same for all the orientations of the fibre relative to the magnetic field. However, this model failed to reproduce the experimental features for reasons which are illustrated in Fgi. 6.20. It becomes clear by examining the spectra from this figure that a "two phase" model (one, producing orientation dependent hyperfine splittings and the other one producing isotropic features) cannot account for the constancy of the hyperfine splittings nor for the gradual variation between the two "extreme" spectra.

However, a "preferential orientation" model could reproduce these features in a satisfactory way. In the fibre model adopted it was assumed that the DNA molecules describe a Gaussian distribution about the fibre axis, so that the probability of a DNA molecule lying on the surface of a cone of semiangle Θ is proportional to $1/\delta \, e^{-\frac{\Theta^2}{2\delta^2}}$, where δ is the angular half width of the distribution (standard deviation).

The position of the radical relative to a DNA molecule can be described in terms of two binding angles illustrated in Fig. 6.19. The "tilt" is the angle between the DNA axis and the molecular z axis (formally defined as a rotation about the molecular y axis. The "twist" describes a rotation of the radical about its own z axis. Originally the molecular z axis is assumed to coincide with the DNA helical axis. A third angle is used to describe the rotation of the radical relative to the DNA helical axis.

In the case of CPZ^+, the molecular reference system (x,y,z) was based on the directions of the principal axes of the g and A tensors so that the z axis was perpendicular to the general plane of the tricyclic system. The axial symmetry of the tensors make the problem independent on the angle of "twist" and this angle was arbitrarily set to zero.

The computer program based on the above fibre model was described in Chapter 5. The algorithm and the mathematical formalism adopted form the object of Section 5.2. and the basic flow chart can be examined in Fig. 5.4.

The principal values of the g and ^{14}N hyperfine tensors used in the computer simulation work, were those obtained from the theoretical simulation of the "gel" spectrum (Section 6.3.3.). Three of these parameters were in fact close to those estimated from the fibre spectra. The trial and error exercise consisted in the visual examination of the X-band and Q-band computed spectra, plotted for a number of orientations of the fibre relative to the magnetic field, for a systematic variation of the adjustable parameters: the title of the radical, the angle of Gaussian misorientation, the linewidth and the type of the lineshape.

A large misorientation angle was required in order to reproduce the asymmetry of the spectra and the correct relative height of the three lines, especially in the "parallel to the field" spectrum. If the Gaussian spread was too low, the relative height of the negative peaks 2 and 3 of the X-band 0° spectrum was reversed and also the triplet feature of the Q-band 0° spectrum had a "downward" slant, in disagreement with the experimental spectrum.

Various degrees of tilt were considered but the fundamental features of the experimental spectra could only be reproduced if one assumed that the plane of the drug was perpendicular or approximately perpendicular to the helix axis. If a finite tilt angle (up to 30°) is introduced, the required Gaussian spread can be reduced, but the spectra recorded at extreme orientations cannot then be fitted using the same set of parameters.

The best fit for all the orientations of the fibre relative to the magnetic field was obtained with the z axis coincident with the fibre axis (corresponding to the plane of the molecule perpendicular to the helix axis) and a Gaussian spread parameter of 40°, in the orientation of the DNA molecules within the fibre. That is to say most of the molecules of DNA lie within a cone of semiangle 40°.

The theoretical spectra from Figs. 6.16. and 6.17. were generated by the computer program set for the "fibre" type of simulation. The tilt and twist were zero and the misalignment parameter was equal to 40 degrees. The principal g and A tensor values were those given in Section 6.3.3. The lineshape was Gaussian and a linewidth equal to about 8.7 Gauss. (The fit was improved if a small differential broadening of the three hyperfine components similar to that discussed in Section 6.3.3. was introduced, so that the widths of the three component lines were 8.7, 8.7 and 9.7 Gauss. respectively.) The angular steps used for the averaging angles ALFA and BETA (see Section 5.5.1.) were 4 and 15 degrees respectively, corresponding to a total of 515 component spectra. The third angle was automatically kept constant due to the coincidence of the symmetry axes of the DNA and the CPZ$^+$ tensors. A refinement of the above steps did not result in changes in the lineshape.

6.4.4. Discussion.

The computer simulations presented above explain the experimental fibre spectra in terms of a strongly immobilized CPZ$^+$ radical having its plane preferentially oriented perpendicular to the DNA helical axis. The good fit

to the experimental spectra obtained at both X and Q-band frequencies for different orientations of the fibres relative to the magnetic field shows that the model adopted is essentially correct.

The perpendicularity of the general plane of the CPZ^+ molecule to the helical axis has been suggested before by Ohnishi and McConnell (Ref. 4.) but their suggestion was based on a limited evidence. The present results show that the equality of the observed splittings in the "parallel to the field" and "complete random" cases is insufficient to demonstrate this perpendicularity because there is a considerable degree of misorientation within the specimen. In fact the observed splittings proved to be approximately constant for all the orientations.

However, the present computer simulation work proved that the perpendicularity of the drug molecule to the helical axis (the same as for intercalation) is indeed a possible explanation. The computer spectra show clearly that the effects of a limited degree of molecular orientation on the ESR spectra are the constancy, over a wide range of orientations, of the observed hyperfine splittings and the asymmetry of the lineshapes and these effects should be quite general to any system, provided one hyperfine component is much greater than the others.

One is inclined to believe that the misorientation is derived entirely from the misalignment of the DNA molecules within the fibre. This is substantiated by comparison with X-ray diffraction pictures (see below) where the angular spread of the diffraction spots is increased compared to those from a fibre without the drug. However, one cannot exclude the possibility that a scatter of the orientation of the drug molecules relative to the DNA helices may make a small contribution. Such a situation would be difficult to envisage in the case of intercalation, but it could occur in the case of the binding of the chlorpromazine ion externally on to the DNA, especially if the binding was such that it allowed for some rotation of different parts of the chlorpromazine ion relative to one another (e.g. the long side chain

relative to the ring).

The ESR studies give evidence of the total misalignment, caused either by a variation in the angle at which the chlorpromazine ion binds to the DNA molecule, or by the scatter in the DNA molecules within the fibre. Clearly the latter situation is more likely.

The algorithm for dealing with the alternative situation would be the same and the spectra obtained by assuming a Gaussian scatter in the tilt angle of the radicals about their preferential position perpendicular to the helical axis would be identical to the ESR spectra presented above. Similar spectra are expected from the "convolution" of the two types of misorientation so that the total misorientation parameter was 40°.

In principle it is possible to distinguish between the two causes of the misorientation by looking at the optical dichroism of the fibre (due to the drug bound on to DNA) and the birefringence (due to the DNA alone) and this possibility is investigated in the next section and in Chapter 8.

6.4.5. Comparison with other Techniques.

One advantage of investigating fibres is the possibility of correlating information derived from various techniques. The ESR results coupled with a theoretical synthesis, are consistent with a preferred orientation of the chlorpromazine ion perpendicular to the fibre axis, but it is also apparent that valuable information might be obscured by a large degree of misorientation which exists in both fibres and in the previous flow experiments. It was found necessary to obtain a confirmation of the existence of this considerable degree of misorientation by evidence from other techniques and in the same time to investigate the cause of the misorientation.

One technique that provided evidence for the misalignment of the helices in the fibre was the X-ray diffraction (XRD). This technique can reveal the effect of the drug on the helical parameters of the DNA and on the

molecular packing inside the fibre (Ref. 3. p 108 and Ref. 15.). An X-ray fibre diffraction pattern consists of spots arranged on "layer lines" (see Fig. 8.5.). The spacing of the layer lines is related to the reciprocal of the helix pitch. The "meridional" reflections (occuring at the top and bottom of the diffraction pattern) correspond to the repeat of the DNA base-pairs along the helical axis. The average lateral separation of the helices in the fibre can be calculated from the separation of the spots along the "equator" (horizontal axis) of the pattern.

Searl cameras with toroidal focussing, mounted on an Elliott G x 6 rotating anode generator were used. The diffraction patterns were recorded at the same relative humidities as those used in the ESR experiments. The patterns were measured against the 0.34 nm calibration ring of a polycrystalline powder of Vaterite, with which the fibres were sprinkled. A computer program was available for the necessary conversions and the correction for the flatness of the film (Ref. 17.).

The XRD patterns obtained from the DNA-CPZ[+] fibres (P/D = 6) were diffuse, with the reflections extended into arcs (Fig. 6.21). The angular spread of this diffraction pattern, as measured from a circular densitometer trace recorded at the radius of the meridional reflections, was estimated to be equal to 25° (half width at half height) but the extent of the misalignment varied from pattern to pattern. The value cannot be taken to represent exactly the misalignment of the helices in the fibre, but rather it is an underestimate. Reference to the simple XRD theory (Ref. 15.) shows that the meridional reflection, by not intersecting the sphere of reflection, is not expected to produce a diffraction spot unless there was a scatter in the orientation of the helices inside the fibre.

One can see an advantage of the ESR over the XRD technique; while the diffraction patterns for higher degrees of misalignment become blurred and uninformative, the quantitive of ESR work , aided by computer simulations is still possible.
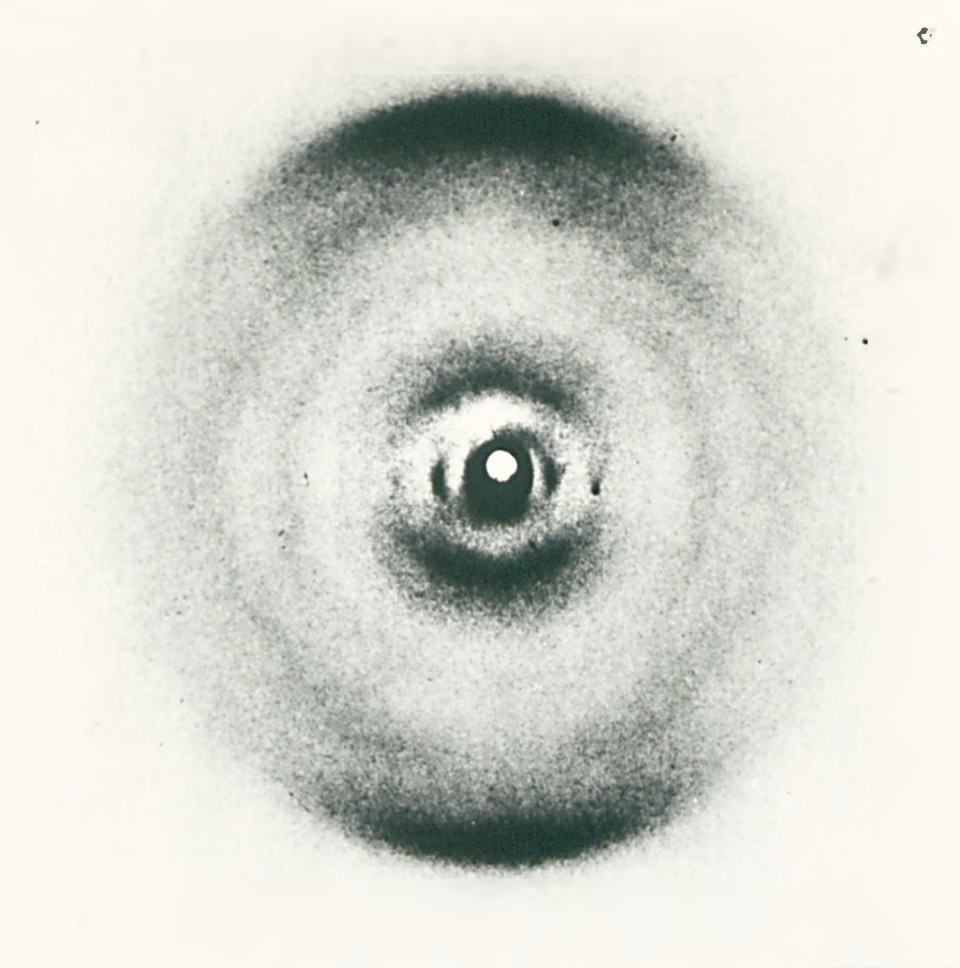
FIG. 6. 21 X-RAY DIFFRACTION PHOTOGRAPH

FROM A DNA-CPZ$^+$ FIBRE (P/D=6), ILLUSTRATING

THE ANGULAR EXTENTION OF THE PATTERN.

Other techniques that provided support for the conclusions of the ESR investigation were the optical dichroism and the birefringence of the fibres, which will be presented in a more detailed fashion in Chapter 8.

For the purpose of this discussion it is necesssry to define the dichroic ratio (D) of a DNA/CPZ^{+} fibre as the ratio of the absorptions at the CPZ^{+} maximum absorption peak (in the visible) recorded perpendicular $(A_{\perp})$ and parallel $(A_{\parallel})$ to the fibre axis.

$$D = \frac{A_{\perp}}{A_{\parallel}}$$

In a perfectly oriented fibre with the drug molecules perpendicular to the fibre axis, D should tend to infinity because the electronic transition dipoles responsible for the absorption lie in the plane of the chromophore so that $A_{\parallel} = 0$. The experimental values measured from these fibres are about 1.5, showing a considerable departure from the ideal case. The theoretical calculations presented in Chapter 8 are in complete agreement with the predicted total misalignment of 40° in the fibres (see also Fig. 8.2.).

There is little reference to this kind of misorientation of the fibres in the literature. Arnott (Ref. 17.) describes various types of disorder in the packing of the nucleic acid helices in a fibre but the helices are considered to be aligned parallel to the fibre axis. However, an estimation of the orientation of the DNA molecules in oriented films has been reported (Ref. 18.). The authors, who used polarised infra-red spectroscopy to measure the angle θ between the helix axis and particular transition moments, worked in terms of a model which assumed a fraction of "perfectly oriented" helices and the remaining randomly oriented. They found that the fraction f of perfectly oriented chains for calf thymus DNA varied, within this model, between 23 and 49% (being greater at low relative humidities). It was calculated that 40° of Gaussian misalignment would correspond to a figure

of $f = 50\%$ which is comparable to the degree of order achieved in the quoted experiment.

As regards the cause of the large misalignment in the DNA/CPZ$^+$ fibres it was thought that part of it might be just the result of the interference of the CPZ$^+$ with the helical structure due to the relatively low initial P/D ratio (6) and possibly due to the adverse effect of the lowering of the pH following the decay of some of the CPZ$^+$ radicals in solution.

One drawback of the ESR technique lies in the large number of fibres of relatively high CPZ$^+$ content that are needed with the present sensitivity of the spectrometer. However, a large batch of DNA/CPZ$^+$ fibres was prepared with the following changes which take into account the points raised above:

1) The initial P/D ratio of the solution (of ionic strength 0.05 N NaCl) was 12. The pH of this solution stabilized around the value of 6.5.

2) The stock solutions were used cold (4°C) and the complex was centrifuged immediately after preparation, at the increased speed of 50,000 rpm, at about 4°C. It was estimated that the proportion of the initial CPZ$^+$ that remained as CPZ$^+$ in the gel was equal to approximately 25%, thus corresponding to a P/D ratio of 48.

3) A large number of fibres was made from the freshly prepared gel. The negative birefringence of each individual fibre was measured as a test for the orientation and only those fibres yielding a value greater than 0.05 (which corresponded to about 20% of the fibres) were used in the ESR experiment. The X-band spectra were recorded for a series of orientations of the fibres, as described above.

The spectrum recorded with the magnetic field parallel to the fibre axis, together with the computer simulation of the same spectrum are presented in Fig. 6.22. Despite the rather low signal-to-noise ratio it is apparent that the orientation inside the fibres has been substantially improved, as seen from the triplet feature being more regular than in the previous case
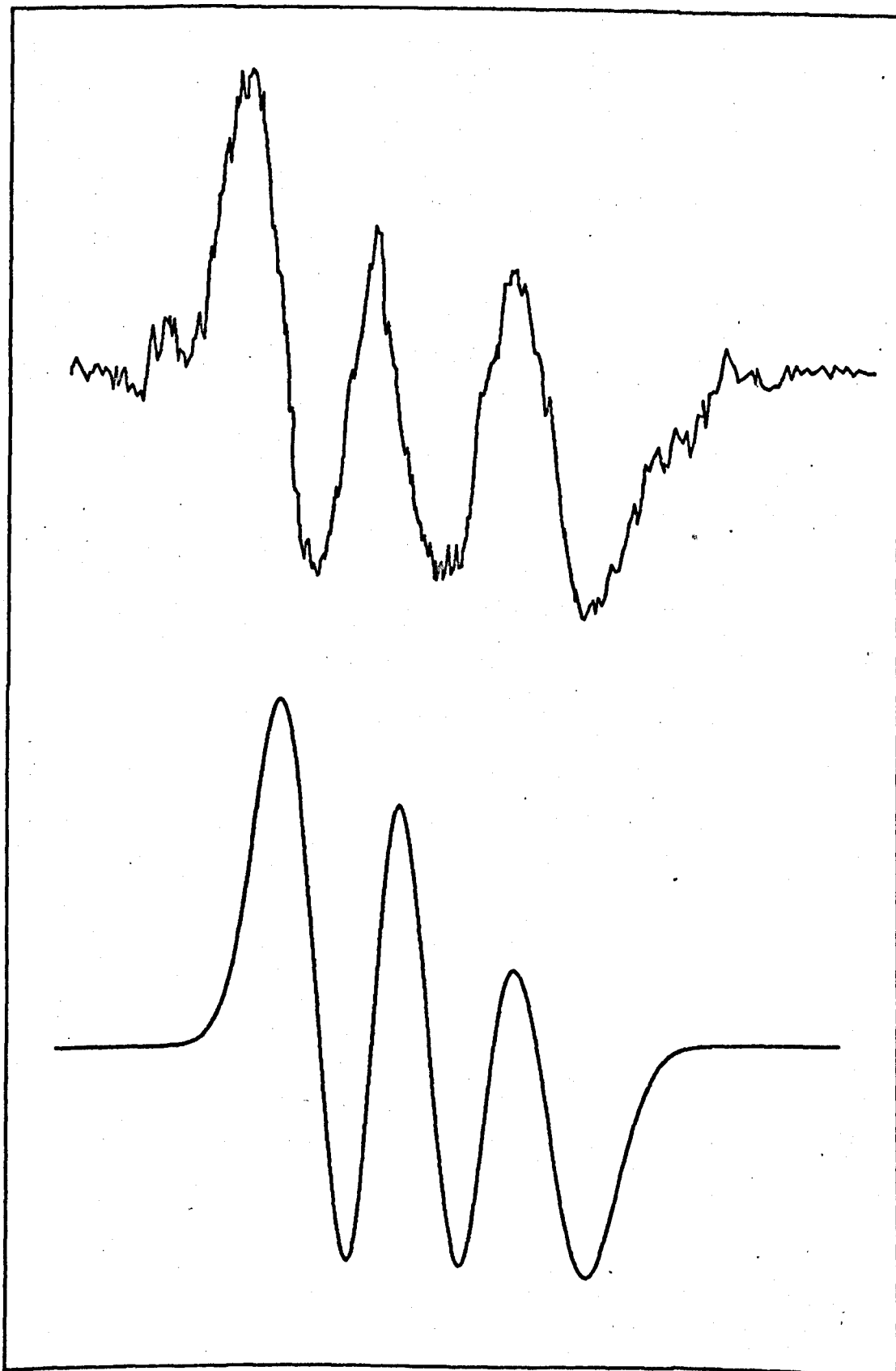
FIG. 8. 22 THE ESR SPECTRUM FROM A BATCH OF WELL ORIENTED DNA-CPZ$^+$
FIBRES (P/D 12) RECORDED AT X-BAND WITH THE FIELD PARALLEL TO THE
FIBRE AXIS, AND THE COMPUTER SIMULATED SPECTRUM.
(ANGULAR MISALIGNMENT 27 DEG., LINEWIDTH 9.2, 8.7, 8.7 GAUSS)

(Fig. 6.16.). The computer simulation of the spectra demonstrated that a good fit at all the orientations of the fibre can be achieved if the drug is assumed to be bound perpendicular (or approximately perpendicular) to the helical axis and the Gaussian misalignment parameter was 27°. Deviations from the rigid perpendicularity to the helical axis of up to 20° produce little detectable changes in the lineshape. The full batch of fibres produced spectra corresponding to a Gaussian parameter increased to 30°.

The optical dichroism measurements carried out in parallel yielded values about $D = 4 \pm 1$, which, compared to the theoretical calculations, correspond to Gaussian parameters of $23 \pm 4°$, in a very good agreement with the ESR results.

It is felt that the considerable reduction of the misalignment in the fibres was achieved mainly due to the use of a larger initial P/D value. Apart from bringing stronger evidence for the preferential orientation of CPZ^+ perpendicular to the fibre axis, this experiment showed that better orientations can be achieved by using the fibre, rather than the flow technique.

6.5. Conclusions.

The orientational study performed on the $DNA-CPZ^+$ demonstrated the preferred orientation of the CPZ^+ radicals with their general planes perpendicular to the DNA helical axis, without, however, favouring at this stage any particular mechanism of binding (intercalation vs. external binding).

The considerable degree of misorientation which existed both in the fibres and in the reported flow experiment (Ref. 4.) was pointed out, but it became apparent that better orientations can be achieved in the fibres. The disorder was assigned to the misalignment of the DNA helices in the fibre and this was found consistent with evidence collected by other techniques. The misalignment was described quantitatively in terms of a Gaussian

distribution of the orientation of the DNA helices about the fibre axis. The good fit to the experimental ESR spectra (and indeed, to the optical dichroic ratios) supports the accuracy of the theoretical fibre model.

The orientational study was made possible by the knowledge of the principal values of the g and ^{14}N hyperfine tensors, which were determined from the study of the "powder" type of spectrum of the DNA-CPZ$^+$ gel.

The experimental techniques used in this study: the "fibre" ESR technique, aided by computer simulations of the ESR spectra and correlated to X-ray diffraction and optical studies and simulations, are thought to set a model of work generally applicable to systems with one axis of symmetry.

The significance of the results obtained with DNA-CPZ$^+$ complexes will be discussed in Chapter 9.

REFERENCES.

1. D. C. BORG, G. C. COTZIAS: Proc. Natl. Acad. Sci. US., 48, 617-623, (1962).

2. D. C. BORG, G. C. COTZIAS: Proc. Natl. Acad. Sci. US., 48, 623-627, (1962).

3. V. A. BLOOMFIELD, D. M. CROTHERS, I. TINOCO: Physical Chemistry of Nucleic Acids, Harper and Row, (1974).

4. S. OHNISHI, H. M. McCONNELL: J. Amer. Chem. Soc., 87, 2293, (1965).

5. F. N. H. ROBINSON: J. Sci. Instrum., 42, 653-654, (1965).

6. A. CARRINGTON, A. D. McLACHLAN: Introduction to Magnetic Resonance, A Harper International Edition, (1969).

7. H. D. KEITH et al: Biochim. Biophys. Acta., 300, 379-419, (1973).

8. B. C. GILBERT, P. HANSON, R. O. C. NORMAN, B. T. SUTCLIFFE: Chem. Comm., 6, 161-164, (1966).

9. H. M. McCONNELL, R. E. ROBERTSON: J. Phys. Chem., 61, 1018, (1957).

10. L. H. PIETTE, I. S. FORREST: Biochim. Biophys. Acta., 57, 419-420, (1962).

11. C. LANGERCRANTZ: Acta Chem. Scandinavica, 15, 1545-1556, (1961).

12. L. H. PIETTE, P. LUDWIG, R. N. ADAMS: Anal. Chemistry, 34, 916-920, (1962).

13. L. H. PIETTE et al: Biochim. Biophys. Acta, 88, 120, (1964).

14. B. H. J. BIELSKI, J. M. GEBICKI: Atlas of ESR Spectra, Academic Press, (1967).

15. B. K. VEINSTEIN: Diffraction of X-rays by Chain Molecules, Elsevier, (1966).

16. H. PORUMB: Private Communication, (1976).

17. S. ARNOTT: Trans. Am. Cryst. Assoc., 2, 31-56, (1966.

18. J. PILET, J. BRAHMS: Biopolymers., 12, 307-403, (1973).

CHAPTER 7.

COMPLEXES OF CHLORPROMAZINE[+] WITH RIBONUCLEIC ACID.

The ESR study of the interaction of CPZ^+ with the DNA was followed by an investigation of the interaction of CPZ^+ with the RNA. The aim of this investigation was to obtain some insight, by comparison, into the mechanism and eventually the specificity of the binding of the free radical to these species.

The chapter begins with the presentation of the ESR work with the synthetic double stranded RNA Poly I. Poly C (see also Chapter 4.), which yielded two distinct kinds of results, depending on the mode of preparation of the material. In order to explain this fact, the study of two other species of RNA was undertaken: natural transfer RNA and the single stranded synthetic polynucleotides PolyI and Poly C. The results reveal the different behaviour of CPZ^+ towards these species and to the DNA.

7.1. Synthetic Double Stranded Polyribonucleotides.

7.1.1. General.

The synthetic Poly I. Poly C was obtained from Sigma Chemicals Company. The species has been characterized by Hodgson (Ref. 1.). The double stranded polynucleotides were obtained in that case by dissolving the single stranded components in water and increasing the ionic strength of the solution to about 0.05 M NaCl. The molar extinction coefficient given for the plateau region at 255 n m was 4900 l mole^{-1} cm^{-1}. Poly I. Poly C was shown to form only double helices in solution (Ref. 2.) unlike other polynucleotides which can form triple helices or other associations.

In the present experiments Poly I . Poly C was either dissolved directly in a 0.001M NaCl solution (the low ionic strength giving the greatest solubility), prior to adjusting the ionic strength to the final NaCl

concentration 0.05 M, or, it was dissolved directly in a 0.05 M NaCl solution. The results obtained with the CPZ^+ complexes from these two preparations were markedly different, although the UV absorption spectra of the two final solutions were the same, and similar to those presented by Hodgson (Ref. 1.). It was realised that the first preparation must have corresponded to a "looped" structure (Ref. 3., p 343), formed as a result of the partial strand separation at the low ionic strength, followed by the rapid reannealing of the strands upon increasing the ionic strength, while the second one corresponded to a regular double stranded structure. Indeed, the absorption spectrum of the low ionic strength solution of Poly I . Poly C (0.001 M NaCl) looked like the sum of the absorption spectra of the individual components Poly I and Poly C (Ref. 1.). The reannealing process induced by the ionic strength can be demonstrated with reference to Fig. 7.1, in which the hypochromic effect that resulted from increasing the ionic strength of such a solution to the intermediate value of 0.03 M, was monitored in time. This effect indicated the slow transition towards a double stranded structure. The specimens obtained from this preparation behaved similarly in all respects to the regular double stranded poly I . Poly C. Only the samples obtained by rapidly increasing the ionic strength from 0.001 M to 0.05 M NaCl (or more) behaved differently (see below). It is thought that the fast reaction conditions, favoured in that case the imperfect pairing of the two strands leading to a structure consisting of double stranded regions interrupted by single stranded "loops" or "bulges" and it is possible that some cross pairing between the molecules also took place (Ref. 1.).

While the conformation of the regular synthetic double stranded RNA is similar to that of the DNA, thus enabling a more direct comparison, the "looped" conformation is closer to that of the biological species, the transfer, messenger and ribosomal RNA (Ref. 3., p 343.).
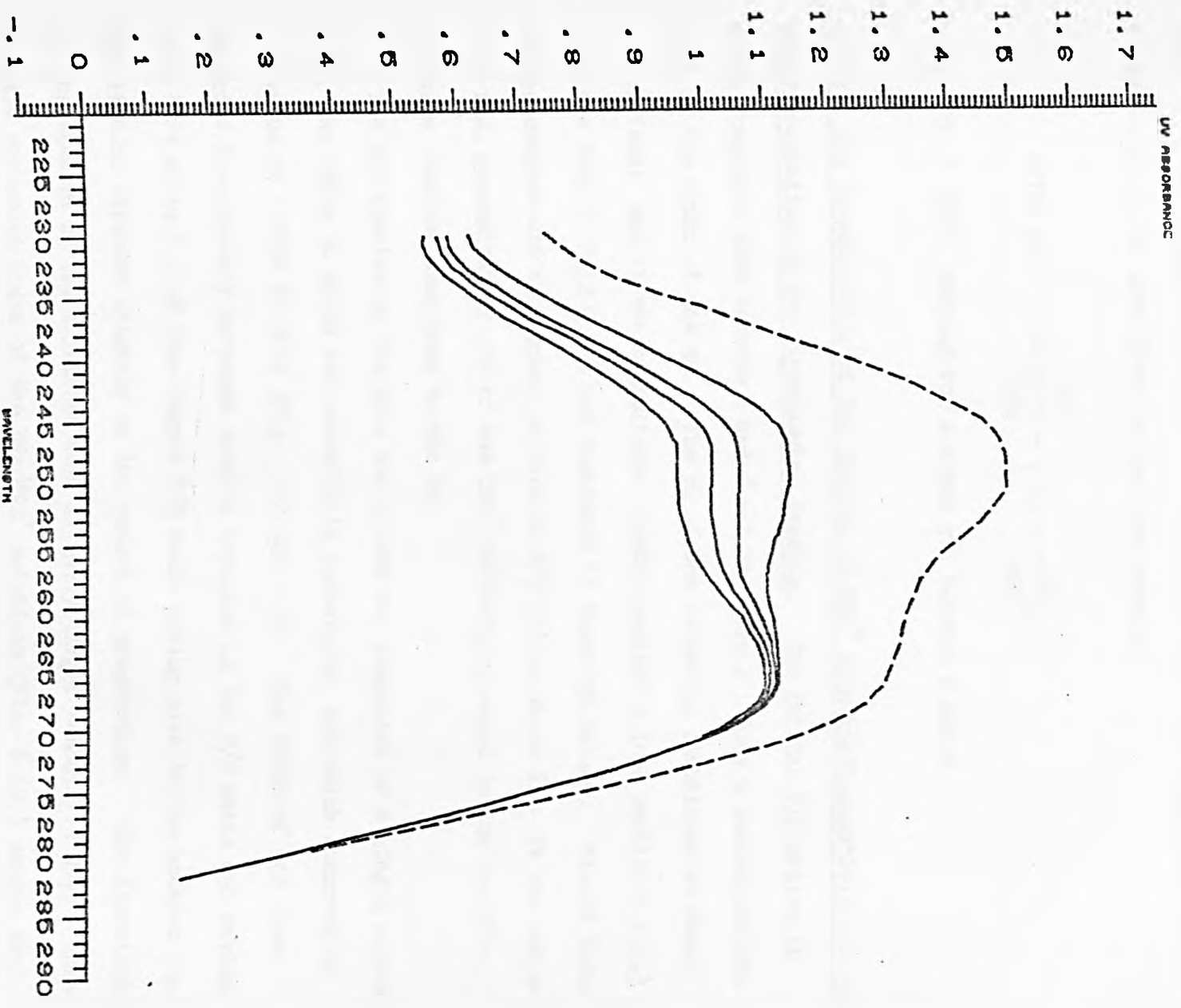
FIG.7.1 ABSORPTION SPECTRA OF AN AQUEOUS POLY I.POLY C SOLUTION
RECORDED AT 9 MINS INTERVALS AFTER INCREASING THE IONIC STRENGTH OF
THE SOLUTION TO APPROX. 0.03 M NACL. DASHED: THE SPECTRUM IN
0.001 M NACL.

UV ABSORBANCE

WAVELENGTH

The CPZ^{+}-RNA complexes were made by the method described in Section 6.2.1. The phosphate-to-radical ratios in the gels were determined by a formula similar to that given in the same section:

$$(P/D) \text{ gel} = 0.62 \frac{A_{255}}{A_{530}} - 3 \left(1 + \frac{SO}{CPZ^{+}}\right)$$

with SO / CPZ^{+} ranging for a fresh gel between 0 and 2.

7.1.2. ESR Investigation of the Complex of CPZ^{+} with the"Looped"Poly I . Poly C. The Presentation of the Experimental Results.

The initial P/D ratios of these complexes were between 2 and 6 and the Poly I . Poly C concentrations were of the order of one mM. The pH of the solutions stabilized at about 5.6 or less; and it was established spectroscopically (see Section 6.2.2.) that the Poly I. Poly C was not denatured at these pH values. Stable forms of the complex did not appear to form at P/D ratios above 6. It was estimated that approximately 50% of the CPZ^{+} initially present in the low P/D mixtures remained complexed to the RNA.

The ESR spectra of the gels and fibres all consisted of a single narrow line, the shape of which was essentially Lorentzian, and which occurred at a g-value of 2.0053 ±0.0002 (Figs. 7.2 and 7.3). The width of the line recorded from freshly prepared samples depended on the P/D ratio and varied from 0.85 mT to 1.0 mT (the larger P/D ratio giving rise to the broader lines) and it also depended slightly on the method of preparation. The linewidths of the spectra of the solutions were slightly larger (about 1.5 mT). These spectra resembled those of the DNA/CPZ^{+} solutions (Fig. 6.13.) except that they were narrower (c.f. 1.8 - 2.0 mT).

The lines from the fibres showed no evidence of anisotropy as the magnetic field orientation was varied relative to the fibre axis. Any change in the temperature or relative humidity of the samples resulted in an
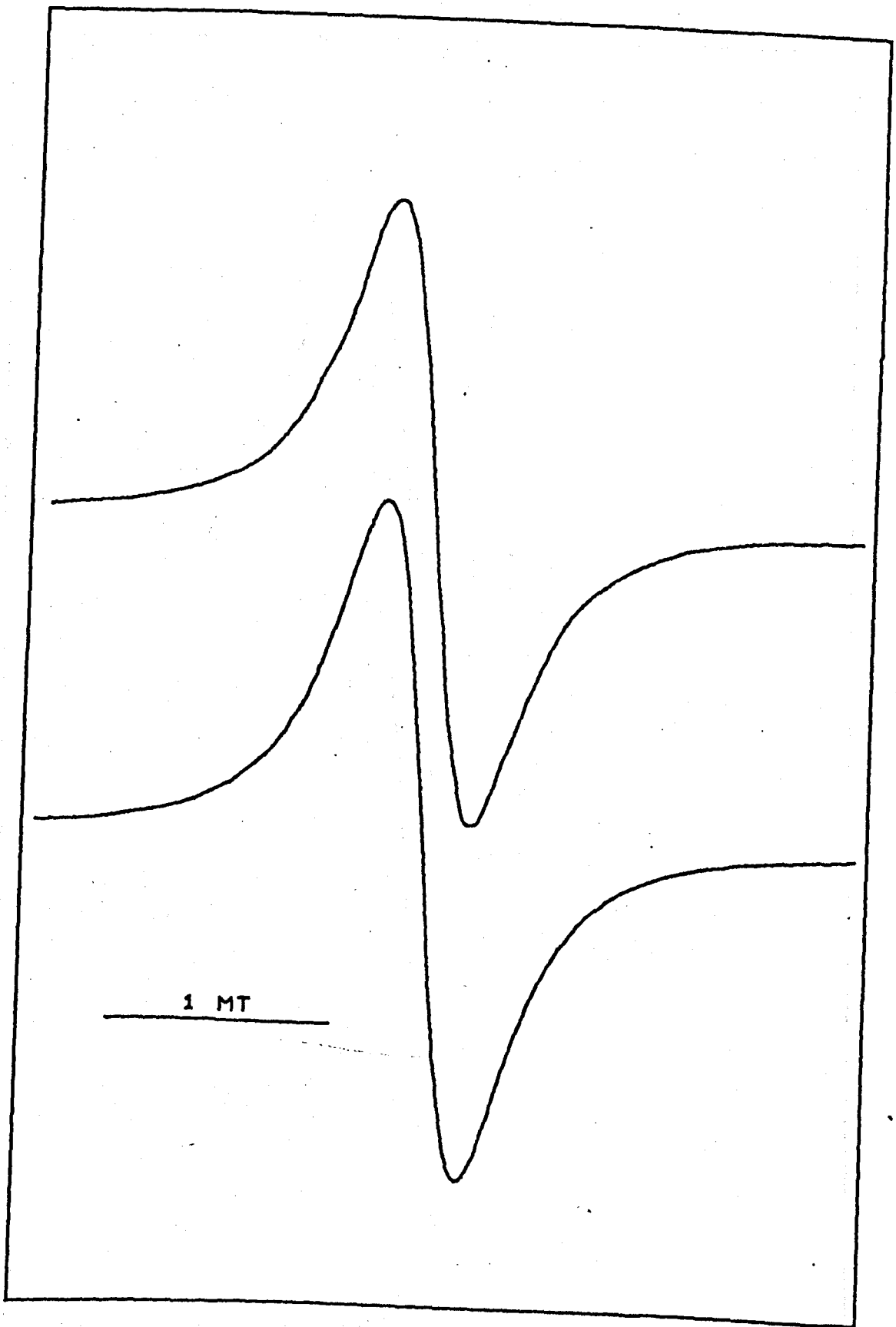
FIG. 7. 2 EXCHANGE NARROWED ESR SPECTRUM FROM POLY I. POLY C FIBRES
RECORDED EXPERIMENTALLY AT X-BAND, AND A THEORETICAL LORENTZIAN
LINESHAPE. (LINEWIDTH 1. 1 MT)
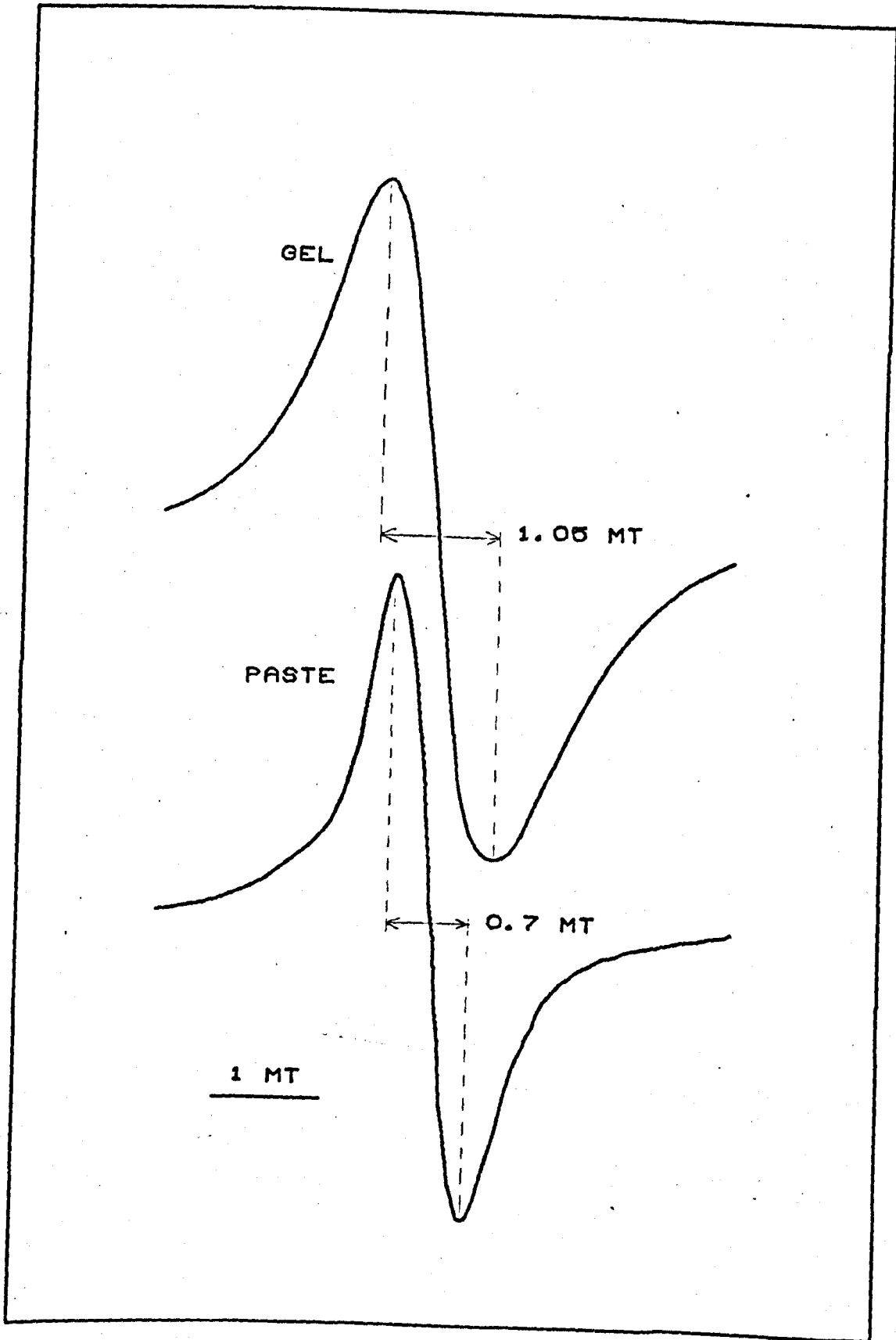
FIG. 7. 3 EXCHANGE NARROWED ESR LINESHAPES RECORDED AT X-BAND
FREQUENCY FROM A POLY I. POLY C GEL AND FROM A DRY PASTE OF PURE CPZ+.

irreversible loss of intensity in the ESR signal and an increase in the line-width. The *maximum* linewidth recorded was 1.83 mT, this spectrum showing the "immobilized" features characteristic of a DNA-CPZ$^+$ gel (Chapter 6). Figure 7.4 shows the width of the signal recorded from this particular *sample over a period of time,* plotted against the corresponding signal intensity (the doubly integrated area under the recorded resonance curve). It can be seen that the final signal intensity represented a drop by about a factor of 6 relative to the original signal intensity.

The signal recorded after cooling a sample at various temperatures between room temperature and 4.2 K was identical to that recorded from the same sample immediately prior to cooling, except for the expected increase in intensity.

Interpretation of the Experimental Results. The observed reduction in the intensity of the ESR signal with the time can be explained as arising from the dilution of the CPZ$^+$ radical, as various molecules decay to the dia-magnetic species. The observed dependence of the linewidth on concentration, and the fact that an increase in linewidth was observed as the concentration decreased as the radicals decayed, indicates that the single narrow line arose from an exchange narrowing process between molecules in close contact (see Section 2.4.4.).

To demonstrate the possibility of exchange narrowing taking place between closely packed CPZ$^+$ radicals, concentrated pastes of pure CPZ$^+$ were obtained by rapid mixing of CPZ hydrochloride and sodium persulphate pastes. The CPZ$^+$ tends to form aggregates, the colour of which is remarkably stable when in highly concentrated form. The dried amorphous pastes gave ESR signals consisting of single narrow lines with widths between 0.5 mT and 0.7 mT (Fig. 7.3.).

Thus the explanation of the CPZ$^+$/Poly I . Poly C spectra in terms of an

WIDTH OF THE EXCHANGE NARROWED LINE
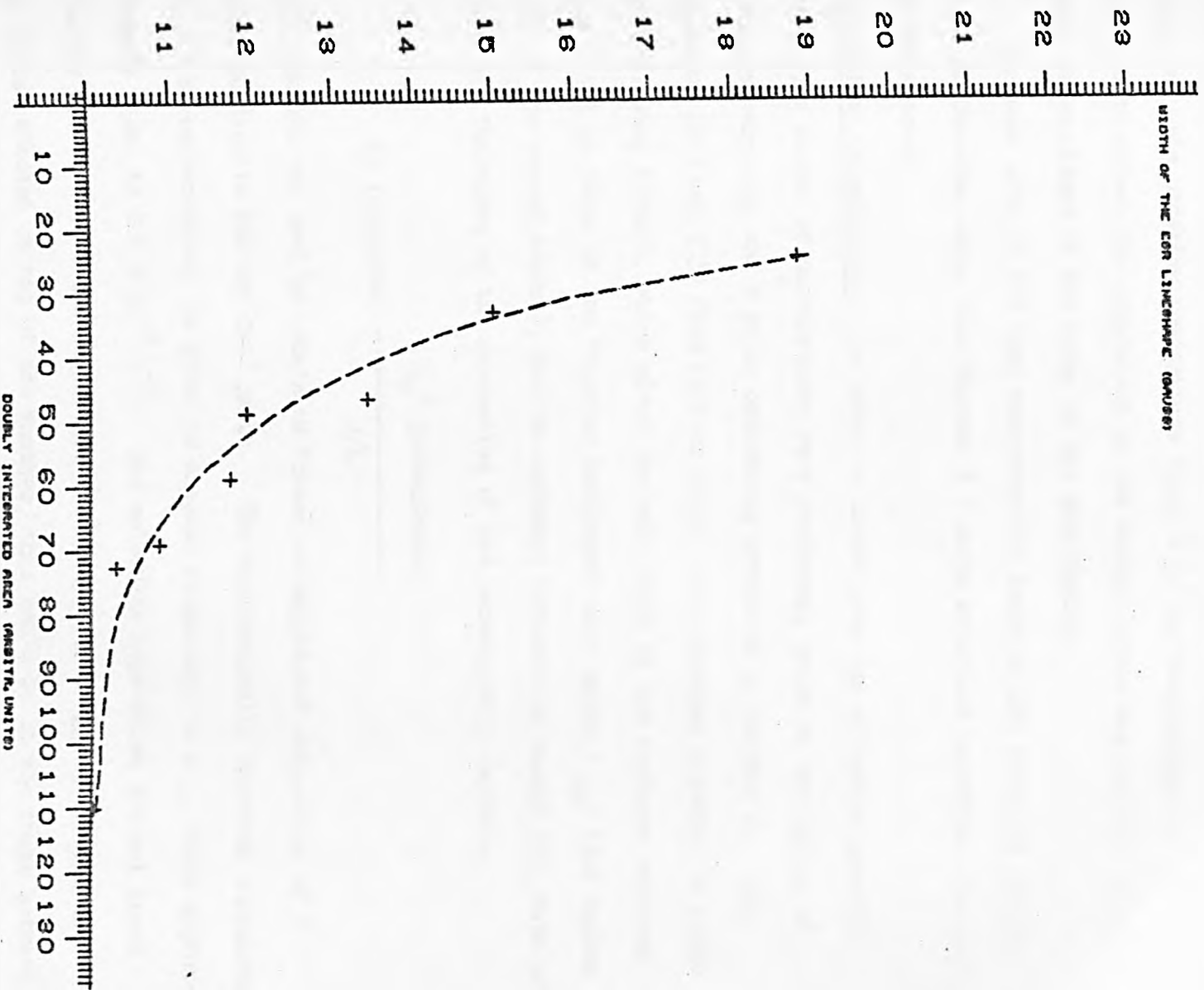
FIG.7.4, ILLUSTRATING THE INCREASE IN THE LINEWIDTH OF THE EXCHANGE
NARROWED ESR SIGNALS RECORDED FROM POLY I.POLY C FIBRES, UPON THE
DECAY OF THE RADICAL IN TIME (2 WEEKS).

exchange narrowing mechanism is substantiated by the observation of similar spectra from the dried CPZ^+ pastes. The low temperature behaviour of the lineshape is consistent with this interpretation. Indeed, while being above any spin ordering temperature (Ref. 4.), the temperature is only expected to affect the population of the energy levels and not the relative order of magnitude of the terms of the Hamiltonian.

The same drug at the same concentration bound to DNA produced broader lines of Gaussian shape (see Chapter 6.) which exhibited hyperfine structure and anisotropy.

Theoretical Calculations. In order to investigate the situation quantitatively, a series of calculations were performed, based on the theory of exchange narrowing and dipolar broadening presented in Chapter 2. The equations (24) and (25) from Section 2.4.2. were combined together to yield the following formula, which gives the half width of the exchange narrowed line ($\Delta\omega$) in terms of the "dipolar broadened" half width (ω_p) (the square root of the second moment), and the exchange interaction energy (J), both of which are functions of the separation of the paramagnetic centres:

$$\Delta\omega \text{ (observed)} = \frac{\omega_p^2 \text{ (calculated)}}{J/\hbar}$$

This formula was used to obtain an "order of magnitude" estimation of J corresponding to the dry CPZ^+ paste. The experimentally observed linewidth of 0.5 mT corresponded, in terms of angular frequency, to a $\Delta\omega$ value approximately equal to $4.4 \times 10^{-7} \text{ s}^{-1}$. The molecular separation was not known exactly but it was estimated that in a closely packed aggregate with the molecules stacked on top of one another, this could be in the range between 0.34 and 0.5 n m. The calculated "dipolar" half widths (ω_p) for these two separations (using Equation (22) from Section 2.4.2.) were equal to 73.7 and 23.2 mT respectively, so that the exchange interactions required to overcome these large dipolar effects were equal to 6.3×10^{-4} eV (approximately 10^{-22} J)

and 6.9×10^{-5} eV (approximately 10^{-23} J) - from the above formula. The contribution of the hyperfine splitting to the second moment of the line-shape has been neglected, as being very small compared to that of the dipolar effect.

The first figure calculated above corresponds, in terms of temperature, to approximately 7.2 K, so that close to 4.2 K one would have expected to detect a phase transition (the sample becoming ferromagnetic) (Ref. 4.). Such a transition, which was not detected experimentally, would have resulted in a large broadening of the lineshape (due to the internal magnetic fields), similar to the effect observed in the case of the DPPH radical (Ref. 5.). The second figure quoted above is in agreement with the observed behaviour of the sample and its magnitude compares favourably with values obtained from other systems (Refs. 6, 8.). Thus, the results of this calculation provides not only an upper limit for the value of the exchange interaction energy (10^{-23} J) but also a lower limit for the separation of the CPZ^{+} molecules (approximately 5 Å). However, these calculations should be regarded only as approximative, in view of the crudeness of the assumptions, e.g. the simple cubic lattice approximation.

As the exchange interaction depends on the overlap of the wavefunctions, one expects its magnitude to diminish very quickly with the increased sep-aration of the paramagnetic centres, so that the linewidth is determined only by the dipolar interaction at the larger separations. Exchange effects do not occur in the DNA/CPZ^{+} case, as demonstrated by the Gaussian character of the lineshapes and by the anisotropy of the spectra. It is interesting to show that the measured linewidth of these spectra (approximately 0.87 mT) can be accounted for by a dipolar broadening effect corresponding to a lattice constant of 1.38 n m, value which compares favourably (as an average) with the separation of about 4 n m of the radicals along the helix and the close lateral packing of the helices. On the other hand the Poly I. Poly C/

CPZ^+ system described above displays all the characteristics of exchange narrowing and on the basis of the calculations above one expects for this system a close packing of the radical molecules, with a molecular separation comparable to that in the dry CPZ^+ paste.

Conclusions. If the CPZ^+ radicals were distributed uniformly along the Poly I . Poly C molecules, then at the concentrations used, the separation between neighbouring ions would be too large (especially in the P/D = 6 case, where it would be around 2.2 n m) for any exchange interaction to occur. One would then expect a similar type of spectrum to that observed for the equivalent DNA preparations. The narrow line, therefore, leads to the postulate that the CPZ^+ binds to the Poly I . Poly C in clusters giving rise to the exchange narrowed lines. From the observation that a 6 fold decrease of the radical concentration resulted in a limiting spectrum similar to that of a DNA-CPZ^+ gel (where exchange narrowing does not occur) it is inferred that the number of radical molecules in a cluster is equal to about six.

There does not seem to be any evidence to suggest a preferred orientation of the CPZ^+ molecules or clusters relative to the fibre axis, either from the fibre ESR spectra or from the measured dichroic ratios, which were close to one in all the cases.

X-ray diffraction and birefringence measurements which were carried out in the same time showed that the degree of orientation of the RNA in these fibres was worse when compared to that in the regular double stranded Poly I . Poly C fibres (see Fig. 8.6.), but the basic helical structure seems to have been preserved. One noticeable feature of the XRD pattern from Fig. 8.6b is the build-up of the intensity in the centre of the pattern, particularly the intensity of the first layer line (which has the appearance of a streak), being stronger than that of the others, contrary to the pattern observed with the other nucleic acids. According to the helical X-ray diffraction theory (Ref. 7.) the odd-numbered layer lines could only be expected to be stronger than the even-numbered ones if the set of dyad axes

(perpendicular to the helical axis), which relate the two strands in all the double-stranded nucleic acids were lost. Such a situation could result either from the separation of the two strands or from the filling of the deep groove with drug molecules so that the double helix acquires the appearance of a single helix, and both these structures could well occur in this particular complex.

The formation of remarkably stable clusters along the Poly I . Poly C in the "looped" conformation is particularly interesting, especially as the complexes with the DNA and with the regular double stranded Poly I . Poly C behave in quite different manners.

7.1.3. Regular Double Helical Poly I . Poly C.

The binding of the CPZ^{+} to the "regular" double helical Poly I . Poly C (see Section 7.1.1.) can be deduced from the change in the colour of the solution. This change, which has accompnaied the binding of the CPZ^{+} to all the nucleic acid species mentioned up to now (Sections 6.2.2. and 7.1.2.) is taken as an indication that a favourable interaction, that allowed for a close contact of the chromophores, took place between the CPZ^{+} and the nucleic acids in question.

However, considering the stabilization of the colour of the radical in solution and gel, a different pattern is encountered with the "looped" structure, although, like in that case, a P/D dependence, with a distinct behaviour at low and high P/D ratios is observed: while red coloured gels can be obtained in the case of large P/D ratios (greater than about 6), completely transparent gels are obtained from small P/D ratios. This behaviour associates the increase in the concentration of the drug with the accelerated decay of the radicals and infers that the decay consisted in a a reaction between the radicals themselves, probably of the "dismutation" type, as mentioned in Section 6.1.2. It is possible, in view of the noticed

tendency of this drug to form aggregates (Section 7.1.1.), that aggregation (or dimerization) of CPZ^+ along the regular Poly I . Poly C chain does occur at low P/D ratios, but the particular configuration of these aggregates, as imposed by the drug-polynucleotide interactions and by the conformation of the polynucleotide chain, is so that the decay reaction is favoured.

When making fibres from the red coloured gels of high P/D ratios it was realised that the colour faded quickly as the gel dried, so that one ended up with fibres that were almost transparent. The extremely small radical concentration in these fibres made it impossible to record any ESR signal from them. However, the weak intensity of the colour was just suitable for optical dichroism measurements and the results obtained by taking advantage of this fact are presented in Chapter 8.

The decay of the CPZ^+ radicals bound on to the regular Poly I . Poly C observed upon drying the fibres (and hence upon the helices packing closer together) is an interesting property of this complex, that provides more information about the binding forces. A possible explanation is that the radical molecules are determined, as a result of the packing of the helices, to break their interactions with the exterior of the helix and are pushed towards the interior of the helical groove, where they are free to move along the groove and have the chance to mutually interact and decay. This hypothesis is consistent with the optical dichroism results (presented in Chapter 8) and also with the finding that the intermolecular separation of the helices, as measured from the X-ray diffraction pattern from Fig. 8.6a was the same as in the specimen without drug (at the same relative humidity).

7.1.4. Final Remarks on Poly I . Poly C.

The main findings connected with the Poly I . Poly C/CPZ^+ complexes were collected in a schematic form in the table from Fig. 9.1. Some of the conclusions, that have already been presented in the above sections, were also entered in the table. Reference to this table will be made with the

occasion of the general discussion that will follow in Chapter 9.

The only difference between the above two Poly I . Poly C preparations that can be invoked to account for the different results obtained, is the conformation of the polynucleotides. It was shown in Section 7.1. that the so-called "looped" Poly I . Poly C was suspected to contain single stranded bulges, because chance was given in the initial stage of its preparation to the two strands to come apart.

The evidence suggests that the "looped" structure favoured the formation of clusters of radicals, which displayed the property of exchange narrowing. The formation, in a very reproducible manner, of "exchange narrowing" clusters along the "looped" Poly I . Poly C is interesting, especially in view of the remarkable stabilization of the radical in these complexes, which might be of interest in practice. It is possible that the clustering is made possible by a definite steric feature existent in the "looped" conformation and/or by the possibility of the radicals to bind to particular chemical groups of the Poly I or Poly C that now became exposed in the single stranded regions.

In order to investigate these possibilities, it was decided to study the interaction of the CPZ[+] with the natural transfer RNA, which has a "looped" structure itself (see below) as well as with the single stranded Poly I and Poly C species.

7.2. Transfer RNA and Single Stranded Polynucleotides.

Transfer RNA (tRNA). The transfer RNA's are the molecules which transport the specific amino acids to the ribosome, which is the site of the protein synthesis in the cell.

The tRNA molecules are folded up in a branched structure, known as the "clover leaf pattern" (Ref. 3., p 433), consisting of double stranded regions and single stranded loops. The molecular weight of the known tRNA species is relatively small (about 30,000) and the base sequence, apart from some

regularities, depends on the tRNA species concerned.

The material used in the present investigation was the tRNA fraction from yeast. It was obtained from Sigma Chemicals Co. (Type III) and it was used without further purification. Solutions of a weak yellow colour were readily obtained by dissolving the material in aqueous NaCl solutions (0.05 M).

No change in the position of the visible absorption band of the radical was detected upon mixing CPZ^+ and tRNA solutions, suggesting that the interactions between the two species were not particularly strong. The radical was weakly stabilized upon mixing, if the P/D ratios were small, but the colour faded almost instantly if large P/D ratios were prepared. The preferential stabilization of the radical by the tRNA at small P/D ratios ressembled the behaviour of the "looped" Poly I . Poly C, rather than that of the "regular" species.

It was impossible to obtain the sedimentation of a gel by ultracentrifugation, because the molecular weight was too small. At the same time, the membrane filtration method (Section 6.2.1.) couldn't be used successfully either, because the chemical decay of the radical molecules was much faster than the rate of filtration.

Weak ESR signals could be obtained from solutions of P/D less than about 4. The signals ressembled the unresolved isotropic hyperfine spectra of the DNA/CPZ^+ solutions (Fig. 6.13.). The linewidths of 1.7 - 2 mT (measured with some uncertainty due to the small signal to noise ratio) fell in between the values obtained in the case of the DNA and of the "exchange narrowing" complex formed with the Poly I . Poly C.

In conclusion, the interaction of CPZ^+ with the tRNA is weak, as seen from the poor stabilization of the colour of the radical and the lack of colour change upon mixing the two species. However, similarities of the behaviour of tRNA with that of the "looped" Poly I . Poly C have been noted,

particularly the distinct behaviour at low and high P/D ratios and the linewidths of the ESR signals being smaller than that in the DNA case. It is thus possible that CPZ$^+$ follows the same basic pattern of binding (see the table from Fig. 9.1.) to both these polynucleotide species (tRNA and "looped" Poly I . Poly C).

Single Stranded Poly I and Poly C.   The single stranded polyribonucleotides Poly I and Poly C were obtained from Sigma Chemicals Co.   The two species have been characterised (Ref. 1, 2.).   Particularly it has been noted that Poly C becomes protonated at low pH values (about 4 - 5) and can form double stranded associations.   A self association of Poly I also occurs under high ionic strength conditions (1 M NaCl).

Complexes of Poly C and Poly I with CPZ$^+$ were made as described above, but the colour of the radical, for all the P/D ratios, faded rapidly (in fact more rapdily than in the case of the aqueous pure CPZ$^+$ solutions), and completely transparent gels were obtained.   A similar behaviour was observed using Poly A.

This behaviour shows (with reference to Section 7.1.4.) that the affinity of CPZ$^+$ to particular chemical groups in the single stranded polynucleotides cannot be made responsible for the stability of the complex obtained between CPZ$^+$ and the Poly I . Poly C in the "looped" conformation.   One is led to the general conclusion that a well defined double stranded structure (not necessarily a regular double helix) is required for the binding and the stabilization of the radical on to the nucleic acids.   This topic, together with the possible biological significance of the above results will be discussed in Chapter 9.

REFERENCES.

1. A. R. HODGSON: PhD Thesis, London University (King's College), (1969).

2. S. ARNOTT, D. W. L. HUKINS, S. D. DOVER, W. FULLER, A. R. HODGSON:
    J. Mol. Biol., 81, 107-122, (1973).

3. V. A. BLOOMFIELD, D. M. CROTHERS, I. TINOCO: Physical Chemistry of
    Nucliec Acids, Harper and Row, (1974).

4. C. KITTEL: Introduction to Solid State Physics (4th Edition), John
    Wiley and Sons Inc., (1976).

5. D E. DUGDALE: (University of Keele), Private Communication,
    (1976)

6. J. R. BESWICK, D. E. DUGDALE: J. Phys. C: Solid State Phys., 6, 3326-
    3340, (1973).

7. B. K. VEINSTEIN: Diffraction of X-rays by Chain Molecules, Elsevier,
    (1966).

8. P. W. ANDERSON, P. R. WEISS: Revs. Modern Phys., 25, 269-276, (1953).

CHAPTER 8.

OPTICAL PROPERTIES OF THE NUCLEIC ACID - CHLORPROMAZINE FIBRES.

8.1. Introduction.

This chapter describes the optical properties, birefringence and linear dichroism of the nucleic acid - chlorpromazine[+] fibres. The value of the optical measurements lies in the fact that they can confirm the existence of a preferred orientation of the drug molecules in the fibre and provide independent measurements of the degree of order in the fibre (reference to this method has been already made in Chapter 6.).

The investigation of the optical properties was carried out using techniques and equipment developed by H. Porumb (Ref. 1.). It was possible to present the theoretical results in a quantitative way by performing computer simulations of the birefringence and dichroism, by using an extension of the FIBRE computer program. (The task was divided between a number of subroutines, not included in the Appendix.)

The theoretical section is followed by a presentation of the experimental results obtained with three different kinds of nucleic acid - CPZ[+] fibres; DNA; regular double stranded RNA (Poly I . Poly C), and the rarely occuring form of "stretched" DNA (Ref. 2.). The evidence provides support for the approximate perpendicularity of the CPZ[+] molecule to the DNA helical axis but suggests that CPZ[+] adopts external modes of binding to both the DNA and the double stranded RNA.

8.2. Theoretical Simulations of the Fibre Dichroism and Birefringence.

8.2.1. The Dichroism.

The absorption of plane polarized light by a chromophore (drug molecule) is proportional to the square of the cosine of the angle between the direction of polarization of the light and the relevant electronic transition moment

(Ref. 3.). The same fibre model which was developed in connection with the interpretation of the ESR results (Chapter 6) was adopted, i.e. the drug molecules were considered to be bound rigidly on to the nucleic acid molecules, which were assumed to have a Gaussian distribution of orientations about the fibre axis. The computations were carried out using the FIBRE computer program described in Chapter 5. The algorithm operated cylindrical averaging routines at the level of both the fibre and the nucleic acid helix, in which the individual contributions of each molecule to the absorptions of light polarized perpendicular and parallel to the fibre axis were accumulated separately, by taking into account the weight of each orientation (see Section 5.3.). The two results were divided into one another to yield the dichroic ratio D.

Fig. 8.1. represents the calculated dichroic ratios for drug molecules bound in fibres of various Gaussian half-widths, against the degree of tilt of the drug molecule, relative to the nucleic acid helical axis. The tilt is the angle between the normal to the plane of the drug and the helix axis. The absorption is considered to be due to an electric transition moment with the coordinates (1, 0, 0) in the molecular frame (Section 5.3.), which is so that the angle between the helical axis and the transition moment is the complement of the angle of "tilt". The curve from Fig. 8.1. referring to a perfectly oriented fibre, reproduces the features of the theoretical calculations performed by Fraser (Ref. 3.). It should be noted that as the orientation of the electric transition moment in the chromophore deviates from the above one, the crossover point moves towards 90° of tilt, after which the curves do not intersect the D = 1 line and the reversal of the dichroism will not occur.

Except for a few cases, the exact orientation of the electric transition dipole in the chromophore is not known. In the case of planar or approximately planar π electron systems, such as Proflavine (Refs. 4., 5.),

OPTICAL DICHROISM

OF FIBRES OF VARIOUS MISALIGNMENTS

(ABSORPTION DUE TO A SINGLE TRANSITION DIPOLE IN THE PLANE OF THE CHROMOPHORE)
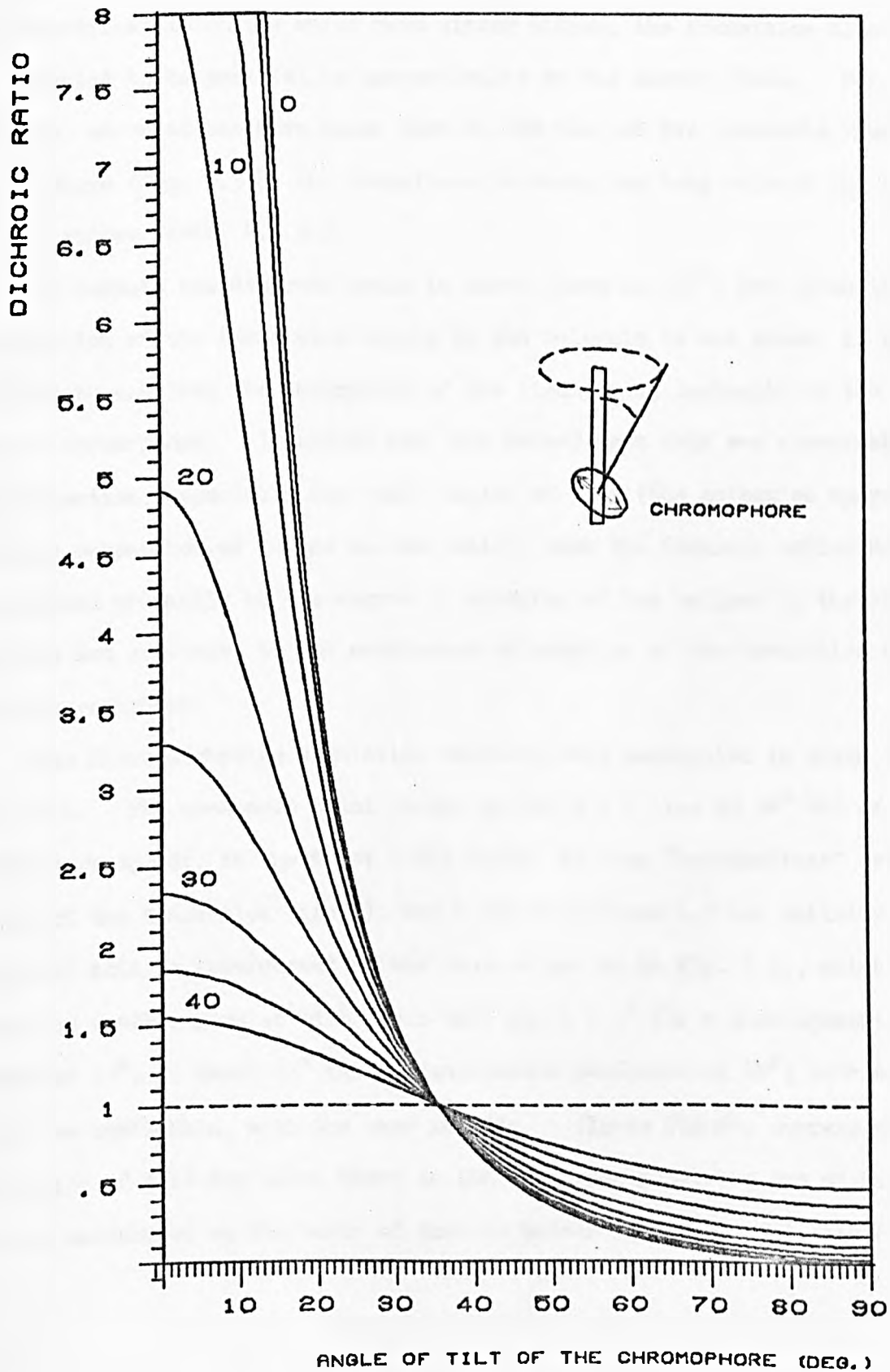
FIG. 8. 1

Ethidium Bromide (Ref.6.) or Phenothiazine (Ref. 7.), the visible absorption bands were shown to correspond to strongly allowed π - π * transitions, with the transition dipoles lying in the general plane of the chromophores. In symmetrical molecules which have mirror planes, the transition dipole is expected to be parallel or perpendicular to the mirror plane. For example, calculations have shown that in the case of the symmetric Proflavine chromophore (Fig. 9.3.), the transition is along the long axis of the tricyclic system (Refs. 4., 5.).

To compute the dichroic ratio in cases (such as CPZ[+]) for which the orientation of the transition dipole in the molecule is not known, it was decided to consider the absorption of the light being isotropic in the plane of the chromophore. It turned out (see below) that this was a reasonable approximation, especially for small angles of tilt (the molecules approximately perpendicular to the helical axis), when the dichroic ratios are determined primarily by the degree of ordering of the helices in the fibre, and are not sensitive to the particular orientation of the transition dipole in the chromophore.

The fibre dichroism simulation based on this assumption is shown in Fig. 8.2. The crossover point occurs on the D = 1 line at $54°$ $44'$ of tilt (This corresponds, in the first model above, to some "intermediate" orientation of the transition dipole), and D varies between 0.5 and infinity. The vertical axis is intercepted at the same values as in Fig. 8.1., which means that for small angles of tilt (less than about $7.5°$ for a misalignment parameter of $15°$, or about $25°$ for a misalignment parameter of $40°$) both models would be applicable, with the same results. (These figures correspond to the angle of tilt for which there is 10% discrepancy between the dichroic ratios calculated on the basis of the two models from Figs. 8.1. and 8.2.

OPTICAL DICHROISM OF FIBRES

OF VARYING DEGRES OF MISALIGNMENT

(ABSORPTION ISOTROPIC IN THE PLANE OF THE CHROMOPHORE)
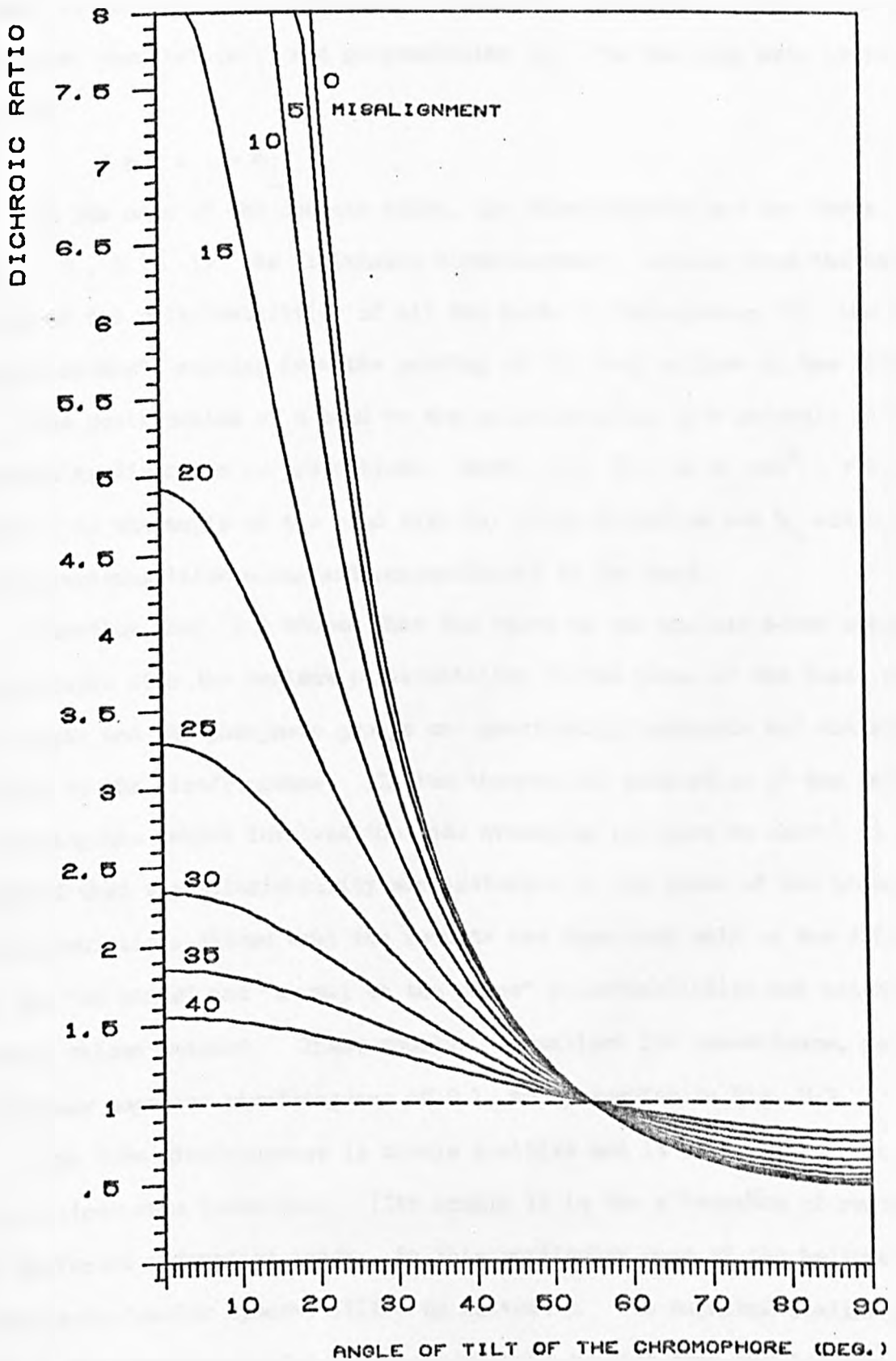
FIG. 8.2

8.2.2. Birefringence.

The birefringence of a long object (e.g. a nucleic acid molecule or fibre) is defined as the difference between the refractive indices for light polarized parallel ($n_{||}$) and perpendicular ($n_\perp$) to the long axis of the object:

$$\Delta n = n_{||} - n_\perp$$

In the case of the nucleic acids, the birefringence has two terms (Refs. 8., 9.): 1) the "intrinsic birefringence", arising from the anisotropy of the polarizabilities of all the bonds in the system; 2) the "form birefringence", arising from the packing of the long helices in the fibre.

The contribution of a bond to the polarizability of a molecule in a particular direction is proportional (Refs. 10., 11.) to $b_L \cos^2 \Omega + b_T \sin^2 \Omega$, where Ω is the angle of the bond with the given direction and b_L and b_T are the polarizabilities along and perpendicular to the bond.

Tsvetkov (Ref. 9.) showed that the bases of the nucleic acids are highly anisotropic with the maximum polarizability in the plane of the base, while the sugar and the phosphate groups are practically isotropic and contribute little to the birefringence. In the theoretical simulation of the intrinsic birefringence (which involved the same averaging routines as above) it was assumed that the polarizability was isotropic in the plane of the bases. The calculations showed that the results are dependent only on the difference of the "in plane" and "normal to the plane" polarizabilities and not on the actual values assumed. These results, normalized for convenience, for a maximum negative birefringence of 0.1, are presented in Fig. 8.3.

The form birefringence is always positive and it would arise even if the helices were isotropic. (Its origin is in the alternation of regions of different refractive index; in this particular case of the helices and the intermolecular spaces, filled by solvent.) Its magnitude, although not at all negligible (Ref. 8.) is certainly smaller than the intrinsic term,

INTRINSIC BIREFRINGENCE OF FIBRES

OF VARIOUS MISALIGNMENTS

FIG. 8.3
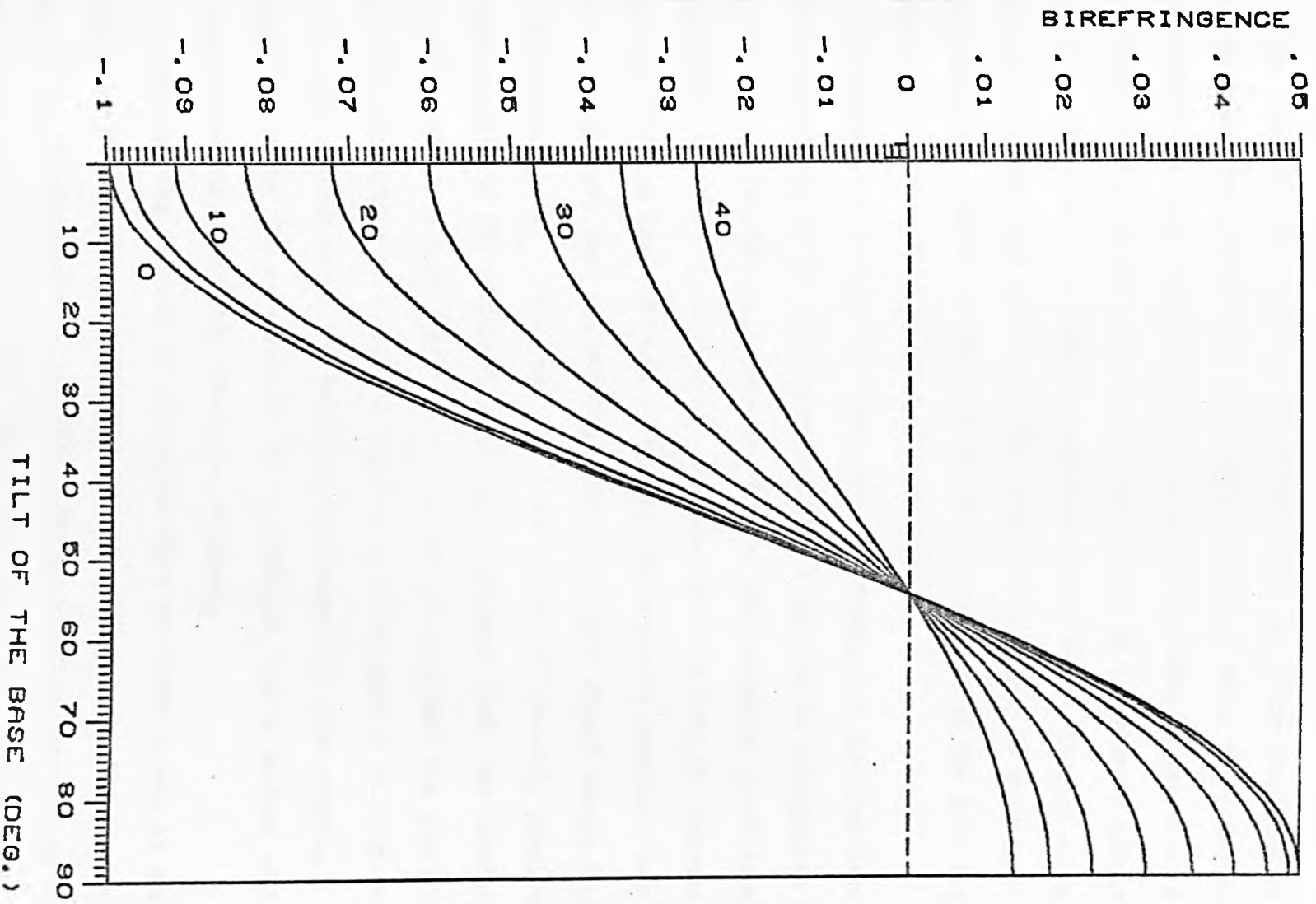
or otherwise one could not account for the negative birefringence of the nucleic acids. In one particular system (Ref. 9.) it was estimated to represent about half (in fact 58%) of the magnitude of the intrinsic term.

The form term was computed by assuming that the fibre consisted of bunches of helices distributed in a Gaussian fashion about the fibre axis. The value of the form birefringence of a bunch was taken to represent a specified fraction of the intrinsic birefringence of a perfectly aligned fibre with zero tilt. A bunch is analogous to a "bond" oriented along the bunch axis, because its polarizability (refractive index) is maximum along this direction. Based on this analogy the calculation of the form term became equivalent to that of the intrinsic term.

It can be seen in Fig. 8.4. that the introduction of the form term, which is sensitive to the misalignment of the fibre but is independent of the base tilt, resulted in the displacement of the crossover point towards lower angles of tilt. For example, choosing the form term to represent arbitrarily 58% of the magnitude of the maximum negative intrinsic term, the theory predicts that the birefringence of a fibre should change sign for 32° of base tilt. This angle is close to the 30° recently predicted in connection with the conformation of the "stretched" DNA, the birefringence of which is close to zero (Ref. 12.). It can be seen that the plots from Fig. 8.4. (normalized to a maximum negative birefringence of 0.1, which is close to the maximum value one recorded experimentally) also provide a reasonable fit for the experimental values obtained from a variety of fibres at the room relative humidity (see next sections).

As regards the swelling of the fibres upon the water uptake at high relative humidities, it is considered that its effect is to decrease both terms of the birefringence in proportion to the dilution, as well as to change the relative contribution of the form term in accordance to the classical formula derived by Weiner for a collection of oriented rods (Ref. 13.).

FIG.8.4
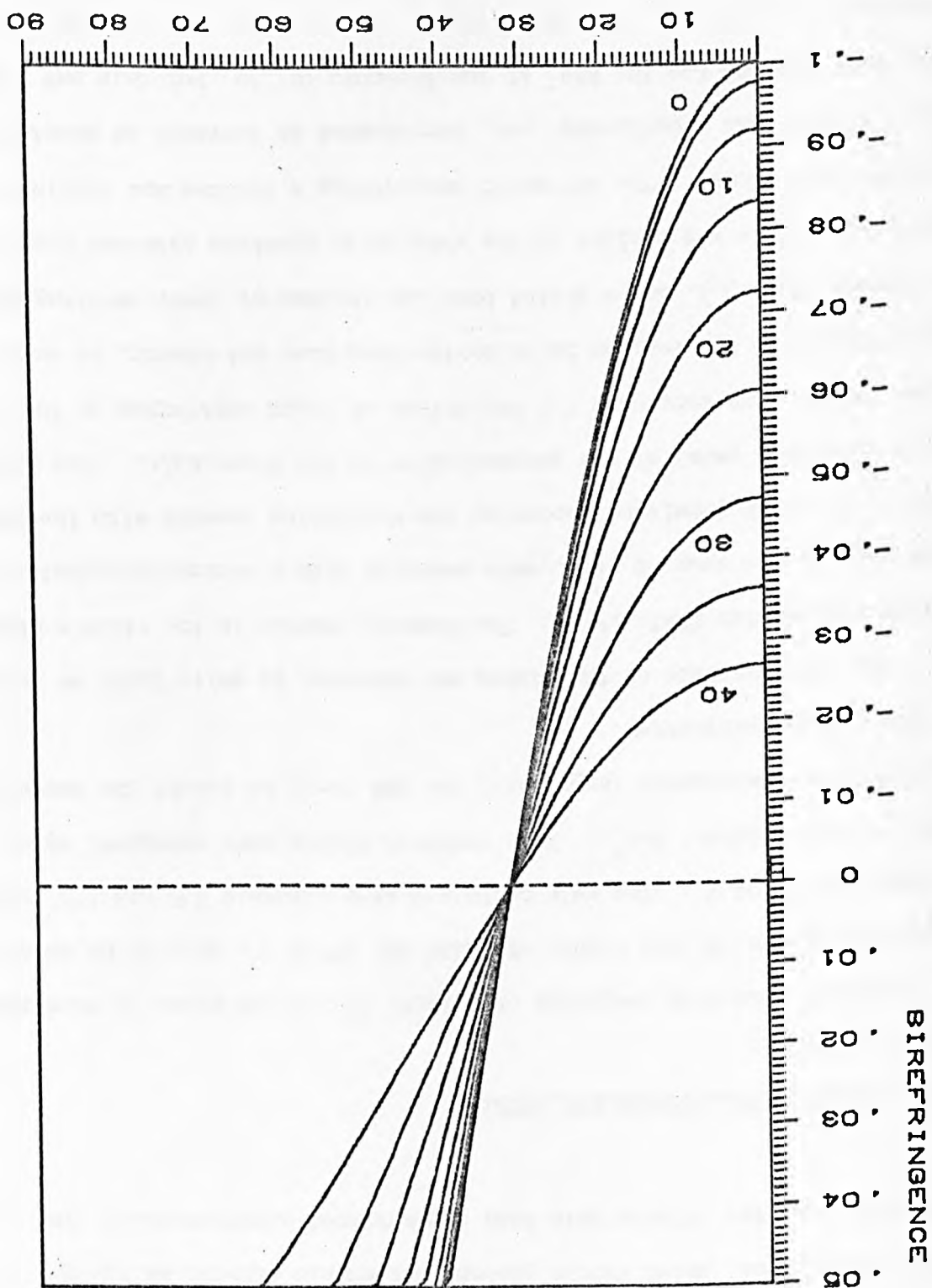
The contribution of the drug molecules to the fibre birefringence was not considered explicitly, but it is thought that, by analogy with the nucleic acid bases, they would have a high polarizability in the plane of their chromophores, which should produce detectable effects at low P/D ratios. Both the above two effects have been demonstrated experimentally (Ref. 1.).

8.3. Experimental Methods and Results.

8.3.1. Methods.

Nucleic acid-drug complexes of initial P/D ratios about 12 were obtained from calf thymus DNA and double stranded RNA (Poly I . Poly C) as described in Chapters 6 and 7. The gels contained approximately 25% and 18% respectively of the original CPZ^+. Well oriented fibres were obtained, which were sufficiently transparent (especially the RNA ones) to permit the measurement of the optical properties.

The birefringence of the fibres was measured in white light by using a Bereck compensator (Ref. 14.). The dichroic ratios in the visible absorption band of the drug, D $(\frac{\perp}{\parallel})$, were measured with a microspectrophotometer (Ref. 1.), which permitted recording the absorption spectra with the incident light polarized parallel and perpendicular to the fibre axis. The absorption spectra were corrected for the effect of light scattering by the specimen, by reference to the regions in which the drug does not absorb, as suggested by Fraser (Ref. 3.), but a tilted baseline (higher at lower wavelengths) was used. This was similar to the absorption spectrum obtained from the nucleic acid alone. The effect of considering a shifted and inclined baseline, rather than a horizontal one, represented an increase of about 30% (for both the DNA and the RNA) in the dichroic ratios, but this had the advantage of yielding a constant D value over a wider range of the absorption band.

9.3.2. Results.

The measured dichroic ratios of the batch of DNA/CPZ[+] fibres were in the region of 4 ± 1. These values are relatively high when compared to those obtained with "intercalating" drugs which bind strictly perpendicular to the helix axis, such as Adriamycin and Daunomycin (D - 3 - 6) (Ref. 1.), or Proflavine (Ref. 16.). The negative birefringence of the same fibres at the room relative himidity (50%) ranged from 0.05 to 0.1 (average 0.06), occasionally higher than that of the DNA in the same conditions (0.06).

One of the DNA/CPZ[+] fibres presented a long, thinner region, corresponding to the "stretched" DNA form (Ref. 2.),in which the bases are thought to be tilted by a larger angle than in any other known forms of the nucleic acids. The dichroism in this region was reversed relative to the normal region (D = 0.64) and the birefringence was close to 0 (in fact it became positive at 0.005). The "stretched" region returned to "normal" upon the exposure of the fibre to a higher relative humidity during 3 days X-ray diffraction run. The birefringence became negative (at -0.07) like the rest of the fibre but it was impossible to measure the dichroic ratio because the drug bleached in the intervening period.

The dichroic ratios of the RNA.CPZ[+] fibres were relatively high, at about 2 - 2.4 and these values were similar to those obtained from the "intercalating" drugs Adriamycin and Daunomycin bound on to the RNA. The measured negative birefringence ranged between 0.053 and 0.073 (average 0.06).

8.4. Interpretation of the Results.

8.4.1. DNA/CPZ[+] Fibres.

The dichroic ratios in the three cases above were significantly different from one (the value expected for complete disorder), showing that there was a considerable degree of orientation of the drug molecules in the fibres

in all cases. In fact the properties of the DNA/CPZ^{+} fibres were comparable to those obtained with the "intercalating" drugs. This comparison can be taken as a further evidence for the preferential orientation of the CPZ^{+} with its plane perpendicular to the DNA helical axis, as suggested by the ESR results (Chapter 6).

The quantitative analysis of the dichroism results shows that the limits within which this perpendicularity has been demonstrated are the same as those obtained from the simulation of the ESR spectra. Indeed, the measured dichroic ratios (4 $\pm$ 1) correspond, with reference to Fig. 8.2., to Gaussian misalignment parameters of about 23 $\pm$ 4°, 19 $\pm$ 5° and about 0° if the assumed tilt angles of the drug molecule relative to the helical axis were 0°, 20° and 30° respectively. The third case, predicting a perfectly aligned fibre, can be ruled out as it disagrees with the X-ray diffraction patterns (Fig. 8.5.), which show the existence of a considerable degree of misalignment.

This clearly excludes the possibility of the CPZ^{+} being bound along the groove of the DNA helix (e.g. along one of the phosphate chains),because this would impose a tilt angle equal or greater than the angle of ascent (30°) of the DNA helix (see also next section).

On the other hand, the misalignment angle predicted in the first case is in very good agreement with the value obtained from the simulation of the ESR spectra (27°), on the basis of the same binding model. Like in that case, the measured dichroic ratio reflects the total misorientation, which could be considered to arise from the convolution of the misalignment of the helices with a scatter in the angle at which the drugs bind to the helix. The birefringence value itself corresponded to a misalignment parameter of the B-DNA helices of 25° (although this value is dependent upon the rather arbitrary normalization of the theoretical plots from Fig. 8.4.).

The second case, which is still acceptable, shows that the results can be accounted for if there was a finite tilt of about 20° of the drug molecules

and it is thought that such changes in tilt might well occur with changes in the DNA conformation upon hydration, without being detectable. It will be remembered that neither the ESR nor the optical investigation showed noticeable variations with the relative humidity but some X-ray diffraction patterns of the P/D 12 batch at low relative humidities (close to the room conditions) revealed the coexistence of both the A and B conformation of DNA (Fig. 8.5.).

In conclusion, the dichroism results confirmed the findings of the ESR investigation: The preferred orientation of the drug molecule relative to the helix axis with a tilt angle in the range $0 - 20^{\circ}$ and the possibility of a scatter in the binding angle making a small contribution to the total misorientation. It is not possible to decide firmly on the basis of these results whether the binding of CPZ^+ to DNA is "externally" or by "intercalation", but one is inclined to believe that an external mode of binding would fit better the behaviour inferred from the above results as well as those of the ESR investigation. Particularly such a mode of binding would allow for departures from the rigorous perpendicularity of the drug molecule to the helical axis and in this way it would allow for the binding of CPZ^+ to both the B and A forms of the DNA. Such a situation would not require alterations of the classical ideas on intercalation (see below) and would also provide a simple explanation (see below) for the orientational transition that takes place in the DNA upon "stretching".

8.4.2. RNA and "Stretched" DNA Fibres.

The results which are to be discussed in this section are interesting both for the binding of CPZ^+ on to these species and also in relation to the general aspects of drug binding to nucleic acids. Particularly, the results confirm that CPZ^+ as well as the "intercalating" drugs bind to the RNA, and
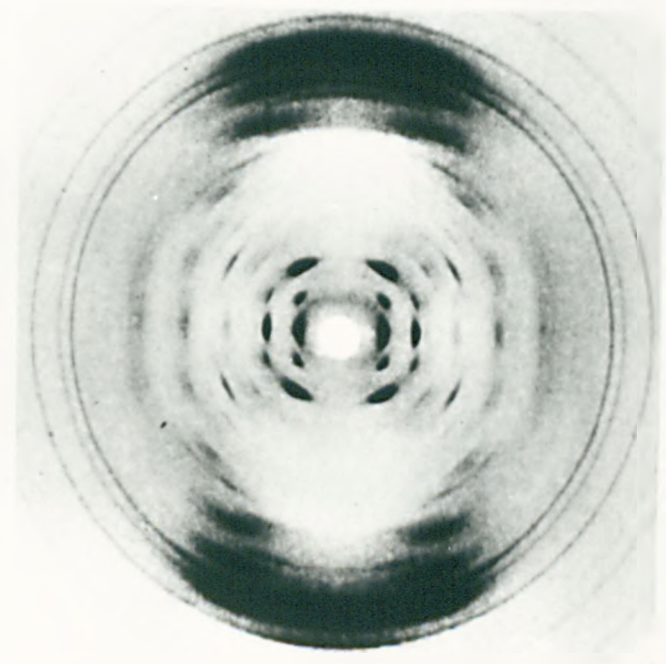
FIG. 8.5 X-RAY DIFFRACTION PHOTOGRAPHS FROM A DNA-CPZ$^+$ FIBRE
(P/D 12), AT A). 92 %, AND B). 66 % RELATIVE HUMIDITY.
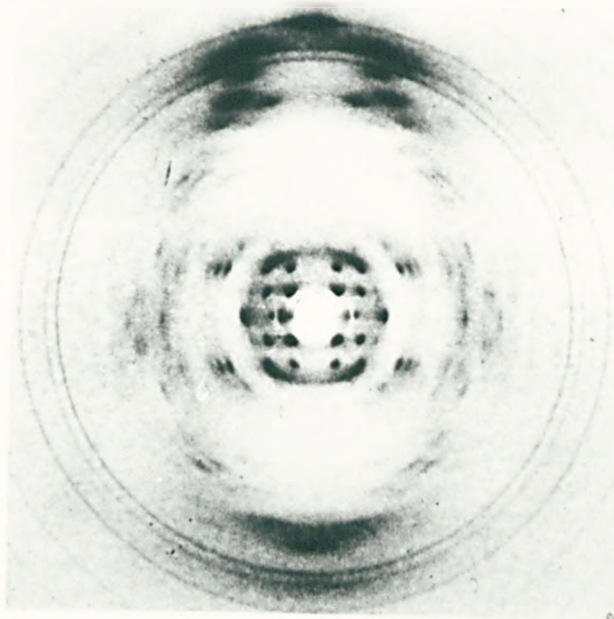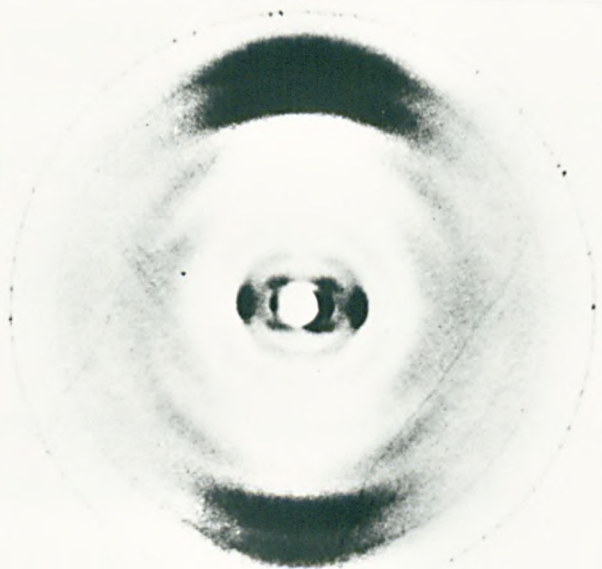
FIG. 8.6 X-RAY DIFFRACTION PHOTOGRAPHS FROM FIBRES OF COMPLEXES
OF CPZ$^+$ WITH POLY I. POLY C IN A). REGULAR DOUBLE HELICAL CONFIGU-
RATION, AND B). LOOPED (PARTIALLY DENATURED) CONFIGURATION.
(RELATIVE HUMIDITY : A). 92 % , B). 75 %)

show that they adopt an ordered distribution inside the fibre; facts little emphasised in the literature.

It will be remembered, however, that the intercalation is thought to be possible only in the B form of the DNA (Ref. 15, 16.) and not the A form or the similar two forms (with tilted bases) of the Poly I . Poly C (Ref. 17.).

The X-ray diffraction patterns of the Poly I . Poly C/CPZ[+] fibres (Fig. 8.6) show that the RNA assumed the 12 fold helix conformation (Ref. 17.), characterised by a tilt of the bases of about 12° measured between the normal to the base and the helical axis (N.B. the authors used a different definition of the tilt) and an angle of ascent of the phosphate backbone of about 32°. The angle of ascent is the angle made by the tangent to the continuous helix drawn at the radius of the phosphate groups, with the plane perpendicular to the helical axis.

A comparison of the measured dichroic ratios (2 - 2.4 for both the CPZ[+] and the "intercalating" drugs - Ref. 1.) with the theoretical calculations shows that the results cannot be accounted for in terms of the molecule being "sandwiched" between the RNA base pairs with a tilt angle of about 12°, because this would require a too large misalignment ($30 - 35^{\circ}$), the existence of which is not supported by the appearance of the X-ray diffraction patterns.

On the other hand, the results can easily be accounted for if one assumes that the tilt angle was the same as the angle of ascent of the 12-fold helix (32°) and the Gaussian parameter was equal to 10 - 20°. (N.B. The birefringence value would fit a misalignment parameter of about 20°). It seems reasonable to suggest that due to the close packing of the helices the CPZ[+] and the "intercalating" drugs are determined to fill the grooves of the RNA, where they adopt an angle of tilt equal to the ascent angle of the groove. It is possible that the molecules, while exhibiting a weak nonspecific attraction towards the negatively charged backbones, are quite free to move

along the groove of the RNA and this ability to move (and hence to interact with each other and with the solvent)could be correlated with the fast decay of the CPZ^+ radical bound in the RNA fibres.

In the "stretched" DNA fibre, the reversal of the dichroism upon stretching shows that the drug molecules, rather than leaving their binding sites and becoming randomly oriented (as one would expect on the basis of the intercalation model), remained bound in a regular fashion on to the DNA but their orientation relative to the helical axis suffered a dramatic change. The comparison of the theoretical and experimental results brings out an interesting point.

On the one hand, it is predicted that the dichroism should reverse for a tilt angle of the molecule greater than $54°$ 44', in the "absorption isotropic in the plane" model (which is the more likely), or, in the "single transition" model, for a tilt greater than $35°$ 16'. A dichroic ratio of 0.64 implies that the angle of tilt should be considerably higher than the smallest of these two figures (perhaps about $72°$). On the other hand, the birefringence becomes zero for an angle of tilt of the bases equal to about $32°$.

This situation decisively rules out the possibility of the drug molecules being stacked on to the nucleic acid bases so that they would move together upon stretching, and infers the existence of an external mode of binding. An interesting possibility would be the one by which the molecules didn't have to leave their original binding sites on the "normal" DNA during the transition to the "stretched" conformation but just suffered a rotation together with the groups on which they were bound (e.g. the phosphate groups on the bases), so that the drug molecules, while being sensitive to the movement of the bases, undergo a change in their tilt angles that is larger than the change of the tilt of the bases themselves.

8.4.3. Conclusions.

In addition to confirming the ESR results on the binding of CPZ^+ to the DNA, the present investigation showed that the interaction of CPZ^+ with the three different kinds of nucleic acid can be better understood in terms of an external mode of binding on to the nucleic acids, as opposed to intercalation. One cannot exclude the possibility that the binding involves the same basic interactions in all the three cases (such as electrostatic attraction to the phosphate chains), possibly supplemented by other stabilizing forces (hydrogen bonding, hyprophobic effect), the balance of which would determine in each case the preferential orientation of the drug, (and, indirectly, the chemical stability of the radical).

REFERENCES.

1. H. PORUMB: PhD Thesis, Keele, (1976).

2. M. H. F. WILKINS, R. G. GOSLING, W. E. SEEDS: Nature, 167, 759-760, (1951).

3. R. D. B. FRASER: J. Chem. Phys., 21, 1511-1515, (1953).

4. L. L. INGRAHAM, H. JOHANSEN: Arch. Biochem. Biophys., 132, 205-209, (1969).

5. H. HO, Y. J. I'HAYA: Int. J. Quart. Chem., 2, 5, (1968).

6. P. U. GIACOMONI, M. LE BRET: FEBS Letters, 27, 227-230, (1973).

7. H. H. MANTSCH, J. DEHLER: Canad. J. Chem., 47, 3173-3178, (1969).

8. V. A. BLOOMFIELD, D. M. CROTHERS, I. TINOCO: Physical Chemistry of Nucleic Acids, Harper and Row, (1974).

9. V. N. TSVETKOV: Polymer Sci. USSR, 4, 1456, (1963).

10. N. H. HARTSHORNE, A. STEWART: Crystals and the Polarizing Microscope, E. Arnold, (1970), (4th Edition).

11. W. E. SEEDS: PhD Thesis, London (1951).

12. C. NAVE: Private Communication.

13. WEINER, (quoted by Ref. 10.).

14. A. N. WINCHELL: Elements of Optical Mineralogy, Wiley, (1949).

15. W. FULLER, M. J. WARING: Ber. Dtsch. Bunsenges. Phys. Chem., 68, 805-808, (1964).

16. D. M. NEVILLE, JR., D. R. DAVIES: J. Mol. Biol., 17, 57-74, (1966).

17. S. ARNOTT et al: J. Mol. Biol., 81, 107-122, (1973).

CHAPTER 9.

CONCLUSIONS.

In this chapter the affinity and specificity of the radical cation of CPZ in relation to DNA and the possible biological implications of these studies is discussed.

The chapter is continued with a discussion of related pieces of work performed with other drugs. The limitations of the method developed are pointed out, and improvements, both on the instrumentational and experimental side, are suggested. Possible extensions of the ESR work with CPZ^+, as well as with other drugs, will be outlined, together with suggestions for further work.

9.1. The interaction Between CPZ^+ and the Nucleic Acids.

9.1.1. Discussion of the Behaviour of CPZ^+ to Various Nucleic Acid Species and Possible Biological Significance.

The experimental results relevant to this discussion were collected together in the table from Fig. 9.1. The observed change of the colour of the CPZ^+ radical upon its interaction with the DNA (see Section 6.2.2.) as well as the stabilization of the colour are consistent with a strong binding of CPZ^+ to the DNA. The observed independence of the stabilizing effect and the invariance of the character of the ESR spectra with the P/D ratio suggest that the binding of CPZ^+ to DNA takes place in individual fashion, rather than in aggregate, at all the P/D ratios. At the same time, the formation of complexes of a well defined geometry, as revealed by the orientational study performed on fibres (Section 6.4.), implies that the binding is specific, i.e.

TYPE OF NUCLEIC ACID OR POLY-NUCLEOIDE	DOES THE COLOUR OF THE SOLUTION CHANGE UPON MIXING	IS COLOUR STABILIZED IN SOLUTION AND GEL LARGE P/D (>6)	SMALL P/D (<6)	IS COLOUR PRESERVED UPON DRYING THE FIBRE	TYPE OF COMLEX DEDUCED BY ESR	CONCLUSIONS
CALF THYMUS DNA	YES	YES (EQUALLY)	YES	YES	ORIENTED	-STRONG BINDING IN INDIVIDUAL FASHION. -THE SAME PATTERN OF BINDING AT ALL P/D.NO AGGREGATES (NO AGGREGATES) -BINDING RESULTS IN STABILIZATION OF THE RADICAL.
LOOPED POLY I.POLY C	YES	YES (LESS THAN DNA)	YES (BETTER THAN DNA)	YES	EXCHANGE NARROWING AGGREGATES	-WEAK BINDING AS INDIVIDUALS AT LARGE P/D. -FORMATION OF AGGREGATES ALLOWED BY THE LOOPED CONFORMATION, IN WHICH THE RADICALS ARE STRONGLY STABILIZED.
REGULAR DOUBLE HELICAL POLY I.POLY C	YES	YES (AS ABOVE)	NO	NO	-TOO WEAK FOR ESR. -SOME ORIENTATION BY DICHR.	-WEAK BINDING AS INDIVIDUALS AT LARGE P/D. -AGGREGATES POSSIBLY FORMED AT LOW P/D, LEADING TO MUTUAL DECAY OF THE RADICALS.
T-RNA	NO	NO	WEAKLY	(IMPOSSIBLE TO OBTAIN GELS)	NO EXCHANGE NARROWING IN SOLUTION.	-THE SAME PATTERN AS THE LOOPED POLY I.POLY C, EXCEPT WEAKER BINDING BOTH OF THE INDIVIDUALLY BOUND RADICALS AND THE AGGREGATES. THE AGGREGATION DOES NOT GIVE EXCHANGE NARROWING BUT RESULTS IN SOME STABILIZATION OF THE COLOUR.
SINGLE STRANDED POLY I POLY C	NO	NO	NO	—	—	- NO BINDING. THE BINDING AND THE PROTECTION OF THE RADICAL THUS REQUIRE THE CHEMICAL GROUPS DISPOSED IN A WELL DEFINED CONFORMATION.

FIG.9.1 COMPARISON OF THE AFFINITY AND SPECIFICITY OF CPZ^+ TO VARIOUS NUCLEIC ACID SPECIES.

it probably involves the simultaneous formation of more than one chemical link.

In comparison, the RNA species display distinct behaviours at low and high P/D ratios (see Fig. 9.1.), which are consistent with the formation of drug aggregates under the low P/D (high drug concentration) conditions. The affinity of the drug molecules to each other is in that case greater than the affinity of the individual drug molecules to the nucleic acids. The tendency of the drugs with extended chromophores to form aggregates in concentrated solutions is well documented: it is manifested by the planar acridines (Ref. 1., p 429) and it has also been shown to occur in the case of the chlorpromazine analogues Thionine and Toluidine, both of which are "bent" tricyclic structures containing nitrogen and sulphur atoms in the central ring (Ref. 2.).

The experimental results show that the effects (such as the stabilization of the radical) resulting from the formation of aggregates along the various types of RNA molecules are different in each case, probably depending on the particular geometry of the aggregate; geometry which would be determined in turn by the local interactions and the conformation of the binding site on the nucleic acid molecule. In this context it is necessary to understand the physical basis of the observed stabilization or destabilization of the radicals upon their binding to the nucleic acids. From the data available, it appears that the decay of the radical species involves a chemical reaction between two radical molecules or possibly a reaction involving water, or both (see Chapter 6.). Thus if the stereochemistry of the binding of the drug is such that the chemical groups involved in these reactions are protected from water or from contact with other molecules, the binding would result in the stabilization of the radical. This seems to be the case with the CPZ^+-DNA interaction. The opposite holds for the destabilization effect, in which case the nucleic acid can act as a catalyst, enhancing the rate of decay. This seems to be the situation in the case of the low P/D complexes of CPZ^+ with the regular double stranded Poly I . Poly C.

A particularly stable complex was formed between CPZ^+ and the partially denatured ("looped") Poly I . Poly C. The ESR investigation of these complexes (see Chapter 7) demonstrated that they consisted of clusters of about six radical molecules. The unpaired spins of these radicals interacted in such a way as to produce exchange narrowed ESR signals, similar to the signals obtained from dry pastes of pure CPZ^+. The colour and the strength of the ESR signals of these pastes were also persistent. It is insufficiently clear which particular feature of the "looped" structure of the nucleic acid was responsible for the formation of the CPZ^+ clusters. It is, however, significant that "exchange narrowing" complexes were not obtained with regular double stranded Poly I.Poly C (where the low P/D ratios resulted in an accelerated decay of the radicals rather than in clustering) nor with natural transfer RNA (where the binding of the radicals, both as individuals and aggregates, was weaker, as deduced from the fact that the interaction produced no detectable colour change).

It is thus apparent that a particular conformation of the binding site and possibly a particular base composition is required in order to produce the clustering of the drug molecules. The conformational requirement was also underlined by the observed inability of CPZ^+ to form stable complexes with the single stranded polyribonucleotides. It is suggested that more information in respect of base specificity should be obtained by repeating the experiments with synthetic double stranded polyribonucleotides of a different base composition and with natural RNA from other sources. In this context it is also suggested that the base specificity of the $DNA-CPZ^+$ interaction be investigated using DNA species which are rich in particular base compositions. For example, the binding of CPZ^+ to Micrococcus Lysodeikticus DNA (72% Guanine and Cytosine) and Clostridium Perfringens (30% G + C) could be studied. (N.B. Calf thymus DNA has 50% G + C content.)

The formation of persistent complexes between CPZ^+ and the nucleic

acids may have a direct significance for the biological function of this drug. It will be recalled that the drugs from the class of Phenothiazine tranquilizers to which CPZ belongs, have a long, persistent effect after administration (Ref. 3.). At the same time, it has been shown (see Chapter 1) that the biologically active form of these drugs was that of cation radical. While it does not seem justified to consider the binding of CPZ^+ to the nucleic acids as being the mechanism of action of the drug, it is clear that the formation of stable complexes with either the DNA or RNA could account for the observed persistence of the drug in the organism. It should be noted that the presence of nucleoprotein and enzyme systems complexed with the nucleic acids in the living cell are likely to create an environment rather devoid of water, similar to the environment existent in the fibres, which would favour the stability of the cation radicals. It is also possible that the binding of these radicals to the nucleic acids is responsible for disturbances in the replication of the nucleic acids which are detected as side effects (deficient regeneration of the skin); effects which are similar to those caused by other drugs which form complexes with the nucleic acids (mentioned in Chapter 4).

In connection with possible extensions of the present work, it should be pointed out that the drug Promethazine (see Fig. 4.1.) appears to be more effective and have a more prolonged action than CPZ. It is suggested that the interaction of this drug with the above types of nucleic acids should be studied, in order to detect if there is any change in the affinity of this drug, compared to that of CPZ^+, to a particular nucleic acid species; affinity that could be correlated with the superior chemotherapeutic activity of this drug. The radicals Promethazine and the related Promazine (Fig. 4.1.), both of which have more symmetrical molecules than CPZ, have already been mentioned in Section 6.3.5., where it was suggested that the study of their ESR spectra in solution could lead more easily to an interpretation of the isotropic hyperfine structure, than is the case with CPZ. The

British Pharmaceutical Codex (Ref. 3.) lists a number of insufficiently well characterized coloured compounds obtained from Promethazine by treating the drug with different acids or bases. It seems possible that some of these might be free radicals and it is thus suggested that an extension of the ESR solution work to the study of these compounds would be appropriate.

9.1.2. Intercalation vs. External Binding.

The results of the ESR investigation of DNA-CPZ$^+$ fibres demonstrated the preferred orientation of the CPZ$^+$ molecule with the general plane of the tricyclic system perpendicular to the helical axis, as for intercalation. The accuracy with which this orientation was established was $\pm 20^\circ$ in the angle of tilt, the uncertainty arising chiefly from the considerable degree of misorientation existing inside the fibres. The best orientation was achieved with a batch of fibres of P/D ratio 12, and corresponded to a Gaussian misalignment parameter of 27° (see Section 6.4.). These parameters were confirmed by the quantitative analysis of the optical dichroism results obtained from the same fibres.

However, from the available data, there is not enough evidence that could support the hypothesis of the intercalation of the bent CPZ$^+$ chromophore between the basepairs of the DNA. In saying so, one has in view the following facts:

i) CPZ does not cause the unwinding of the supercoiled closed circular DNA. Ultracentrifugation studies performed by Waring (Ref. 4.) showed that in the case of the "intercalating" drugs (see Chapter 4), the local unwinding caused by intercalation propagates and causes the reversal of the supercoiling existing in this DNA species, the magnitude of this effect being proportional to the D/P ratio. Such effects were not observed with chlorpromazine. However, the studies reported were carried out with the native CPZ species, so that these results might not be directly relevant to the intercalation of the CPZ$^+$ cation radical.

ii) The pitch of the DNA helix as measured from the separation of the layer lines from the fibre X-ray diffraction pattern (Fig. 8.5.) does not show the expected 1-3Å increase relative to the pitch of a control DNA fibre. Neither do the CPZ analogues Toluidine and Thionine (Ref. 2.) cause a similar effect. The analogy with these two compounds was included because, contrary to the native or oxidised CPZ species, they bind to the DNA with a high affinity and it was hoped that a detectable effect would be observed. It should be noted that the changes in the helical pitch expected with CPZ$^+$ are at the limit of accuracy of the measurements and it is felt that a detailed and careful X-ray diffraction investigation of a larger number of DNA-CPZ$^+$ fibres is essential.

While it does not seem justifiable to rule out decisively the hypothesis of intercalation, the possibility of external binding of CPZ$^+$ to the DNA was also investigated. An experiment with molecular models showed that CPZ$^+$ can be fitted externally on to the DNA, so that its general plane was perpendicular to the helical axis. In the tentative model from Fig. 9.2., the molecule is "sitting" on the phosphate backbone with its chromophore accommodated in the large DNA groove, oriented approximately perpendicular to the helical axis. The structure is stabilized by an electrostatic interaction between the protonated terminal dimethyl-amino group of the CPZ sidechain and a phosphate group of the backbone. The ring nitrogen (possibly being also positively charged) is close to another phosphate group, while the surface of the chromophore forms a hydrophobic contact with the apolar core of the DNA helix. An attractive feature of this model is that the sulphur atom of the ring (which is the one which acquires an oxygen atom upon conversion of the radical to the sulphoxide) is in close contact with the core of the helix, so that there wouldn't be room to accommodate an extra oxygen atom. This could explain the way DNA stabilizes the radical (i.e. by protecting the sulphur position from external attack) as

FIG. 9.2 TENTATIVE MODEL FOR THE EXTERNAL ATTACHMENT OF THE CPZ RADICAL ONTO THE B-DNA. THE STRUCTURE IS STABILIZED BY ELECTROSTATIC INTERACTIONS WITH THE PHOSPHATE BACKBONE AND BY HYDROPHOBIC EFFECT.
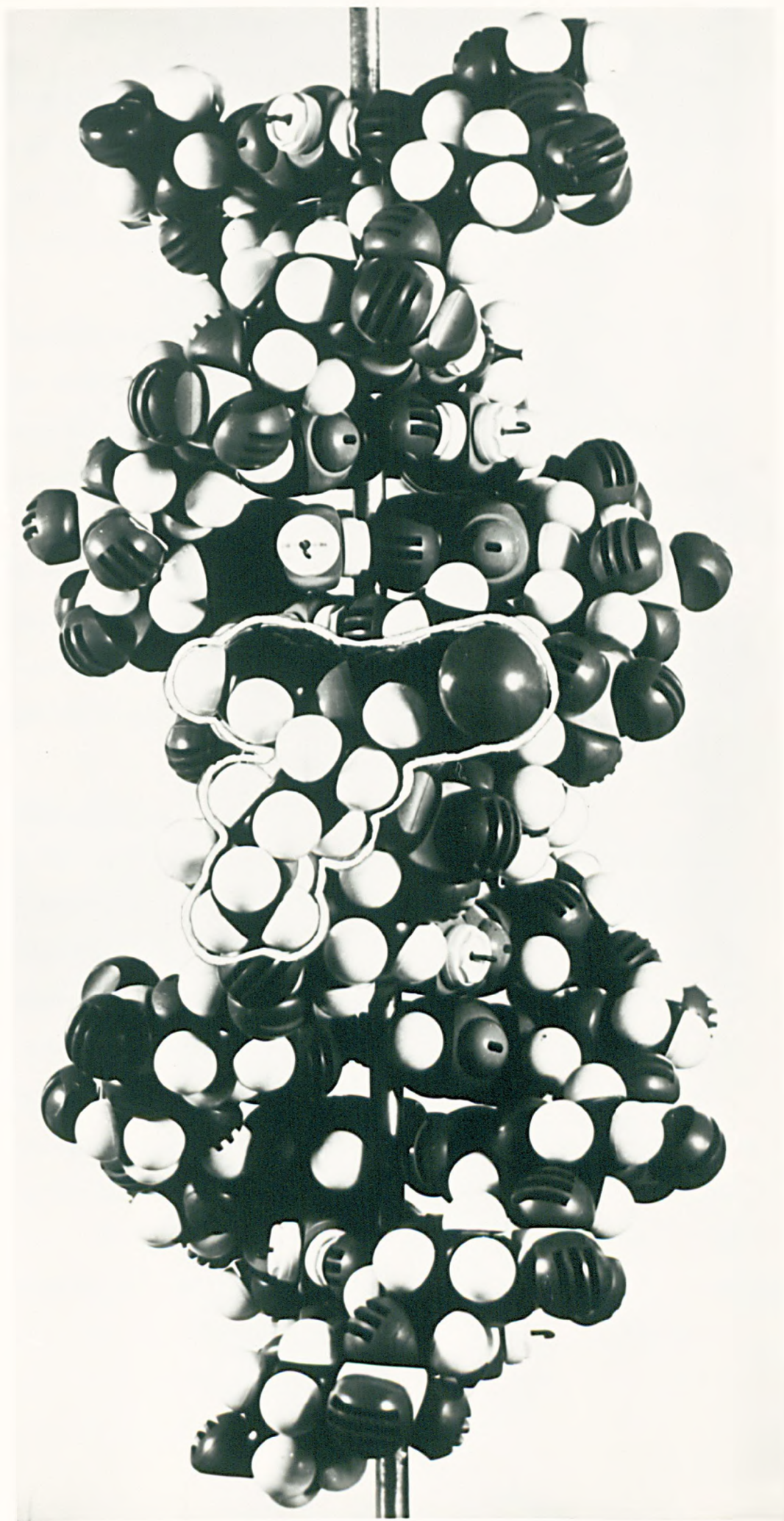
well as the reason why the sulphoxide has low affinity to the DNA. The *conformation* ~~configuration~~ of the CPZ$^+$ molecule itself was the same as that reported previously (Ref. 5.). As this investigation was far from being exhaustive, it is possible that other satisfactory models might also exist.

It is considered that the major limitations in the present ESR determinations arise from the finite degree of ordering of the specimens. It would be clearly of a great advantage if the orientation of CPZ$^+$ relative to the helical axis was known with a greater accuracy. It was shown that the ordering could be improved if larger P/D (i.e. smaller drug concentrations) were used, but in this way one approached the sensitivity limit of the apparatus. The enhancement of the sensitivity of the spectrometers (e.g. by fitting a solid state phase locked microwave source to the X-band spectrometer) is suggested as an instrumentational improvement for the future.

9.2. Other Pieces of Work.

Following the objectives outlined in Section 4.3., it was attempted (without being able to complete the work) to apply the methods developed in connection to the DNA-CPZ$^+$ interaction to study the interaction between the DNA and compounds that are generally assumed to intercalate. Such a study is necessary, since although the intercalation is accepted as a possible mode of binding, there has been so far no direct proof of its existence. The evidence was usually indirect, coming from measurements of hydrodynamic properties of solutions or measurements of X-ray diffraction patterns, etc. (Ref. 1., p429). The increase of the helical pitch as measured from X-ray diffraction patterns is one of the strongest tests for intercalation, although . it should be admitted that this is by no means the only binding mechanism that could result in the elongation of the DNA helix; an external mode of binding could impose the same changes.

It was thought that the quantitative ESR method developed above, possibly coupled with optical dichroism measurements, could provide strong orientational evidence for or against intercalation.

9.2.1. The Binding of the Phenazine Radical to DNA.

The first radical investigated was 5-Methyl Phenazine[+]. Its molecule (Fig. 9.3.) is a tricyclic structure, containing two Nitrogen atoms in the central ring. According to the criteria presented in Section 4.1.1., this molecule should be planar and could intercalate.

The radical was obtained from Phenazine Methosulphate by reduction with Sodium Borohydrate in anaerobic conditions (because the oxygen reverses the reaction) (Ref. 6.). All the reagent solutions were deaerated by bubbling oxygen-free nitrogen gas through them. It was found convenient to mix the reagents in a syringe, thus protected from contact with the air. Good yields of radical were obtained provided the concentrations of the reagents were small (approximately 10^{-4} M); higher concentrations resulting in the precipitation of the material.

The ESR spectrum of a Phenazine[+] solution consisted of seven major hyperfine lines (separated by approximately 0.66 mT), each line presenting a partially resolved structure consisting of about 13 lines. This spectrum was similar to that reported previously (Ref. 6.).

Complexes of Phenazine[+] with DNA in 0.05 M NaCl/0.01 M sodium acetate buffer (pH 6.0) were made and fibres obtained by the methods already described. The P/D ratios ranged between 4 and 16. The ESR spectra of DNA-Phenazine[+] solutions and gels consisted of a single, fairly broad line (of width 1.62 mT), without resolved hyperfine structure (Fig. 9.4.). In this respect the spectra differ from the solution spectra previously reported (Ref. 6.), which showed a resolved seven-line structure, the overall spread of which was comparable to that presently observed. It is possible that
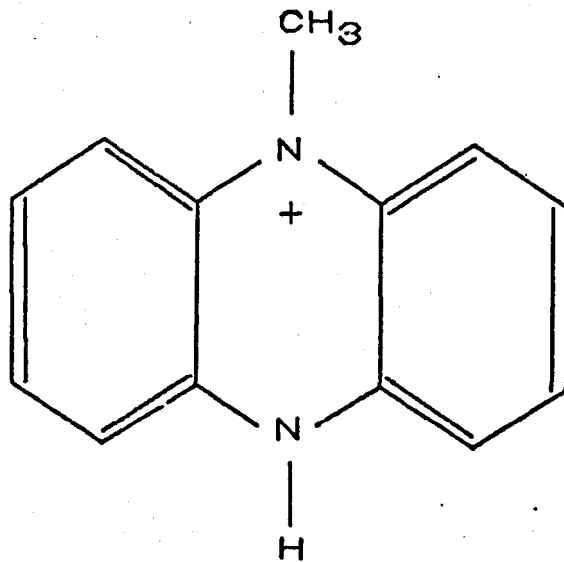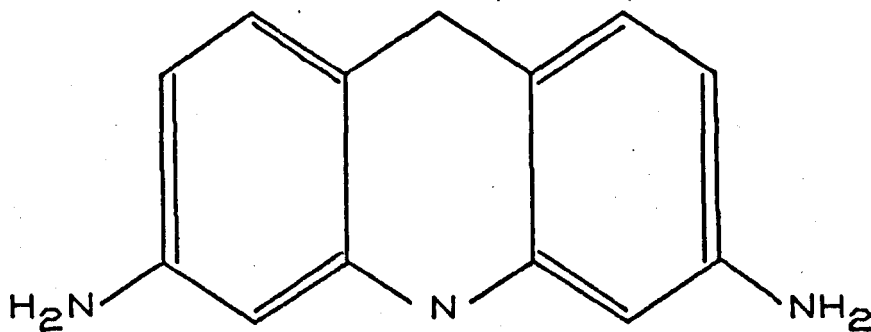
FIG. 9. 3 THE CHEMICAL FORMULAE OF THE DRUGS 5-METHYL PHENAZINE AND PROFLAVINE.
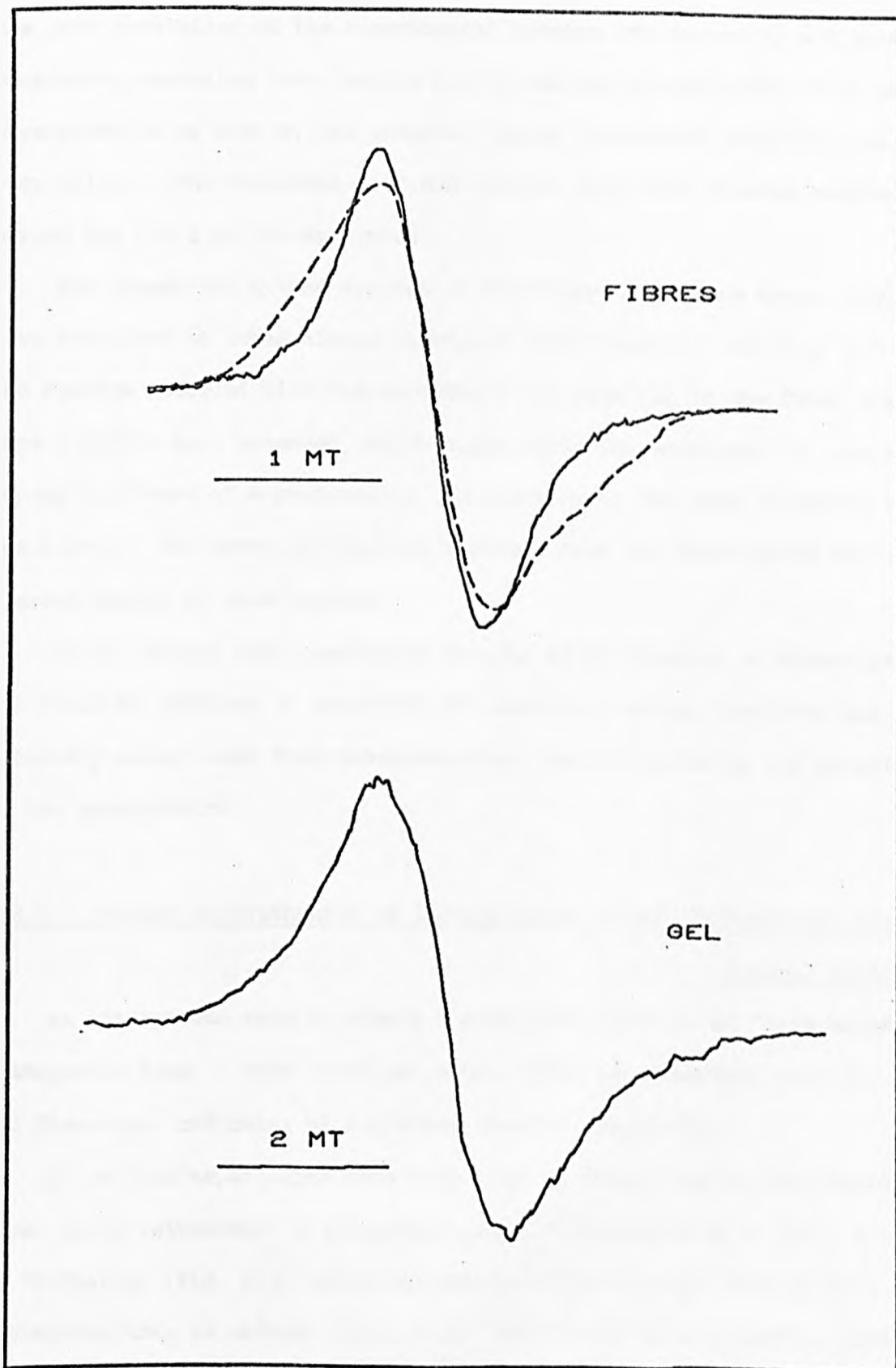
FIG. 9.4 X-BAND ESR SPECTRUM RECORDED FROM A GEL AND FIBRES OF THE COMPLEX OF DNA WITH THE PHENAZINE RADICAL.
(——PERPENDICULAR, ---PARALLEL)

the poor resolution of the experimental spectra was caused by a dipolar broadening mechanism (see Section 2.4.2) and can be correlated with the precipitation of some of the material, which inevitably occurred upon complexing. The observation of ESR signals from more diluted samples was beyond the limit of the apparatus.

The X-band and Q-band spectra of the fibres made from these complexes also consisted of broad single lines, of width about 2.1 mT (Fig. 9.4.). The spectra recorded with the magnetic field parallel to the fibre axis were slightly more extended, which might imply the existence of some anisotropy and hence of a preferential orientation of the drug molecules inside the fibre. The X-ray diffraction patterns from the same fibres revealed a great degree of misalignment.

It is thought that conclusive results on the binding of Phenazine to DNA could be obtained by improving the method of making complexes and fibres (possibly using lower drug concentrations) and by improving the sensitivity of the spectrometer.

9.2.2. Attempt to Synthesise an Intercalating Nitroxide Probe for the Nucleic Acids.

An attempt was made to attach a nitroxide group to an "intercalating" diamagnetic drug. Such a radical would offer the advantage over the CPZ^+ and Phenazine$^+$ radicals, of a greater chemical stability.

In particular, attempts have been made to attach the five-membered spin label 22-55 Tetramethyl 3 pyrroline 1 oxyl 3 carboxylic acid (Fig. 3.1e) to Proflavine (Fig. 9.3) using the catalyst Dicyclohexyl Carbodiimide in Tetrahydrofuran as solvent (Ref. 7.). Proflavine Hemisulphate (obtained from Sigma Chemicals Co.) was converted to Proflavine by treatment with a 20% NaOH solution. The condensation reaction was expected to result in the formation of a rigid peptide link between the two molecules. These

experiments have so far produced an insufficient yield to be useful in practice. However, recent work elsewhere has suggested that a more appropriate coupling reagent is NN[1] - Thionyldiimidazole (Ref. 8.).

This reaction would result in the formation of a freely rotating link, so that the radical obtained could be used to produce information on the motional freedom associated with the different binding sites. It is thought that depending on the conformation of the particular binding site, the attachment of this radical to the DNA would either result in a restriction of the mobility of the nitroxide group, or it would cause the group to adopt a rigid preferred orientation. An orientational ESR study performed on fibres, coupled with molecular model building could thus provide information about the particular geometry of the binding site. It is suggested that the synthesis of the proflavine radical be pursued and once the technique is established it should be a relatively simple exercise to synthesize derivatives of the dyes Toluidine and Thionine, both which have "bent" molecules. The binding of these molecules with a range of nucleic acids should then be studied by ESR, using fibres and solutions. It is hoped that such studies, complemented by X-ray diffraction and optical measurements could provide valuable information in relation to the general aspects of drug binding to nucleic acids and in particular to intercalation.

REFERENCES.

1. V. A. BLOOMFIELD, D. M. CROTHERS, I. TINOCO: Physical Chemistry of Nucleic Acids, Harper and Row, (1974).

2. T. PORUMB: Project, King's College, London, Biophysics Department, (1973).

3. BRITISH PHARMACEUTICAL CODEX, 1956, The Pharmaceutical Press, London.

4. M. J. WARING: Prog. Mol. Subcell. Biol., 2, 216-231, (1971).

5. R. M. METZGER (Mississippi) : Private Communication, (1976).

6. K. ISHIZU et al.: Biochemistry, 8, 1283, (1969).

7. G. JONES (Chemistry Department, University of Keele): Personal Communication, (1976).

8. J. R. DODD: Chem. Comm., 13, 520, (1975).

APPENDIX.

```
C=========================================================================
C
C                    PROGRAM FOR ESR LINESHAPES.
C
C
C          TO COMPUTE ESR SPECTRA FOR-
C1- SOLUTIONS.UP TO 10 ISOTROPIC HYPERFINE INTERACTIONS.SPIN DEPENDENT WIDTH
C2- SINGLE CRYSTALS.A SINGLE HYPERFINE INTERACTION.THE A AND G TENSORS COLINEAR
C3- POWDER SPECTRUM OF THE ABOVE TYPE OF MOLECULES
C4- FIBRE SPECTRUM.THE FIBRILS IN THE FIBRE ARE MISALIGNED ( GAUSSIAN SPREAD
C     DELTA ). THE ORIENTATION OF THE  LABEL RELATIVE TO THE FIBRIL IS DESCRIBED
C     BY TWO ANGLES ( THE TILT THETA AND THE TWIST PSI ).
C     THE PROGRAM CYLINDRICALLY AVERAGES EACH FIBRIL AND THEN THE WHOLE FIBRE.
C     NO= 1,2,3,4,  LABEL THE ABOVE TYPES OF SPECTRA.
C
C    DATA-
C CONTENTS OF THE CARD -------------------------------------- THE FORMAT
C
C               MASTER CARD-
C NO,ISHAPE,IADD,IPRINT,RA,IREPET                                = 4I1 F6 I1
C (NO=THE TYPE OF SPECTRUM. ISHAPE=0-LORENTZIAN,1-GAUSSIAN,2-BOTH,FIRST 0,THEN
C  REPEATED WITH 1. IADD=0 FOR NORMAL  OPERATION,=1 FOR ADDING THIS SPECTRUM
C  TO PREVIOUS ONE. IPRINT=1 / 0 TO PRINT / NOT TO PRINT INTERMED.RESULTS.
C  RA= THE NORMALIZED SPECTRUM WILL BE MULTIPLIED BY THIS NUMBER. IREPET=0 FOR
C  ORDINARY  OPERATION,=1-OPENS THE SECTION PREPARED FOR OPTIONALLY ALTERING
C  PARAMETERS IN SYSTEMATIC MANNER ).
C               2ND GENERAL CARD
C THE RANGE AND THE STARTING FIELD VALUE (IN GAUSS)                = 2F10
C
C             FOR ISOTROPIC SPECTRA-
C FREQ(GHZ),G,DH(WIDTH),N( THE NUMBER OF HYPERFINE INTERACTIONS)   = 3F10 I2
C A(SPLITTING IN GAUSS),I(NUCLEAR SPIN)                            = 2F10
C AFTER ATOM 1-WIDTH OF EACH LINE (IF DH=0.)                       = 8F10
C             FOR ANISOTROPIC SPECTRA-
C ANGLES IN DEGREES: FIELD-FIBRE,MISALIGNEMENT,TILT OF LABEL,
C                               TWIST OF LABEL.(ONLY IF NO=4)      = 4F10
C FREQ(GHZ), DH(LINEWIDTH), I(NUCLEAR SPIN)                        = 3F10
C WIDTH OF EACH LINE ( IF DH=0.)
C PRINCIPAL G AND A TENSOR VALUES                                  = 6F10
C THE STEPS IN DEGREES( SEE TEXT)-ASTEP,BSTEP,FSTEP / ASTEP,BSTEP
C                               IF NO= 4 / NO=3                    = -F10
C THE   POLAR ANGLES (IN DEGREES )- IF NO=2                        = 2F10
C               BLANK CARD OR NEXT SET OF DATA.
C
      REAL A1(1000),B(1000 ),X(1000),A(10),  I(10), DHH(8)
      REAL AA(1000),B3(1000)
      REAL MARKX(4),  MARKY(4)
      DIMENSION GPX(1020),GRY(1020)
      COMMON NN(100),MSIGN(100),MS,IPOINT(100)
      IRUN=0
      IRJ =0
      PI   =4.0 *ATAN(1.0)
      DO 200 L=1,6
200   DHH(LL)=0.0
C/////////// READ MASTER CARD.
999   READ(7,500)NO,ISHAPE,IADD,IPRINT,RA,IREPET
```

```
C//////// TEST FOR END.
      IF(NO.EQ.0)STOP
C  ISHAPE CONTROLS THE TYPE OF LINESHAPE.
      ISHAP1=ISHAPE
      IF(ISHAPE.EQ.2)ISHAP1=0
      READ(7,203)RANGE,START
      RNSTOR=RANGE
      SRSTOR=START
C//////// TEST FOR TYPE.
      IF(NO-2)2,201,201
2     CONTINUE
C  THE SECTION FOR ISOTROPIC HYPERFINE SPECTRA (NO=1)
C========================================================================
C//////// READ INPUT DATA.
      READ(7,3)FREQ,G,DH,N
      FRSTOR = FREQ
      IF(N.EQ. 0) GOTO 44
      DO 4 L=1,N
      READ( 7, 5)A(L),I(L)
      IF(DH.NE.0.0 .OR. L.NE. 1) GOTO 4
C IF DH=0 READ WIDTH ASSOC.WITH EACH HYP.LINE OF ATOM NO.1
      READ(7,100) DHH
4     CONTINUE
C  ALL PARAMETERS ARE READ
C  WRITE PARAMETERS
44    CONTINUE
      IRUN=IRUN+1
C  WRITE HEADING
      WRITE(2,903)
      WRITE(2,707)IRUN
      WRITE(2,700)  N
700   FORMAT(30H ISOTROPIC HYPERFINE SPECTRUM. ,I3, 6H NUCLEI. )
      WRITE(2,701)G,FREQ
701   FORMAT( 4H G= ,F9.6, 7H FREQ.=, F10.7, 4H GHZ  )
      IF(ISHAP1.EQ.0)WRITE(2,293)
      IF(ISHAP1.EQ.1)WRITE(2,505)
      IF(DH.NE.0.0)WRITE(2,198)DH
      LLL=2.0*I(1)+1.01
      IF(DH.EQ.0.0) WRITE(2,101) (DHH(LL),LL=1,LLL)
      IF(N.NE.0)WRITE(2,61)(A(L), I(L), L=1,N)
61    FORMAT(40H HYPERFINE SPLITTINGS AND NUCLEAR SPINS: /(13X,F10.3,
     1  1X,F10.1))
C//////// COMPUTE THE SPECTRUM.
      CALL SPECTR(N,A,I,FREQ,G,DH,DHH,1.0,AA,BB,X,1000,1.,ISHAP1,IPRINT,
     1  RANGE,START)
      GOTO 301
C========================================================================
C
C  THE SECTION FOR  ANISOTROPIC  SPECTRA STARTS HERE.
C
201   CONTINUE
C INITIATE PARAMETERS.
      ALFA=0.0
      DELTA=0.0
      GAMMA=0.0
      THETA=0.0
      FI=0.0
      PSI=0.0
      ASTEP= 1.0
      BSTEP= 1.0
```

```
      FSTEP=1.0
C//////// READ INPUT DATA.
      IF(NO.EQ.4)READ(7,492)GAMMA,DELTA,THETA,PSI
      READ(7,292)FREQ,DH,I(1)
      FRSTOR =FREQ
      IF(DH.EQ. 0.0) READ(7,100) DHH
      READ(7,199)GX,GY,GZ,AX,AY,AZ
      IF(NO.EQ.2)READ(7,203)AFIX,BFIX
      IF(NO.EQ.3)READ(7,203)ASTEP,BSTEP
      IF(NO.EQ.4) READ(7,292) ASTEP,BSTEP,FSTEP
C  ALL PARAMETERS KNOWN.
6003  CONTINUE
      IRUN=IRUN+1
C  SECTION TO WRITE TITLES AND PARAMETERS .
      WRITE(2,903)
      WRITE(2,707)IRUN
      IF(NO.EQ.2)WRITE(2,501) AFIX,BFIX
501   FORMAT(48H ANISTROTROPIC SPECTRUM.THE FIELD MAKES ANGLES     .
     1 F7.2,5H AND , F7.2,33H WITH THE MOLECULAR AXES Z AND X.      )
      IF(NO.EQ.3)WRITE(2,303)ASTEP,BSTEP
903   FORMAT( 17H POWDER SPECTRUM.
     1        / 80H THE ANGLES ALFA AND BETA OF H WITH THE MOLECULAR AXES
     1Z AND X VARY IN STEPS OF ,F5.1, 5H AND ,F5.1, 9H DEGREES.)
      IF(NO.EQ.4)WRITE(2,804)GAMMA ,DELTA ,THETA , PSI
804   FORMAT( 41H FIBRE SPECTRUM.THE ANGLE (FIBRE,FIELD)= ,F6.1,
     2 32H DEGREES                                    /
     2 16X, 27H MISALIGNEMENT IN THE FIBRE= ,F6.1,9H DEGREES.    /
     2 16X, 33H ORIENTATION OF THE MOLECULE.TILT= ,F6.1,9H DEGREES.  .
     2 7H TWIST=          ,F6.1, 9H DEGREES.   )
C  WRITE  THE TYPE OF LINESHAPE AND WIDTH
      IF(ISHAP1.EQ.0)WRITE(2,293)
      IF(ISHAP1.EQ.1)WRITE(2,506)
      IF(DH.NE.0.0) WRITE(2,198) DH
      LLL=2.0*I(1)+1.01
      IF(DH.EQ.0.0) WRITE(2,101) (DHH(LL),LL=1,LLL)
      WRITE(2,505 )FREQ,I(1),GX,GY,GZ,AX,AY,AZ,ASTEP, BSTEP, FSTEP
505   FORMAT(/ 29H K.FREQ.    N.SPIN      G TENSOR           HYP.TENSOR
     1          STEP(ALFA) STEP(BETA)STEP(FI)                    /
     2 2X,F8.5,2X,F4.2,1X,3(1X,F6.4,1X), 3(1X,F6.2,1X),3(3X,F5.1,3X)/)
      IF(IPRINT .EQ. 1)WRITE(2,509)
509   FORMAT(/ 113H  NO  ALFA      BETA      FI      SPLITTING  G  SPIN  FI
     1ELD       WIDTH       PROB.GAUSS WEIGHT ORIENT. TOTAL WEIGHT      /)
CC//////// SET UP ANGULAR RANGES, INCLUDING PARTICULAR CASES.
C//////// CALCULATE COMMON PARAMETERS.
      DOLOWF=0.0
      DOHIF =359.9
      IF(NO.NE.4.OR.(THETA.EQ.0.0 .AND.GX.EQ.GY.AND.AX.EQ.AY)
     1   .OR.(THETA.EQ.0.0.AND.DELTA.EQ.0.0.AND.GAMMA.EQ.0.0))DOHIF=0.0
C//////// SPLIT ACCORDING  TO TYPE.
      IF(NO-3) 390, 391, 395
395   CONTINUE
C  FIBRE CASE ( NO=4 )
C  THE ANGLE OF ROTATION ABOUT THE FIBRE AXIS.
         DOLOWB=0.0
         DOHIB =359.9
C  EXCEPTION IF THE FIBRILS  ARE PERFECTLY ORIENTED
      IF(DELTA.EQ.0.0)DOHIB=0.0
C  THE ANGLE OF INCLINATION OF THE FIBRIL IN THE FIBRE
         DOLOWA=0.0
         DOHIA =180.0
```

```
      IF(DELTA.LT. 60.0) DOHIA= 2.5 *DELTA
      IF(DELTA .EQ. 0.0)DOHIA =0.0
C  CONVERSIONS
      GAMMAR= GAMMA*PI / 180.0
      THETAR = THETA*PI / 180.0
      PSIR=PSI*PI /180.0
      SP2=SIN(PSIR)
      CP2=COS(PSIR)
      STO=SIN(GAMMAR)
      CTO=COS(GAMMAR)
      ST2=SIN(THETAR)
      CT2=COS(THETAR)
      GOTO 394
391   CONTINUE
C  THE POWDER CASE (NO=3)
      DOLOWA=0.0
      DOHIA = 90.0
      DOLOWB=0.0
      DOHIB =180.0
C  AXIAL SYMMETRY NEEDS NO BETA  VARIATIONS :
      IF(GX.EQ.GY.AND.AX.EQ.AY  )   DOHIB=0.0
      GOTO 394
390   CONTINUE
C  THE CASE OF A SINGLE CRYSTAL   (NO =2)
      DOLOWA=AFIX
      DOHIA  =AFIX
      DOLOWB=BFIX
      DOHIB =BFIX
      GOTO 394
C  THE LIMITS OF THE  DO LOOPS  IN REAL DEGREES  HAVE BEEN SET.
394   CONTINUE
C  THE INTEGER  LIMITS  AND  STEPS  OF THE DO  LOOPS .
      IA1=(DOLOWA+500.0)*10.0
      IA2=(DOHIA +500.0)*10.0
      IB1=(DOLOWB+500.0)*10.0
      IB2=(DOHIB +500.0)*10.0
      IF1=(DOLOWF +500.0)*10.0
      IF2=(DOHIF  +500.0)*10.0
      IASTEP= ASTEP *10 + 0.5
      IBSTEP= BSTEP *10 +0.5
      IFSTEP= FSTEP *10 +0.5
C  INITIATION .
      COUNT=0.0
      SP   =0.0
C///////// SET UP ORIENTATION ALFA (T1).
      DO 205 IALFA=IA1,IA2,IASTEP
      ALFA = FLOAT(IALFA)/10.0 -500.0
      ALFAR= ALFA *PI/180.0
      ST1=SIN(ALFAR)
      CT1=COS(ALFAR)
C THE GAUSSIAN PROBABILITY  (PA)
      PA=1.0
      IF(NO .NE.4 .OR. DELTA .EQ. 0.0 )GOTO 888
      ARG= -(ALFA/DELTA)**2 / 2.0
C TERMINATE THE LOOP IF THE ARGUMENT GETS TOO SMALL.
      IF( ARG .LT. (-20.0)) GOTO 205
      PA = EXP(ARG ) / DELTA
888   CONTINUE
      P= ABS( SIN (ALFAR) )
C///////// THE WEIGHT OF THIS ORIENTATION.
```

```
      WEIGHT =P*PA
C TERMINATE THE LOOP IF THE WEIGHT IS 0 EXCEPT IF THE SPECTRUM IS NOT PART OF A
C SUMMATION WHEN SET WEIGHT=1.
      IF(WEIGHT .EQ.0.0 .AND. DOHIA .EQ. 0.0) WEIGHT=1.0
      IF(WEIGHT .EQ. 0.0 ) GOTO 205
C//////// SET UP ORIENTATION BETA (F1)
      DO 206 IBETA= IB1,IB2,IBSTEP
      BETA =FLOAT(IBETA)/10.0 -500.0
      BETAR=BETA *PI/180.0
      SF1=SIN(BETAR)
      CF1=COS(BETAR)
C//////// SET UP ORIENTATION FI (F2).
      DO 204 IFI=IF1,IF2,IFSTEP
      FI=FLOAT(IFI)/10.0-500.0
C  CONVERT FROM DEGREES TO RADIANS.
      FIR=FI*PI/180.0
C
C//////// CALCULATE THE COORDINATES OF THE MAGNETIC FIELD IN THE MOLECULAR FRAME
      IF(NO.EQ.4)GOTO 392
C  THIS IS THE CASE OF A SINGLE CRYSTAL OR POWDER.
      XL = ST1*CF1
      YL = ST1*SF1
      ZL = CT1
      GOTO 202
392   CONTINUE
C  THIS IS THE FIBRE CASE.
      SF2=SIN(FIR)
      CF2=COS(FIR)
      XL= -ST0*(CP2*(CT1*CF1*CT2*CF2 -SF1*CT2*SF2 -ST1*CF1*ST2) -SP2*
     1(CT1*CF1*SF2 +SF1*CF2 )) +CT0*(CP2*(-ST1*CT2*CF2  -CT1*ST2 )+
     2ST1*SF2*SP2 )
      YL= -ST0*(CP2*(-CT1*CF1*SF2 -SF1*CF2) +SP2*(-CT1*CF1*CT2*CF2 +
     1SF1*CT2*SF2 +ST1*CF1*ST2 )) +CT0*(ST1*(CT2*CF2*SP2 +    SF2*CP2)
     2 +CT1*ST2*SP2 )
      ZL= -ST0*(CT1*CF1*ST2*CF2 - SF1*ST2*SF2 + ST1*CF1*CT2) +
     1CT0*(-ST1*ST2*CF2 +CT1*CT2)
202   CONTINUE
C//////// CALCULATE THE SPLITTING AND G VALUE.
      A(1)= SQRT( (AX*XL)**2 +(AY*YL)**2 +(AZ*ZL)**2 )
      G = GX*XL**2 + GY*YL**2 + GZ*ZL**2
      SP =SP + WEIGHT
      COUNT= COUNT + 1.0
C  ALL THE  PARAMETERS  WERE CALCULATED. WRITE  THIS PARTIAL  RESULT .
      IF(IPRINT.EQ.1)WRITE(2,507 )COUNT,ALFA,BETA,FI  ,A(1),G ,
     1     PA ,P, WEIGHT
507   FORMAT(1X, F4.0,3(  F7.2),   1X,F8.3,2X,F8.5,27X ,
     1     1PE11.3 ,2X, 2(E11.3,2X) / )
C//////// BUILD UP THE SPECTRUM.
      CALL SPECTR(1,A,I,FREQ,G,DH,D4H,WEIGHT,AA,BB,X,1000,COUNT,ISHAP1,
     1     IPRINT ,RANGE,START)
204   CONTINUE
206   CONTINUE
205   CONTINUE
C  WRITE  THE SUMOF  THE WEIGHTS.   DIVIDE  THE SPECTRA BY THIS .
      IF(IPRINT .EQ. 1)WRITE(2,998) SP
      WRITE(2,237) COUNT
      IF(SP.EQ. 0.0) GOTO 301
C//////// NORMALIZE THE SPECTRUM.
      DO 25: IH=1,1000
      AA(IH)=AA(IH)/SP
```

```
251   BB(IH)=B3(IH)/SP
301   CONTINUE
C
C     ==============================================================================
C
C THE TWO SECTIONS REJOIN HERE
C
C///////// PLOT THE SPECTRUM (BB).
      IF(IPRINT .EQ. 1) WRITE(2,903)
      CALL GRAPHS(X,BB,1000,1,0,2,GRX,GRY)
C MARK THE G VALUES
      MARKY(1)=0.0
      MARKY(2)=0.0
      MARKY(3)=0.0
      MARKY(4)=0.0
      MARKX(1)=(6625.0 *FREQ / 2.0036 ) / 9.2731
      IF( NO.EQ. 1) GOTO 7020
      MARKX(2)=(6625.0 *FREQ / GX      ) / 9.2731
      MARKX(3)=(6625.0 *FREQ /  GY     ) / 9.2731
      MARKX(4)=(6625.0 *FREQ / GZ      ) / 9.2731
      GOTO 7021
7020  MARKX(2) = (6625.0 *FREQ / G    )/ 9.2731
      MARKX(3) = MARKX(2)
      MARKX(4) = MARKX(2)
7021  CONTINUE
      CALL GRAPHS(MARKX,MARKY,4,2,6,2,GRX,GRY)
      WRITE(2,707)IRUN
C CLEAR THE STORAGE ARRAYS.
      IF(IRUN.EQ. 1) GOTO 65
      IF (IADD.EQ.1) GOTO 400
65    DO 1 L=1,1000
      A1(L)=0.0
    1 B(L)=0.0
400   CONTINUE
C ADDUPTHE ARRAYS.
      DO 250 IH=1,1000
      A1(IH)=A1(IH) + AA(IH)*RA
250   B(IH) = B(IH) + B9(IH)*RA
C PLOT THE SUM SPECTRUM IF REQUIRED.
      IF( IADD .EQ. 0) GOTO 7022
      WRITE(2,903)
      CALL GRAPHS(X,B ,1000,1,0,2,GRX,GRY)
      CALL GRAPHS(MARKX,MARKY,4,2,6,2,GRX,GRY)
      IR=IRUN-1
      WRITE (2,905) IR,IRUN
7022  CONTINUE
C REPEAT WITH A DIFFERENT LINESHAPE IF ISHAPE=2 .RESET THE ORIGINAL CONDITIONS.
      IF(ISHAPE.NE.2 .OR. ISHAP1.NE. 0 )GOTO 70
      ISHAP1 = 1
      GOTO( 44,6003,6003,6003),NO
70    CONTINUE
      IF(ISHAPE.EQ.2 .AND. ISHAP1.EQ.1 )ISHAP1 = 0
C
C     ==============================================================================
C
C  IF IREPET=1 ONE CAN REPEAT THE RUN WITH PARAMETERS ALTERED INSIDE THE PROGRAM
      IF(IREPET .EQ. 0)GOTO 999
C
C  THIS IS THE SECTION TO COMPUTE BOTH X BAND O BAND SPECTRA.
      IF(FREQ.NE.FRSTOR )GOTO 6007
```

```
C   ONE PASSES THROUGH THESE STATEMENTS ONLY AT THE FIRST RUN.
C   ===========
C   THE ALTERNATIVES FREQUENCY ,RANGE AND STARTING FIELD MUST BE GIVEN HERE
C                       AS FRONEW, RNNEW, SRNEW.
      FRONEW= 30.
      SRNEW=   10600.
      RNNEW=  200.
C   ==========
      IF((FREQ.LT.20.0.AND.FRONEW.LT.20.0).OR.(FREQ.GT.20.0.AND.
     1   FRONEW.GT.20.0)) GOTO 6007
C   SAFETY MARGIN IF BOTH FREQUENCIES ARE OF THE SAME TYPE IS INCLUDED .
C   ALSO RETURN TO ORIGINAL FREQUENCY.
      FREQ = FRONEW
      RANGE=RNNEW
      START=SRNEW
      GOTO ( 44,6003,6003,6003),NO
 6007 FREQ=FRSTOR
      RANGE=RNSTOR
      START=SPSTOR
      IRU=IRU+1
C
C START BRANCHING AS DIRECTED BY THE COUNTER IRU. ONE CAN ALTER ANY PARAMETER
C ( EXAMPLES- IRU=0 , GAMMA=GAMMA+5. , IF( )GOTO 7002 , ISHAP1=1 , ETC. )
      GOTO(7001,7002,7003,7004,7005,7006),IRU
 7001 CONTINUE
      IRU= 0
      GOTO ( 44,6003,6003,6003),NO
 7002 CONTINUE
      GOTO ( 44,6003,6003,6003),NO
 7003 CONTINUE
      GOTO ( 44,6003,6003,6003),NO
 7004 CONTINUE
      GOTO ( 44,6003,6003,6003),NO
 7005 CONTINUE
      GOTO ( 44,6003,6003,6003),NO
 7006 CONTINUE
      STOP
C
 292  FORMAT(3F10.5)
 492  FORMAT(4F10.5)
 199  FORMAT(6F10.5)
 203  FORMAT(2F10.5)
 500  FORMAT(4I1,F6.0,      I1)
 3    FORMAT(3F10.5,I2)
 5    FORMAT(2F10.5)
 100  FORMAT(8F10.5)
 903  FORMAT( 1H1//  )
 101  FORMAT(12H LINEWIDTHS: /(12X,F10.5))
 198  FORMAT(12H LINEWIDTH=  ,F6.2 ,  7H GAUSS. )
 293  FORMAT(/23H LORENTZIAN LINESHAPE. )
 506  FORMAT(/21H GAUSSIAN LINESHAPE.    )
 998  FORMAT(/ 76X, 20HSUM OF THE WEIGHTS=   .1PE15.5/)
 233  FORMAT( 76X,F6.0,1X,11HCOMPONENTS   )
 737  FORMAT(120X, 7HRUN NO ,I3)
 805  FORMAT(24H THE SUM OF THE SPECTRA  ,I2,5H AND  ,I2)
      END
      SUBROUTINE SPECTR(N,A,I,FREQ,G,D,DHH,P,AB,B,X,NP,
     1        COUNT,ISHAPE,IPRINT ,RANGE,START)
C
C CALCULATES AND ACCUMULATES  ESR SPECTRA FROM SUCCESIVE CALLS.
```

```fortran
C  RETURNS THE ACUMULATED  ABSORPTION AND DERIVATIVE SPECTRA.
C   THE ACUMULATOR  IS CLEARED IF COUNT .LE. 1.0
C INPUT PARAMETERS=N(NUMBER OF NUCLEI),A(SPLITTING IN GAUSS),I(NUCLEAR SPIN),
C FRED(GHZ),G VALUE,D(LINEWIDTH),DHH(SPIN DEPENDENT WIDTH,IF DH=0.),P(WEIGHT),
C ISHAPE(0=LORENTZIAN,1=GAUSSIAN),IPRINT(0=NO PRINTOUT OF INTERMEDIATE RESULTS),
C NP(NUMBER OF POINTS).
C
      REAL A9(1),B(1),X(1)
      REAL A(10), I(10), M(10), DHH(8)
      INTEGER JA(10), JB(10)
C
      IF( COUNT .GT.1.0 ) GOTO 301
C  AT COUNT 1 PERFORM THE FOLLOWING -
C  CLEAR THE ARRAY AB
      DO 300 L=1,NP
300   AB(I)=0.0
C  CALCULATE THE STEP
      STEP=RANGE / FLOAT(NP)
C SET REST OF A AND I TO 0
66    NN=N+1
      IF(N.EQ.10)GOTO 131
      DO 6 L=NN,10
      A(L)=0.0
    6 I(L)=0.0
C SET THE LIMITS OF THE DO LOOPS FOR THE NUCLEAR SPINS.
131   DO 7 L=1,10
      JA(I)=          (10.0-I(L) )*10.0 +0.002
7     JB(I)=          (10.0+I(L) )*10.0 +0.002
      LA1=JA(1)
      LB1 =JB(1 )
      LA2=JA(2)
      LB2 =JB(2 )
      LA3=JA(3)
      LB3 =JB(3 )
      LA4=JA(4)
      LB4 =JB(4 )
      LA5=JA(5)
      LB5 =JB(5 )
      LA6=JA(6)
      LB6 =JB(6 )
      LA7=JA(7)
      LB7 =JB(7 )
      LA8=JA(8)
      LB8 =JB(8 )
      LA9=JA(9)
      LB9 =JB(9 )
      LA10=JA(10)
      LB10=JB(10)
C  CALCULATE CONSTANTS
      PI=4.0*ATAN(1.0)
      CONSTG=SQRT(2.0/PI)
      CONSTL=2.0/(PI*SQRT(3.0))
C
301   CONTINUE
      DH=D
      HF=(6625.0 *FRED /G) /9.2731
C
C  SET UP COMBINATIONS OF NUCLEAR SPIN COMPONENTS BY NESTED DO LOOPS.
      L=0
      DO 99 L1=LA1,LB1,10
```

```fortran
      LM=LM+1
      M(1)=L1    /10.0 - 10.0
      DO 98 L2=LA2,LB2,10
      M(2)=L2    /10.0 - 10.0
      DO 97 L3=LA3,LB3,10
      M(3)=L3    /10.0 - 10.0
      DO 96 L4=LA4,LB4,10
      M(4)=L4    /10.0 - 10.0
      DO 95 L5=LA5,LB5,10
      M(5)=L5    /10.0 - 10.0
      DO 94 L6=LA6,LB6,10
      M(6)=L6    /10.0 - 10.0
      DO 93 L7=LA7,LB7,10
      M(7)=L7    /10.0 - 10.0
      DO 92 L8=LA8,LB8,10
      M(8)=L8    /10.0 - 10.0
      DO 91 L9=LA9,LB9,10
      M(9)=L9    /10.0 - 10.0
      DO 90 L10=LA10,LB10,10
      M(10)=L10 /10.0 - 10.0
C
C  CALCULATE THE POSITION OF THE HYPERFINE LINE
      RESULT=0.0
      IF(N.EQ. 0) GOTO 81
      DO 8 L=1,N
    8 RESULT=RESULT+ A(L)*M(L)
   81    CONTINUE
      RESULT=HF+RESULT
      IF( D.EQ. 0.0) DH=DHH(LM)
C
C  PRINT THE RESULT IF REQUIRED
      IF(IPRINT .EQ. 0)GOTO 120
C THIS IS THE FORMAT  IF THERE ARE MORE NUCLEI
      IF(N.EQ. 1)GOTO 210
      WRITE(2,9) (M(L),L=1,N)
    9 FORMAT(//36H POSITION OF HYPERF.LINE FOR SPINS:  /(16X,F4.1))
      WRITE(2,11)RESULT
   11    FORMAT( 22H THIS LINE OCCURS AT  ,1PE15.6,8H  GAUSS. )
      WRITE(2,110) DH
  110    FORMAT(1H+  ,46X,6HWIDTH= ,F6.2 , 7H GAUSS.   )
      GOTO 120
C
C  THIS IS THE FORMAT IF THERE IS  ONLY ONE NUCLEUS
  210    CONTINUE
      WRITE(2,211) M(1), RESULT, DH
  211    FORMAT( 40X, F6.1, 2X, 1PE13.5, 0PF6.2 )
C
C CALCULATE LINE SHAPES
C
  120    CONTINUE
C
      DO 51 IH=1,NP
      X(IH)= START + FLOAT(IH-1) + STEP
      H=X(IH)
      IF(ISHAPE.EQ.1)GOTO 500
C  LORENTZIAN LINESHAPE
      AB(IH)=AB(IH)*(1.0 / (1.0 + 4.0*((H-RESULT)**2)/ (3.0*DH**2)))*
     1   ( CONST  / DH ) *P
      GOTO 501
  500    CONTINUE
```

```fortran
C  GAUSSIAN LINESHAPE
       ARG= ( -2.0)* (( H-RESULT)**2 )/ (DH*DH )
       IF( ARG .LT. (- 30.0) ) GOTO 600
       AR(IH) = AB(IH) + (CONSTG /DH)  * EXP( ARG) *P
600    CONTINUE
501    CONTINUE
C
51     CONTINUE
C ONE HYP: LINE IS COMPLETED
C
90     CONTINUE
91     CONTINUE
92     CONTINUE
93     CONTINUE
94     CONTINUE
95     CONTINUE
96     CONTINUE
97     CONTINUE
98     CONTINUE
99     CONTINUE
C
C   CALCULATE THE FIRST DERIVATIVE
C
       B(1)=0.0
       DO 68 IH=2,NP
       IHH=IH-1
       B(IH)=( AR(IH)- AB(IHH))/ STEP
68     CONTINUE
C
C ALL LINES COMPLETED. RETURN THE ARRAYS TO THE MAINPROGRAM
       RETURN
       END
       SUBROUTINE GRAPHS(X,Y,M,ICALL,ISIGN,IPRINT,A,B)
C THE SUBROUTINE STORES SUCCESIVE PLOTS ( LABELED ICALL=1,2,....,IPRINT ) OF
C M X-Y POINTS AND PRINTS OUT THE COMBINED GRAPH WHEN ICALL=IPRINT.OTHERWISE THE CHOICE
C OF SYMBOLS IS CONTAINED IN THE ARRAY MM (THE DATA STATEMENT BELOW).
C A AND B HAVE TO BE DIMENSIONED IN MAINPROG  WITH THE EXPECTED TOTAL NUMBER
C OF POINTS(A AND B STORE THE X AND Y COORDS FROM SUCCESIVE CALLS.)
C ALSO MAINPROG SHOULD HAVE COMMON NN(100),MSIGN(100),MS,IPOINT(100)
       DIMENSION A(1),B(1)
       DIMENSION X(1),Y(1)
       INTEGER ARRAY(105, 44)
       COMMON NN(100),MSIGN(100),MS,IPOINT(100)
       INTEGER XAX,YAX,SIGN,MM(44)
       REAL VERT( 9),0317(6)
       DATA MM / 1H .1H*,1HX,1H.,1H+,1H1,1H2,1H3,1H4,1H5,1H6,1H7,1H8,
      1 1H9,1HA,1HB,1HC,1HD,1HE,1HF,1HG,1HH,1HI,1HJ,1HK,1HL,1HM,1HN,
      2 1HO,1HP,1HQ,1HR,1HS,1HT,1HU,1HV,1HW,1HY,1HZ,1H-,1H=,1H(,1H),1H//
       IF(ICALL.NE.1)GOTO 4
       DO 6 I=1,100
    6  NN(I)=0
       MS=0
4      CONTINUE
       IF(ICALL.GT.100)GOTO 500
       KO= ICALL
       IF(M.EQ.0)GOTO 500
       IF(NN(KO).NE.0)GOTO 130
       NN(KO)=M
       IS=ISIGN
```

```
        IPR=IPRINT
        IF(ICALL.LT.1.OR.IPRINT.LT.1.OR.M.LT.1.OR.ISIGN.LT.0)GOTO 500
        IF(IS    .EQ. 0)IS   =ICALL  + 1
        IF(IS.EQ.45)WRITE(2,502)
502     FORMAT(  92H WARNING FROM THE PLOTTING SUBROUTINE: THE 44 SIGNS EX
       1HAUSTED.THE LAST SIGN,/.WILL BE USED.          )
        IF(IS.GT.44)IS=44
        MSIGN(KO)=MM(IS)
        IPO1 = MS+1
        IPOINT(KO)=IPO1
          MS  = MS+ NN(KO)
        IPO2=MS
        J=0
        DO 1 I=IPO1,IPO2
        J=J+1
        A(I)=X(J)
        B(I)=Y(J)
1       CONTINUE
        IF(ICALL.LT.IPR  )RETURN
51      AMAXA=A(1)
        AMINA=A(1)
        AMAXB=B(1)
        AMINB=B(1)
        DO 52 I=1,MS
        IF(A(I).GT.AMAXA)AMAXA=A(I)
        IF(A(I).LT.AMINA)AMINA=A(I)
        IF(B(I).GT.AMAXB)AMAXB=B(I)
        IF(B(I).LT.AMINB)AMINB=B(I)
52      CONTINUE
        XSCALE =(AMAXA-AMINA) /100.
        YSCALE =(AMAXB-AMINB) / 40.
        IF(XSCALE.EQ.0.0  .OR. YSCALE.EQ.0.0 )GOTO 500
        XAX=MM(40)
        YAX=MM( 6)
        DO 30 I=1,105
        DO 30 J=1, 44
30      ARRAY(I,J)= MM( 1)
        IF( AMAXA+AMINA) 60,61,61
60      I = -AMINA / XSCALE  + 5.5
        DO 65 J=1, 44
65      ARRAY(I,J)=YAX
        GOTO 69
61      I = 1
        DO 62 J=1, 44
62      ARRAY(I,J)=YAX
69      IF(AMAXB+AMINB) 70,71,71
70      J = AMAXB / YSCALE  + 1.5
        DO 75 I=1,105
75      ARRAY(I,J)= XAX
        GOTO 79
71      J=44
        DO 72 I=1,105
72      ARRAY(I,J)=XAX
79      CONTINUE
        J=44
        DO 80 I=5,105,20
80      ARRAY(I,J)=MM(23)
        DO 53 II=1,ICALL
        IF(NN(II).NE.0)GOTO 120
        I= -AMINA/XSCALE +5.5
```

```fortran
      J=    AMAXB/YSCALE +1.5
      ARRAY(I,J)=MM( 1)
      GOTO 53
120   SIGN=MSIGN(II)
      IDO1=IPOINT(II)
      IDO2=IPOINT(II)+NN(II)   -1
      DO 122 L=IDO1,IDO2
      I= ( A(L) -AMINA )/XSCALE+5.5
      J= ( AMAXB -B(L) )/YSCALE+ 1.5
      ARRAY(I,J)=SIGN
122   CONTINUE
53    CONTINUE
      DO 109 I=1,9
  109 VERT(I)=AMAXB - (AMAXB-AMINB)*(I-1)/8.
      DO 110 I=1,6
110   ORIZ(I)= AMINA +(AMAXA -AMINA)*(I-1) / 5.
      WRITE(2,90) VERT(1),((ARRAY(I,J),I=1,105),J=1,5),VERT(2),
     1 ((ARRAY(I,J),I=1,105),J=6,10),VERT(3),((ARRAY(I,J),I=1,105),
     2 J=11,15),VERT(4),((ARRAY(I,J),I=1,105),J=16,20),VERT(5),
     3 ((ARRAY(I,J),I=1,105),J=21,25), VERT(6), ((ARRAY(I,J),I=1,
     4 105),J=26,30),VERT(7),((ARRAY(I,J),I=1,105),J=31,35),VERT(8),
     5 ((ARRAY(I,J),I=1,105),J=36,40),VERT(9),((ARRAY(I,J),I=1,105),
     6 J=41,44),(ORIZ(I),I=1,6)
90     FORMAT (      / 1X,1PE9.2,1X,105A1,4(/11X,105A1),
     1 7(/1X,F9.2,1X,105A1, 4(/ 11X,105A1)) / 1X,E9.2,1X,105A1 /
     2 3(11X,105A1 / )/
     3 9X, E10.3, 5 ( 10X, E10.3 ) )
      RETURN
130   CONTINUE
      WRITE(2,131)KO
131   FORMAT(/ 59H ERRONEOUS CALL OF SUBROUTINE GRAPHS.ATTEMPT TO USE IC
     1ALL= ,I3,  7H TWICE. /)
      RETURN
500   CONTINUE
      WRITE(2,501)
501   FORMAT(/40H ERRONEOUS INPUT TO PLOTTING SUBROUTINE   /)
      RETURN
      RETURN
```